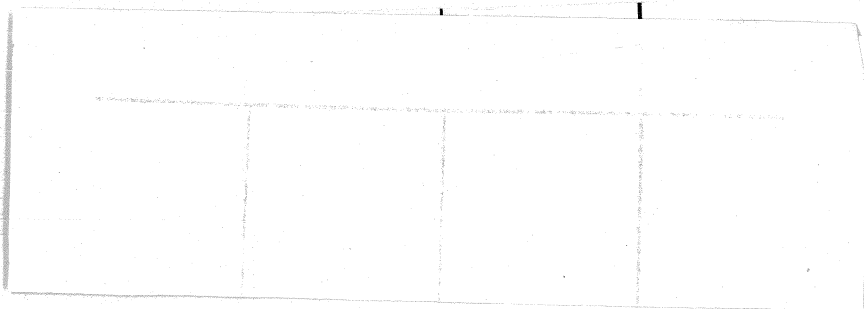


12074

**STUDIES ON PERICARDIAL CALCIFICATION:
PREVENTION VIA SURFACE MODIFICATION
AND DRUG DELIVERY**



A Thesis Presented

by

SINDHU C.V.

to

**The Division of Biosurface Technology
in partial fulfilment of the requirements
for the degree of
Doctor of Philosophy**

**SREE CHITRA TIRUNAL INSTITUTE FOR
MEDICAL SCIENCES AND TECHNOLOGY
THIRUVANANTHAPURAM**

MARCH 1998

CERTIFICATE

I, Sindhu C.V. hereby certify that I had personally carried out the work depicted in the thesis entitled “**Studies on Pericardial Calcification: Prevention via Surface Modification and Drug Delivery**” except where external help sought are acknowledged.

Date 2 April, 1998


SINDHU C.V.

DECLARATION

Dr. Chandra P. Sharma,
Division of Biosurface Technology,
Biomedical Technology Wing,
Sree Chitra Tirunal Institute for
Medical Sciences and Technology,
Thiruvananthapuram - 695 012, Kerala, India.

This is to certify that Mrs. Sindhu C.V. in the division of Biosurface Technology of this Institute, has fulfilled the requirements of the regulations relating to the nature and prescribed period of research for the Ph.D. degree of the Sree Chitra Tirunal Institute for Medical Sciences and Technology, Thiruvananthapuram, Kerala, India. The work relating to her thesis entitled "**Studies on Pericardial Calcification Prevention via Surface Modification and Drug Delivery**" was carried out under my direct supervision.

5/6/98

Chandra Sharma

The thesis
entitled
Studies on Pericardial Calcification Prevention
via Surface Modification and Drug Delivery

Submitted by
Sindhu .C.V.
for
Doctor of Philosophy
of
SREE CHITRA TIRUNAL INSTITUTE
FOR
MEDICAL SCIENCES AND TECHNOLOGY
THIRUVANANTHAPURAM

Evaluated and Approved
by

.....

.....

TABLE OF CONTENTS

	Page
ACKNOWLEDGEMENTS	x
LIST OF TABLES	xi
LIST OF FIGURES	xii
SCHEMES	xviii
SYNOPSIS	xix
CHAPTER I GENERAL INTRODUCTION	1
1.1 Criteria for Heart valve Implantation.	1
1.2 Mechanical Heart valve Prosthesis	2
1.3 Bioprostheses	4
1.3.1 Advantages and disadvantages	11
1.4 General Features of Calcification	11
1.4.1 Physiologic versus Pathologic Calcification	13
1.5 Multifactorial Aspects of Bioprosthetic Calcification	16
1.5.1 Implant Material Factors	16
1.5.2 Host Biologic Factors	19
1.5.3 Stress Localization of Bioprosthetic Calcification	23
1.6 Prevention of Bioprosthetic Calcification	24
1.6.1 Detergent Pretreatment for Inhibiting Calcification	25
1.6.2 Surface Modifications to Prevent Tissue Calcification	26
1.6.3 Controlled release, Site specific Drug Delivery	30
1.7 Polyethylene Glycol (PEG) - A Novel Material to Improve Biocompatibility	33
1.8 Conclusion	35
1.9 Scope and need of the present Investigation	36

CHAPTER 2 MATERIALS AND METHODS

2.1	Materials	39
2.2	Cell Extraction	41
2.3	Chemical Crosslinking	43
2.3.1	Glutaraldehyde fixed BP - GATBP	45
2.3.2	Hexamethylene Diisocyanate fixed bovine pericardium	45
2.3.3	Ethyl -3- (3-Dimethyl amino propyl carbodiimide treated BP	45
2.3.4	Bis(Polyoxy ethylene) bis (glycidyl ether) treated BP	48
2.4	Surface Modification of BP via PEG	48
2.4.1	PEG grafting via free aldehyde group of GA (PEG - GABP)	48
2.4.2	PEG.CHO-BP	50
2.4.3	PEG.NH ₂ -GABP	50
2.4.4	PEG grafting on hexamethylene diisocyanate crosslinked BP (PEG.HMDIC-BP)	51
2.5	Double crosslinking technique of BP	51
2.6	Characterization of PEG grafted Pericardium	52
2.6.1	Percent Grafting of PEG	52
2.6.2	PEG Leaching Studies	53
2.6.3	Determination of the degree of hydration	53
2.6.4	Octane Contact Angle Studies	54
2.7	In vitro Degradation Studies with Enzymes	57
2.7.1	Mechanical Properties	58
2.8	In vitro Calcification Experiments	58
2.9	Development of Chitosan/Polyethylene vinyl acetate Co-matrix	59
2.9.1	Preparation of Aspirin Loaded Chitosan Beads	59
2.9.2	Preparation of Aspirin/Heparin Co-matrix Systems	60
2.9.3	Dissolution Studies	60
2.9.4	Assay of released drugs: Metachromic Toluidine blue assay for heparin	61
2.9.5	Ferric Ion Quantitation	62

2.9.6	Magnesium ion Estimation	62
2.9.7	Platelet Adhesion Studies with Washed Platelets	63
2.9.8	Thromboplastin time	64
2.10	In Vivo Studies	65
2.10.1	Implant and Explant Studies	65
2.10.2	Extraction and Analysis of Alkaline Phosphatase (AP)	67
2.10.3	Histopathology	68
2.10.4	Haematoxylin and Eosin Staining	68
2.10.5	von Kossa Method for Calcification	68
2.11	Scanning Electron Microscopy (SEM)	70
2.12	Statistical Analysis	73

CHAPTER 3 RESULTS AND DISCUSSION

CHAPTER 3.1	EFFECT OF ALTERNATIVE CROSSLINKING TECHNIQUES ON THE ENZYMATIC DEGRADATION OF BOVINE PERICARDIUM AND THEIR CALCIFICATION	74
3.1.1	Enzymatic Degradation of Crosslinked Pericardium	75
3.1.2	Changes in contact angle, Platelet adhesion and calcium deposition due to various crosslinking techniques.	87
CHAPTER 3.2	INFLUENCE OF POLYETHYLENE GLYCOL GRAFTINGS ON THE IN VITRO DEGRADATION AND CALCIFICATION OF BOVIN PERICARDIUM	
3.2.1	Enzymatic degradation of PEG modified tissues through various chemical treatments.	97
3.2.2	Calcium deposition to PEG modified tissues (Via Chemical treatment)	103
3.2.3	Enzymatic degradation of PEG grafted BP versus PEG molecular weight	110
3.2.4	Effect of molecular weights of PEG on tissue calcification and cell adhesion	117

4.3.1	Site specific drug delivery	191
4.4	Future Outlook	193
4.4.1	In vitro wear testing	193
4.4.2	Circulatory Animal Models	193
4.4.3	Development of the tissue engineered valves	194

BIBLIOGRAPHY	195
---------------------	-----

APPENDICES

Appendix A	List of Publications from this work	213
Appendix B	List of abbreviations	214

ACKNOWLEDGEMENTS

*I am greatly indebted to express my deep gratitude to my thesis guides **Dr. Chandra P. Sharma**, Head, Division of Biosurface Technology and **Dr. Thomas Chandy** for their invaluable guidance, constant encouragement, effective criticism and support through out my graduate carrier.*

*I also wish to express my deep sense of gratitude to my doctoral advisory committee members, **Dr. Mira Mohanty** and **Dr. Sankar Kumar** of this institute for their patience, useful suggestions motivation throughout the course of this work and for teaching course related to histology, tissue material interactions, blood compatibility etc.*

*I am grateful to **Prof. K. Mohandas**, Director, **Dr. R. Sivakumar**, Head, **Mr. A.V. George**, Registrar and **Prof. V.V. Radhakrishnan**, Dean of the Institute for providing facilities for my work and administrative help for completing this effort. It is my obligation to thank all officials involved in granting financial help from **Department of Biotechnology** and **Council of Scientific & Industrial Research**, New Delhi for the fulfilment of this work. Being the Head of the **Department of Pathophysiology**, **Dr. Mira Mohanty** has also allowed me to utilize many of the facilities in her laboratory. I also thank **Mrs. Sulekha Baby**, **Dr. Annie John**, **Dr. T.V. Kumari** and **Mrs Usha Vasudev** for their help.*

*It is my pleasure to thank my friends and colleagues in my division **Mr. Willi Paul** and **Mr. L. Rowsen Moses** for their kind advice, discussions, help & cooperation.*

*I also appreciate **Dr. A.V. Lal** and **Dr. Umasankar** for their help in animal experiments. I wish to acknowledge **Mr. R. Sreekumar** for scanning electron micrographs, **Mrs. Vasanthi** and **Mr. Liji Kumar** for their fine art work and photographic supports.*

It is my proud privilege and pleasure to express my sincere thanks to my husband, parents and relatives for their supports, constant encouragement and patience to finish this work.

There are many others who have helped me. Though their names are not mentioned here I am thankful to all whose help I have received directly or indirectly.

LIST OF TABLES

Table Number	Caption	Page
3.1.I	Contact angle, platelet adhesion and amount of calcium deposited to various treated bovine pericardial tissues.	92
3.2.I	Percent of PEG grafting and amount of calcium and phosphorus deposited to PEG-6000 grafted bovine pericardium.	105
3.2.II	Data on PEG-modified bovine pericardium.	106
3.2.III	Percentage of PEG grafting, Mechanical properties (Tensile Strength) and water of hydration of GA fixed and various PEG grafted pericardial tissues.	112
3.2.IV	Octane contact angle, platelet adhesion and calcium deposited after 50 days of calcification to various PEG modified pericardium.	122
3.3.I	Octane contact angle, platelet adhesion and calcium deposited after 21 days of calcification to various double crosslinked pericardium.	144
3.4.I	Adhesion of platelets to glass as a function of released aspirin.	156
3.4.II	Plasma thromboplastin time (PTT) as a function of released heparin.	157
3.4.III	Effect of Fe^{3+} / Mg^{2+} ions released from the chitosan / PE(VA c) co-matrix on pericardial calcification.	167
3.5.I	Amount of calcium deposited on bovine pericardium (Group I to IV) after 21 days and 6 months rats subcutaneous Implantation.	181
3.5.II	Alkaline phosphatase activity of retrieved samples (Group I to Group IV) after 72 hrs. and 21 days represented as the nano mole of para-nitrophenol liberated per minute for mg protein.	184

LIST OF FIGURES

Figure Number	Caption	Page
1.1	Tilting disc model of Chitra heart valve prosthesis; from ultra high molecular weight polyethylene (UHMW-PE) disc and metallic cage of Haynes - 25 alloy.	3
1.2	Bioprosthesis gross photograph	5
1.3	Calcified bioprosthesis (From a colour Atlas of Heart Failure by L.M. Shaprio, K.M. Fox)	12
2.1	Schematic drawing of apparatus for contact angle measurements by the inverted bubble method. Drop of n-octane at the tissue water interface.	55
2.2	3 weeks old wistar rat after subcutaneous implantation.	66
2.3	Interaction between the incident electrons and the sample surface.	69
3.1.1	Effect of various enzymes on the tensile strength of SDS-BP as a function of time. Bar indicates 95% confidence limits.	76
3.1.2	Effect of enzymes on the tensile strength of GATBP as a function of time. Bar indicates 95% confidence limits.	76
3.1.3	Effect of various enzymes on the tensile strength of HMDIC-BP as a function of time. Bar indicates 95% confidence limits.	77
3.1.4	Effect of various enzymes on the tensile strength of EDC treated BP as a function of time. Bar indicates 95% confidence limits.	77
3.1.5	Effect of various enzymes on the tensile strength of GLE treated BP as a function of time. Bar indicates 95% confidence limits.	78
3.1.6	Scanning electron micrographs of crosslinked bovine pericardium. Surface morphology of (A)SDS treated, (B) its 30 days collagenase digested, (C) glutaraldehyde fixed BP, (D) its collagenase digested, (E) HMDIC treated BP, (F) its 30 days collagenase digested.	80

3.1.7	Effect of various enzymes on per cent elongation of SDS-BP as a function of time. Bar indicates 95% confidence limits.	78
3.1.8	Effect of various enzymes on per cent elongation of GATBP as a function of time. Bar indicates 95% confidence limits.	82
3.1.9	Effect of various enzyme digestion on per cent elongation of HMDIC-BP as a function of time. Bar indicates 95% confidence limits.	82
3.1.10	Effect of various enzymes on per cent elongation of EDC treated BP as a function of time. Bar indicates 95% confidence limits.	83
3.1.11	Effect of various enzymes on per cent elongation of GLE treated BP as a function of time. Bar indicates 95% confidence limits.	83
3.1.12	Scanning electron micrographs of adhered platelets to bovine pericardial surface (A) SDS treated BP, (B) GA treated BP, (C) HMDIC treated BP, (D) EDC treated BP and (E) GLE treated BP.	88
3.1.13	Scanning electron micrographs of bovine pericardium after 30 days incubation in calcium phosphate solution (A) SDS treated BP, (B) GA treated BP, (C) HMDIC treated BP, (D) EDC treated BP, (E) GLE treated BP.	90
3.1.14	Amount of calcium deposited on various treated surfaces as a function of time on exposure to calcium phosphate solution. Bar indicates 95% confidence limits.	95
3.2.1	Effect of collagenase digestion in the tensile strength of PEG grafted bovine pericardium as a function of time. Bar indicates 95% confidence limits.	99
3.2.2	Effect of collagenase digestion on percent elongation of PEG grafted BP as a function of time. Bar indicates 95% confidence limits.	99
3.2.3	Scanning electron micrographs of crosslinked bovine pericardium, surface morphology of (A) GA treated BP, (B) its 30 days collagenase digested, (C) PEG grafted BP via GA, (D) its collagenase digested, (E) PEG grafted BP via HMDIC and (F) its collagenase digested.	101
3.2.4	Amount of calcium deposited on PEG grafted bovine pericardium as a function of time on exposure to calcium phosphate solution. Bar indicates 95% confidence limits.	108

3.2.5	Amount of phosphorus deposited on PEG grafted bovine pericardium as a function of time on exposure to calcium phosphate solution. Bar indicates 95% confidence limits.	108
3.2.6	Scanning electron micrographs of bovine pericardium after 30 days incubation in calcium phosphate solution (A) PEG grafted BP via GA, (B) PEG-CHO grafted BP, (C) PEG-NH ₂ grafted BP via GA, (D) PEG grafted BP via HMDIC.	103
3.2.7	Effect of Trypsin digestion on the tensile strength of PEG grafted bovine pericardium, as a function of time. Bar indicates 95% confidence limits.	111
3.2.8	Effect of various enzymes on the tensile strength of PEG-20,000 grafted BP as a function of time. Bar indicates 95% confidence limits.	111
3.2.9	Scanning electron micrographs of various PEG grafted bovine pericardium. (A) PEG-600 grafted BP, (B) PEG-1500 grafted BP, (C) PEG-4000 grafted BP, (D) PEG 6000 grafted BP, (E) PEG-20,000 grafted BP and (F) its 30 days collagenase digested BP.	114
3.2.10	Amount of calcium deposited on PEG grafted bovine pericardium as a function of time on exposure to calcium phosphate solution. Bar indicates 95% confidence limits.	116
3.2.11	Scanning electron micrographs of various PEG grafted pericardium after 30 days in vitro calcification. (A) GATBP, (B) PEG-600 grafted BP, (C) PEG-1500 grafted BP, (D) PEG-4000 grafted BP, (E) PEG-6000 grafted BP and (F) PEG-20,000 grafted BP.	118
3.2.12	Scanning electron micrographs of platelet adhered PEG grafted surfaces. (A) PEG-1500 grafted BP, (B) PEG-4000 grafted BP, (C) PEG-6000 grafted BP, (D) PEG-20,000 grafted BP.	120
3.3.1	Scanning electron micrographs of double crosslinked pericardium after 60 days collagenase digestion (A) GATBP (B) GA.PEG.EDC.PEG-BP, (C) EDC.PEG.GA.PEG-BP, (D) GA.PEG.HMDIC.PEG-BP and 3(E) HMDIC.PEG.EDC.PEG-BP.	127
3.3.2	Effect of collagenase on the tensile strength of double crosslinked BP as a function of time. Bar indicates 95% confidence limits.	129

3.3.3	Effect of collagenase digestion on the percent elongation of double crosslinked BP as a function of time. Bar indicates 95% confidence limits.	129
3.3.4	Scanning electron micrographs of 60 days calcified double crosslinked pericardium (A) GA.PEG.EDC.PEG-BP, (B) EDC.PEG.GA.PEG-BP, (C) GA.PEG.HMDIC.PEG-BP and (D) HMDIC.PEG.EDC.PEG-BP.	134
3.3.5	Amount of calcium deposited on double crosslinked BP as a function of time. Bar indicates 95% confidence limits.	136
3.3.6	Effect of calcification on the tensile strength of double crosslinked BP's as a function of time. Bar indicates 95% confidence limits.	136
3.3.7	Scanning electron micrographs of retrieved double crosslinked BP after 21 days rats subcutaneous implantation (A) GATBP, (B) GA.PEG.EDC.PEG BP, (C) EDC.PEG.GA.PEG-BP, (D) GA.PEG.HMDIC.PEG-BP, (E) HMDIC.PEG.EDC.PEG-BP.	138
3.3.8	Histologic demonstration of double crosslinked pericardium stained with von Kossa after 21 days post implantation (A) GATBP, (B) GA.PEG.EDC.PEG-BP, (C) EDC.PEG.GA.PEG-BP, (D) GA.PEG.HMDIC.PEG-BP, (E) HMDIC.PEG.EDC.PEG-BP.	140
3.3.9	Histologic demonstration of double crosslinked BP stained with haemotoxylin-eosin after 21 days rat subcutaneous implantation (A) GATBP, (B) GA.PEG.EDC.PEG.BP, (C) EDC.PEG.GA.PEG-BP, (D) GA.PEG.HMDIC.PEG-BP, (E) HMDIC.PEG.EDC.PEG-BP.	142
3.4.1	Scanning electron micrographs of (A) Aspirin loaded chitosan beads embedded in heparin loaded PE(VAc), (B) Surface morphology of aspirin loaded chitosan beads. (C) Its ultrastructure, (D) Surface morphology of co-matrix before SBR coating and (E) Surface morphology of co-matrix after SBR coating.	149
3.4.2	Schematic diagram of Aspirin/Heparin loaded chitosan/Polyethylene vinyl acetate matrix (A), and an enlarged cross section (B) and structure of drugs used.	151
3.4.3	Release of aspirin (Asp) from Chitosan/PE(VAc) co-matrix (14.45 mg/cm ²) as a function of time. Bar indicates 95% confidence limits.	153

3.4.4	Release of heparin (Hep) from Chitosan/PE(VAc) co-matrix (11.44 $\mu\text{g}/\text{cm}^2$) as a function of time. Bar indicates 95% confidence limits.	153
3.4.5	Initial phase of aspirin release from Chitosan/PE(VAc) co-matrix (11.45 mg/cm^2) as a function of time. Bar indicates 95% confidence limits.	154
3.4.6	Initial phase of heparin release from Chitosan/PEt(VAc) co-matrix (11.44 mg/cm^2) as a function of time. Bar indicated 95% confidence limits.	154
3.4.7	Scanning electron micrographs of bovine pericardium after 30 days of in vitro calcification (A) Surface morphology of GA treated BP, (B) Surface morphology of GA treated BP with Aspirin heparin delivery, (C) Calcium phosphate deposits with trapped fibrinogen threads.	160
3.4.8	Amount of calcium deposited to bovine pericardium against the released Hep/Asp as a function of time. Bar indicates 95% confidence limits.	163
3.4.9	Initial phase of ferric ion release from Chitosan/PE(VAc) co-matrix as a function of time. Bar indicates 95% confidence limits.	163
3.4.10	Initial phase of magnesium ion release from Chitosan/PE(VAc) co-matrix as a function of time. Bar indicates 95% confidence limits.	165
3.4.11	Scanning electron micrographs of bovine pericardium after 30 days of in vitro calcification (A) Surface morphology of calcified GA treated BP, (B) Inhibition of calcification on GATBP.	166
3.5.1	Scanning electron micrographs of explanted pericardium (A) GATBP, (B) PEG grafted BP, (C) PEG grafted BP with aspirin/heparin delivery (D) PEG grafted BP with ferric/magnesium ions delivery.	170
3.5.2	Scanning electron micrographs of calcified BP after 6 months of implantation (A) GATBP, (B) PEG grafted BP, (C) PEG grafted BP with aspirin/heparin delivery, (D) PEG grafted BP with ferric/magnesium delivery.	172

- 3.5.3 Histological demonstration of calcified pericardial samples stained with von Kossa after 21 days post implantation (A) GATBP, (B) PEG grafted BP, (C) PEG grafted BP coimplanted with aspirin/heparin loaded co-matrix, (D) PEG grafted BP co-implanted with ferric/magnesium loaded co-matrix, (E) PEG grafted BP co-implanted with ferric/magnesium loaded co-matrix 21 days post implantation stained with Perl's Prussion blue. 174
- 3.5.4 Histological demonstration of calcified pericardial samples after 6 months of post implantation stained with von Kossa (A) GATBP, (B) PEG grafted BP, (C) PEG grafted BP co-implanted with aspirin/heparin delivery, (D) PEG grafted BP coimplanted with ferric/magnesium delivery. 177
- 3.5.5 Histological demonstration of implanted pericardium after 21 days subcutaneous implantation stained by haemotoxylin-eosin staining (A) GATBP, (B) PEG grafted BP, (C) PEG grafted BP co-implanted with aspirin/heparin delivery. (D) PEG grafted BP coimplanted with ferric/magnesium delivery. 179
- 4.1 Schematic controlled release co-matrix situated at the valve-annular junction in bioprosthetic heart valve conduct with selective release at the affinity site. 192

Scheme

1. Simplified representation of monomeric glutaraldehyde reaction with amino groups on collagen to form crosslinks. 44
2. Representative reaction of hexamethylene diisocyanate with the amino group on collagen to form ureum crosslinks. 44
3. The sequence of reactions for the carbodiimide method to crosslink tissue. 46
4. Proposed mechanism of crosslinking for polyepoxy compounds to collagen showing the amino group on collagen undertaking a nucleophilic displacement of the epoxy function to form cross-links. 46
5. The proposed mechanism of PEG grafting to glutaraldehyde treated BP (GABP). 47
6. The proposed mechanism of PEG aldehyde grafting to BP. 47
7. The proposed mechanism of PEG amine grafting to glutaraldehyde treated BP. 49
8. The proposed mechanism of PEG grafting to hexamethylene diisocyanate crosslinked BP. 49

**STUDIES ON PERICARDIAL CALCIFICATION :
PREVENTION VIA SURFACE MODIFICATION
AND DRUG DELIVERY**

Synopsis

by

Sindhu C.V.

for the Ph.D degree

of

Sree Chitra Tirunal Institute for Medical Sciences & Technology

Thiruvananthapuram, Kerala.

November, 1997

Diseased heart valves can be replaced by either mechanical or bioprosthetic heart valves. Major disadvantages with the use of mechanical valve is the need for continuous anticoagulant therapy to minimize the risk of thrombosis and thromboembolic complications. These problems led to the effort to develop tissue derived bioprostheses with improved biocompatibility. Calcification and biodegradation are frequent causes of the failure of more than 60% bioprostheses, derived from glutaraldehyde (GA) pretreated bovine pericardium (BP).

The introductory chapter gives an overview of bioprosthetic tissue calcification, aetiological factors involved and its preventive strategies. Clinical and experimental studies revealed that bioprosthetic mineralization occurs as the result of an interactive process involving three broad categories of determinants including implant material factors, host metabolic factors and stress localization. The most important host factor is younger age and the chief implant factors are glutaraldehyde pretreatment, material stress, adsorption of calcium binding serum proteins, alkaline phosphatase enzymes, surface porosity and water content, surface adhered organic or cellular debris etc. This chapter also provides an insight to the basic approaches, like surface modifications and target drug delivery, being tried to reduce bioprosthesis associated calcification. Unfortunately, the exact mechanism of induction and propagation of this disease process is not well defined, and hence the method to prevent calcification. This study deals with the efforts in developing a biostable and calcium resistant material from bovine pericardium.

The general experimental techniques, highlighting the use of each for evaluating and correlating various parameters of tissue calcification and their relevance to biocompatibility are elucidated in chapter 2. Cell extracted bovine pericardia were fixed with various single and double crosslinkers such as glutaraldehyde, carbodiimide, diisocyanate, glycidyl ether etc. and were modified with polyethylene glycol (PEG). Modified pericardia were evaluated and prescreened through in vitro calcification, mechanical property after enzyme digestion, octane contact angle measurement, and platelet adhesion studies. For the controlled delivery of anticalcifying drug combinations such as aspirin/heparin and $\text{Fe}^{3+}/\text{Mg}^{2+}$, a co-matrix system from chitosan and polyethylene vinyl acetate (PEVAc), was developed. The calcification was evaluated in in vitro by incubating pericardium

samples in metastable calcium phosphate solutions. Selected modified pericardial samples were coimplanted with co-matrix system in 3 week old Wistar rats and the retrieved samples were evaluated for alkaline phosphatase activity, and for the presence of calcium by biochemical, histological and scanning electron microscopic techniques.

Chapter 3.1 discusses, the in vitro calcification and enzymatic degradation of bovine pericardia (BP) after a series of treatments with bifunctional tissue cross-linkers such as glutaraldehyde, carbodiimide (EDC), hexamethylene diisocyanate (HMDIC) and glycidyl ether (GLE) as a function of exposure time. GA and HMDIC cross-linked BP retained maximum stability in collagenase digestion compared to noncrosslinked BP. The ability of α -chymotrypsin, bromelain, esterase, trypsin and collagenase to modulate the degradation of SDS, GA, HMDIC, EDC and GLE treated BPs were also investigated. Incubation of various enzymes to this crosslinked pericardia variably reduced the tensile strength of these tissues. In vitro calcification studies showed a substantial reduction in the calcification profile of EDC crosslinked BP as compared to other crosslinked surfaces. Further, the blood compatibility of crosslinked tissues were established by platelet adhesion and octane contact angle measurements. Finally, scanning electron microscopic evaluation of calcified and enzyme degraded samples had also substantiated these observations.

Chapter 3.2 discusses the influence of polyethylene glycol graftings on the degradation and calcification of bovine pericardium. PEG (Mol. Wt. -6000) was grafted on bovine pericardium via different functionalities such as free -CHO of glutaraldehyde fixed BP, -NCO of hexamethylene diisocyanate treated BP and free NH_2 of tissue. The calcification profile of PEG modified BP through aldehyde linkages of GA and isocyanate functionalities of HMDIC had shown significant reduction. The mechanical properties of these PEG modified tissues after collagenase digestion and calcification were also investigated. PEG grafted through glutaraldehyde and HMDIC linkages had shown better mechanical stability compared to other means of PEG grafting. Further, different molecular weight polyethylene glycols (PEG-600,1500,4000,6000 and 20,000) were grafted on GA fixed BP via utilizing their free aldehydic groups. The grafting and leaching percentages of all PEG substrates were noted. Calcification of PEG- 20,000 grafted BP was significantly decreased compared to low molecular weight PEG grafts and glutaraldehyde treated BP(control). The mechanical property of PEG-20,000 modified

tissues were retained after enzyme digestion and calcification. The biocompatibility aspects of grafted substrates were also established by monitoring the platelet adhesion, octane contact angle and water of hydration, percentage of PEG. Scanning electron micrographs of calcified BP, digested BP and platelet adhered BP also supported the above observations.

Chapter 3.3 deals with double crosslinking of bovine pericardium with selected effective tissue fixatives such as glutaraldehyde, carbodiimide, hexamethylene diisocyanate. Using their alternative combinations, further surfaces were modified by high molecular weight PEG. The tensile strength and scanning electron micrography of calcified and collagenase digested tissues had shown significant reduction for GA-EDC and GA-HMDIC combinations. From these in vitro prescreened surfaces, certain selected tissue modifications were then evaluated through subcutaneous implantation in 3 weeks old Wistar rats for 21 days, and retrieved samples were examined through biochemical and histological means for presence of calcification and biodegradation. The biocompatibility aspect of pericardial tissues have also been observed through octane contact angle and platelet adhesion studies. These observations proposed that these bifunctional crosslinking techniques may provide biostability and anticalcifying effects to pericardial tissue.

Chapter 3.4 represents the development of chitosan / polyethylene vinyl acetate co-matrix for the controlled release of drugs having synergistic effects. Aspirin/heparin were embedded in chitosan and polyethylene vinyl acetate comatrix to develop a prolonged release form. The in vitro release profile of these drugs from the co-matrix system were monitored in Tris HCl buffer pH 7.4, using a UV-spectrophotometer. The amount of drug release was much higher initially, which was substantially modified with styrene butadiene coatings to have a slow release profile. From SEM studies it appears that the drug diffuses out slowly to the dissolution medium through the micropores of the co-matrix. The released aspirin / heparin from the comatrix system had indicated calcium antagonistic effects, in addition to their antiplatelet and anticoagulant functions. Similar system was also developed from ferric chloride loaded chitosan beads and magnesium chloride loaded PEVAc. These results proposes the possibility of delivering drug combinations having synergistic effects for therapeutic applications.

Chapter 3.5 comprises results of certain selected (as represented below) groups after subcutaneous implantation in Wistar rats and their evaluation for calcification and alkaline phosphatase activity.

Group I. Glutaraldehyde treated pericardium - GATBP

Group II. PEG -20,000 grafted pericardium - PEG GABP

Group III. PEG grafted pericardium coimplanted with aspirin/heparin loaded co-matrix.

Group IV. PEG grafted pericardium coimplanted with Fe^{3+} / Mg^{2+} ions loaded co-matrix.

Biochemical estimation and electron microscopic and histological staining techniques had shown reduction in calcification and biodegradation of modified samples (group III to IV) compared to the controls (group I). Further AP activity was also markedly reduced in PEG modified and drug delivered cases. It is also noted that the low levels of aspirin/heparin combinations could synergistically inhibit the pericardial calcification in addition to their antithrombotic effect. Another approach in which there was a combined release of Fe^{3+} / Mg^{2+} ions from co-matrix, there was substantial inhibition of deposition of calcium and alkaline phosphatase activity. It may be hypothesised that the PEG grafting at the tissue interface and in parallel with antiplatelet therapy may interfere with the cellular adhesion, activation and extrinsic alkaline phosphatase activity; and the mineralization process.

Finally, Chapter 4 contains the conclusion and future outlook to develop applications. Hence, to summarise, a novel tissue - polymer hybrid material from bovine pericardium and polyethylene glycol was developed. This hybrid material has shown significant reduction in calcification, platelet adhesion and biodegradation. In addition, the low levels of antiplatelet drug combinations could inhibit calcium nodulation on tissues. So, it is concluded that a combination therapy via surface modification and prolonged release of the antiplatelets - may be a possibility towards increasing the functional lifetime of tissue derived prosthesis.

CHAPTER I

GENERAL INTRODUCTION

Heart valves are thin translucent structures containing mostly collagen and proteoglycans and small amount of elastin which are subjected to continuous repetitive mechanical stress for the lifespan of an individual. A variety of pathological processes can lead to heart valve malfunction. These include genetic diseases of the connective tissues where crosslinking of collagen is impaired, rheumatic fever, and a variety of infectious diseases. A major cause of ultimate failure is calcification, a common sequela to problems involving the cardiovascular system. The pathogenesis of calcific aortic stenosis is still a matter of controversy. Calcification of the annulus fibrous of the mitral valve is a frequent finding in older patients at necropsy. Dysfunction is usually associated with degenerative changes of the tissue substances which require surgical correction or replacement with a prostheses. Heart valve prostheses have been used successfully since 1960.²⁰⁶ Of the more than 50 different type of cardiac valve introduced over the past 35 years, many have been discarded due to their lack of success and of those remaining several modifications have been made. The **mechanical** and **bioprosthetic** heart valves are the most common types used at present.

1.1 Criteria for heart valve Implantation

The ideal cardiac valve substitute remains the goal for those seeking to improve the clinical results of replacement surgery. The generally accepted characteristics of the ideal heart valve substitute should:^{116, 206} be fully sterile at the

time of implantation and be non-toxic, be surgically convenient to insert at or near the normal location in the heart, conform to the heart structure rather than conforming to the valve, show a minimum resistance to flow so as to prevent a significant pressure drop across the valve, have minimal reverse flow necessary for valve closure so as to keep the incompetence of the valve at low levels, show long resistance to mechanical and structural wear, be long-lasting and maintain its normal functional performance, cause minimum trauma to blood elements and the endothelial tissue of the cardiovascular structure surrounding the valve, show a low probability for thromboembolic complications without the use of anticoagulants, be sufficiently quiet so as to not disturb the patient, be radiographically visible, and have an acceptable cost. No cardiac valve prosthesis currently available completely satisfies these criteria.

The challenge of replacing the natural heart valve with a prosthetic device continues to be a formidable one. Materials do not exist that can duplicate the flexibility of natural valves in which the orifice and leaflets can deform in harmony with myocardial action. Nor is it possible for man to match nature's ability to remodel and heal in order to maintain and preserve the function of an artificial device. In spite of the magnitude of the challenge, the replacement of a diseased valve with a prosthetic contrivance offers a better prognosis than today's medical treatments.

1.2 Mechanical Heart Valve Prosthesis

Mechanical heart valve prosthesis, composed of rigid biomaterials (polymers, metals or LTI carbon) employ a poppet occluder which responds passively to changes in intracardiac pressure and flow.^{116, 188, 206} Many of the observed complications of

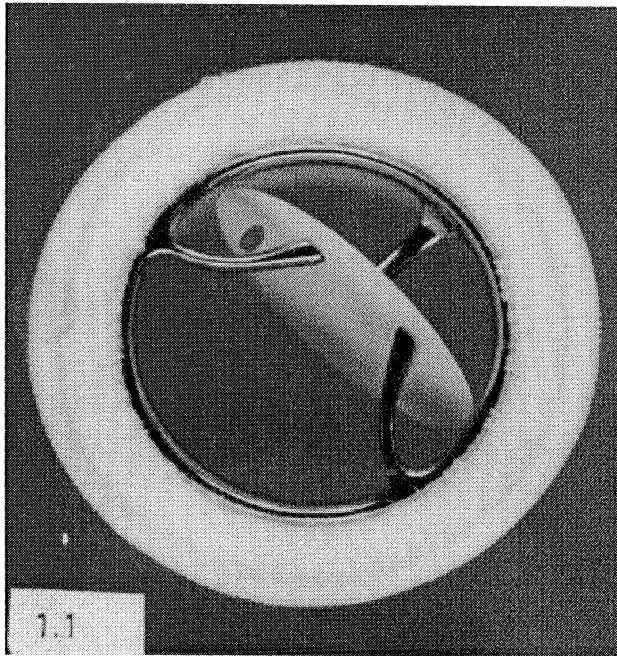


Figure 1.1 Tilting disc model of Chitra heart valve prosthesis; from ultra high molecular weight polyethylene (UHMW-PE) disc and metallic cage of Haynes-25 alloy.

mechanical valve prostheses can be explained by a close inspection of their functional components. A wide variety of valve models are, regularly used in clinical practice, which consists of either a caged ball,¹⁰⁶ caged disc, or tilting disc¹² (either mono or bileaflet in design). The turbulent flow characteristics and nonendothelialized surfaces typical of current mechanical prostheses cause the bulk of intrinsic failures. The most serious problem and complications associated with heart valve prostheses are local thrombosis,¹³⁴ distant thromboembolism,¹²⁹ tissue over growth, infection, tearing of sewing sutures, red cell destruction (haemolysis),¹⁶⁴ valve failure due to material fatigue or chemical change, damage to the endothelial tissue lining of the vessel wall adjacent to the valve, and leaks caused by failure of the valve to close

properly and complications of therapy intended to reduce these problems. The choice between prosthesis of different design and manufacture has therefore often to be made on the basis of their thrombotic and embolic characteristics. It is thus important for the cardiac surgeon to have reliable information about thrombogenicity of individual prosthesis in order to make a logical choice. Thromboembolism, tissue overgrowth, red cell destruction and endothelial damage are directly related to the fluid dynamics associated with the various prosthetic heart valves. The other problems are directly related to fluid mechanics. These complications led to the effort to develop tissue derived bioprosthetic cardiac replacement valves.

1.3 Bioprostheses

Biological valves can be grouped into three categories: aortic valve allografts, aortic valve xenografts and valves constructed from non-valvular tissue of auto-, allo- or xenogenic origin. Interest in the clinical use of tissue valves was kindled by Lam, Aram and Munnell who, in 1952, successfully implanted fresh aortic allografts in the descending thoracic aorta of dogs.¹⁰¹ In 1962, the first successful clinical orthotopic implantation of allograft valve in the aortic position was accomplished by Ross.¹⁶⁵ The main problem with these cadaveric allografts, as far as may be ascertained, is that they are no longer living tissue and therefore lack that unique quality of cellular regeneration typical of normal living system. This makes them more vulnerable to long term damage. A variety of biological tissue have been used for the manufacture of heart valve substitutes such as fascia lata,¹⁷⁸ dura mater,⁴³ pericardium,⁹¹ peritonium,⁵⁰ tissue to implanted silastic⁵⁸ and vena cava.¹⁵⁸

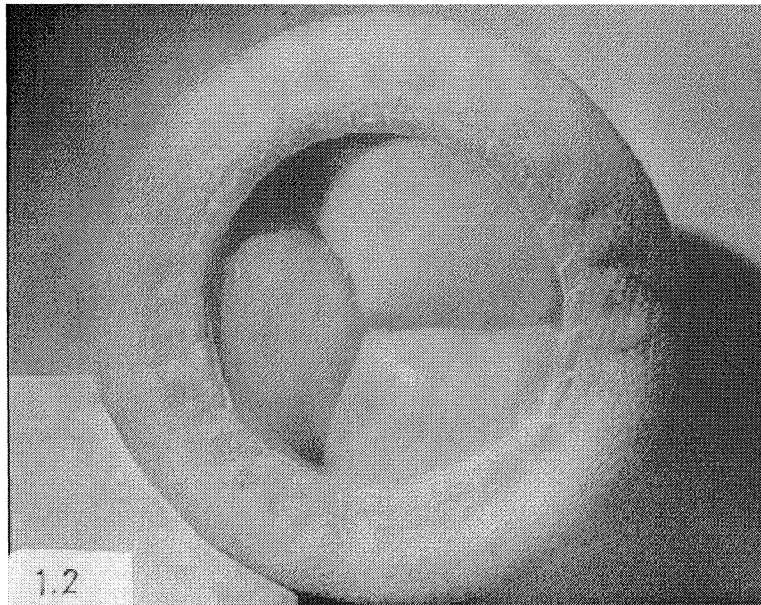


Figure 1.2 Bioprosthesis gross photograph

The next stage in the development of tissue valve substitute was the use of autologous fascia lata either as free or on frame mounted leaflets.^{9,178} The failure of this technique was due to the inadequate strength of this tissue when subjected to long-term cyclic stressing in the heart. In parallel with the work on fascia lata valves, alternative forms of tissue leaflet valves were, being developed from dura mater.⁴³ The allogeneal dura mater has the necessary qualities for use in the preparation of artificial cardiac valves. It has an almost uniform thickness and pliability in the 'avascular' areas. Its tensile strength is satisfactory and uniform for a particular area. Another alternative approach is to transplant the patients' own pulmonary valve into the aortic position. This transplantation technique is however, limited in that it can only be applied to one site.⁶⁰

Glutaraldehyde (GA) preserved porcine bioprostheses have been used as cardiac valve substitutes since 1971. The introduction of GA for the fixation of

biological tissues by Carpentier and colleagues²³ in 1969 facilitated the use of bioprosthesis, both porcine and bovine pericardium, as a satisfactory alternative to mechanical valves. In 1971 Reis *et al*¹⁶² described a valve substitute using an explanted GA treated porcine aortic valve which was mounted on to a frame having a rigid base ring with flexible posts, and was commercially available as the Hancock Porcine Xenograft.¹³⁵ It remains one of the two most popular valve substitutes of this type, the other being the Carpentier-Edwards bioprosthesis introduced commercially by Edward Laboratories.^{92,93,94} The porcine bioprostheses available now for implantation as cardiac valve substitutes are new generations from previous porcine valves. The previous generation prosthesis, the Hancock standard and the Carpentier-Edwards standard, are high pressure GA fixed prosthesis.²² The new generation bioprosthesis are essentially treated with low pressure GA fixation and have been in use since 1982. Carpentier and colleagues^{22,23} introduced the Carpentier-Edwards suprannular porcine bioprosthesis to reduce fatigue lesions and improve hemodynamics and provided the Hancock II porcine valve in 1982. The Medtronic-Intact pressure free GA fixed porcine bioprostheses had also been introduced which claimed to have given patients an excellent quality of life with a low rate of serious thromboembolism, essential lack of thrombosis, and freedom from anticoagulant related haemorrhage.

In this type of prostheses the use of the intact biologically formed valve obviates the need to manufacture individual valve cusps.^{9,17} Whilst this has the obvious advantage of reduced complexity of construction, the latter problem did not

occur in the production of three leaflet calf pericardial valves developed by Ionsecu et al.^{90,91} The majority of pericardial bioprosthesis are fabricated from bovine parietal pericardium, with the exception of the Polystan valve in which porcine parietal pericardium is used. There are also attempts to develop leaflet valves from man-made materials such as block polymers or modified polyurethanes.¹⁶⁰

The third possibility, bovine pericardium, seemed to possess the advantage of the cadaver and porcine valves over the mechanical valves, in terms of a lower thrombogenicity. Its availability made it more convenient than the homografts. Its ease of construction on unobstructive stents, and therefore better haemodynamics than the porcine valve, pointed towards a very promising venue. Parietal pericardium is composed of three layers: a serosal layer, which consists of mesothelial cells, their basement membrane, and a narrow submesothelial space; the fibrosa, which contains collagen bundles, elastic fibers, nerves, blood vessels and lymphatics; and the epipericardial connective tissue, which has more loosely arranged collagen and elastic fibers. Fibroblasts are present in the fibrosa and epipericardial tissue; few histocytes and mast cells are also seen. Clusters of adipose tissue cells are present, especially in the epipericardial connective tissue layer. In pericardial bioprosthesis the epipericardial tissue layer corresponding in orientation to the inflow surface is extremely rough because of its content of large, coarse bundles of collagen. The serosal surface is lined by mesothelial cells with numerous microvilli, which characteristically are much longer and numerous than those present in valvular endothelial cells. During preimplantation processing the mesothelial cells are largely

lost and then the serosal surface appears smooth because it is composed of exposed basement membrane and underlying collagen fibrils. The collagen bundles in parietal pericardium are overlapping and multidirectional rather than highly oriented and layered. The waviness or crimp, of the collagen bundles is more pronounced, and the mean diameter of the collagen fibrils is larger in parietal pericardium (about 100nm) than in porcine aortic valves. Elastic fibers in pericardium are larger but less numerous than those in any of the layers of porcine aortic valves. Biochemical studies have shown that 90% of the protein in bovine pericardium is collagen, mostly Type I.¹⁷⁶

The collagen molecule is a generic term for a family of extracellular proteins which are essentially polymers of amino acids. Nineteen types of collagen have been identified.^{42,137,143,167} They differ genetically, chemically and immunologically. At the most basic level, a collagen molecule consists of three chains of poly (aminoacids or polypeptides) arranged in a trihelical configuration ending in non-helical carboxyl and amino terminals, one at each end. These nonhelical ends are believed to contribute to most of the antigenic properties of collagen.⁵² Collagen molecules assemble to form micro fibrils to give the collagen fibre. In their natural state, the collagen trihelical configurations are held in place by direct chemical bonds, hydrogen bonds and water bridge cross-links.^{20,105} Associated with collagen tissue are elastin and proteoglycans, mucopolysaccharides attached covalently to protein cores. They are believed to modulate collagen fibrillogenesis, fill space, bind and organize water, and repel negatively charged molecules in these collagenous tissue fibers. The amino

acids in collagen contain pendant groups such as amines (NH₂), acids (COOH) and hydroxyls (OH) and together with the amide bond of the polymer, are points for possible chemical reactions on collagen.^{137,143,167} Additionally, water molecules surrounding the collagen molecules form another source of entry for reaction, since they can be displaced upon dehydration, exposing previously concealed groups for potential cross-linking.

Fresh pericardium, as such, can be used for the manufacture of tissue valves but may fail due to immunological rejection and biodegradation. These problems can be reduced via crosslinking the tissue with tissue fixatives. The crosslinking can prolong the materials original structural and mechanical integrity and remove or at least neutralize the antigenic properties attributed to these materials.¹⁴² These supplementary links reinforce the tissue to give a tough and strong but viable material that maintains the original shape of the tissue.

Physical and chemical methods for the treatment of collagenous tissue are available. The process of stabilizing tissue involves the chemical agent or physical process initiating, ideally, irreversible and stable intra - and intermolecular chemical bonds between collagen molecules. Preferably, the agent promotes bond between the functional groups of the amino acids. Chemical methods typically utilize bifunctional chemicals that interact with collagen at two different sites.⁹⁹ The functional groups of the chemical agent react with those on the amino acid residues of collagen, such as the -amino function on lysine and hydroxylysine or the carboxyl function on aspartic and glutamic acids, to give rise to 'cross-links' between the collagen molecules.¹⁹⁶ A

drawback of chemical agents is the potential toxic effects, a recipient may be exposed to form residues and/or chemicals resulting from a reversal of the cross-links. Physical methods include drying, heating or exposure to ultraviolet, plasma glow or gamma radiation. Unlike chemical cross-linking, these methods do not introduce toxic chemicals into the tissue, but this does not preclude undefined side-effects that may arise due to these processes.

The efficiency and extent of these reactions depend on the thickness of layers of collagenous tissue which defines the magnitude of penetration and are a function of parameters such as the concentration of the reagent, and the time and the temperature of exposure. It is generally accepted that the more exogenous bonds that are generated in the natural biomaterial, the better the durability. Ideally, the treatment should also maintain much of the original character of the tissue, such as its flexible mechanical properties, and should not shrink significantly. Hence the necessity of keeping the tissue near neutral pH, ensuring an aqueous media environment and minimizing denaturation of the collagen. Therefore a balance must be achieved for attaining enough reliable cross-links for the biomaterial to last the lifetime of the recipient, yet permit the biomaterial to perform as it would in its natural state.

For the construction of pericardial xenografts, the stabilized pericardium is attached onto the outer aspect of the dacron cloth covered titanium stent, thus maintaining intact the central opening which is the inside diameter of the fabric.

1.3.1 Advantages and disadvantages

Tissue bioprosthesis gained wide spread use during the mid 1970s. The major advantage of tissue bioprostheses compared to their mechanical counter parts, is that they have a lower incidence of thromboembolic complications.^{91,116,206} Therefore, tissue valves for a large part can be used without anticoagulants. Furthermore, tissue valves are silent in operation, produce minimal blood trauma, patient inconvenience and anxiety, have central flow path and financial advantages.

Despite the generally satisfactory haemodynamic performance of tissue valves, reports on clinical experience with tissue valves increasingly indicate time dependent structural changes such as **calcification** (figure 1.3) and leaflet wear, leading to valve failure, and subsequent replacement.^{75,114,174} 'Cuspal mineralization', however is a significant limitation to their long term success, with calcification accounting for over 60% of failures.^{2,136} Despite the clinical importance of this problem, its pathogenesis is incompletely understood, and there is at present no effective therapy.

1.4 General Features of Calcification

Calcification is a normal or physiological, event in the formation of bone, dentin and tooth enamel, but calcific deposits are unusual in functional soft tissues. Dystrophic , pathologic calcification, defined as the accumulation of crystalline calcium phosphate in necrotic or otherwise altered tissues, is a relatively common phenomenon in cardiovascular diseases.^{163,169,171,204} These initially diffuse calcific deposits increase in number and size, eventually coalescing to form calcific nodules in the tissue collagen (intrinsic calcification). The nodular calcium deposits leads to a

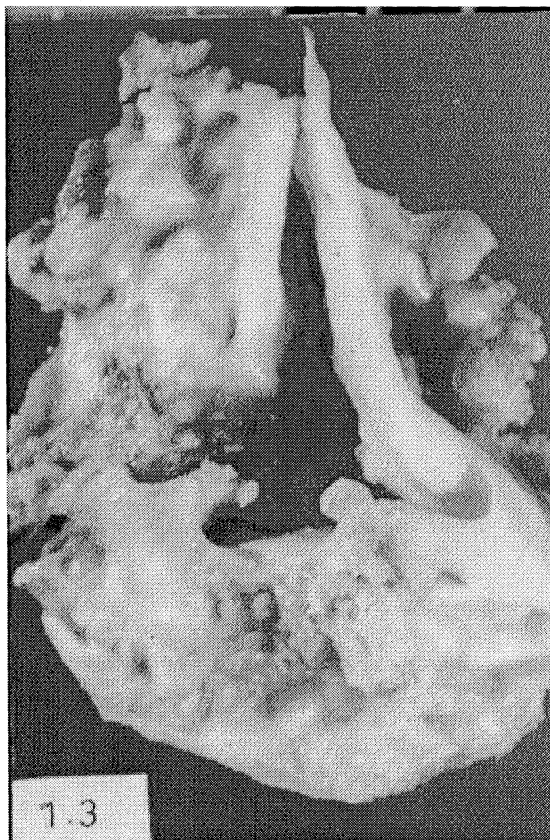


Figure 1.3 Calcified bioprosthesis (From a colour Atlas of Heart Failure by L.M. Shaprio, KM Fox).

predominance of either of two outcomes, stiffening of the cusps which causes valvular stenosis, or ulceration and tearing of the cusps which causes valvular regurgitation.^{72,113,205} Although both phenomena often coexist in a given prosthesis, the clinical symptomatology is usually due to regurgitation. Calcific deposits on the external surface of the cusps (extrinsic calcification) occasionally are seen, arising from the ulceration of intrinsic deposits. Extrinsic calcification, not contributory to prosthesis failure, is frequently associated with bacterial endocarditis in which the mineral deposits occur within the inflammatory cells of the vegetations or within the

bacteria themselves. Extrinsic calcification can also occur independently within superficial platelet thrombi. It has also recently been suggested that insudation of blood and molecular blood constituents, such as fibrin - an amyloid may further contribute to overall cuspal mineralization.

Although calcification is functional, thus physiological, phenomenon in the skeleton and dental structures, extraskeletal and extradental calcification is pathologic.² Pathological calcification may be subdivided into two types: meta static in hypercalcemic subjects, and the other type seen usually in association with tissue damage.¹⁷² Clinically important dystrophic calcification termed as “calcific diseases” by Anderson,² include, atherosclerosis, senile aortic valve stenosis, crystal deposition arthritis,² dental calculus,²⁰⁵ ischemic myocardial calcification¹⁶⁹ and the dysfunctional calcification of implanted medical devices such as valvular grafts, cardiac assist devices,⁴¹ bioprosthetic heart valves,¹⁷³ soft contact lenses¹⁶⁶ and intrauterine contraceptive devices.⁸⁴ Although the mechanism leading to pathological calcification are incompletely understood, there are parallels and interrelationships with physiological mineralization.

1.4.1 Physiologic versus Pathologic Calcification

Bone is composed mainly of mineral (65%) and structural protein collagen in a highly organized functional array.¹⁵⁵ Long bone growth has been demonstrated to occur as a result of cellular proliferation of osteoblast precursors at the cartilaginous epiphyseal growth plate associated with the eventual death of these proliferating

columns of cells. This is followed by mineralization of their vascular fragments; these have been termed matrix vesicles.^{3,62,63} The resulting mineral is subsequently deposited in the extracellular matrix, and is there noted to also occur in association with collagen.⁶³ The predominant crystalline mineral phase present in the bone is hydroxyapatite, although there has been much speculation concerning the presence of other unstable calcium phosphate salts as precursors.^{62,63} It has been hypothesized that mineral is deposited initially as amorphous calcium phosphate, undergoes a phase transition to brushite $\text{CaHPO}_4 \cdot 2\text{H}_2\text{O}$, which then recrystallize as octacalcium phosphate $(\text{Ca}_8\text{H}_2 [\text{PO}_4]_6 \cdot 5\text{H}_2\text{O})$ finally forming hydroxyapatite $\text{Ca}_{10} [\text{PO}_4]_6 (\text{OH})_2$.

The localization of ultrastructural mineral deposits in calcified bioprosthesis to vesicular cell fragments and collagen is comparable to bone.^{10,190} Although there is much debate as to the interrelationship of the two sites and mechanisms of development of mineral deposition, there is little doubt that both exist and that in the case of endochondral bone formation, matrix vesicle mineral deposition occurs first.³ Of additional interest is the predominance of Type I collagen as the most abundant protein in both bioprosthetic heart valve tissue¹⁷⁴ and bone.⁸³ Type I protein is present in both dermis and tendon and this observation has suggested the hypothesis that the molecular alignment created by extensive intermolecular collagen crosslinks enhance the propensity to calcify. The hypothesis may also be of relevance with regard to chemically induced crosslinkages, such as those created by glutaraldehyde in bioprosthetic heart valve tissue and the tendency of this biomaterial to calcify.¹⁷⁴

Regulation of mineral deposition in the extracellular matrix of bone has been hypothesized to be locally controlled by an interaction of naturally occurring promoters and inhibitors of mineral deposition. The principal promoting molecules are thought to be the acidic phospholipids which may function to promote calcification either by their own individual effects or through the formation of calcium-phospholipids-phosphate complexes, which may also be of importance in the formation of initial mineral deposits.^{18,152} The principal naturally occurring inhibitors of hydroxy appetite formation identified thus far are pyrophosphate⁵⁵ and proteoglycan¹⁶ and phosphocitrate.¹⁸⁶ Though it has been hypothesized that bone mineral formation is regulated by the enzyme alkaline phosphatase, which hydrolyzes pyrophosphate and therefore leads to the selective removal of this inhibitor, this intriguing hypothesis is still under investigation. There are a number of other matrix proteins present in mineralized bone, but their role in mineral regulation is at present unclear. These include the collagen-binding protein, osteonectin and the vitamin K dependent calcium binding protein, osteocalcin which is also present in bioprosthetic heart valve calcification.¹²²

In bone, after the initial cellular proliferation and calcification of osteoid matrix, extracellular calcification and remodeling via osteoclast activity is the predominant process in development and growth. Bone morphogenesis and geometrical organizations are thought to be due, in part, to the effects of local mechanical stresses, and the response of the mineralizing matrix to these stresses.¹⁸⁷ This hypothesis known as Wolff's law, states that "Every changes in the form of

function of bone or in their functions alone, is followed by certain definite changes in their internal architecture and equally definite changes in the external conformation in accordance with mathematical laws. In essence, the internal architecture and geometry correspond to the best mechanical arrangements possible to resist functional stresses with the least amount of material. The cellular and extracellular regulatory mechanism which accounts for bone remodeling, is according to Wolff's law hypothesis.²⁰³ Perhaps similar process also explain in part the stress localization noted in bioprosthetic heart valve failures in which the calcified deposits are most intense at the commisural and annular attachments, which are sites of greatest mechanical stress.¹⁸⁶ However, unlike bone, in preserved bioprosthetic valves there appears to be little to no remodeling of valvular mineral, and no additional connective matrix is laid down during the development of the pathological calcification.

1.5 Multifactorial Aspects of Bioprosthetic Calcification

Clinical and experimental studies reveals that bioprosthetic mineralization occurs as a result of an interactive process involving three broad categories of determinants, namely implant material factors, host biologic factors and stress localization.

1.5.1 Implant Material Factors

Fresh biological tissues as such can be used for the manufacture of the tissue valve, but may fail due to immunological rejection and biodegradation. These defects can be reduced by crosslinking the tissues with tissue crosslinking agents.

Reaction of Glutaraldehyde with collagen

Glutaraldehyde (1,5 pentane dialdehyde) has been used since antiquity for the tanning of leather and for the past 30 years as a tissue fixative.^{176,204} Two basic reactions most likely account for the unique structural stability of connective tissue treated with GA.^{126,127} The free aldehydic group of monomeric and/or polymeric (aldol condensation or hydrated cyclic aldehydes) GA react with primary amines of lysine, hydroxylysine or N- terminal amino acid residues present in the protein to form a Schiff base. The Schiff base is then reduced to form a secondary amine linkage which is extremely stable at physiological temperature and pH. The types of reaction products vary from simple Schiff base to complex pyridinium Chromophores.^{119,128} Pretreatment of porcine aortic valve leaflet or bovine pericardium with GA results in a noticeable color change of these materials from white to tan, which is thought to reflect the formation of cyclic-chromophores due to aldehyde -amino reactions. Bioprosthetic heart valve tissue is typically pretreated at pH 7.4 so that the tissue will be exposed to physiologic pH during fixation; which may prevent material damage due to extremes of pH. The glutaraldehyde pretreatment procedures have three net results: material stability is enhanced, tissue thromboresistance is maintained, and antimicrobial sterility is also reasonably preserved.¹²⁰ Cheung et al³⁸ proposed that high concentrations of glutaraldehyde promote rapid surface cross-linking of the tissue, generating a barrier that impedes or prevents the further diffusion of GA into the tissue bulk. There is also some dispute as to whether fixation is complete as the

depth of tissue increases, hence GA's cross-link effectiveness is dependent upon pH, temperature and concentration used. Studies have shown that low or zero pressure fixation is best retaining the original character of tissue.^{19,54,126} Despite the problems with implant calcification, GA remains the reagent of choice for bioprosthetic heart valve fabrication because of these considerations.

But, observations have shown that brief exposure to GA may result in less calcification. Diminished calcification following brief GA exposure may simply occur because the material is inadequately cross-linked and therefore fails to calcify. Bioprostheses prepared in such a way also fail due to material instability. The chemical and biological studies suggested that local cytotoxicity of GA crosslinked bioprostheses may be due to unstable GA polymers that persist in the interstices of crosslinked tissues.⁶⁷ One cannot distinguish whether the release of GA was due to the reversibility of the GA crosslinks or the breakdown of the collagenous matrix. The release of glutaraldehyde from the prosthesis may be due to (1) the degradation of GA crosslinks by some unidentified hydrolytic mechanism (2) the reversibility of some of GA crosslinks and (3) the release of uncrosslinked GA and its derivatives. Recent studies in a rat model have confirmed the immunogenicity of GA treated bovine pericardium, with both a cytotoxic and a humoral response observed.^{45,116} The glutaraldehyde treatment of tissues is thought to be one of the causes for calcification. Calcification appears linked to both GA crosslinking of collagen molecules and the presence of devitalized cellular debris. During the fabrication of tissue - derived heart valve materials, cells are ruptured, but the cellular debris is largely retained.

These cell remnants have been microscopically associated with earlier crystal formation.¹⁷⁰

Surface charge was studied as another factor in calcification. GA treatment on tissue reduces the positively charged moieties and thereby increases net negative charge. Since calcium ions has a positive charge, negatively charged protein will attract calcium ions.²⁵

1.5.2 Host Biologic Factors

Age of the host is an important factor involved in calcification.

A. Age and Vitamin D Effects

The rate of clinical and experimental bioprosthetic tissue calcification is dependent on host metabolic factors.^{116,118,119} Calcification in particular and valve failure in general are markedly accelerated in children, adolescents, and young adults.^{116,117,118,119} This age effect has been observed in rat studies with a sixfold greater calcium accumulation in implants in three week old male weanling rats compared to those in 6 month old retired breeders.¹¹⁶ It has been reported that serum phosphate levels have been significantly higher in the younger animals than in the older ones, although the direct correlation is not possible with serum phosphate levels at sacrifice with tissue calcium or phosphorus. Further, an age dependent difference in serum levels of the vitamin K dependent calcium binding bone protein, osteocalcin, with higher osteocalcin has been observed levels in younger animals. However, the serum osteocalcin levels also did not correlate with bulk mineral measurements in the

explanted cusps, and vitamin K antagonism did not affect the valve calcification.^{56,122}

One possible explanation for age effect may be due to the difference in parathyroid hormone metabolism which exist between immature and adult animals, as reflected by the serum phosphate levels.^{116,118,119} However, the age dependent endocrine interaction with this disease process is complex and may be related to vitamin D metabolism as well.

B. Vitamin K dependent Calcium Binding Proteins

Calcium binding proteins containing-carboxyglutamic acid result from post translational carboxylation of specific glutamic acid residues by several protein specific vitamin K dependent carboxylases.^{56,126,182} Carboxyglutamic acid (Gla) is normally present in the protein osteocalcin, the most abundant noncollagenous protein found in the tissue. Gla proteins have been shown to be present in all cardiovascular calcification, including those present in arteriosclerosis, calcific aortic stenosis, cardiac assist device calcium deposits and calcified bioprosthetic heart valves.¹²³ These osteocalcin proteins are not normally present in vascular tissue, and in the case of calcified heart valve leaflets, the tissue levels of Gla protein have been demonstrated to correlate with mineral accumulation. Calcium binding proteins containing amino malonic acid have been shown to be present in calcified cardiovascular tissue, but are not present in nonmineralized samples.¹⁹¹ However, the pathophysiological role of proteins containing aminomalonic acid is not well understood.

C. Cellular and Immunological Effects

Redistribution and accumulation of intracellular calcium may occur during cell contact with a biomaterial. The nucleus of calcification appears as a result of adhesion and death of cells which contain calcium, phosphate, phospholipids, lipoproteins and enzymes.⁴⁸ As a result of cell death, membrane fragments forming a vesicular matrix appear in the media and calcium phosphate crystals are formed in this matrix. Adsorption of these structures onto implant surface generates nuclei of calcification. Neither nonspecific inflammation nor specific immunologic responses appear to mediate bioprosthetic tissue calcification.^{45,48,116} Inflammation doesn't induce either mineral deposition or resorption.

D. Calcium-Magnesium ATPase Enzymes

Calcification of cells or cell fragments is due to distortion of normal physiology. Normally living mammalian cells maintain an intracellular calcium concentration which is approximately one ten thousandth that of extracellular level. In physiological states, despite passive entry of calcium into cells through several types of calcium channels.^{51,114,116} This steep gradient is maintained by the outward pumping activity of several ATP dependent calcium buffering mechanisms. Cell death causes both increased calcium influx and decreased efflux. Thus increased calcium influx may be coupled with the activity of alkaline phosphatase or other intracellular phosphatases leading to the hydrolysis of phosphoesters. Thus it appears that this causes an increase in phosphorus nodulation which itself may be an initiating mechanism for calcium phosphate crystallization in cardiovascular implants.⁵¹

E. Alkaline phosphatase (AP)

Levy et al¹¹⁶ have proposed that alkaline phosphatase, an enzyme also associated with matrix vesicles involved in bone mineral nucleation, is present in fresh bioprosthetic tissue at sites of initial mineralization. Alkaline phosphatase has been hypothesized to facilitate the initiation of bone mineralization both by the hydrolysis of phosphoesters, thereby raising regional phosphate concentrations, and by the hydrolysis of inhibitors of calcification such as pyrophosphate. It is assumed that alkaline phosphatase acts as matrix vesicles for sequestration of calcium ions to the phosphorus nodules and subsequent mineralization of bioprosthetic tissues.

An enrichment of alkaline phosphatase within the matrix vesicles suggests an important role for this enzyme in the initiation of calcification; following nucleation, AP activity declines progressive bone mineralization. However some studies have shown that AP catalytic activity is not absolutely required for matrix vesicles calcification.⁵⁹ The fact that the enzyme was found distributed widely in tissues that normally do not undergo mineralization, has raised questions as to the specificity of the relationship between AP and calcification.¹⁴¹

Earlier observation have demonstrated AP activity in glutaraldehyde-pretreated porcine aortic valve tissue¹³⁰ and glutaraldehyde pretreated pericardial bioprosthetic tissue¹⁹⁶ after glutaraldehyde fixation AP activity is only detectable by histochemistry, and is not extractable using the established butanol extraction procedure.¹⁹⁷ Further more, subdermal implant studies have demonstrated peak

extractable AP levels in GATBP after 72 h implantation, coinciding with onset of calcification. AP activity declined thereafter, while bulk mineral increased.¹⁹⁶

F. Role of Phospholipids

Acidic phospholipids such as phosphatidyl inositol and phosphatidyl serine are present in high levels in cells at the mineralizing front in bone and in pathological calcification.^{42,116,118,153} However, phospholipids and phosphoproteins form a nucleation complex with calcium and phosphate, which may initiate bone mineralization. These acidic phospholipids may function to promote calcification either by their individual effects or through the formation of calcium-phospholipid-phosphate complexes.^{150,153}

G. Role of Collagen and Elastin

Collagen oriented calcification is usually noted to occur significantly later and perhaps secondary to cell oriented calcific deposits.⁴² It has also been observed that calcification of collagen is prominent following long-term implantation. Hence, it is conceivable that collagen calcification may occur independently of cell oriented mineralization observed in the media of aortic homografts in rat subdermal explants. It is apparent that both cell-oriented and elastin calcification occur and these phenomena may be mechanically related.

1.5.3 Stress Localization Of Bioprosthetic Calcification

Primary stress-mediated valvular dysfunction produces some bioprosthetic valve failure by mechanisms apparently related to collagen degradation. Gross calcific deposits are noted to begin in the areas of leaflet flexion, where dynamic force

and related material stress are maximal. The pattern of mineralization correlates with the magnitude of stress and with the mode of tissue deformation^{116,187}. This type of mechanical stress is not a prerequisite for the nucleation of calcific deposits in bioprosthetic heart valve tissue.

The exact mechanism responsible for stress acceleration of calcification is unknown. However, it is well understood that collagen is a prominent site of calcification in clinical and experimental bioprosthetic valve implants. Electrical energies generated by the intermittent mechanical deformation of collagen due to the piezoelectric nature of this protein, may regulate calcium accumulation directly.^{125,172,185} Since calcific nodules grow between disrupted tissue planes, material stress could result in the disruption of tissue integrity to a greater extent in hyperdynamic or statically stressed regions, thereby enhancing the formation of potential space for nodular crystal growth.

1.6 Prevention Of Bioprosthetic Calcification

Prevention of bioprosthetic heart valve failure due to calcification possess a number of important challenges. Since calcification is a multifactorial process its therapy also require drug action at different stages of the disease process. Inhibition of the pathophysiological events may be possible by either altering the implant through pretreatment procedures used to prepare the bioprosthesis or by altering the host or implant through the use of an anticalcification agent. Both approaches raise important issues concerning possible untoward effects. Implant modifications may

deleteriously alter the material strength or adversely affect the biocompatibility of the prosthesis. Administration of anticalcification agent may have untoward effects on normal calcium metabolism and bone physiology. Basically, three types of approaches have been tried for the inhibition of bioprosthesis calcification. They are (1) extraction of cell debris and lipids from the tissues,^{44,149} (2) surface modification of tissue prosthesis with detergents, diphosphonates, - amino oleic acid or metallic ions etc.^{5,36,44,65,86,,95,156,175,185} and (3) target delivery of anticalcification agents.

1.6.1 Detergent Pretreatment For Inhibiting Calcification

Detergent pretreatment of bioprosthetic heart valve tissue inhibits subdermal bioprosthetic leaflet calcification and delays the onset of circulatory deposits in some but not all studies.^{44,116,148} Devitalized cellular elements have been demonstrated to be important to the initiation of bioprosthetic calcification and it has been hypothesized that the acidic phospholipids present in cell membrane structures promote calcification in direct analogy to physiological bone development in which acidic phospholipids are present in the mineralizing front.^{44,116,152} It has been reported that sodium dodecyl sulphate (SDS) pretreatment effects for porcine aortic valve bioprosthesis, but not bovine pericardial valve.⁸⁶ The exact reason for this is not well understood. SDS pretreatment may provide some preferential anticalcification effects for porcine pericardial valves. In addition, another concern about the detergent pretreatment approach is that the structural integrity of the tissue may be harmed by this type of chemical exposure and could result in delamination of the bioprosthetic cuspal tissue. The mechanisms responsible for the SDS-anticalcification effects are

unknown. However, the possible mechanism of inhibition may be due to either the extraction of membrane lipids or net surface charge modification or removal of endogenous AP.^{44,148}

1.6.2 Surface Modifications to Prevent Tissue Calcification

Surface modification has extensively investigated by various investigators^{5,36,65,95,144,148,173} via immobilization or crosslinking of bioprosthetic tissues with anticalcifying agents to develop a biocompatible calcium resistant interface. Modified surface can be achieved by preincubating bioprosthetic tissues in phospho citrate, diphosphonates,^{97,111} detergents like SDS,⁸⁶ protamine sulfate,⁶⁵ Aluminium ions, Ferric ions^{115,197} etc.

A. Diphosphonate Preincubation

Diphosphonates are analogous of pyrophosphate and are thought to inhibit both physiological and pathological calcification by binding to hydroxy apatite and sterically restricting crystal growth. However, unlike pyrophosphate, these compounds are resistant to enzymatic degradation by AP. Studies of Levy et al^{16,97,115} have shown that preincubation of ethane hydroxy diphosphonate (EHDP) can completely inhibit the patho physiological events of bioprosthetic heart valve calcification in either circulatory or subdermal implantation.

Amino hydroxy diphosphonate (APD) can crosslink to cuspal tissue proteins via residual aldehydic group of glutaraldehyde pretreated bioprosthesis.¹⁹⁹ Such

modified tissue have inhibited the AP activity which directly associated with the progression of GABP calcification. Recent studies have also shown that sodium/calcium EHDP in 1:1 ratios are most effective in inhibiting calcification without any adverse effects.^{39,116} The administration of diphosphonates have shown severe untoward effects like osteomalacia and calcium imbalance. However, these adverse effects can be avoided by pretreatment of prosthetic tissues with diphosphonates since their concentrations are minimal on the tissue surface.

B. 2-Amino Oleic Acid (AOA)

Levy et al³⁶ have indicated that 2-amino oleic acid is effective in preventing or treating bioprosthetic heart valve calcification, which is preincubated in glutaraldehyde. Further studies have shown that 2-Amino Oleic acid is effective for inhibiting bioprosthetic heart valve (BPHV) leaflet. But not aortic wall calcification.³⁶ The difference in tissue composition or difference in binding mechanism may account for their variations in anticalcification effect on the two types of tissues. Further, it appears that AOA may not necessarily alter the pathophysiology of aortic wall mineralization, which involves elastin calcification. The mechanism of AOA inhibition of calcification may be due to extraction of calcifiable proteins and phospholipids from the crosslinked tissues. It can further be hypothesized that the AOA pretreatment of BPHV cusps permanently alters the conformation of its structural protein resulting in an unfavourable structure for the deposition of calcium phosphate crystal thereby inhibiting the process of mineralization.^{36,191} It is assumed that AOA covalently bind to GA pretreated bioprosthetic tissues, presumably as the

result of an aldehyde-amino reaction. Due to the nonavailability of free-CHO group in GA treated BPHV when crosslinked with AOA, inhibit calcification.

C. Surface Modification using Protamine sulphate and Antibiotics

In glutaraldehyde treated bioprosthetic tissue, GA- protein reaction involves mainly lysine residues and such tissues calcify. The mechanism of this potentiation of this calcification is most closely associated with the crosslinkages and tissue stability resulting from the reaction. The significant reduction in the content of basic amino acids due to the reaction with glutaraldehyde, has led to the hypothesis that the impaired balance between positively and negatively charged, affinity sites to calcium ions.^{25,65} It is suggested that protamine sulfate can modify the surface charge and subsequent calcification. It was demonstrated previously in a study of bovine pericardial tissues implanted subdermally in rats²⁵ that gentamycin mitigates calcification of the tissues. Gentamycin is hypothesized to bind by its amino groups to free aldehyde groups of tissue bound GA, sustaining its anticalcification effects.

D. Infusion of Trivalent Metal Ions or Drugs

Studies have shown that preincubation of glutaraldehyde pretreated bovine pericardium with Al^{3+} or Fe^{3+} effectively inhibit pathological calcification in the long term rat subdermal model.^{14,115,185,198} But other trivalent metal ions like La^{3+} and Ga^{3+} tested have no anticalcification behaviour. It is also assumed that AP is a key enzyme in the mineralization process and preincubation of FeCl_3 and AlCl_3 have substantially inhibited the enzyme activity and tissue calcification. A possible mechanism may be

the coordination of Al^{3+} to oxygen atoms in the growth sites of hydroxyapatite crystals slows down or retards the calcification process by delaying the proper formation of hydroxyapatite.^{14,15}

Anticalcification requirement of trivalent metal ions are the possession of a high ionic charge and a small ionic radius¹⁸⁵ and have closest fit in the radius to Calcium. A hard metal ion is one with high positive charge, small radius and the electrons which easily removed or polarized. The hard metal ions prefer to react with hard bases, in this case the oxygen atoms on the phosphate ion of the forming hydroxyapatite utilizing this concept, we can explain the anticalcification behaviour or lack of it for the metal ions Al^{3+} , Fe^{3+} , Ga^{3+} , La^{3+} and Gd^{3+} .^{183,198}

All the five trivalent metal ions fit the high ionic charge requirement. However, their reaction is determined not only by ionic charge but also by the ionic radius and the effective charge of the metal ions. A synergy of three factors such as high charge, small ionic radius and effective positive charge are felt more strongly by the oxygen atoms, leading to stronger electrostatic interactions. Fe^{3+} and Al^{3+} ions are most viable candidates for calcification prevention as far as trivalent metal ions are concerned. The metals like Fe^{3+} ions and Mg^{2+} ions and their combination have substantially reduced pericardial calcification.²⁸ It is assumed that ferric ions may slow down or retard the calcification process by delaying the proper formation of hydroxyapatite, while Mg^{2+} disrupt the growth of these crystals by replacing calcium ions.

Aminoglycoside antibiotics such as neomycin and gentamycin on incubation with polyurethane in a metastable calcium phosphate solution, in vitro have shown to interfere with calcium binding.^{25,35,191} The exact mechanism of antibiotics to reduce the calcification is not well understood. However, it appears that neomycin and gentamycin may block calcium ion entry channels or conversely they may block a surface bound calcium ion fractions, which has subsequently been mobilized through channels stimulating agents. It has also been indicated that low levels of daily intake of ethyl alcohol may reduce the deposition of tissue associated calcification.²⁸ Further studies have shown that certain anesthetic drugs may also interfere with the cellular exchange of calcium and their mobility.

1.6.3 Controlled release, Site Specific Drug Delivery

Controlled release of anticalcifying drug continues to be a field of extensive investigation.^{107,116,121} However, several criteria may be necessary for formulating an optimal circulatory design. The drug should be delivered directly into the valve cusps to minimize or eliminate a washout effect by the blood stream, the duration drug delivery should be maximally prolonged while remaining therapeutically effective against cuspal calcification, but avoid causing untoward effects. The anticalcification agent used should have an affinity for the cuspal tissue so that sufficient levels of the drug will be present in the valve cusps. It is observed that blood material interaction may also affect performance of controlled release matrices both from the point of view of drug washout as well as deposition of thrombosis, plasma proteins and formed elements. Rapid circulatory removal of released drug can adversely influence

attaining adequate therapeutic levels of an anticalcification agent. This can be minimized by the approach of releasing the drug at the site of application. Controlled release drug delivery implants for use in the cardiovascular system have been the subject of several previous studies. Local polymer delivery systems have been tried with several drugs such as Ferric Chloride, Aluminium Chloride, Diphosphonates etc. In many cases a constant effective nontoxic level of the drug at a particular body location is needed. Optimal orthotopic valve replacement would utilize a controlled release matrix containing EHDP around the attachment ring of valve. This arrangement results in drug delivery at the valve annular attachment area, a site where calcification often appears to originate and is most intense, and where there is no intervening blood flow.

A. Controlled Release of Diphosphonates

Calcification of glutaraldehyde treated bioprosthetic heart valve can be prevented by controlled release of diphosphonates.^{66,116} Polymeric matrices for the controlled release drug delivery of EHDP have been studied by dispersion of this compound in a biocompatible polymer, ethylene vinyl acetate (EVA). In this system the EHDP powder has been dispersed in varying concentrations in EVA, and has provided a wide range of release rate and duration.

Levy et al⁶⁶ have coimplanted the bioprosthetic cusps with EVA-EHDP matrices using the rat subdermal implant system. It appears that the site specific controlled release of EHDP successfully inhibits bioprosthetic cusp calcification at a dose that was 1% of that required for daily injection and there are no demonstrable

adverse effects on bone, calcium metabolism or overall growth in the controlled release treated animals.

B. Controlled Release of Metal ions

Superior anticalcification efficacy has been noted for both Al^{3+} and Fe^{3+} matrices.^{31,150} Further, it has been proposed that the mechanism of action of Al^{3+} may be due to localization Al^{3+} within the devitalized cells of glutaraldehyde pretreated bioprosthesis. $\text{Al}_2(\text{NO}_3)_3$ and FeCl_3 have been incorporated into silastic 6605-41 and Biomer by solvent casting. Release kinetic studies from this system have shown, that all formulations exhibited an initial burst release, followed by an exponentially decreasing release rate. Further, the release rate has been more rapid from Biomer matrices containing Al^{3+} and Fe^{3+} than from the silastic 6605-41.

Improved anticalcification efficacy has been noted for Fe^{3+} matrices. Previous work has shown^{31,151} that regional controlled release of both Al^{3+} and Fe^{3+} effectively inhibited tissue calcification. Further, the ferric ion loaded chitosan matrix appears to be a suitable system towards preventing bioprosthesis associated calcification. The combination of initial burst effect and the pseudo zero- order kinetics in the subsequent release phase suggests an important advantage of this drug delivery system.

C. Drug Combination Therapy

Release of single drug leads to certain unwanted side effects, since more concentrations of the drug is needed for therapy. It has been seen that Fe^{3+} ions and Al^{3+} ions have superior anticalcification effects on prolonged delivery. However,

despite the very low doses of Al^{3+} used, Al^{3+} is of concern as a central nervous system toxin, which may have a casual role in Alzheimer's disease and other neurological disorders.^{14,39} Hence, the release of Fe^{3+} ions appears to be a suitable system for prevention of tissue calcification. But, high amounts of ferric ion release in the blood, for prolonged period may also be toxic since they may accumulate in the liver, bone marrow or reticuloendothelial tissues etc.

Levy et al^{85,112} have proposed a synergistic effects between Al^{3+} and EHDP and Fe^{3+} and EHDP for preventing bioprosthetic valve calcification. Recent studies have also indicated that synergism of Fe^{3+} ions and Mg^{2+} ions prevent the tissue calcification.²⁸ Hence, the synergism of drug combination with low levels of the drug with least side effects, appear to be a promising therapy for preventing tissue calcification.

1.7 Polyethylene glycol (PEG) - a novel material to improve biocompatibility

Polyethylene glycols (PEGs), are versatile polymers having mostly hydrophilic and hydrophobic properties.¹²⁴ PEGs possess a variety of properties pertinent to biomedical and biotechnical application. PEG is a water soluble polymer that exhibits properties such as protein resistance, low toxicity, and immunogenicity. These properties have been attributed to its segmental flexibility and its polar but uncharged chemical composition.

Although PEG exhibits a high degree of biocompatibility, it lacks the mechanical properties necessary to replace materials such as polyurethane and silica. However, grafted PEG chains on the surface of these relatively rigid materials can make them more biocompatible. One feature of grafted PEG surfaces is their low degree of protein adsorption. The key of this phenomenon is the mobility of this grafted chains. Moreover, since the flexible PEG chains can readily adapt their conformation to fit the surface topology of a protein, there is very little tendency for the protein to undergo significant conformational changes. In addition the electrical neutrality of PEG may diminish the difference in its interaction with hydrophobic or hydrophilic parts of the protein surface.

Modifications of proteins by PEG has been used to reduce the immunogenicity of various enzymes. The covalent attachment of activated PEG to available lysines in peptides and proteins presumably masks antigenic epitopes and may mimic glycosylation in increasing clearance time in the circulation.¹²⁴ PEGs were conjugated to various proteins or lipids to produce various delivery systems for drugs, cytokines and enzymes.⁴⁷ Using PEG modified adenosine deaminase, children with adenosine deaminase deficiency were successfully treated. Neither toxic effect nor hypersensitivity reactions were observed. Furthermore, PEGs conjugated to liposomes significantly prolonged their biological properties.

Usually polymers like polytetra methylene glycol (PTMG), PEG etc. having ether soft segment have metal ion chelation (calcification). It is well documented that

polyurethanes, with a poly ether soft segment, can selectively and quantitatively extract anions containing heavy metals from aqueous solution.^{74,76} Complexation is thought to occur through electrostatic interaction between the polarizable ether oxygens and the positively charged metal ions. In this case polyether conformation, i.e. chain mobility and flexibility, is likely to be a principal requirement. Several other requirements must be met for stable complexation, including a 'fitting size' of the cation, a suitable number of oxygen atoms in the ring, lack of steric hindrance and cationic charge of the ion.¹⁵³ It has been suggested that cation is complexed at the center of a coil composed of the polyether.⁷⁴ Calcium is a relatively large ion, and it has no fixed apparent ionic radius.⁷⁶ The coordination number for calcium ligand interaction varies from 6 to 12. Because of this lack of stereochemical demand, variability of co-ordination number, size and crosslinking agent between organic molecules. Low molecular weight acyclic, linear polyethers have also been shown to complex calcium.⁸⁹

1.8 Conclusion

The pioneering work of Carpentier and colleagues resulted in the development of cardiac valve bioprosthesis derived from non-human tissues.²³ Bioprosthesis are now widely used due to their advantages over mechanical valve prosthesis such as low thrombogenicity, less hemolysis and gradual deterioration in contrast to the catastrophic failure of mechanical prosthesis. Chemically crosslinked biological tissues have been used to prolong the original structure and mechanical integrity of

the material. The most successful method, glutaraldehyde has questionable durability and results in calcification of the bioprosthesis. Present research directions point to the use of short time exposure to low concentrations of glutaraldehyde with biological tissue.¹⁰⁸ Bioprosthetic heart valve calcification is an important clinical and experimental problem. The propensity of bioprosthetic tissue to calcify is dependent on tissue preparation, host biologic factors and mechanical deformation during functioning. Since calcification is a multi factorial process, therapeutic strategy may require drug action at different stages of calcium phosphate deposition. Further, it is also understood that the calcification of tissue valves, artificial hearts and ventricular assist systems occur in association with the deposition of devitalized cells and cellular debris and perhaps adhered blood platelets.⁷⁵ Hence, a combination approach is needed to prevent tissue associated calcification and thrombosis. Promising therapeutic approaches are surface modification of the implant by pretreatment with anticalcifying drugs and controlled delivery of the drug combination to the implant site, while avoiding systemic side effects. Unfortunately the mechanism of induction and propagation of this disorder is not well defined and hence the method to prevent calcification.

1.9 Scope and need of the present investigation

Review of scientific literature on bioprosthetic heart valve has unequivocally shown the relevance of surface modification of the bovine pericardium to develop an anticalcifying and nonthrombogenic bioprosthesis for long run.

The earliest event in mineralization of bioprosthetic connective tissue cells are hypothesized to result from glutaraldehyde induced cellular “devitalization” and resulting disruption of cellular calcium regulation. Moreover, membrane bound organellar and plasma membranes themselves contain considerable phosphorus, largely as phospholipids. Further, alkaline phosphatase (AP) an enzyme also associated with matrix vesicles involved in bone mineral nucleation, is present in BP tissue mineralization sites. AP may hydrolyse cellular phosphoesters to increase the regional phosphate concentrations. These source of phosphorus are the observed sites of early bioprosthetic mineralization.

Preliminary studies from our laboratory have selected bovine pericardium as a feasible biological tissue, having the least calcification profile among biological tissues such as dura mater, fascia lata and bovine pericardium.²⁷ Hence, bovine pericardium has been chosen for the studies presented here. This study proposes the various stages of development of a biostable and anticalcifying material from bovine pericardium. The following detailed investigations were undertaken to bring the conclusions presented (elaborated in the preceding chapters) in this work.

1. The role of various tissue fixing agents like glutaraldehyde, carbodiimide, hexamethylene diisocyanate and polyglycidyl ether, have been investigated for their calcification profile and biostability. Combinations of tissue fixatives have been selected and tried for improved biostability and reduced calcification.

2. A novel tissue- polymer hybrid material from bovine pericardium and polyethylene glycol have been developed, which has shown significant reduction in calcification and biodegradation.
3. The in vitro formulation and evaluation of polymer co-matrix systems from polyethylene vinyl acetate and chitosan, for the controlled delivery of drug combinations having synergistic effects in inhibiting calcification. Several drug combinations such as aspirin/heparin or ferric/magnesium have been released from the co-matrix system and evaluated for prevention of tissue calcification and thrombosis.
4. The novel tissue- polymer hybrid material has been subcutaneously implanted in rats along with drug delivery co-matrices. The combination of surface modifications with synergistic anticalcifying drug delivery appears to be a suitable method for preventing calcification and thrombosis in bioprosthesis.

CHAPTER II

MATERIALS AND METHODS

2.1 Materials

This chapter deals with the experimental protocols used in this study

Tissue

Bovine pericardium was the tissue material used for these investigations. Whole hearts of 10-18 months old calves, with intact pericardia were collected fresh from the local slaughterhouse. The hearts were transported to the laboratory in cold saline, and the pericardia were gently removed. Fat and excess tissues were stripped from the bovine pericardium and processed within 4 hours of slaughter. This was easily accomplished without damage to the pericardium, the fat being gently lifted and the adherent loose connective tissue was cut with a scalpel, leaving a smooth tissue surface. Two incisions were made in the pericardium along a line, joining the aortic root and the apex of the heart (across the area that overlies the atrium and longitudinally) defining the orientation of the tissue after excision from the heart.^{104,178} An 8cm square of ventral tissue was then cut with scissors midway between the aorta and apex and the orientation sutures. The tissues were washed in four changes of sterile saline and stored frozen, prior to tissue treatments.

Polymers

Chitosan ($\alpha(1\rightarrow4)$ 2-amino-2deoxy - β - D - glucan) which is one of the abundantly available polysaccharides in nature, was obtained as a gift from the

Central Institute of Fisheries, Technology (Cochin, India). Chitosan derived from prawn shell chitin by greater than 85% deacetylation of particle size 1-3mm and inherent viscosity 5.13 dl/g measured at a concentration of 0.5 g/dl in 2% acetic acid at 30°C was used as received. Poly (ethylene–vinyl acetate), 60% ethylene, polystyrene-butadiene (Poly-sciences, Warrington, USA), heparin sodium injection I.P, 25,000 IU in 5ml (Biological E. Limited, Hyderabad) and aspirin from Sigma, St. Louis, MO, USA. Calcium, phosphorus, alkaline phosphatase and iron combination kits were from Miles India Ltd. Baroda, India.

Enzymes and proteins

Sodium dodecyl sulfate (SDS), Phenyl methane sulphonyl fluoride (PMSF), Ethyl-3 (3-Dimethyl amino propyl) carbodiimide (EDC), bis (Polyoxy ethylene) bis (glycidyl ether) (GLE), Glutaraldehyde (GA), Tris (hydroxy methyl amine-methane), Lot 16H5724, Ferric Chloride Lot 81H3472 and the enzymes used for the degradation study - chymotrypsin (bovine pancreas, Type I .S, 3x crystallized and lyophilized, 64 units/mg protein, Lot 91H–7195), esterase (Type I) porcine liver suspension in 3.2M (NH₄)₂SO₄, pH 8.0, 335 units/mg protein, lot 103H-701). Bromelain (pineapple stem, lyophilized powder, 10 units/mg protein, Lot 93-H-0325), collagenase (Type I activity greater than 289 collagen digestion units/mg solid, Lot 94-H-1032) and trypsin (Type III bovine pancreas, 11,100 units/mg protein Lot 25 H0 357) were obtained from Sigma Chemicals, USA.

Albumin (Human, fraction V, 96-99% pure), γ -globulin (Human, Cohn fraction II), fibrinogen (Human, Essentially plasminogen free No F-4883) were obtained from Sigma Co, USA. All proteins were dissolved in 0.1 M phosphate buffer, pH 7.4

Tissue crosslinkers, antiplatelet drugs and other chemicals

Polyethylene glycol 600,1500, 4000, and 6000, sodium azide isopropanol were obtained from BDH Chemicals Ltd., Poole, England. Hexamethylene diisocyanate (Merck Schuchardt, Hohenbrumbei, Munchen). Polyethylene glycol 20,000 (Sisco Research Laboratories, India), Potassium dihydrogen orthophosphate, dipotassium hydrogen orthophosphate, Disodium hydrogen phosphate, Hydrochloric acid, Sodium chloride and sodium citrate were of analytical reagent grade from chemical division, Glaxo Laboratories (India) Ltd, Mumbai. Calcium Chloride dihydrate, Sodium phosphate dibasic, (Sarabhai M Chemicals, Mumbai), Magnesium Chloride (Ranbaxy Laboratories Ltd., India) Polyoxy ethylene (20) sorbiten monolaurate (Tween 20) (Sd Fine Chem. Ltd. India) Dimethyl sulphoxide (DMSO) [Spectrochem Mumbai] and all other chemicals were of analytical reagent grade.

2.2 Cell extraction

Calcification appears to be linked to both glutaraldehyde crosslinking of collagen molecules and the presence of cellular debris. Glutaraldehyde crosslinking has been shown to accelerate calcification of collagenous materials in a juvenile rat

model.¹⁷⁹ During processing and GA treatment of tissue derived heart valve materials, cells are ruptured, but the cellular debris is largely retained. This cell remnants have been microscopically associated with early crystal formation.^{44,116}

Calcific deposits on the external surface of the cusps occasionally are seen, arising from the ulceration of intrinsic deposits. Such external deposition of calcium is found within the inflammatory cells, bacteria, superficial platelet thrombi etc. Hence, one of the major problems still to be addressed is the development of an appropriate tissue treatment for the removal of cell debris while maintaining its structural integrity.

The following procedure has found to be suitable to remove the tissue associated cell debris and subsequently their calcification . Selected pericardial sacs were used for various chemical treatments, where the tissues were decellularized and crosslinked, as indicated else where.^{44,149} Decellularization method consists of a selective removal of cellular components from the pericardial stroma such as cells and nuclear membranes and the DNA protein. This procedure involves the extraction of tissues with two different detergents, Triton X-100 and SDS.

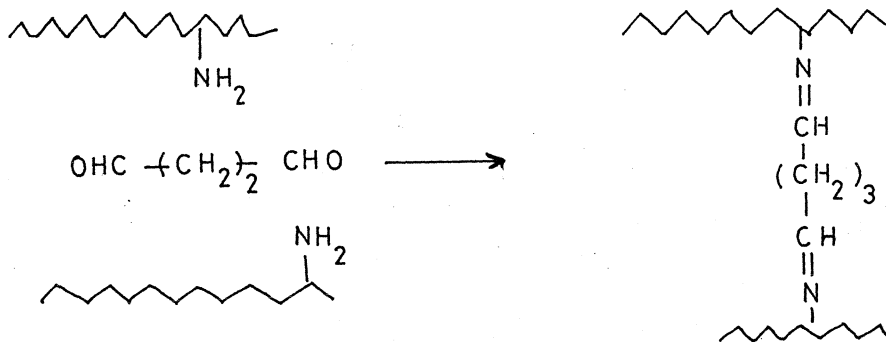
Triton X-100, a nonionic surfactant was used initially to treat the fresh pericardium at a concentration of 0.1% in saline, with the addition of 1mM PMSF as proteinase inhibitor, to prevent degradation of the extracellular matrix. The pericardial samples were immersed in the surfactant solution and soaked overnight at

room temperature. This treatment was aimed at removing the cellular membrane and proteins by disrupting their lipids. After the first detergent step, the tissues were washed with distilled water to remove the traces of detergent and to prevent the possible blocking action of the second detergent used.

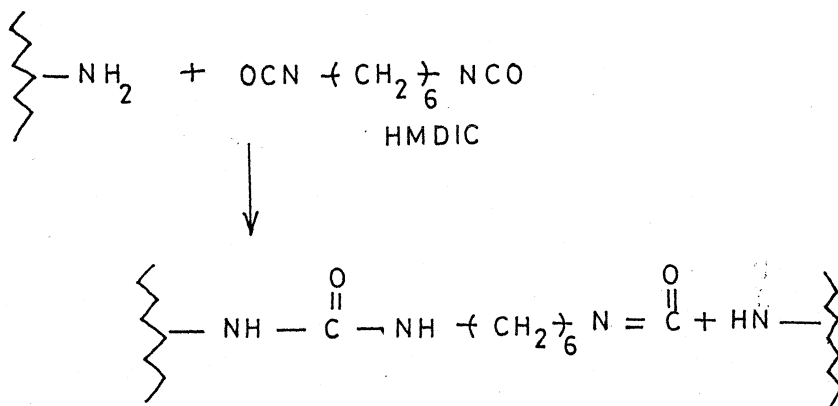
The second detergent treatment was performed with 0.5% SDS with 1mM PMSF in saline for 72 h at room temperature in a mechanical shaker at 100rpm.^{44,149} The SDS detergent was used for dissolving the nuclear envelope, and subsequently removing it. The SDS was then completely removed by several rinsings with large amounts of distilled water. After this decellularization process, the pericardial sacs were cut into dumbbell specimens and 1x1 square cm samples according to the ASTM standard D 1708.^{6,149} The decellularization process was immediately followed by collagen crosslinking and PEG immobilization by different techniques. The cell extracted pericardium is denoted as SDS-BP.

2.3 Chemical crosslinking

The predominant chemical agents that have been investigated for the treatment of collagenous tissue for bioprosthesis are glutaraldehyde,^{67,146,147,196} carbodiimide,^{104,147,196} hexa methylene diisocyanate^{140,146} polyepoxy compounds¹⁸⁴ and their combinations. The functional groups of the chemical agents react with those on the amino acid residues of collagen, such as the ϵ -amino function on lysine and hydroxylysine or the carboxyl function on aspartic and glutamic acids, to give rise to



Scheme . 1 Simplified representation of monomeric glutaraldehyde reaction with amino groups on collagen to form cross-links.



Scheme.2 Representative reaction of hexamethylene diisocyanate with the amino group on collagen to form ureum cross-links

'crosslinks' between the collagen molecules. A series of selected collagen crosslinking agents alone and in combinations were used to crosslink BP tissues as represented below.

2.3.1 Glutaraldehyde fixed BP-GATBP

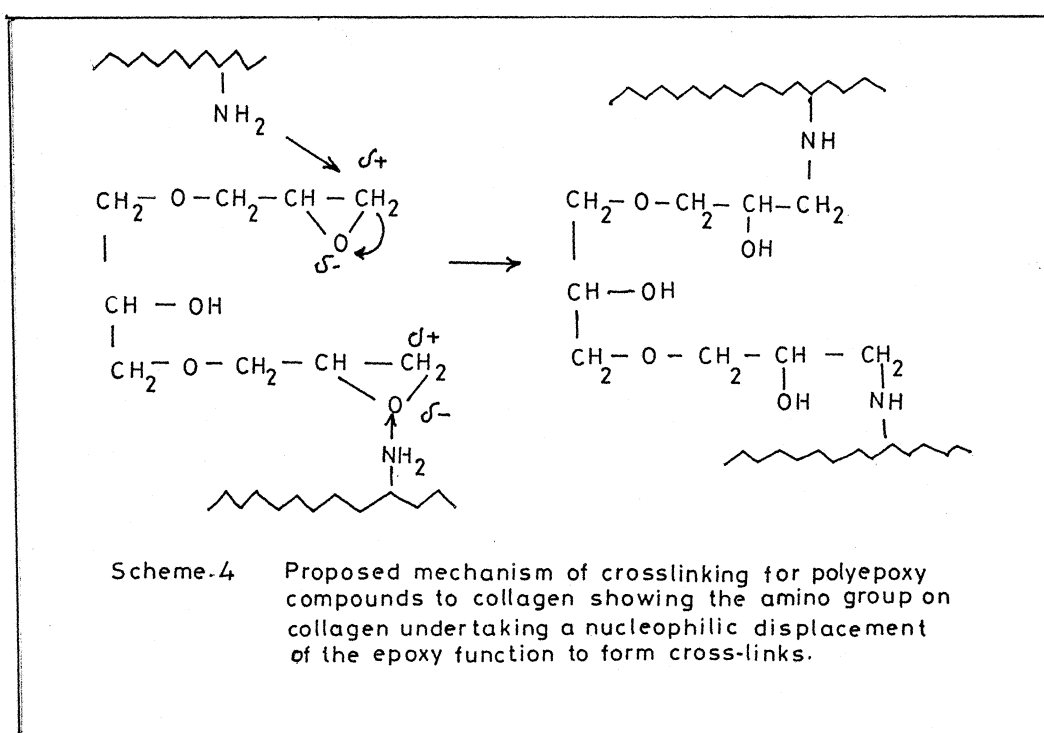
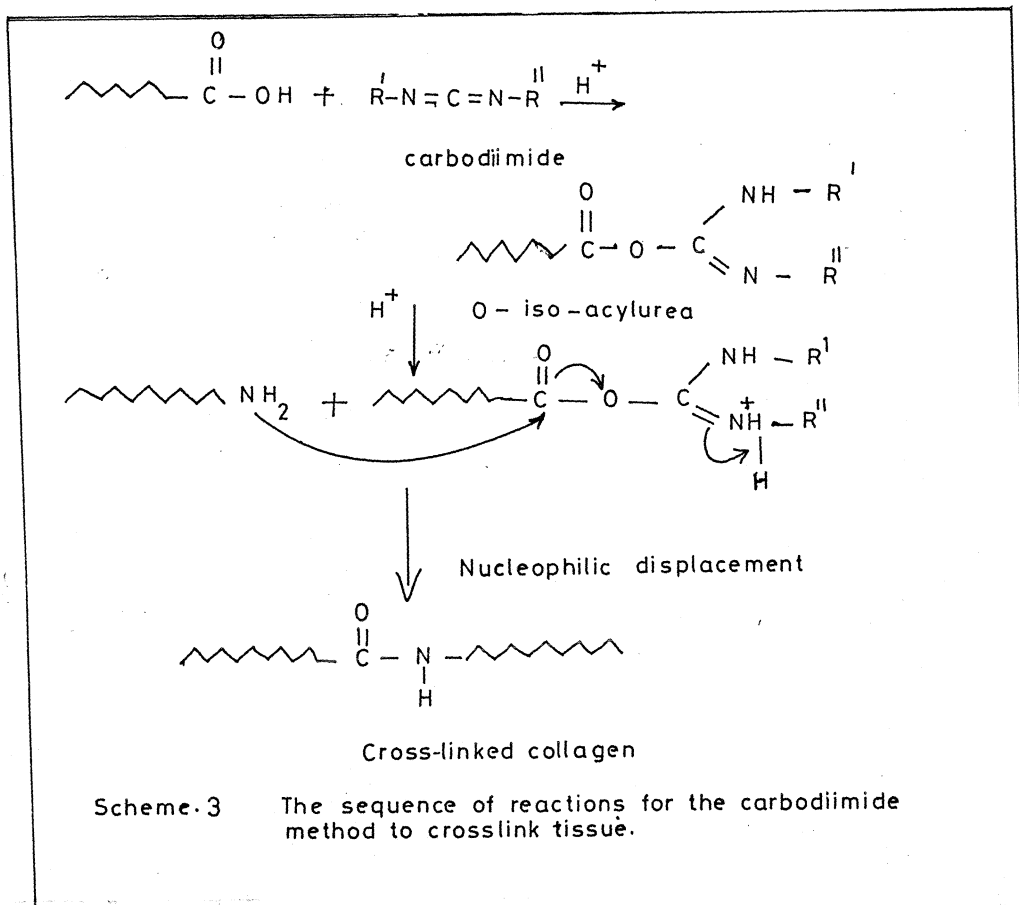
Tissue fixation with GA was carried out with 0.6% glutaraldehyde in 0.1 M phosphate buffered saline (pH 7.4) and transferred after 24h.^{151,196} Further, they were exposed to 0.2% GA for two weeks at 4°C, then washed with plenty of distilled water to remove residual glutaraldehyde and used for these studies (**scheme 1**).

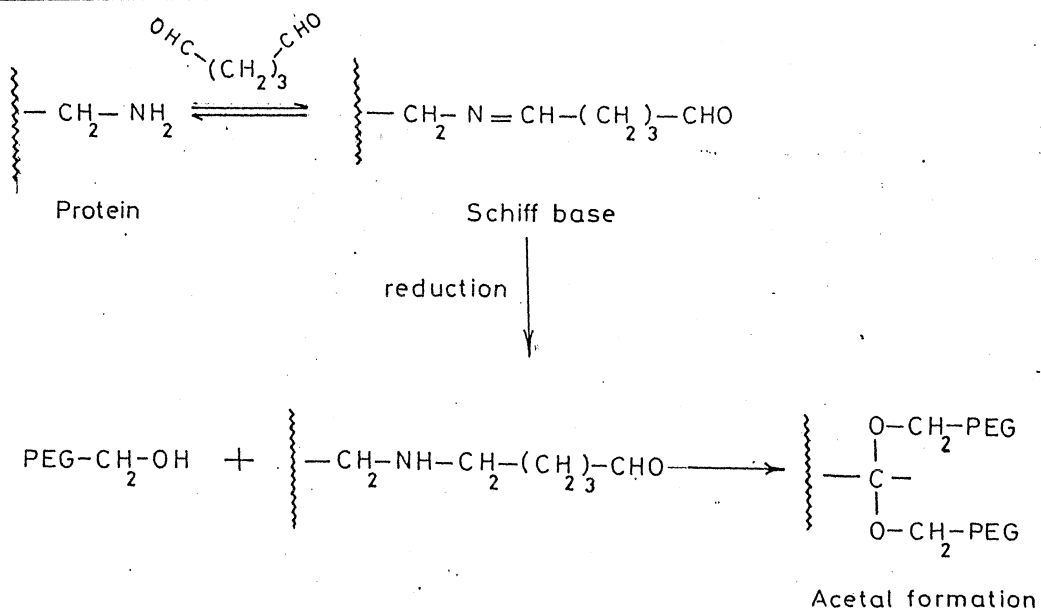
2.3.2 Hexamethylene Diisocyanate fixed bovine pericardium

Decellularized fresh pericardial samples were crosslinked with hexamethylene diisocyanate using a 1.5% (wt/vol) solution of HMDIC in buffer (0.08M Na₂HPO₄ adjusted with NaOH) at pH 9.5 containing 1.0% (wt/vol). Tween 20 for 5h at room temperature to give HMDIC-BP.^{140,146} After crosslinking these samples were washed two times with distilled water, two times with 4M NaCl and four times with distilled water (**scheme 2**).

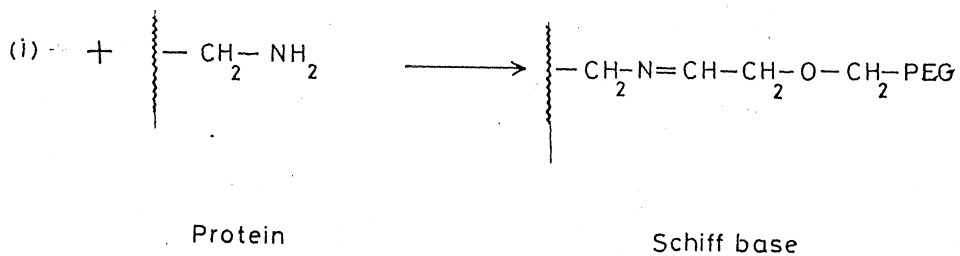
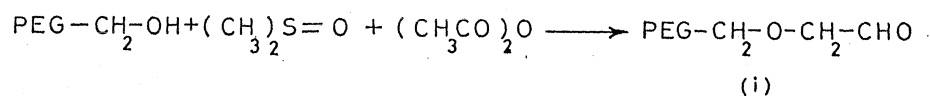
2.3.3 Ethyl-3-(3-Dimethyl amino propyl carbodiimide treated BP (EDC-BP))

Decellularized bovine pericardial samples were immersed in 2.5% EDC solution in phosphate buffer.^{104,147} After 48h, the samples were removed from EDC solution and rinsed with distilled water prior to use (**scheme 3**).





Scheme 5: The proposed mechanism of PEG grafting to glutaraldehyde treated BP (GABP).



Scheme 6: The proposed mechanism of PEG-aldehyde grafting to BP.

2.3.4 Bis(Polyoxy ethylene) bis (glycidyl ether) treated BP (GLE-BP)

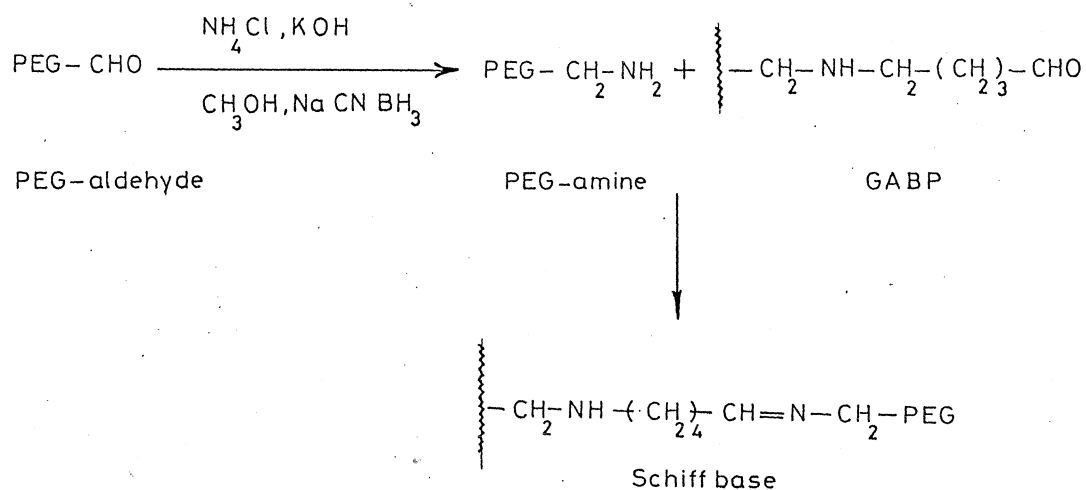
Glycidyl ether fixation was performed by the method of Tang et al.¹⁸⁴ Decellularized BP samples were treated with 4% GLE solution containing 70% ethanol, buffered with sodium carbonate/bicarbonate pH 9.5 at room temperature for 72h. An excess amount of GLE solution was used so that the bulk concentration of GLE remained essentially constant throughout the course of the fixation process. Samples were removed from the fixation solution and quenched in cold distilled water (scheme 4).

2.4 Surface modification of BP via PEG

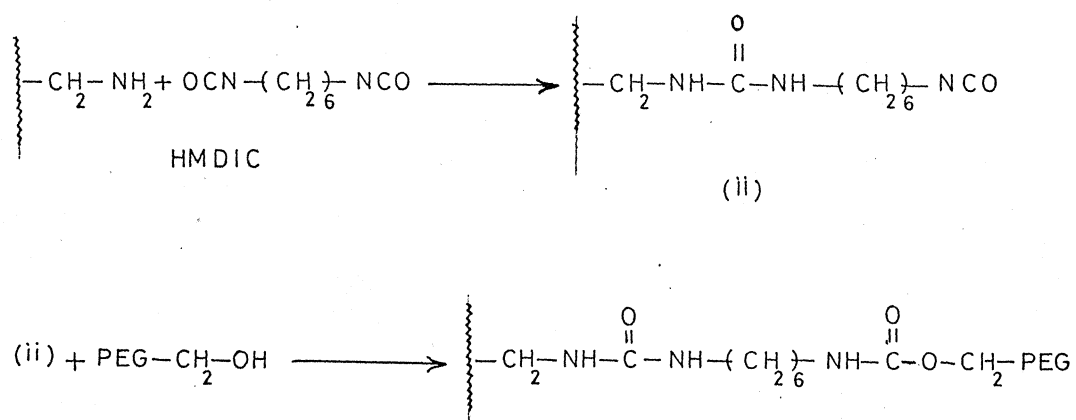
Polyethylene glycol was grafted onto BP surfaces via different functionalities, as represented below.

2.4.1 PEG grafting via free aldehyde group of GA (PEG-GABP)

Decellularized bovine pericardium were exposed in 0.6% GA for 24 hours and were subsequently incubated in 5% solution of polyethylene glycol (PEG-6000) in 0.1M tris-HCl buffer pH 5 for 5 hours.⁷⁹ The PEG grafted samples were then washed with distilled water to remove the unattached PEGs. The possible reaction is demonstrated in scheme 5.



Scheme.7. The proposed mechanism of PEG amine grafting to glutaraldehyde treated BP.



Scheme.8 The proposed mechanism of PEG grafting to hexamethylene diisocyanate crosslinked - BP.

2.4.2 PEG-CHO-BP

Formation of PEG-CHO by DMSO acetic anhydride oxidation

Polyethylene glycol-6000, (5g), was added to 0.4g acetic anhydride in 15ml dimethylsulfoxide and stirred for 30 hours at room temperature⁸⁰. At this point the reaction mixture was added dropwise to 100ml dry ethylether, and reprecipitated two or three times from methylene chloride with ethylether. The yield of PEG-CHO was 4.5g. Five percent solution of PEG-CHO in phosphate buffer pH 7.4 was subsequently exposed with decellularized BP⁸⁰. After 5 hours, the samples were removed and washed with phosphate buffer. The mechanism of the reaction is depicted in **scheme 6**.

2.4.3 PEG-NH₂-GABP

PEG- amine was prepared from PEG-CHO by Potassium hydroxide (0.02g) was added to ammonium chloride (0.36g) in 5ml methanol. After the KOH pellets dissolved PEG-CHO was added and the solution was stirred for 15 minutes. A solution of NaCNBH₃ (0.42g) in 5ml methanol was then added dropwise over 30 min., followed by addition of a second portion of KOH (0.1g). The solution was stirred for 24h, and the product was then precipitated by addition of ether.⁸⁰ 5 % aqueous solution of PEG-amine was then exposed to GABP for 5 hours. Free aldehydic group of GABP forms schiff base bond with PEG-amine, as described in **scheme 7**.

2.4.4 PEG grafting on hexamethylene diisocyanate crosslinked BP (PEG.HMDIC-BP)

Decellularised fresh pericardial samples were crosslinked with hexamethylene diisocyanate (HMDIC) as presented earlier in this chapter. HMDIC crosslinked BP samples were exposed to 5% solution of polyethylene glycol in 0.1M tris HCl buffer pH 5 for about 5 hours. The PEG grafted samples were rinsed with distilled water to remove excess PEG. The possible mechanism is depicted in **scheme 8**.

Polyethylene glycols of different molecular weights (600, 1500, 4000, 6000 and 20,000) were also grafted on the decellularised bovine pericardium via acetal linkages of GABP as reported in **scheme 5**.

2.5 Double crosslinking technique of BP

1. GA-PEG-EDC-PEG-BP

Bovine pericardium were fixed with 0.4% glutaraldehyde, grafted with PEG ,crosslinked with 0.4% EDC (pH 7.4) for 24 hours and finally exposed to PEG solution for 5 hours at pH 5).

2. EDC-PEG-GA-PEG

BP were crosslinked first with EDC and then exposed to PEG, again crosslinked with GA and finally surface modified by PEG.

3. HMDIC-PEG-GA-PEG

HMDIC crosslinked BP were grafted with PEG and fixed with GA again exposed to PEG for surface grafting.

4. HMDIC-PEG-EDC-PEG

HMDIC fixed BP were grafted with PEG and again crosslinked with EDC, then exposed to PEG.

All the above mentioned tissue treatments (GA, HMDIC, EDC tissue crosslinking and PEG - 20,000 grafting) are explained in 2.3 and 2.4

2.6 Charecterization of PEG grafted pericardium

2.6.1 Per cent Grafting of PEG

The percent grafting of PEG on above mentioned samples (Scheme 5 to 8) were determined as follows. The dry weights of the BP samples before and after grafting of PEG were taken. Then, the percent grafting of PEG on BP were determined¹⁷⁶ from the equation represented below.

$$\% \text{ grafting} = \frac{W_2 - W_1}{W_1} \times 100$$

Where, W_1 and W_2 denoted the dry weights of samples before grafting and after grating respectively.

2.6.2 PEG Leaching Studies

The percent of PEG–Leaching from the above mentioned PEG grafted BP samples were determined as follows. The leaching of PEG from PEG-BP was carried out by incubating the samples in Tris. HCl buffer, at room temperature (30⁰C) and a constant shear rate of 100rpm. After 5 days, the samples were removed, dried, weighed and the leaching of PEG was quantitated

$$\% \text{ leaching} = \frac{W_1 - W_2}{W_1} \times 100$$

Where W_1 and W_2 denoted the dry weights of samples before and after PEG leaching.

2.6.3 Determination of the degree of hydration

The PEG grafted BP (different molecular weights) and the cell extracted glutraldehyde crosslinked BP were immersed in distilled water for 24h. They were taken out, and the water on the membrane surface was blotted with a filter paper by applying a uniform force¹⁷⁷ and were weighed to get their wet weights. The weights of the dry tissues were then, determined by drying them to constant weights. The water content was expressed as the ratio of the weight of water in the water swollen tissues to that of the dry tissue.

$$\% \text{ degree of hydration} = \frac{W_1 - W_2}{W_1} \times 100$$

Where W_1 and W_2 are the wet and dry weights of the tissues respectively.

2.6.4 Octane Contact Angle Studies

Theoretical - Polar interactions across tissue/water interface

Here, octane/water method have been selected as a probe for investigating the polar interactions across tissue/water interface.⁴ Consider a drop of n-octane at a tissue-water interface. From figure 2.1, we can write (from Young's equation).

$$\gamma_{sw} - \gamma_{so} = \gamma_{ow} \cos \theta$$

Where γ is the interfacial free energy and the subscripts 's' denote tissue substrate, 'w' water and 'o' n-octane.

These interfacial tension terms can further be written as.^{4,7,73}

$$\gamma_{so} \equiv \gamma_s + \gamma_o - 2 (\gamma_s^d \gamma_o^d)^{1/2} - I_{so} \quad (2)$$

$$\gamma_{sw} \equiv \gamma_s + \gamma_w^l - 2 (\gamma_s^d \gamma_w^d)^{1/2} - I_{sw} \quad (3)$$

Where, γ_s and γ_w^l are the surface tension of tissue and octane saturated water respectively. γ_w^d , γ_s^d , γ_o^d are dispersion components of the surface free energies of w, s and 'o' phases, and I_{so} , I_{sw} are the nondispersive (polar) interactions at the s-o and s-w interfaces.

n-octane has a surface tension of 21.6 dynes/cm at 25°C which is also its dispersion component of the surface tension as octane has no polar component.

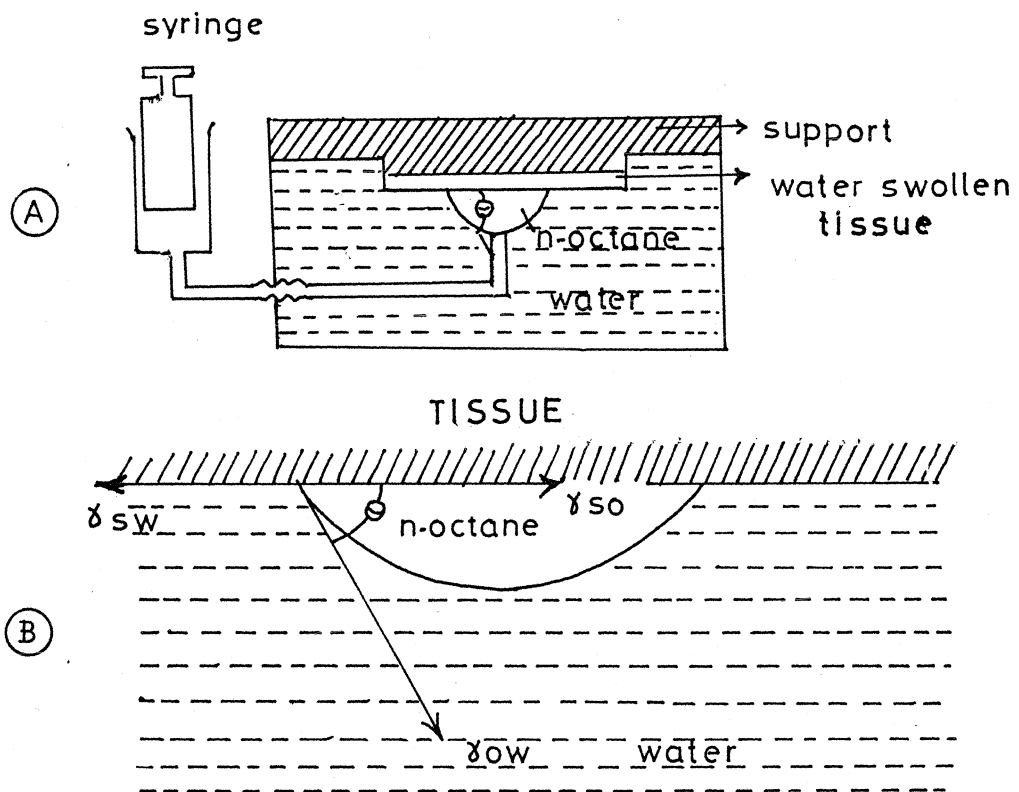


Figure 2.1 Schematic drawing of apparatus for contact angle measurement by the inverted bubble method B-Drop of n-octane at the tissue-water interface

$$\gamma_o = \gamma_o^d = 21.6 \text{ ergs/cm}^2 \quad (4)$$

also, at 25°C, $\gamma_w = 72.1 \text{ ergs/cm}^2$,

$$\gamma_w^d = 21.6 \text{ ergs/cm}^2$$

and $\gamma_w^p = 50.5 \text{ ergs/cm}^2$

$$\text{So, } \gamma_o = \gamma_w^d = 21.6 \text{ ergs/cm}^2 \quad (5)$$

from equation (1), it follows

$$\text{Cos } \theta = \frac{\gamma_{sw} - \gamma_{so}}{\gamma_{ow}} \quad (6)$$

from equations (2), (3) and taking $I_{so} = 0$, equation (6) can be written as

$$\text{Cos } \theta = \frac{\gamma_w^l - \gamma_o - I_{sw}}{\gamma_{ow}} \quad (7)$$

$$\text{or } I_{sw} = \gamma_w^l - \gamma_o - \gamma_{ow} \text{ Cos } \theta \quad (8)$$

$$\gamma_w^l \sim \gamma_w \text{ (the solubility of octane in water is less than 1 ppm)}^{73,87}.$$

$$I_{sw} \equiv 50.51 (1 - \text{Cos } \theta) \quad (9)$$

So, the contact angle θ , can provide a direct measure of polar interactions across the tissue/water interface. For a purely apolar surface in water, $I_{sw} \equiv 0$ and θ will be small, indicating a high polar component to the interfacial free energy. For a very hydrophilic surface, θ will approach 180° , indicating a large I_{sw} and a correspondingly low polar component to the interfacial free energy.

Experimental method

Here, octane/water method has been selected as a probe for investigating the polar interactions across tissue/water interface. In order to develop an understanding

of tissue (BP)-interactions at the solid/liquid interface, which is closest to in vivo conditions, the contact angle of 99.99% pure n-octane on different modified tissue interfaces have been attempted.^{7,87} The modified pericardial tissues were mounted on microscope slides, and were supported in an inverted position in a container. The container was carefully filled with double distilled water until the microscope slide was completely immersed. The goniometer was aligned (Kernco Instruments Co. Inc. Texas) and focused on the tissue-water interface. At this point a microsyringe, containing 99.9% pure n-octane, was lowered into the water. A drop was formed on the syringe tip, positioned underneath the sample surface, snapped from the tip, and allowed to rise to the tissue water interface. The apparent octane tissue contact angle was immediately measured. Angle on both sides of each bubble were measured, assuming symmetry, and at least 10 angles were observed, and expressed as the mean contact angle with standard deviation.

2.7 In vitro degradation studies with enzymes

The enzymes used in these experiments were as listed earlier. The conditions (pH, buffer system etc) and concentrations of these enzymes used for the studies were the same as reported elsewhere.^{32,146,201,202}

In short, bromelain (200mg/lit), chymotrypsin (200mg/lit), collagenase (60mg/lit), esterase (10mg/lit), and trypsin (200mg/lit) were dissolved in 0.1M phosphate buffer pH 7.4 containing 0.03% sodium azide as a preservative. The pericardial tissue strips were immersed in their respective enzyme solutions and kept

at 37°C. The solutions were changed every 24 hours to restore the original level of enzyme activity. At the end of the experimental period, the conditions of the various BP samples were noted and the tensile strengths determined .

2.7.1 Mechanical Properties

The mechanical properties of the wet tissues taken at specific time points, after enzymatic digestion, were measured by the ASTM (6) standard method protocol using a Chatillon universal test stand model UTSE-2. Dumbell shaped specimens were prepared and were tested under wet conditions, having lengths between the grips of 2.5cm, a width of 0.5cm, and employing a crosshead speed of 1 in/min. The tensile stress and tensile strain (percentage of elongation) were calculated.

2.8 In vitro calcification experiments

The calcification experiments were performed as reported earlier.^{26,28,68} In brief, in this system, the calcium concentration (10.3mg/100ml) was similar to mean total serum levels (10mg/100ml), and the ratio of Ca/PO₄ was 1.67 as in hydroxyapatite (HAP). The concentration product of calcium (CaCl₂ 2H₂O) and phosphate (K₂HPO₄) in the incubation solution was 3.95mM², 2.57mM calcium, and 1.54mM phosphate. Each salt solution was prepared in 0.1M Tris-buffer pH 7.4 containing 0.03% sodium azide as a preservative.²⁶ Equal volumes of doubled concentrations of 2.57mM calcium and 1.54mM phosphate were mixed in a screw cap bottle containing the pericardial tissues.

At specified time points, the tissues were removed and rinsed with water to remove excess solution and loosely attached deposits. They were oven dried (24h, 100°C) accurately weighed, and hydrolysed in 2ml of 2N HCl for 48 hours at 60°C, as reported elsewhere.^{26,68} The calcium concentration was determined from HCl hydrolysate, using the colouri metric method of O-cresolphthalein complexone obtained as standard kits.⁸² For that, 1ml of O-cresolphthalein was added in alkaline condition to a known volume of HCl hydrolysate. The blueviolet colour of the complex formed was read against a known calcium standard solution, at 578 nm. For the estimation of phosphorous, ammonium molybdate was added and unreduced phosphomolybdate complex formed were measured at 340 nm.¹⁶¹

2.9 Development of Chitosan/Polyethylene Vinyl Acetate Co-matrix

Controlled release of drug combinations: Drug combinations, such as aspirin/heparin and Ferric/Magnesium were loaded in the co-matrix system. The release kinetics and their synergistic effects on inhibiting pericardial calcification and thrombosis were evaluated.

2.9.1 Preparation of Aspirin Loaded Chitosan Beads

Chitosan beads were prepared as reported elsewhere.^{30,31} Briefly, chitosan dissolved in 2% acetic acid was blown into a NaOH-methanol solution by compressed air through nozzles (0.15mm diameter) and then the regenerated porous beads were washed by hot and cold water successively.

Nishimura *et al*¹⁴³ have loaded adriamycin to chitosan beads and studied their antitumour activity. Here aspirin was loaded to chitosan beads in a similar fashion to investigate the release characteristics. Chitosan beads of uniform size (about 1.0mm diameter) were added to known amounts of aspirin in water (adjusted to pH 7.4), and stirred at room temperature. The preparation was evaporated to dryness.

2.9.2 Preparation of Aspirin/Heparin Co-matrix Systems

A known amount of heparin sodium was dispersed in 15% solution of poly ethylene (vinyl acetate) PE(VAc) in chloroform at room temperature. The solution was spread over a glass plate separated by shims and the solvent evaporated slowly. The aspirin loaded chitosan beads were spread over the partially evaporated solutions and further, more heparin-PE(VAc) was added and the solvent was evaporated completely. By this process a co-matrix system was developed by incorporating aspirin loaded chitosan beads in heparin loaded polyethylene vinyl acetate matrix. These co-matrices were further surface coated with polystyrene-butadiene. The co-matrices were then dipped in 2% solutions of various polystyrene butadiene (5:95), (45:55), (85:15) in toluene.

2.9.3 Dissolution Studies

The release experiments were performed in 50ml 0.1M Tris HCl buffer

pH 7.4 solution taken in a screw cap bottle. Then, the co-matrix containing known amounts of aspirin and heparin was transferred into the bottle, and at appropriate intervals, 2ml samples were withdrawn, filtered and assayed for the aspirin and heparin content using standard protocols. An equal volume of the same dissolution medium was added to maintain constant volume.^{30,31} Each determination was carried out in triplicate and the release results were plotted as the amount and the percentage of cumulative aspirin/heparin release into the dissolution medium from the co-matrix versus time.

Another co-matrix system was also developed with ferric chloride loaded chitosan beads and magnesium chloride loaded polyethylene vinyl acetate. The release profile of Fe^{3+} ions and Mg^{2+} ions in tris HCl buffer, pH 7.4 was determined as that of aspirin/heparin system.

2.9.4 Assay of released drugs: The amount of various drugs released from the co-matrix was determined as represented below.

Metachromic Toluidine blue assay for heparin.

Metachromic toluidine blue assay¹⁸⁰ was used to quantitate the amount of heparin released from co-matrix system developed from aspirin loaded chitosan beads and heparin loaded PE(VAc). 0.005% of toluidine blue solution was prepared in 0.01 N HCl containing 0.2% NaCl. Standard heparin solution was prepared by 50 μ l heparin, diluted to 100ml with 0.2% NaCl. Two and one-half milli liters of 0.005% Toluidine blue solution was pipetted into test tubes containing 0.5ml test samples,

standards (10-70 μ g heparin) and a blank with same volume of saline. All the tubes were agitated for 30 seconds. Hexane (5ml) was then added to each tube and the tubes were shaken vigorously for another 30s. to separate the heparin dye complex.¹⁸⁰ The aqueous layers of all the tubes were removed and absorbances were measured at 631nm, within 30 min. The differences in the absorbances of blank versus tests, provided the free heparin.

Aspirin concentration was measured at 260nm by UV absorbance using spectrophotometer (Shimadzu Spectrophotometer, Japan) against a standard.

2.9.5 Ferric Ion Quantitation

The amount of FeCl₃ release in tris-HCl buffer, pH 7.4 from co-matrix system was estimated by the colourimetric method, by using standard kit from Miles India Ltd. In short, the iron released from the co-matrix system has been reduced in acetate buffer at p^H 4.8 from the ferric to ferrous state by ascorbic acid¹⁸¹. Ferrous ions chelate then with Ferene-S [(3-2-pyridyl)-5,6-bis[2-(5-furylsulphonic acid)]-1,2,4-triazine] forming a stable blue complex. The reaction is read at 578nm.

2.9.6 Magnesium Ion Estimation

The magnesium ions released from the co-matrix was determined as reported earlier.¹⁹² In brief, in alkaline solution, magnesium forms a coloured compound with the dye titan yellow. The amount of colour formed is proportional to the amount of magnesium present. Since the coloured product is actually colloidal in nature and is

not a true solution, polyvinyl alcohol is added to stabilize the colour. To 5ml of the supernatant fluid added 1ml of distilled water, 1 ml of gum ghatti, 1 ml of 0.05 per cent titan yellow and 2 ml of 4N sodium hydroxide. At the same time put up 1 ml of calcium chloride and 5ml of water and 1ml of calcium chloride and 2.5 ml of the standard for use, plus 2.5 ml of water, as blank and standard respectively. Read standard and unknown against the blank were measured at 540nm, using spectrophotometer (Shimadzu Spectrophotometer, Japan)

2.9.7 Platelet Adhesion Studies with Platelet Rich Plasma or Washed Platelets

Calf blood collected anticoagulant solution (1 part 3.8% sodium citrate for 10ml of blood) was centrifuged at 700 xg for 15 minutes.^{11,33} Supernatant PRP was then removed by aspiration and was collected in a plastic tube. The hematocrit (obtained after removing PRP from whole blood) was further centrifuged at 1000 x g for 15 minutes and the white blood cell button was removed. The PRP was again centrifuged at 2000 xg for 10 minutes to separate the platelet button. The platelet button was washed with tyrode solution (0.055M D-glucose, 0.138 M NaCl, 0.012 M NaHCO₃, 0.0018 M CaCl₂, 0.0049 MMgCl₂, 0.0027 MKCl, 0.0036 MNaH₂ PO, pH 7.4) and suspended the cells in the same solution for the adhesion studies. The platelets were then exposed to PEG, modified BP and to crosslinked BP.

Platelet suspensions demonstrated above were exposed to the tissue surfaces for 15 minutes at room temperature, rinsed with 0.1M phosphate buffer, pH 7.4. The

adhered platelets were fixed with 2.5% glutaraldehyde and stained with coomassie Blue G.³³ Number of platelets adhered to the tissue surface were counted using an optical microscope (Nikon, Japan). Different vision fields were read randomly and averaged in a similar fashion for all samples. A minimum of 20 fields were counted from three separate experiments and the data were expressed as the average number of platelets observed per mm² of the surface with standard deviation.

Similarly, platelet adhesion in presence of released aspirin/heparin from the co-matrix to glass surfaces were also performed using tyrode washed platelets.^{11,33} These platelet suspensions were exposed to glass slides in presence and absence of the released aspirin/heparin from the co-matrix system for 15 minutes. The adhered platelets were quantitated as reported earlier.

2.9.8 Thromboplastin time

Thromboplastin time was performed with released heparin to certain specific time intervals, according to the method of Langdell et al.¹⁰² The test system consisted of known amount of released heparin solution, incubating 0.1ml citrated plasma and 0.1ml kaolin- cephalin mixture (equal volume of 4% kaolin in 0.9% NaCl and the working suspension of cephalin, provided by Sigma, USA) at 37°C, for 6 minutes with regular agitation of the incubation mixture to redisperse the kaolin at 2 minutes intervals. At the end of the 6 minutes incubation, 0.1 ml CaCl₂ (0.025M) was added and the clotting time registered.^{29,102} The test was repeated at least five times and the activated plasma thromboplastin time expressed in seconds with standard deviation.

2.10 In vivo studies

We have elected subcutaneous implantation studies in albino rats for evaluating tissue mineralization as reported^{53,116,117,175} by various investigators.

2.10.1 Implant and Explant Studies

Bioprosthetic heart valve calcification has been studied by both subcutaneous and circulatory animal models.^{118,175} Subcutaneous implants of bioprosthetic cusps have been studied in rats^{118,175}, mice¹¹⁶ and rabbits.⁵³ With either bovine pericardial or porcine aortic valve bioprosthetic materials, subcutaneous implants have been noted to have analogous calcific lesions. This approach has the advantage of minimal expense, an extremely accelerated time course in younger animals.

Three weeks old (50-60g) male wistar rats were used for the implantation experiments, with humane care in compliance with established guidelines. The rats were anaesthetized by subcutaneous injection of ketamine and xylazine and four subdermal pouches at least 4cm apart were dissected in the paravertebral area on the dorsal aspect of each rat, as shown in Figure 2.2.

Animals were divided into 4 groups, having 5 animals in each group. They were grouped as represented below and the samples were implanted subcutaneously.

- Group I - Glutaraldehyde fixed BP - GATBP
- Group II - PEG grafted BP
- Group III - PEG-20,000 grafted BP coimplanted with aspirin/heparin loaded co-matrix.

Group IV - PEG-20,000 grafted BP coimplanted with ferric/magnesium loaded co-matrix

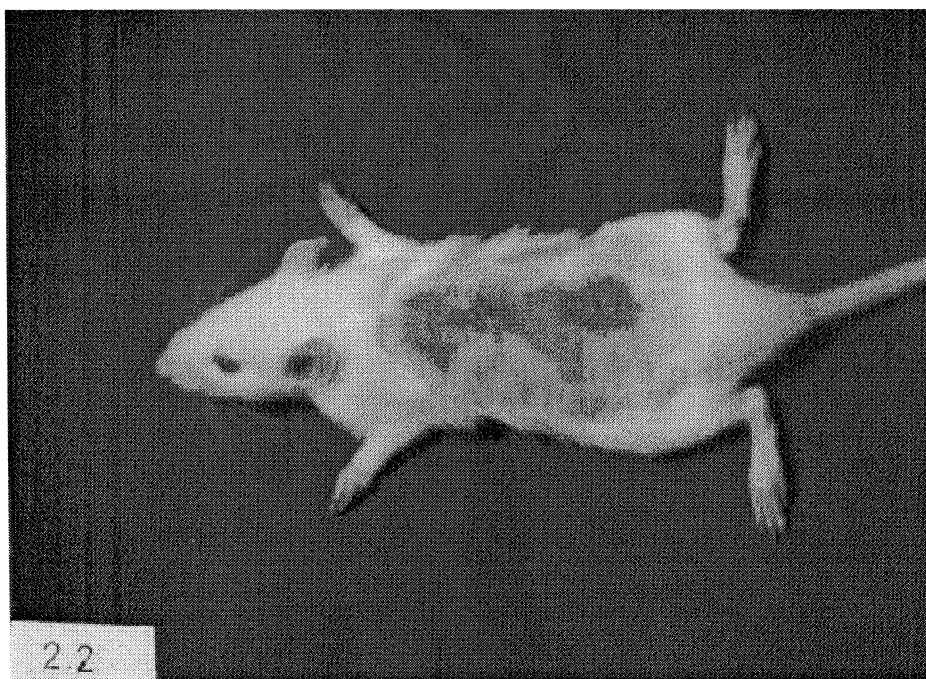


Figure 2.2 3 weeks old wistar rat after subcutaneous implantation.

The rats were sacrificed, after 3, 21, 180 days and explanted tissues were analyzed biochemically for presence of calcium and alkaline phosphatase. Morphological changes were also assessed by light microscopy. The amount of

calcium in the retrieved tissues were determined from HCl hydrolysate, as reported earlier, using O-cresolphthalein complexone method.

2.10.2 Extraction and Analysis of Alkaline Phosphatase (AP)

Explanted pericardial samples (25-30mg) were collected in ice and were homogenized with a mortar and pestle using 2.0ml sec- butanol and 1.0ml distilled water. The liquid was removed and the homogenization and extraction in butanol – water system was repeated twice. Extracts were pooled and centrifuged for 15min. at 1500g at 4°C.^{115,130,131} The aqueous layer was removed and the protein concentration and AP was assayed.

The assay for AP was based on the enzymatic hydrolysis of the substrate P-nitrophenyl phosphate to nitrophenol which was measured quantitatively using visible light spectroscopy.¹¹⁵ A standard kit obtained from Miles lab was used for this assay. In brief, 1 ml of p-nitro phenyl phosphate were pipetted in a cuvette, placed in spectrophotometer and set the reading to zero and immediately add 0.1 ml of aqueous extract of enzyme from tissue. Recorded the absorbance (405 nm) and time every 20 sec. For a duration of 4 min. The slope of the linear portion of the absorbance vs. Time curve provided a rate of formation of p-nitrophenol which, when divided by the protein concentration gave AP activity. The protein concentration in the aqueous layer was determined by phenol reagent method using human serum albumin as a standard.¹²⁷ The AP activity was represented as the nano mole of para-nitrophenol liberated per minute for mg protein (nm/pnp/min/mg protein).

2.10.3 Histopathology

Explanted pericardial tissues were fixed in 10% of buffered formalin for 24h. Tissues were then dehydrated in alcohol (changes of one hour each in 50,70,80,90% and 2 hour each in 100% alcohol following by clearing in 3 changes of chloroform and embedded in paraffin wax.^{8,171} 5 micrometer sections were cut on a rotating microtome deparaffinised, rehydrated and stained with haematoxylin and eosin, von Kossa, (for calcific deposits), Pearl's Prussian Blue (for iron).¹⁷¹

2.10.4 Haematoxylin and Eosin

Deparaffinised sections were immersed in the haematoxylin solution, for 10 minutes, washed well in running tap water, differentiated in acid alcohol for 10 sec. The sections were then stained with 1 per cent eosin (in alcohol) for 1 minute,^{81,171} dehydrated in graded alcohols, cleared, mounted and examined in light microscopy.

2.10.5 von Kossa Method for calcification

Deparaffinised sections were dipped in distilled water, 1% silver nitrate solution was poured onto the section and the section exposed to strong sunlight for 10-60 mins. followed by washing in distilled water.

2.10.5 a Perl's Method For Iron

The released iron from the co-matrix at the tissue (implant) interface was histologically observed by special stain (prussian blue). Deparaffinized sections were rehydrated, for 5 minutes in potassium ferrocyanide solution, followed by in potassium

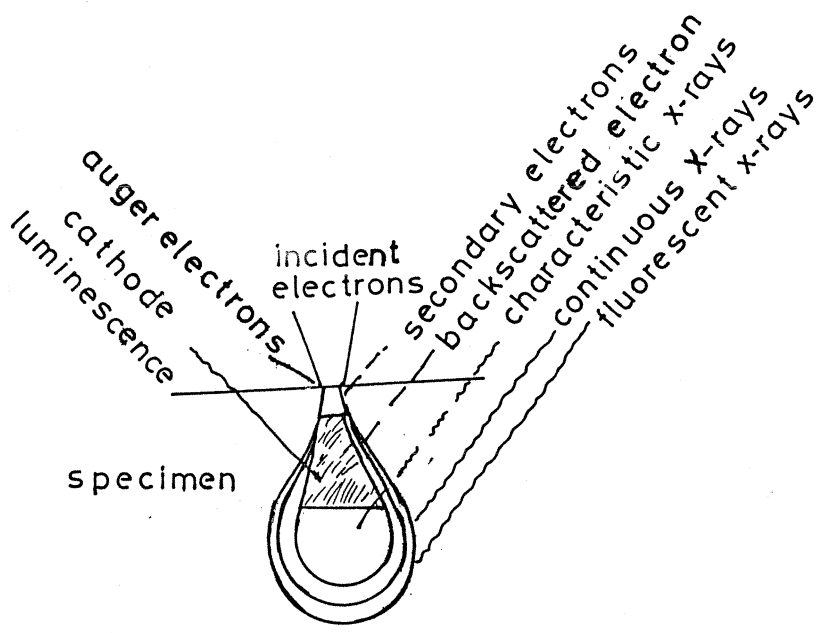


Figure 2.3. Interaction between the incident electrons and the sample surface.

ferrocyanide-hydrochloric acid solution for 20 minutes.^{8,171} They were rinsed well in distilled water and counter stained with nuclear red for 5 minutes. The slides were washed well in running water, dehydrated, and cleared; and observed by light microscopy.

2.11 Scanning Electron Microscopy (SEM)

The role of microscopy in biomaterials surface development consists in the pre-screening of the material for a fast examination of surface topography, observation of obvious defects or particulate contamination before any finer method to be used. SEM is used when the resolution needs to be 1 μm or better or when a greater depth of field is required for three dimensional samples studies.¹⁵⁹

The SEM principle is to scan a fine, high-energy electron beam across a surface to generate its highly resolved image. Both inelastic and elastic interactions between the incident electrons and the atoms of the surface result in the emission of a variety of radiations which are depicted in figure 2.3. In surface topography studies, two types of emissions are of interest: secondary electrons and backscattered electrons. Secondary electrons are the electrons which are weakly bond to the material and are emitted with low kinetic energies (approx. 50 eV). Due to their low energy, secondary electrons are detected only if created near the surface and, therefore, they are sensitive to the surface topography, those have a high spatial resolution. If the incident electron interacts with the nucleus of a sample atom, then it

is scattered in any direction with little loss of energy: Backscattered electrons are constituted of the electrons scattered back out of the sample after one or several scattering events. Those have higher energies than secondary electrons and come from a deeper part of the sample. Their surface topography sensitivity and spatial resolution are therefore less than that of the secondary electrons. The depth of analysis is smaller than 5\AA . The volume of interaction between the incident electrons and the sample is onion-shaped as the incident electrons are scattered and spread (figure 2.3).

The Cathode Ray Tube (CRT) is scanning in synchronism with the scan on the sample. The information given by the SEM is therefore the scan or pixel coordinates in an x-y plane and the corresponding intensities are generated by the set of detectors. SEM allows specimen tilting, completing the information on the topographic features of the sample, and provides different types of information depending on the type of electrons detected.

The samples observed must be able to both withstand vacuum ($2 - 6.10^{-7}$ torr) be electrically and thermally conductive: biological, organic and polymeric materials need to undergo specific and careful preparations to be studied with SEM. In order to avoid charging of non-conductive samples and improve their secondary electron emission, the specimens are coated with a thin layer of carbon or metal such as gold, palladium, platinum or chromium, depending on the magnification and resolution sought. Both vacuum evaporation or sputtering methods are generally used to coat the

sample. Special fixation and drying techniques have been developed to allow the conservation of the size and form of the biological specimen by precipitation, denaturation and crosslinking during both the sputtering and scanning of the sample. Glutaraldehyde and osmium tetroxide are the most popular fixative and post-fixative used. Both fixatives should be diluted in adequate buffer to prevent volume change. However, slight shrinkage of the cell was reported after fixation in glutaraldehyde and a slight increase in volume follows post fixation in osmium tetroxide⁹⁶. Different methods are available for the dehydration of the sample such as chemical dehydration, freeze drying, critical point drying and ambient temperature sublimation, all of which induce shrinkage of the specimens. Surface preparation such as stripping, cutting, cleaving, eroding and etching can be done on the surface to highlight specific characteristics.

A variety of artifacts can be introduced in the sample preparation for SEM. Therefore, great care must be taken to use this technique both qualitatively and quantitatively. Image distortion, and differences in secondary electron emission can be confused with surface features: the former, consisting in the loss of either horizontal or vertical deflection, can result from the charging of the surface, mechanical vibrations, the possible deformation of the sample during its preparation and the charging-up of the electron column interior. Specimen tilt should be strictly avoided when measuring lengths on the pictures or the data should be corrected for the tilt angle applied. Moreover, one should be aware of the effect of all the SEM parameters on both the image quality and the sample integrity: accelerating voltage,

proble current, working distance, objective aperture, astigmatism, gun alignment all contribute mutually to possible artifacts on the image.

Overall, SEM is a rather rewarding technique, offering the viewing of submicroscopic features of any surfaces.

The surface and or internal morphology of bovine pericardial tissues and the drug loaded co-matrix were examined using scanning electron microscope. Dehydration of tissue specimens were carried out with distilled ethanol in a graded series to avoid tissue shrinkage. For dehydration, the tissues were dipped for 15 minutes each in a series of 30, 50, 70, 80, 90, 95 and 100% ethanol. Finally, the samples were critical point dried in liquid CO₂. The samples were mounted onto aluminium stubs using double sided adhesive tape 35nm (350A) vacuum coated with gold film and were observed under the Scanning Electron Microscope. (SEM Model S-2400, Hitachi, Japan).

2.12 Statistical Analysis

Statistical analysis of important observations were also done and probability values (P) for significance were calculated using student's t-test. The mean \pm standard deviation, 't' and 'p' values were calculated for comparing significance of different observations. The mechanical properties of various crosslinked tissues were compared to non-cross linked pericardium and the calcification profile of various modified pericardium were compared to glutaraldehyde treated pericardium. The 'P' values 0.05 were considered as being statistically significant.

RESULTS AND DISCUSSION

CHAPTER 3.1

EFFECT OF ALTERNATIVE CROSSLINKING TECHNIQUES ON THE ENZYMATIC DEGRADATION OF BOVINE PERICARDIUM AND THEIR CALCIFICATION.

The strength, resorption rate and biocompatibility of collagenous biomaterials are profoundly influenced by the method and extent of crosslinking. In any cardiovascular application pericardial materials must sustain dynamic loads for the lifetime of the structure. It has been suggested that the collagen molecules in normal vascular endothelium are stabilized in the fibrils by covalent intermolecular crosslinks which provide the fibrillar matrices with an adequate degree of tensile strength and biostability.¹⁹⁶ Several crosslinking techniques have been explored in different applications with collagenous biomaterials, including physical methods such as uv-irradiation, dehydrothermal, freeze drying etc. and the use of chemical reagents, such as glutaraldehyde, diepoxides diisocyanates, carbodiimides, diisothiocyanates and glycidyl ethers.^{69,88,146,150,184,189,196} However currently very limited basic research exists on the calcification effects of various modified (crosslinked) bovine pericardia and their relationship to other properties.

We compared the in vitro calcification and enzymatic degradation of bovine pericardia (after a series of surface treatments). The ability of α -chymotrypsin, bromelain, esterase, trypsin, and collagenase to modulate the degradation of SDS, GA, HMDIC, EDC and GLE treated BPs, were investigated. Incubation of various

enzymes to these crosslinked pericardia variably reduced the tensile strength of these tissues. Further, the biocompatibility and anticalcifying aspects of pericardial tissues were investigated. It seems that the chemical treatments of pericardial tissues might have altered their physical and chemical configuration and their subsequent biodegradation and calcification.

3.1.1 Enzymatic degradation of crosslinked pericardium

The degradation of SDS-BP, GATBP, HMDIC-BP, EDC-BP and GLE-BP, in the presence of various enzymes, such as bromelain, chymotrypsin, collagenase, esterase and trypsin were studied in vitro in Tris. HCl buffer pH 7.4, as represented in figure 3.1.1 to 3.1.5, respectively. Addition of these enzymes to the system variably reduced the tensile strength of all treated tissues. All the enzymes showed extensive digestion for SDS treated BP, as depicted in Figure 3.1.1. Among the five enzymes studied, collagenase indicated the highest digestion and subsequent degradation of SDS and other crosslinked tissues. SDS treated surfaces were completely digested within 20 days of collagenase treatment or after 40 days of bromelain exposure (Figure 3.1.1). In the case of other enzymes, a substantial reduction in the original tensile strength of SDS-BP (non-crosslinked) also was observed.

Figures 3.1.2 to 3.1.5 show the reduction in tensile strength of GATBP, HMDIC-BP, EDC-BP and GLE-BP as a function of time, due to enzyme digestion. The percentage retention in tensile strengths of glutaraldehyde and HMDIC

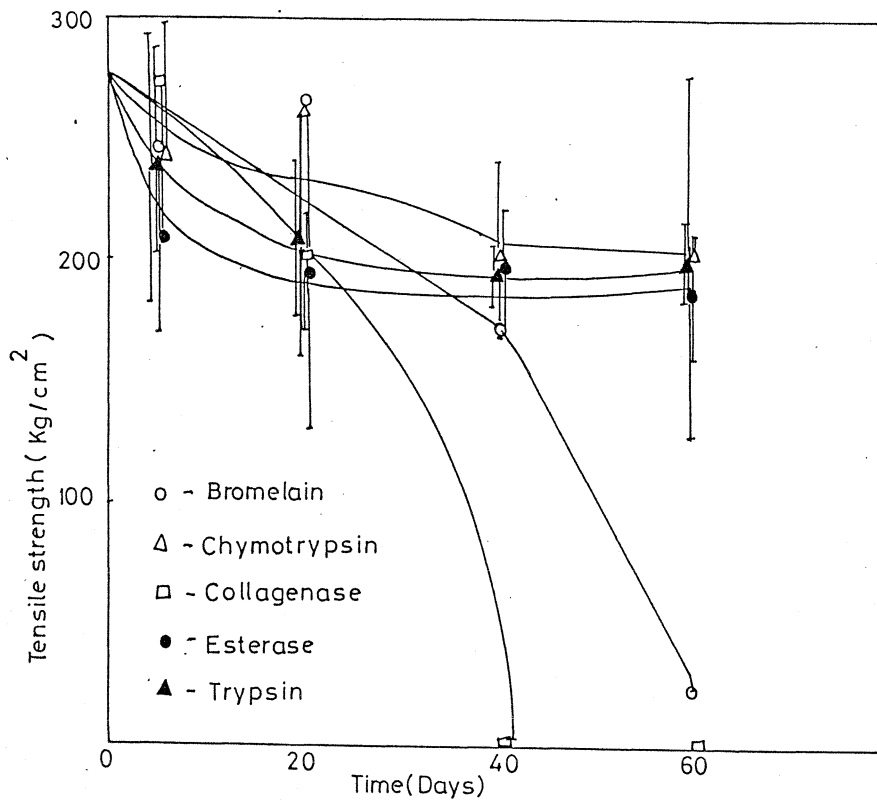


Figure. 3.1.1: Effect of various enzymes on the tensile strength of SDS-BP as a function of time. Bar indicates 95% confidence limits.

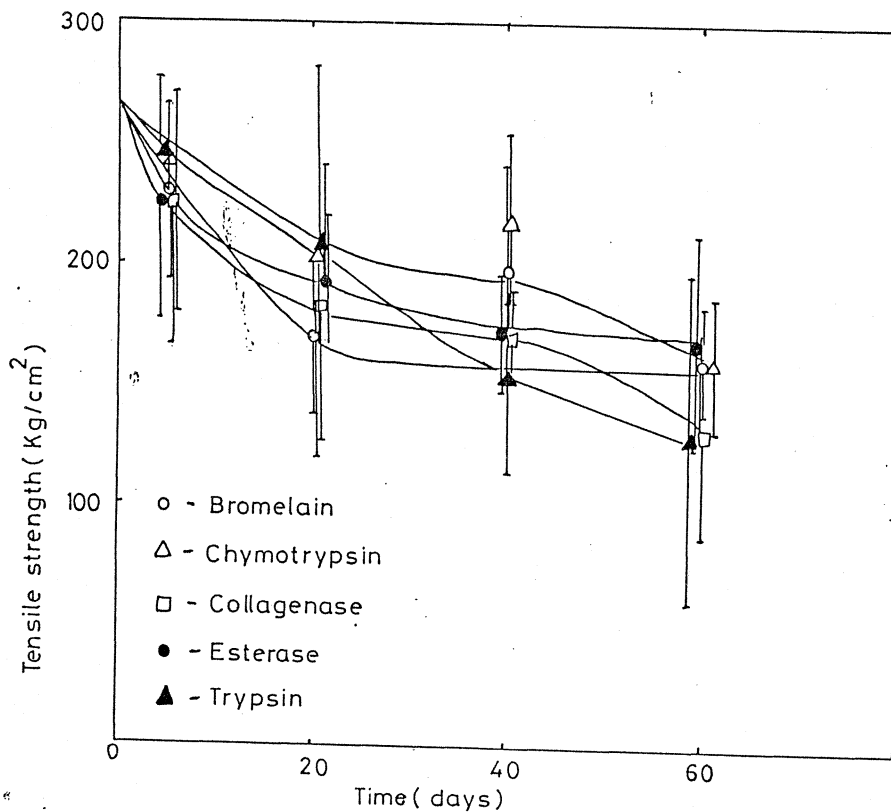


Figure.3.1.2 Effect of enzymes on the tensile strength of GATBP as a function of time. Bar indicates 95% confidence limits.

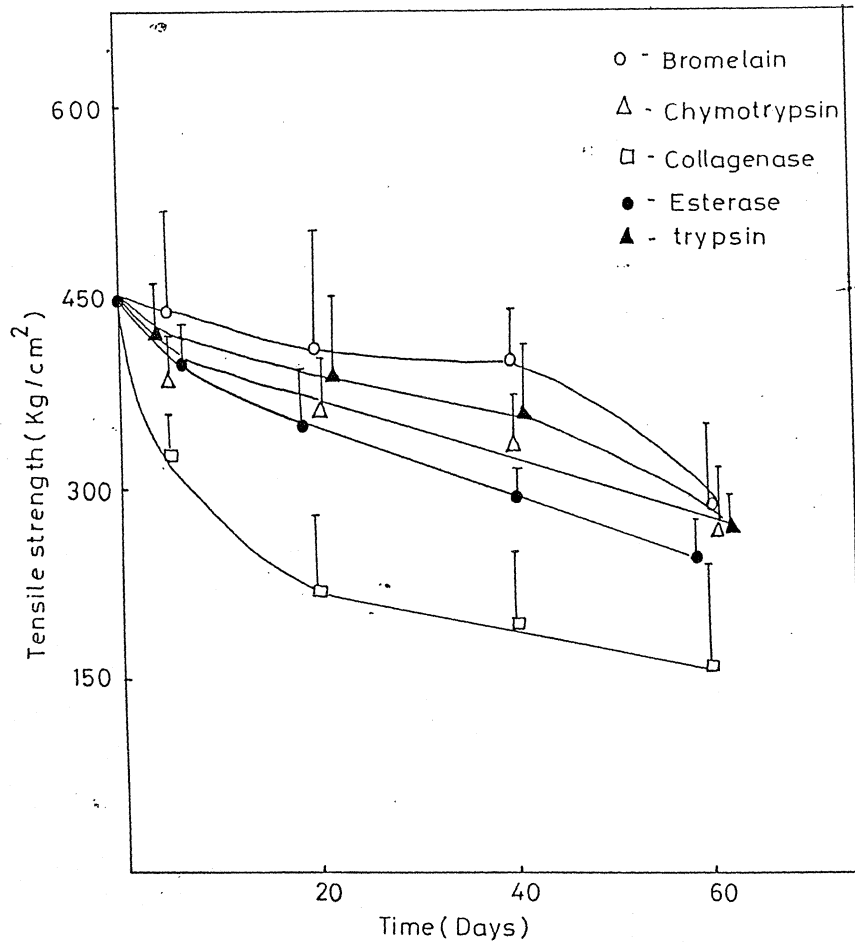


Figure-3.1.3 Effect of various enzymes on the tensile strength of HMDIC-BP as a function of time. Bar indicates 95% confidence limits.

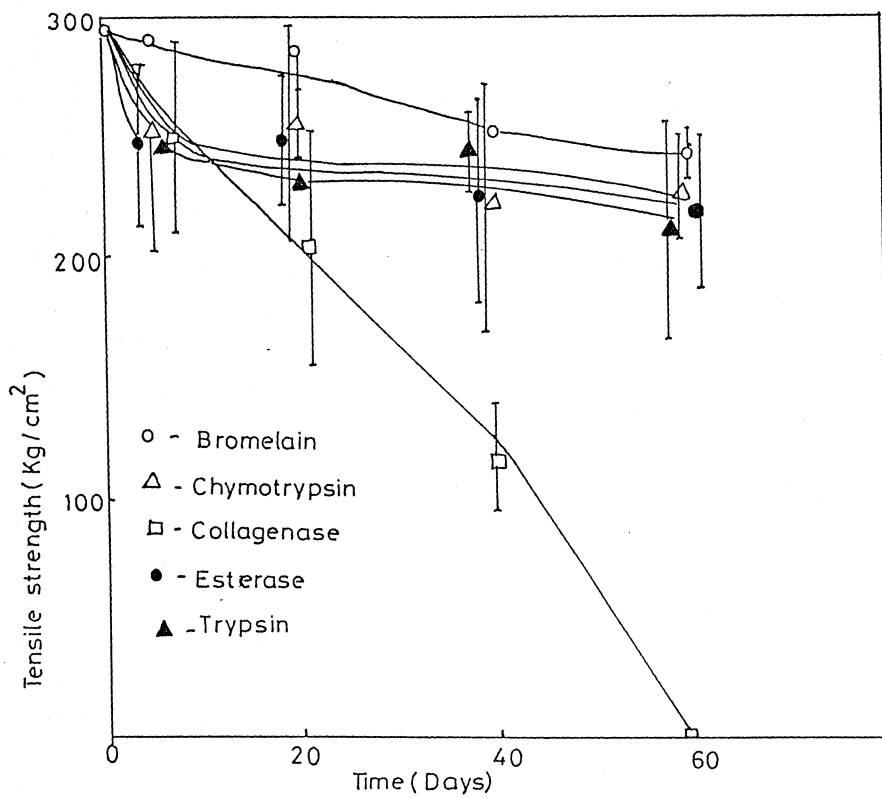


Figure-3.1.4 Effect of various enzymes on the tensile strength of EDC treated BP as a function of time. Bar indicates 95% confidence limits.

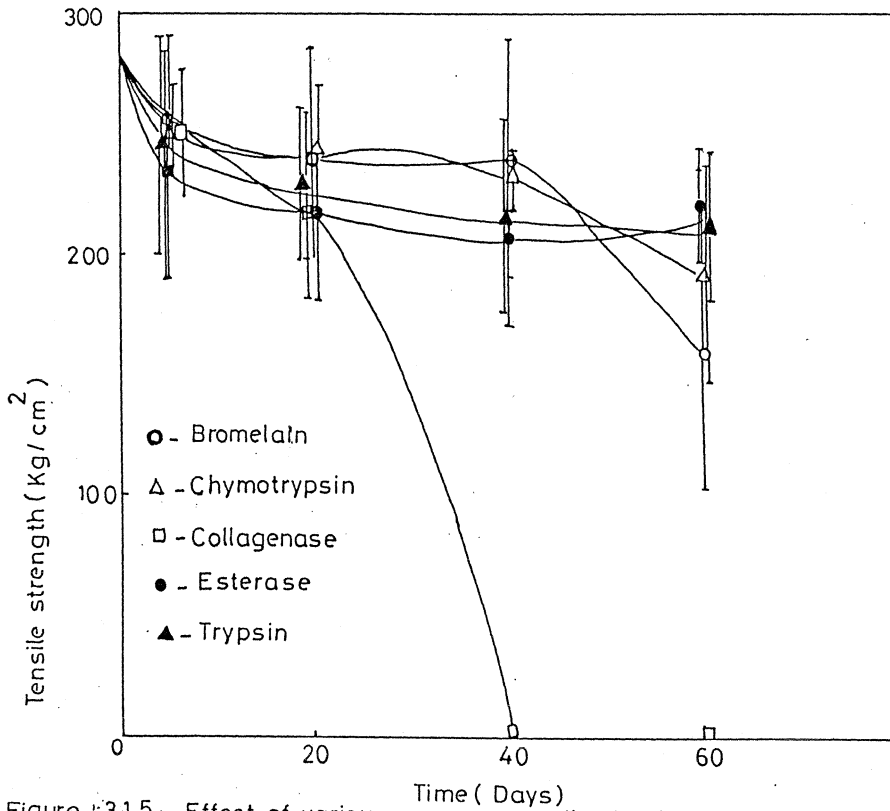


Figure 3.1.5. Effect of various enzymes on the tensile strength of GLE treated BP as a function of time. Bar indicates 95% confidence limits.

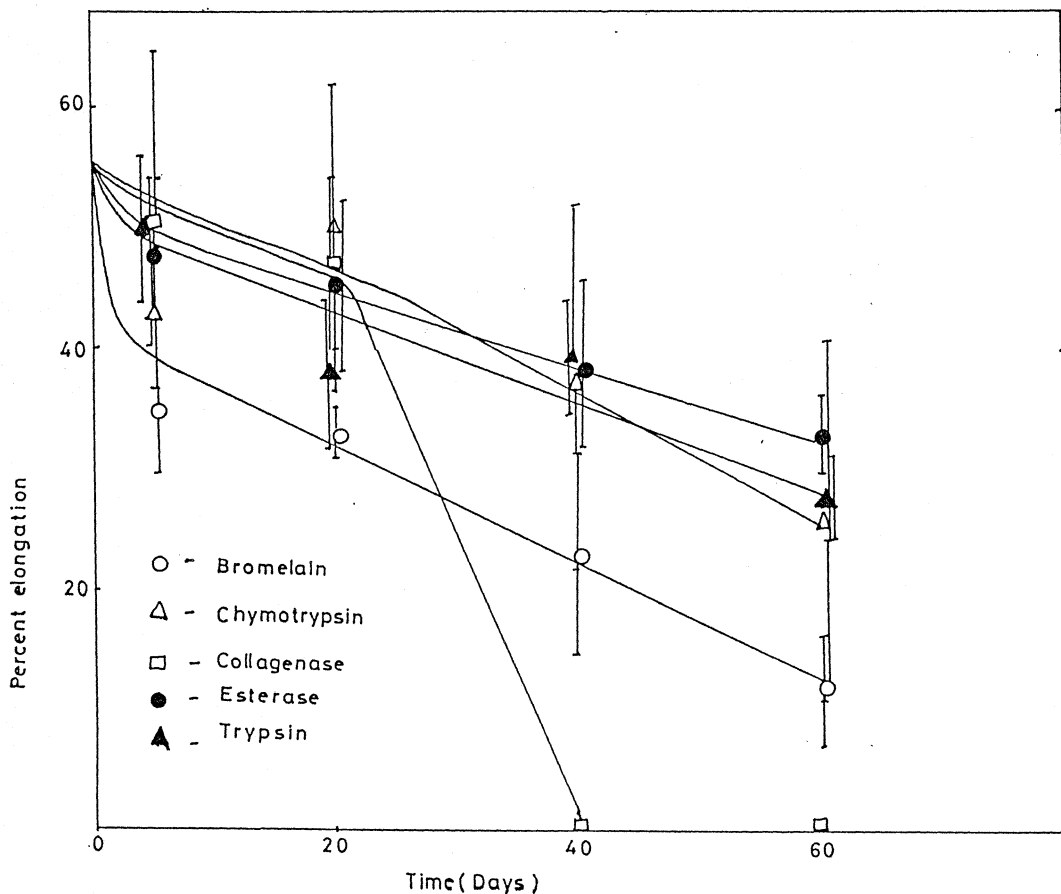


Figure 3.1.7. Effect of various enzymes on Percent elongation of SDS-BP as a function of time. Bar indicates 95% confidence limits.

crosslinked BP were higher, compared to EDC-BP, GLE-BP and SDS-BP. The GLE-BP tissues were completely digested after 20 days of incubation in collagenase (60 mg/lit). Whereas this enzyme could digest EDC-BP only after 40 days, as is evident from figure 3.1.4. In both EDC-BP and GLE-BP, an accelerated degradation was observed with bromelain (200 mg/lit) and chymotrypsin (200 mg/lit) incubation. However, from these substrates, the EDC-BP surfaces showed more stability in bromelain, chymotrypsin, esterase and trypsin compared to GLE-BP.

GATBP and HMDIC-BP tissues demonstrated higher stability in collagenase, or in all other enzyme systems studied, compared to SDS-BP and other crosslinked surfaces. The effect of various enzymes on GATBP and HMDIC-BP shown in figures 3.1.2 and 3.1.3. Collagenase and bromelain demonstrated more degradation on SDS-BP, GLE-BP, and EDC-BP, compared to HMDIC-BP.

Scanning electron micro-graphs of the SDS-BP, HMDIC-BP and GATBP and their 30 days of collagenase-digested tissues are shown in figure 3.1.6. SDS treated and crosslinked surfaces appeared to be smooth (figure 3.1.6. A, C & E) but after enzymatic digestion with collagenase, the SDS-BP had substantially degraded, as is evident from figure 3.1.6.B. However, the GA grafted BP had retained most of its structural integrity HMDIC-BP had shown compact collagen bundles within the pericardium but slight separation of collagen fibers are evident on surface. In other words, the GA & HMDIC modification of BP improved the stability of the pericardial tissue by retarding collagenase digestion (figure 3.1.6 D and F).

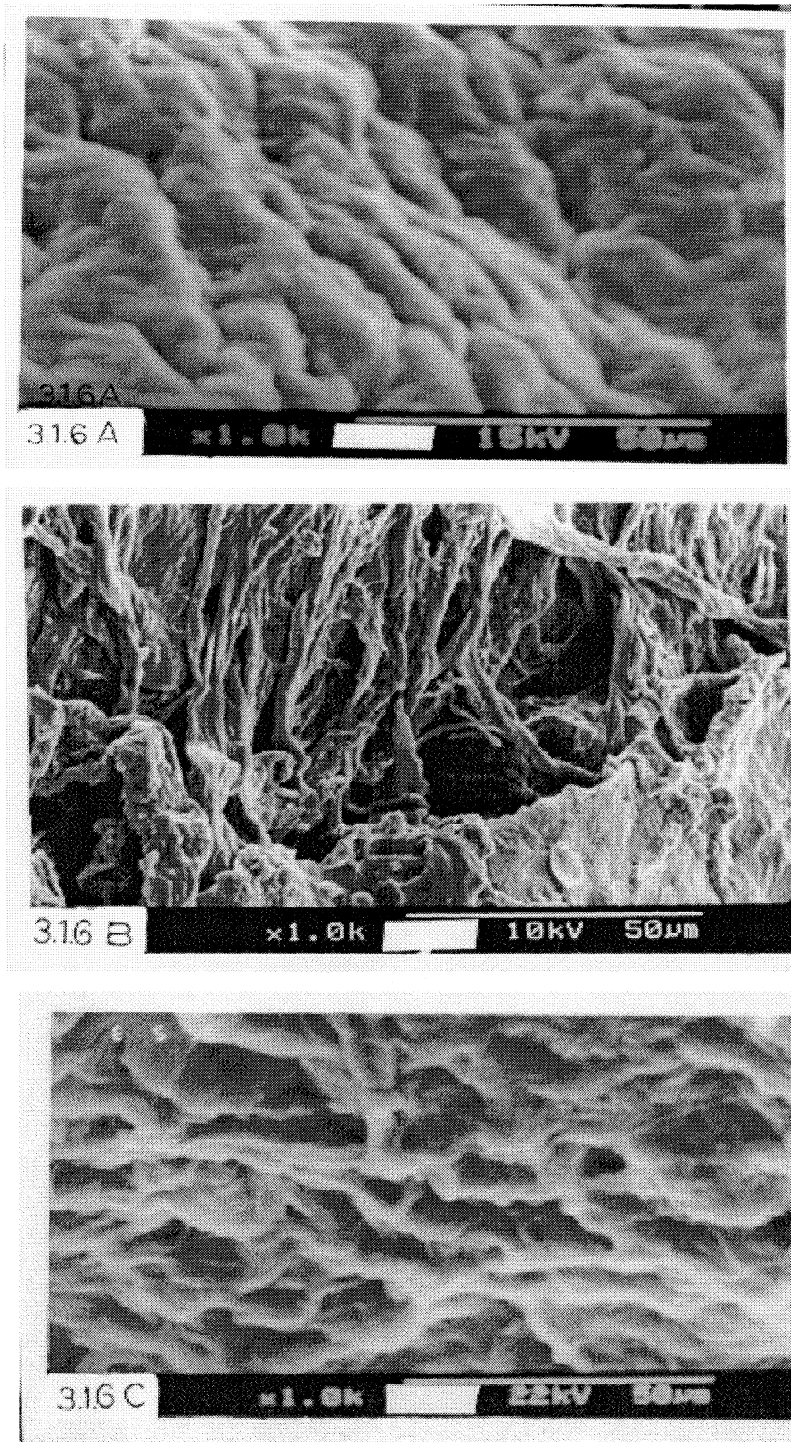
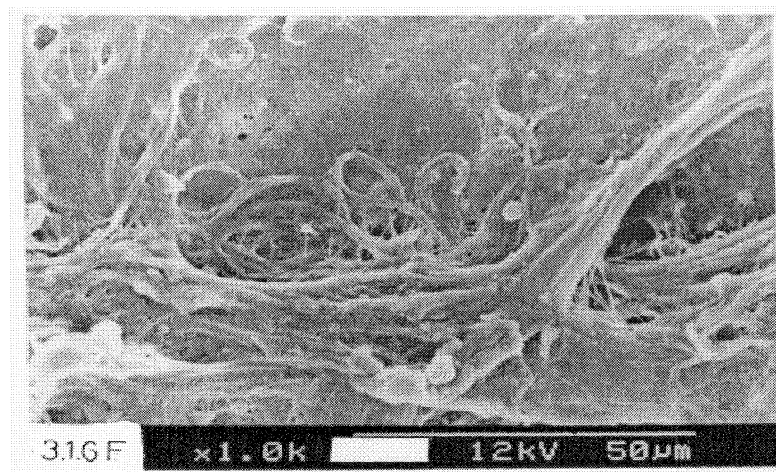
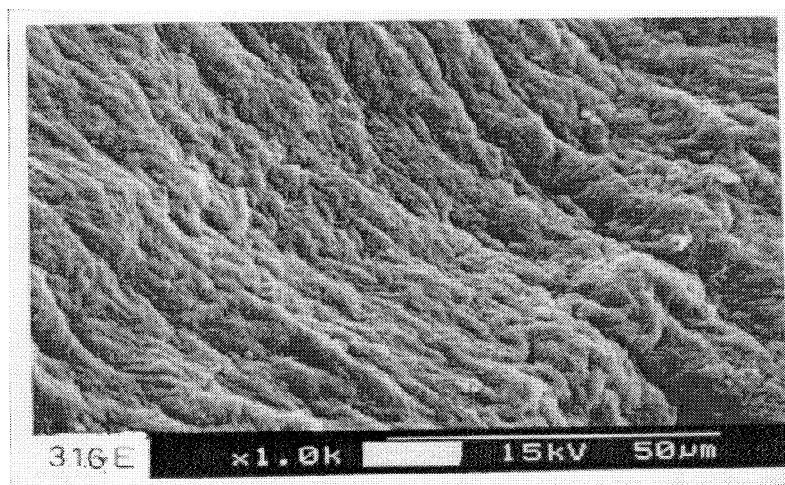
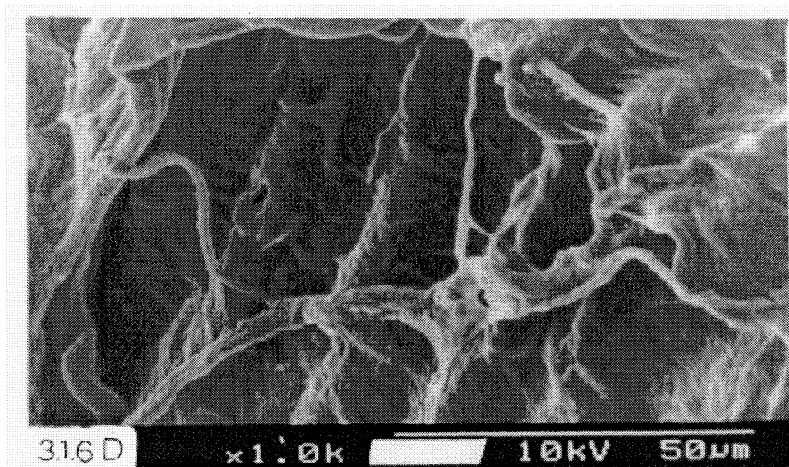


Figure 3.1.6. Scanning electron micrographs of crosslinked bovine pericardium. Surface morphology of (A) SDS-BP (B) its 30 days collagenase digested. (C) Glutaraldehyde fixed BP.



(D) its collagenase digested, (E) HMDIC treated BP and (F) its 30 days collagenase digested BP.

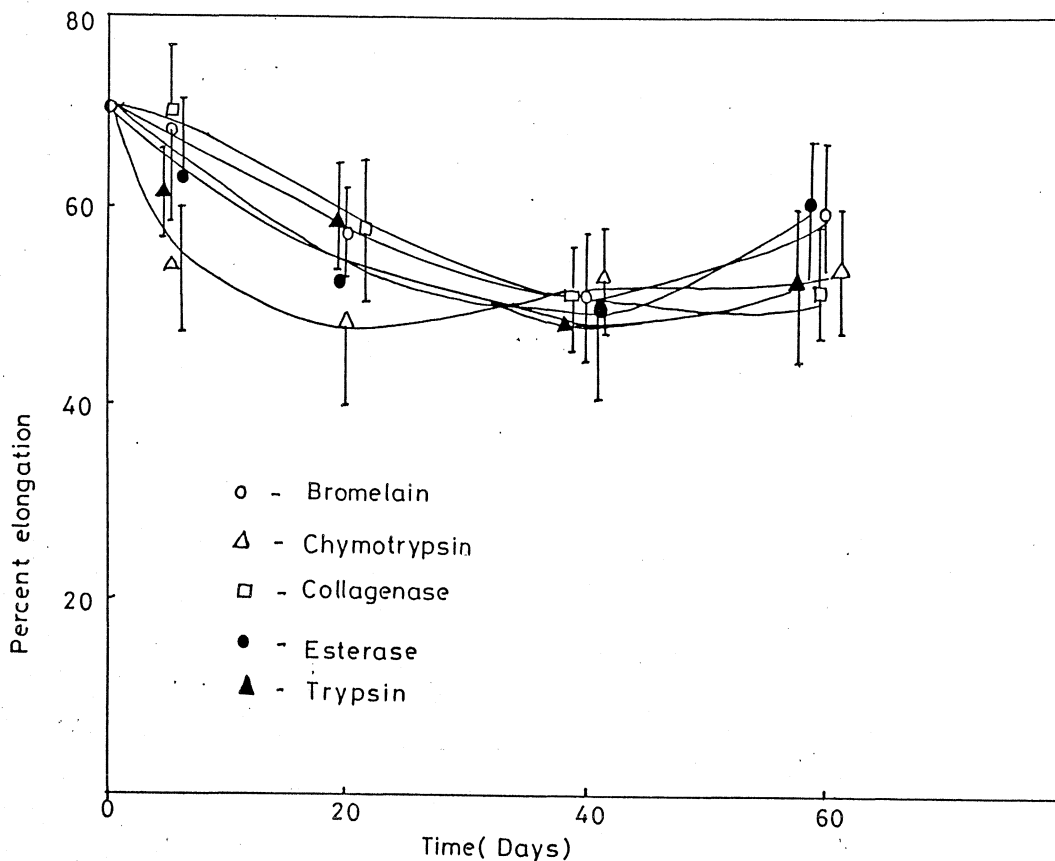


Figure 3.1.8. Effect of various enzymes on percent elongation of GATBP as a function of time. Bar indicates 95% confidence limits.

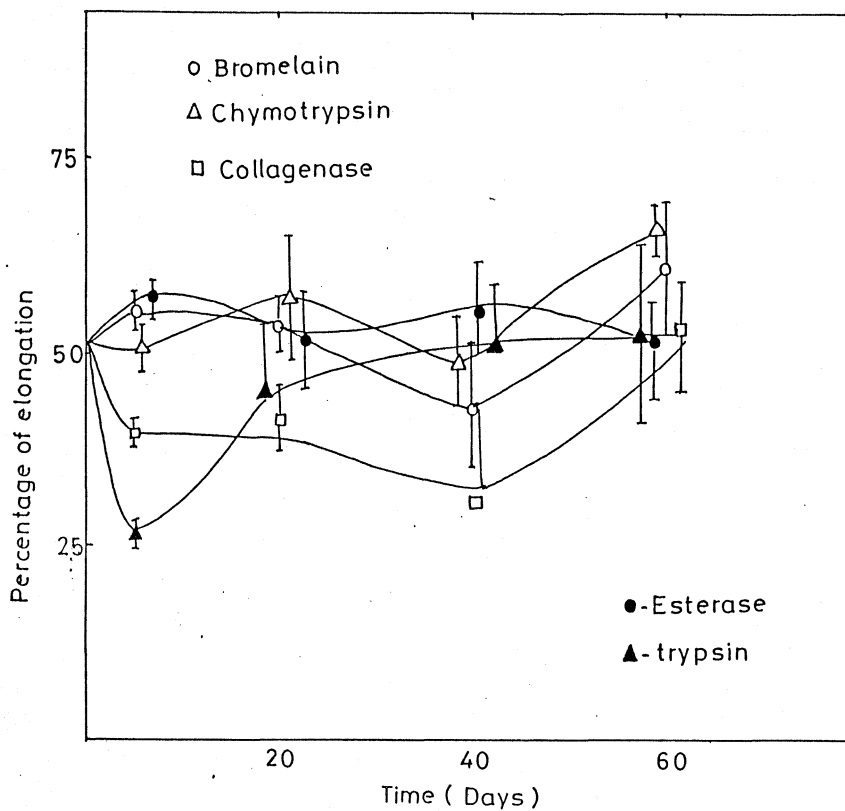


Figure 3.1.9 Effect of various enzyme digestion on percent elongation of HMDIC-BP as a function of time. Bar indicates 95% confidence limits.

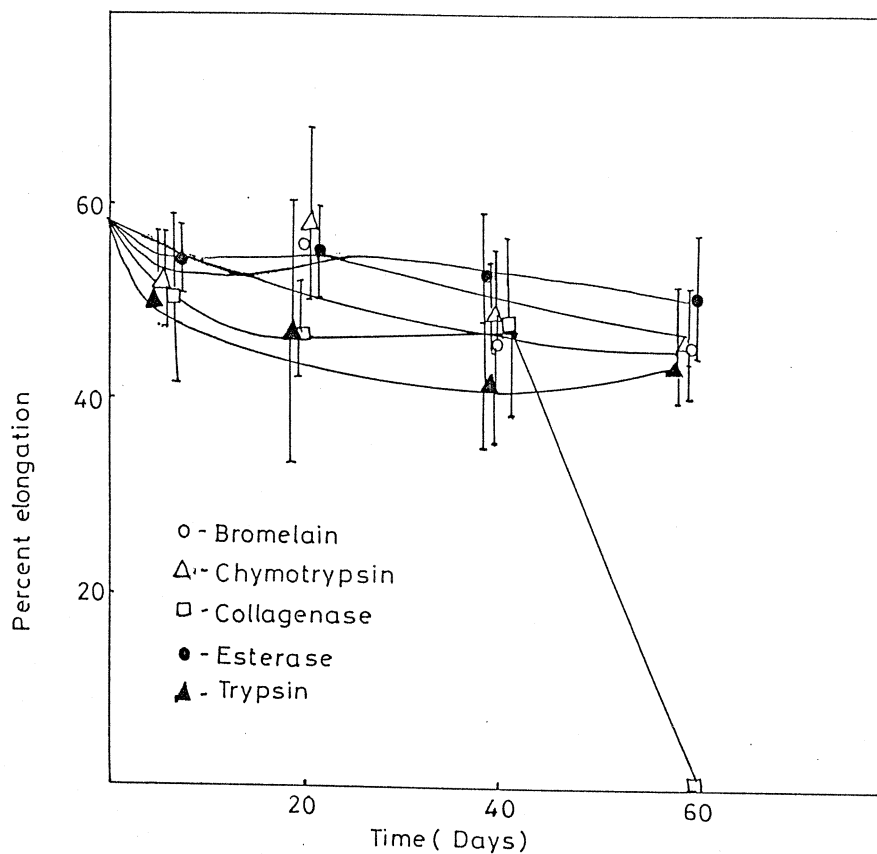


Figure 3.1.10. Effect of various enzymes on percent elongation of EDC treated BP as a function of time. Bar indicates 95% confidence limits.

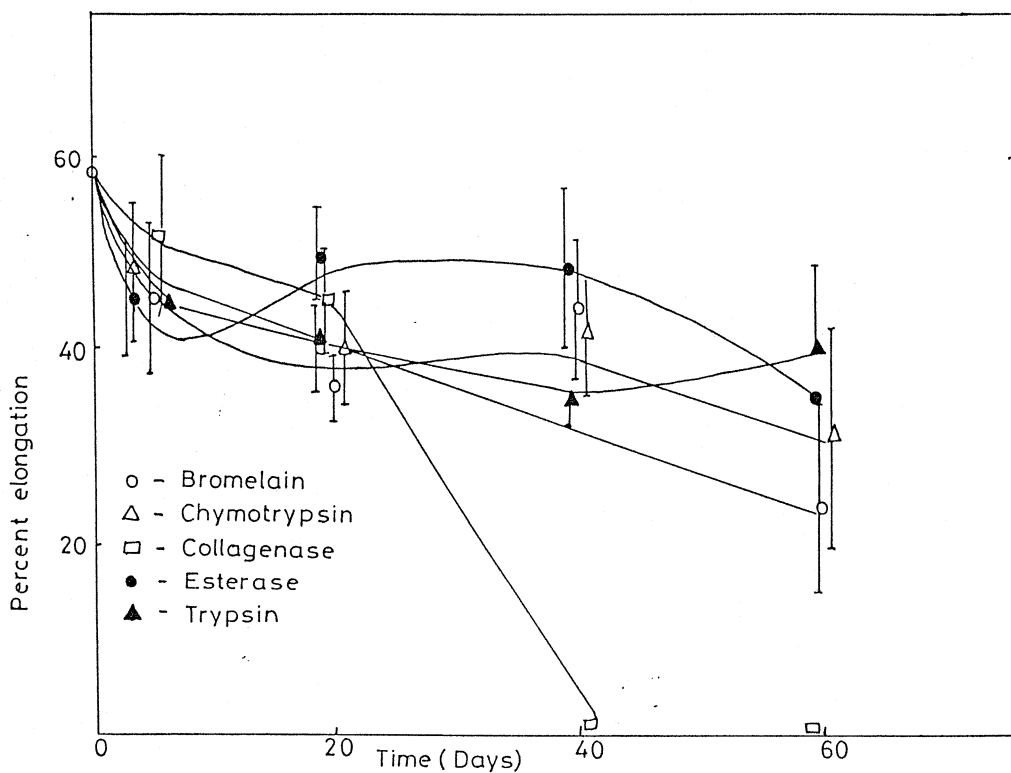


Figure 3.1.11 Effect of various enzymes on percent elongation of GLE treated BP as a function of time. Bar indicates, 95% confidence limits.

The per cent elongation of various crosslinked surfaces under enzymatic digestion of bromelain, chymotrypsin, collagenase, esterase and trypsin, respectively are shown in figure 3.1.7 to 3.1.11. Addition of these enzymes to the crosslinked system, variably reduced the per cent elongation of these tissues. The elongation of SDS-BP reduced substantially with most of the enzyme systems; as is evident in figure 3.1.7, while GATBP and HMDIC-BP did not exhibit much reduction (figure 3.1.8 and 3.1.9) from their original elongation per cent. The original elongation of percent of the GLE-BP and GLE-BP specimen substantially reduced with time, though the changes were not significant with EDC-BP (figures 3.1.10 and 3.1.11). However, GA and HMDIC crosslinked BP retained a maximum percentage elongation in all enzyme systems, compared to those tissues crosslinked with GA, EDC, and GLE.

In this context, glutaraldehyde, and hexamethylene diisocyanate are effective crosslinking reagents for fixing collagen based biomaterials. HMDIC crosslinked BP had shown maximum tensile strength initially, but with time the per cent loss of tensile strength was higher compared to glutaraldehyde fixed pericardium.

Crosslinking is an effective means of controlling the biodegradation rate of collagen based biomaterials. Pericardial bioprosthetic materials have relied on GA crosslinking to improve in vivo stability and resistance to degradation.^{69,88} The GA treatment is nominally intended to reduce immunogenicity of the materials.⁶⁹ Several alternative crosslinking agents have been explored in different applications, including

diepoxides,¹⁸⁹ diisocyanates,¹⁴⁶ carbodiimides,¹⁴⁷ and diisothio-cyanates.¹⁸⁹

Hexamethylene diisocyanate is a difunctional molecule, where the terminal isocyanate groups can react with amines of lysine on collagen to form the urea bond. The cytotoxic effects of HMDIC appears to be tolerable and mechanical properties of HMDIC crosslinked BP is better than glutaraldehyde.

At low concentration, GA produces intramolecular crosslinks in collagen while at higher concentration GA form long polymeric chains of intermolecular crosslinks,⁷⁰ and this reaction is reversible. After implantation of GA crosslinked collagenous biomaterials, large polymers of GA are continuously hydrolysed and this results in the release of free monomeric GA into surrounding tissues, causing cytotoxic effects. Tissues crosslinked with GA have a high strain modular and collagenase resistance time, significantly greater than those obtained for any single crosslinking procedure evaluated in this study. GA crosslinking may inhibit the activity of proteases by sterically restricting them from the substrate interaction, and may also inhibit penetration of the enzyme into the material and, subsequently, its degradation. Uncrosslinked implants (SDS-BP) degraded at a faster rate than crosslinked implants because of the increased susceptibility to enzymes whose activity is diminished by the presence of crosslinks (Figure 3.1.1 to 3.1.5).

Obviously, where cellular ingrowth into the implant is desired, alternative crosslinking methods are needed. Previous investigations have demonstrated that carbodiimides can serve as crosslinkers that produce biostable, biocompatible

interfaces. Further, the carbodiimides are used to crosslink compounds containing amines, phosphates, alcohols and thiols with the formation of amides and esters.¹⁹⁶ Carboxy and amino groups from the same residue are bound to the carbodiimide with the release of water soluble compounds as a byproduct. Here we are dealing with high molecular weight soluble carbodiimide - Ethyl-3-(3-dimethyl amino propyl) carbodiimide (EDC), it may be able to crosslink residues with larger separation distances and thus yield materials with a greater cross-linked density. This may be one of the reasons for its mechanical stability. The materials crosslinked with carbodiimides are relatively resistant to enzymatic degradation and do not produce any toxic substances to leach into host tissues.¹⁴⁷

Pereira et al¹⁵¹ have indicated that polyglycidyl ethers are equally effective as that of GA in fixing tissues. Here we used polyglycidyl ether, such as bis (polyoxy ethylene bis glycidyl ether) GLE to crosslink BP. It seems GLE fixation can block the ξ -amino groups in proteins, mostly forming secondary amines, carboxyl groups, hydroxyl groups and methyl thio radicals in proteins.¹⁸⁴ Thus, GLE binds the same residues as GA, but demonstrates a greater potential for preventing calcification.¹⁵¹

Enzymatic degradation and subsequent changes in mechanical properties of GLE-BP is depicted in figure 3.1.5. These show that GLE-BP materials are more susceptible to degradation. Initial decrease in the tensile strength of these matrices were small, but after 40 days of degradation wide differences from original tensile strength were noted. These changes are due to the enzymatic attack, predominantly

located at the surface of the fiber bundles. Only after multiple chain scission have taken place, where wide variations in mechanical properties observed.

Among the five enzymes studied collagenase showed the highest tissue degradation. It is suggested that the bacterial collagenase are capable of cleaving peptide bonds within the triple helical structure and have a specificity for the Pro-X-Gly-Pro-Y region, splitting between X and Gly.^{78,183} Previous studies have shown that cleavage sites within the molecular architecture of aggregates of tropocollagen molecules are not accessible for collagenase, and enzyme substrate complexes are formed only on the surface.¹⁸³

3.1 2 Changes in contact angle, platelet adhesion and calcium deposition due to various crosslinking techniques.

Table 3.1.1 gives the contact angle, platelet adhesion and calcium deposited (after 60 days of calcification) of various crosslinked tissue surfaces. GA treated BP showed the lowest octane contact angle, and HMDIC and EDC crosslinked BP demonstrated the highest octane contact angle. A reverse pattern was observed with the number of platelets seen on the surface. It is also evident from the Table 3.1.I. that the amount of calcium deposited on EDC-BP had apparently reduced, compared with the SDS treated tissues.

Figure 3.1.12 shows scanning electron micrographs of the platelets on SDS-BP and surface crosslinked bovine pericardia. It appears that platelet adhesion on

EDC crosslinked surfaces reduced compared to SDS-BP and GATBP. Platelets on SDS treated and GATBP surfaces extended long pseudopods leading to their complete spreading while most of the platelets on EDC-crosslinked surfaces retained their discoid shapes. Platelets spreading was maximum on GA treated surfaces. In some cases a few aggregates also were observed.

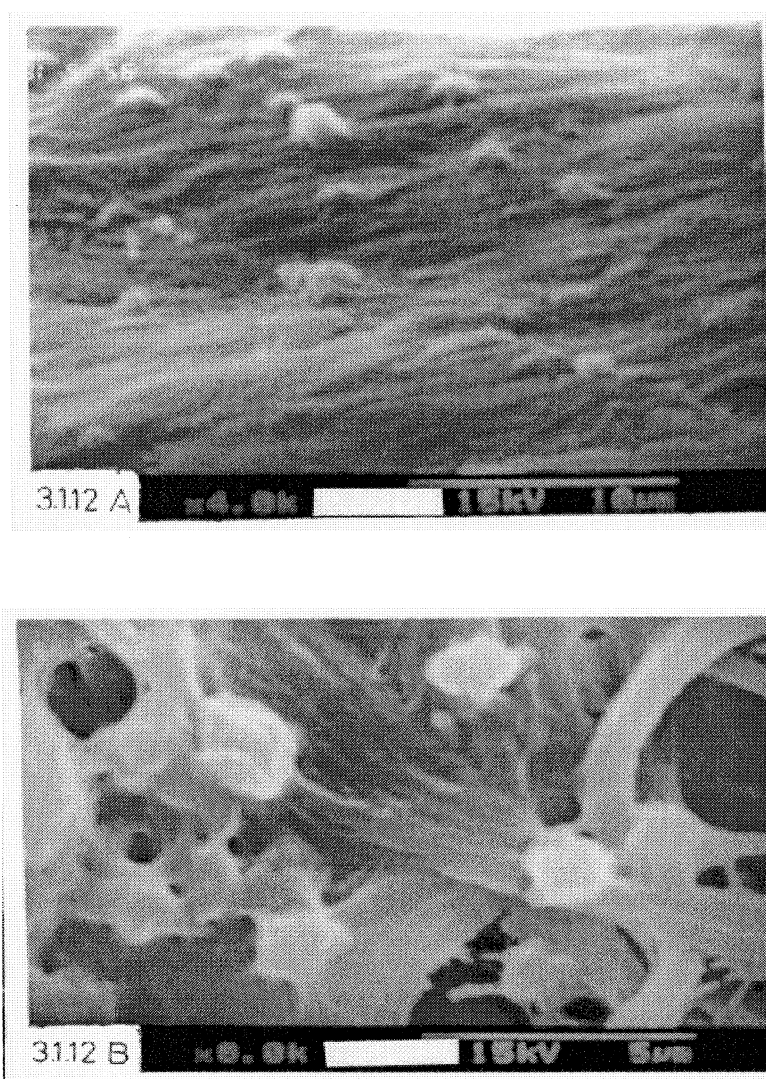
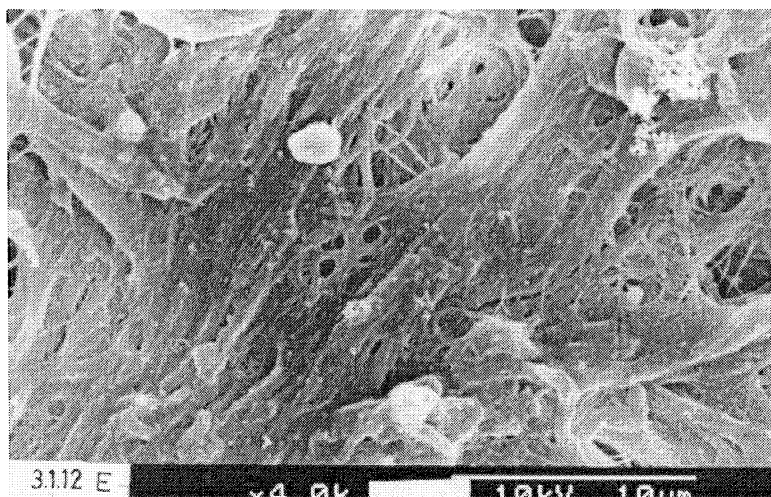
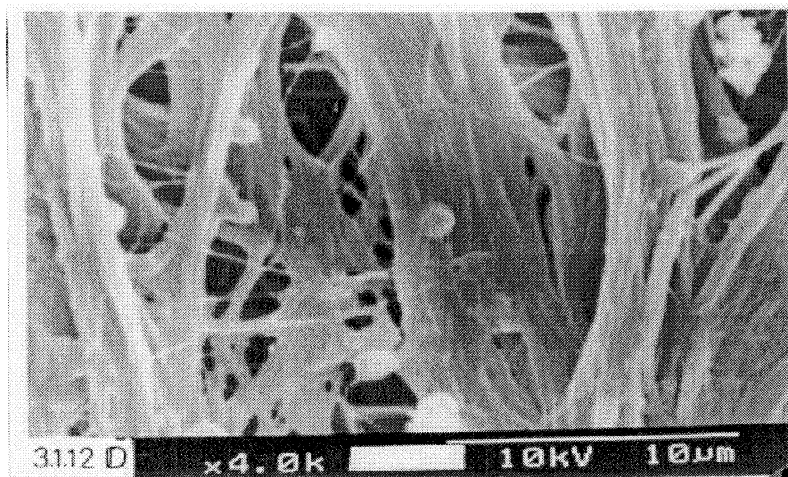
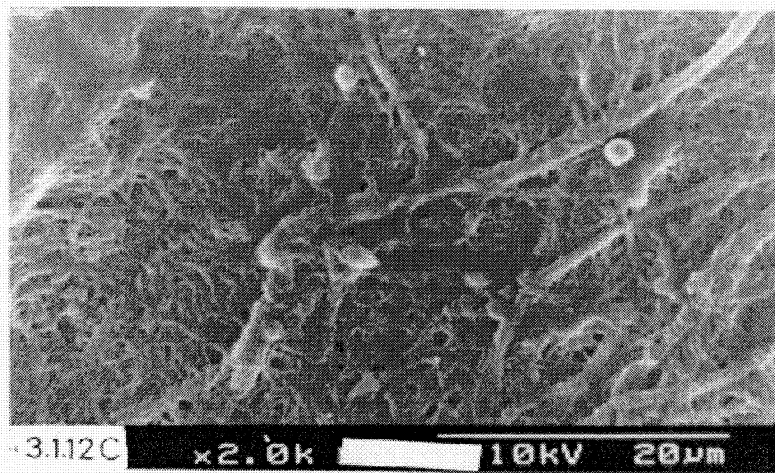


Figure 3.1.12 Scanning electron micrographs of adhered platelets to bovine pericardial surface. (A) SDS treated BP (B) GA treated BP.



(C) HMDIC treated BP (D) EDC treated BP, and
(E) GLE treated BP

Scanning electron microscopy (SEM) of various cross-linked pericardial tissues, (after calcification) and their surface morphology are depicted in figure 3.1.13. The calcium phosphate crystals were evident on most of the surfaces, however, EDC and HMDIC crosslinking variably reduced the calcium nodulation on BP (figure 3.1.13 C and D). Big clusters of calcium phosphate crystals were observed on GLE-BP (figure 3.1.13E), while crystals were rare on EDC-BP (figure 3.1.13 C and D) and were concentrated at particular points.

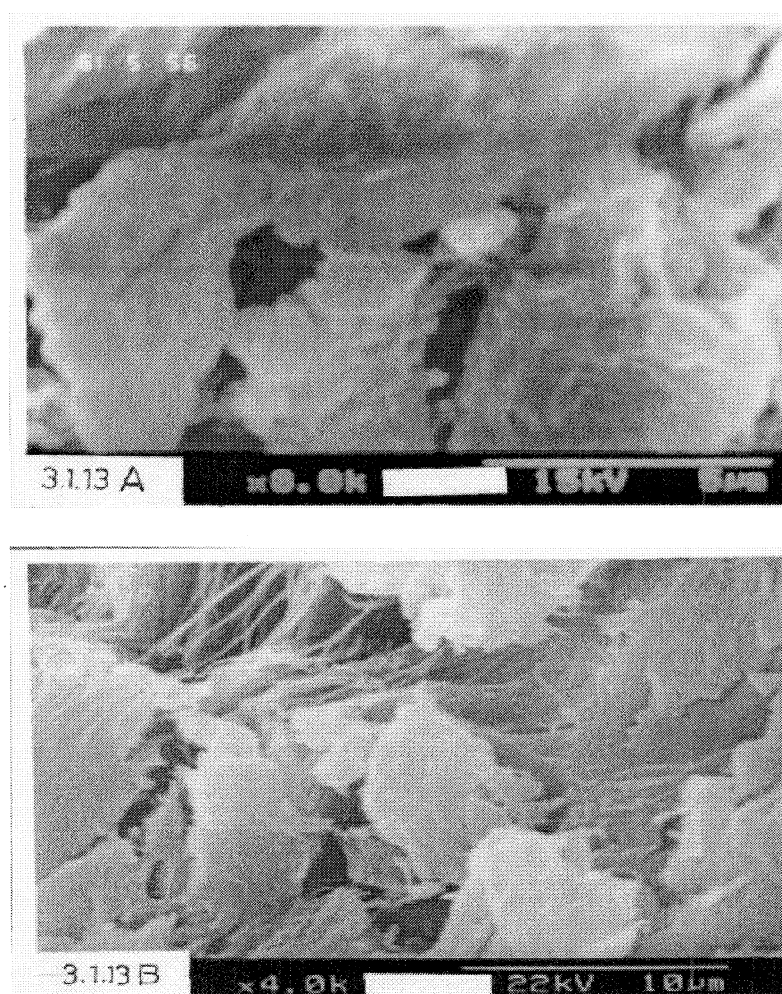
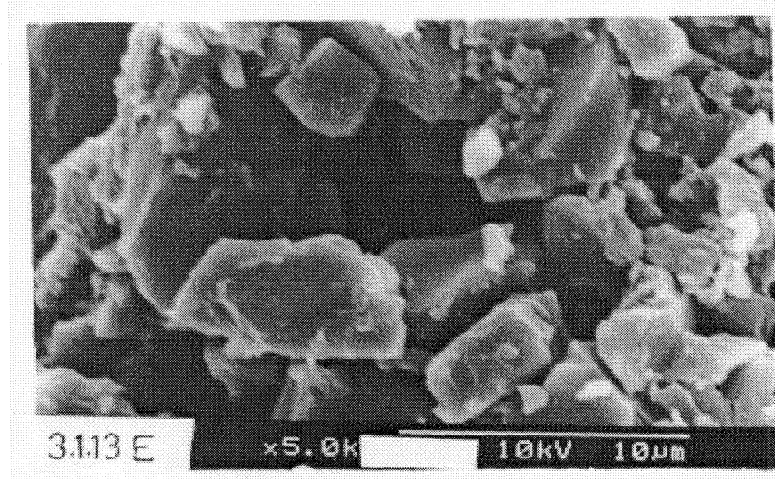
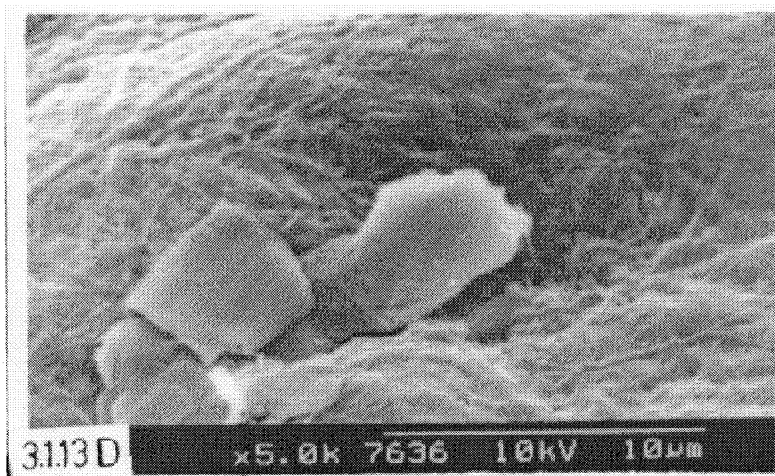
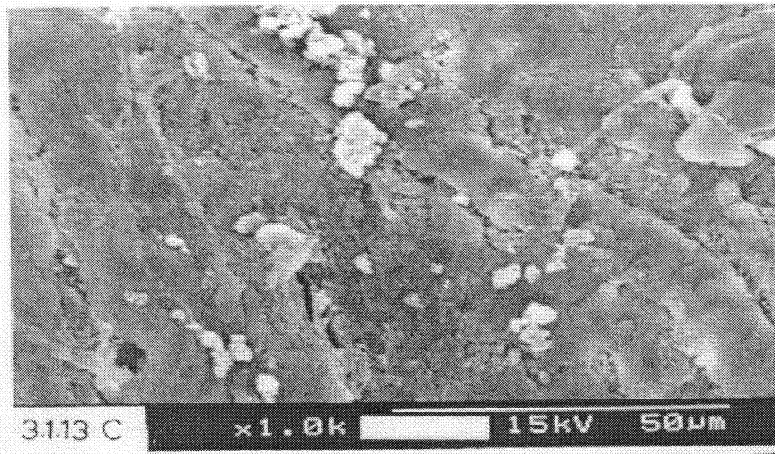


Figure 3.1.13 Scanning electron micrographs of bovine pericardium, after 30 days incubation in calcium phosphate solution (A) SDS treated BP (B) GA treated BP.



(C) HMDIC treated BP (D) EDC treated BP(E) GLE treated BP.

Table 3.1.I. Contact angle, platelet adhesion and amount of Calcium deposited to various treated bovine pericardial tissues.

a	b	c	d
Surfaces	Octane contact angle \pm SD	Mean platelets per $\text{mm}^2 \pm$ SD	Amount of Ca deposited for 60 days in $\mu\text{g}/\text{mg}$ of tissue
SDS-BP	141.0 \pm 3.2	82.3 \pm 9.8	29.2 \pm 1.6
GATBP	137.8 \pm 8.0* (2.0)	58.5 \pm 7.5* (7.7)	120.3 \pm 1.3
HMDIC	155.2 \pm 3.4* (3.2)	18.3 \pm 4.6* (22.8)	10.7 \pm 1.0* (8.0)
EDC-BP	141.2 \pm 2.1 [#] (0.2)	19.4 \pm 2.7* (12.7)	12.8 \pm 1.5* (5.2)
GLE-BP	148.7 \pm 3.2* (4.9)	49.3 \pm 7.5* (13.6)	25.3 \pm 2.2* (2.6)

- a. SDS treated bovine pericardium was exposed to various crosslinking agents (for more details refer experimental section).
- b. Octane contact angle expressed as mean \pm SD (from at least ten observations)
- c. Values denoted as the average of the numbers of platelets attached to the surface per mm^2 with \pm SD (at least 20 observations from triplicate experiments)
- d. Values expressed as mean \pm SD from at least four experiments. * $P < 0.005$, [#] $P < 0.1$ where the all values of crosslinked surfaces are compared \pm SDS-BP, except for calcification. The “t” values are provided in parentheses. ‘P’ values < 0.05 were considered as statistically significant when all values were compared using a student’s t-test.

The amount of calcium deposited on various crosslinked BP specimens incubated in calcium phosphate solution, with time are depicted in figure 3.1.14. The calcium concentration in the SDS and GATBP were significantly higher than EDC and HMDIC crosslinked BP, at all incubation time periods. In other words, the EDC-BP have a dramatic reduction in calcium deposition.

The platelet attachment studies represented in Table 3.1.I have shown that cell adhesion was substantially reduced with EDC-BP and HMDIC-BP, compared to other cases. SEM also revealed that the platelet adhesion (figure 3.1.12) was less on HMDIC and EDC-BP and the cellular morphology was moderately retained. However, platelets attached on GATBP and SDS-BP had extended their pseudopods (figure 3.1.12 A & B). It seems, human platelets possess membrane receptors for a wide variety of materials, including collagen.³⁴ Thus, it is conceivable that the crosslinkers variably modifies or mask the platelet receptor sites for collagen and causes reduction of platelet densities on the surface.

Table 3.1.I also provides information related to octane contact angle to the various above-mentioned surfaces. The octane contact angles of EDC and HMDIC crosslinked surfaces were higher compared to GA treated tissue. The octane contact angle technique has been widely used by various investigators to study the nature of surfaces, and it has been correlated as one of the factors for blood compatibility.^{7,87} This can provide information related to the hydrophilic and hydrophobic nature of the surface, where a higher angle shows an increase in hydrophilic character.⁷

Calcification is the principal cause of clinical failure of tissue valves.^{69,196} The nucleus of calcification appears as a result of adhesion and the death of cells that contain calcium, phosphate, phospholipids, lipoproteins and enzymes. Golomb et al⁶⁸ have compared in vitro calcification studies with in vivo subcutaneous models. It was concluded that this in vitro model was sensitive enough to diagnose biomaterial calcification and could serve as a prescreening method to examine calcification mechanisms. There are many limitations to this in vitro calcification model compared to in vivo conditions.

The available amount of calcium phosphate precipitate in the in vitro model system is limited and depends on the concentration of initial working solutions. In contrast, body homeostasis generates relatively unlimited amounts of calcium phosphate in the subdermal milieu.⁶⁸ Moreover, calcium phosphate precipitate in the in vitro system is randomly deposited (in the biomaterial and the environment) in contrast to the specific pathological calcification. Therefore, the crystalline mineral phase in the in vitro system is completely unpredictable and may not bear any resemblance to that occurring in vivo.^{26,68} However, the proposed model might be helpful in explaining the formation of subsurface and gross deposits.

The deposition of calcium was least with EDC and HMDIC grafted surface compared to other crosslinked surfaces (figure 3.1.13, 3.1.14 and Table 3.1.I). It has been reported that carboxy glutamic acid present in vitamin K-dependent protein are thought to bind with Ca^{2+} ion.¹⁸² In a similar fashion, two neighbouring $-\text{COO}^-$

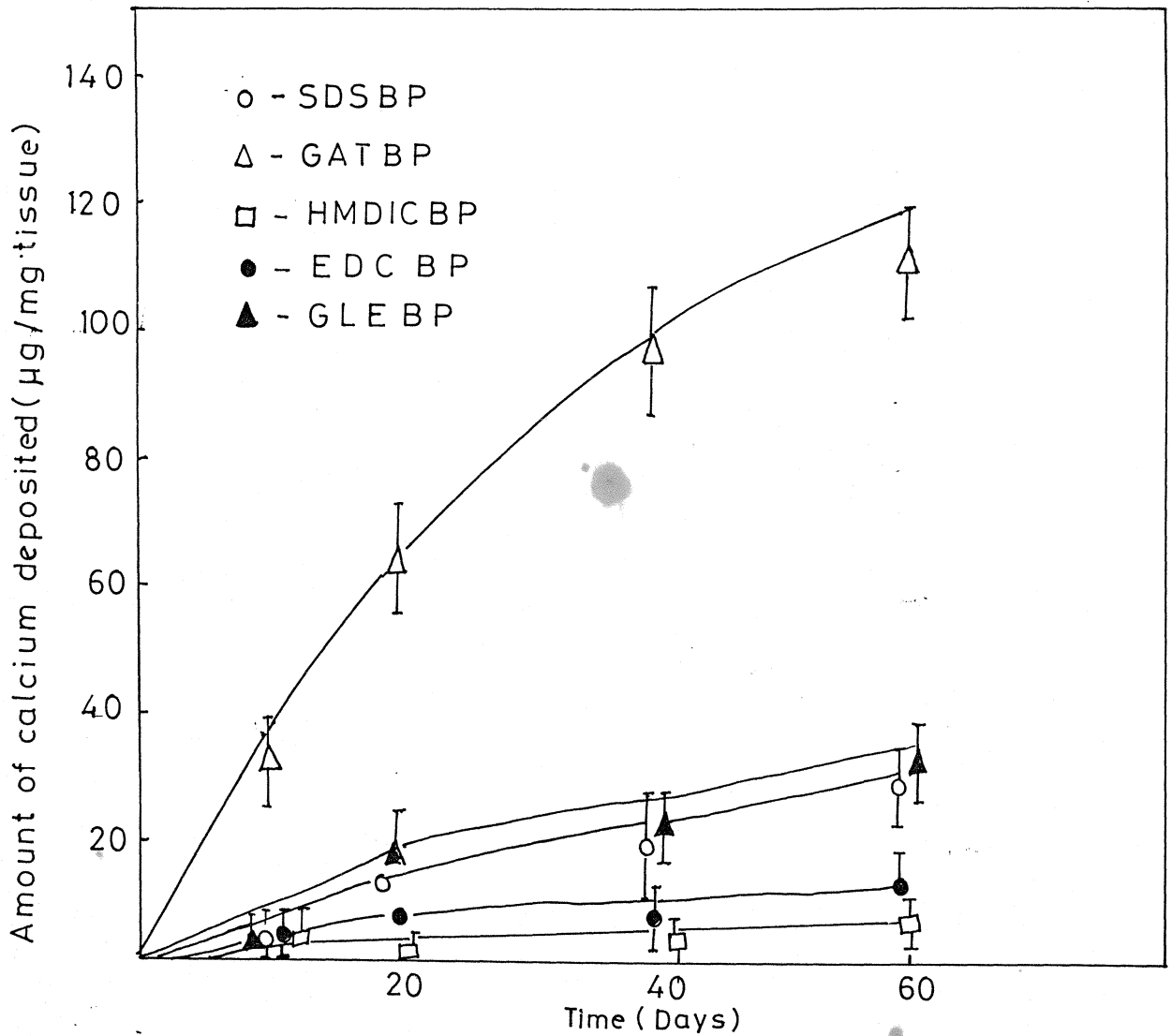


Figure 3.1.14 Amount of calcium deposited on various treated surfaces as a function of time on exposure to calcium deposited solution. Bar indicates 95% confidence limits.

groups present at a specific distance also can bind Ca^{2+} ions. In the case of EDC-BP, long chain carbodiimide effectively can crosslink intra and intermolecular carboxylic acid groups in BP, and subsequently the free $-\text{COO}^-$ groups may not be available for Ca^{2+} binding. This may be one of the reason for the observed reduction in calcium modulation on BP with EDC as depicted in figure 3.1.13 D and Table 3.1.I. The present study proposes that EDC modified and HMDIC crosslinked BP appears to be highly resistant to calcification, while GATBP have shown high resistance to enzyme digestion. From these observations, it is hypothesized that a suitable selection of bifunctional crosslinking techniques on tissues (combination of crosslinkers) may help to develop stable implants of high patency rates. This study also provides an insight to explore other alternative procedures in improving the pericardial tissues towards immuno resistance, biostability and anticalcifications.

CHAPTER 3.2

INFLUENCE OF POLYETHYLENE GLYCOL GRAFTINGS ON THE IN VITRO DEGRADATION AND CALCI- FICATION OF BOVINE PERICARDIUM

Polyethylene glycol (PEG) is a water-soluble polymer that exhibits properties such as protein resistance, low toxicity, and reduced immunogenicity.⁷⁹ The grafting of hydrophilic polyethylene glycol at the blood material interface can increase their surface hydrophilicity reduce protein adsorption, platelet adhesion and can develop a passive nonthrombogenic interface.^{74,133} PEGs are used for improving the blood compatibility of polymers. It has been reported that the deposition of calcium to high molecular weight polyethylene glycol has been substantially less compared to their low molecular weight polymers.⁸⁹ This chapter proposes the selection of a method for grafting PEG on bovine pericardium via various chemical treatments through their stability and calcification profile. Further, the selected crosslinking technique has been used for evaluating a variety of polyethylene glycols having varied molecular weights to choose the best combination for improved calcium resistance and stability.

3.2.1 Enzymatic degradation of PEG modified tissues through various chemical treatments

The initial studies were conducted to compare the efficiency of PEG-6000 grafted BP by different functionalities under enzymatic degradation and in vitro calcification. The degradation profile of PEG modified (via various crosslinkers)

pericardial tissues in the presence of bacterial collagenase was studied in vitro. figure 3.2.1 gives the variation in tensile strength of PEG modified pericardial surfaces with time in collagenase. It is evident from figure 3.2.1 that the PEG. CHO-BP lost their original tensile strength completely within 5 days of collagenase digestion. But, in all other PEG- grafted cases and GATBP retained most of their original tensile strength even after 60 days of collagenase digestion. In other words, the PEG-GABP, PEG-HMDIC BP, and GATBP appeared to be more resistant to bacterial collagenase.

The per cent elongation of various modified BP surfaces under collagenase digestion is shown in figure 3.2.2. Addition of enzyme to the PEG grafted pericardial tissue variably reduced the per cent elongation. The elongation of PEG-CHO BP was completely lost within 5 days of collagenase treatment. Further the per cent elongation was similar to all other modified and GATBP surfaces as is evident from figure 3.2.2.

Scanning electron micrographs of the GATBP, PEG-GABP, PEG-HMDIC-BP (crosslinked surfaces) and their 30 days collagenase digested tissue surfaces are shown in figure 3.2.3. The surface of GATBP (figure 3.2.3A) had been modified by PEG graftings. However, after enzymatic digestion with collagenase, the GATBP degraded more in comparison with PEG modified BP as is evident from figure 3.2.3A and B. SEM studies also indicated that PEG-GABP and PEG-HMDIC, BP had retained most of its structural integrity, (figure 3.2.3 D, E and F) after collagenase digestion. This study proposes the grafting of polyethylene glycol on crosslinked and

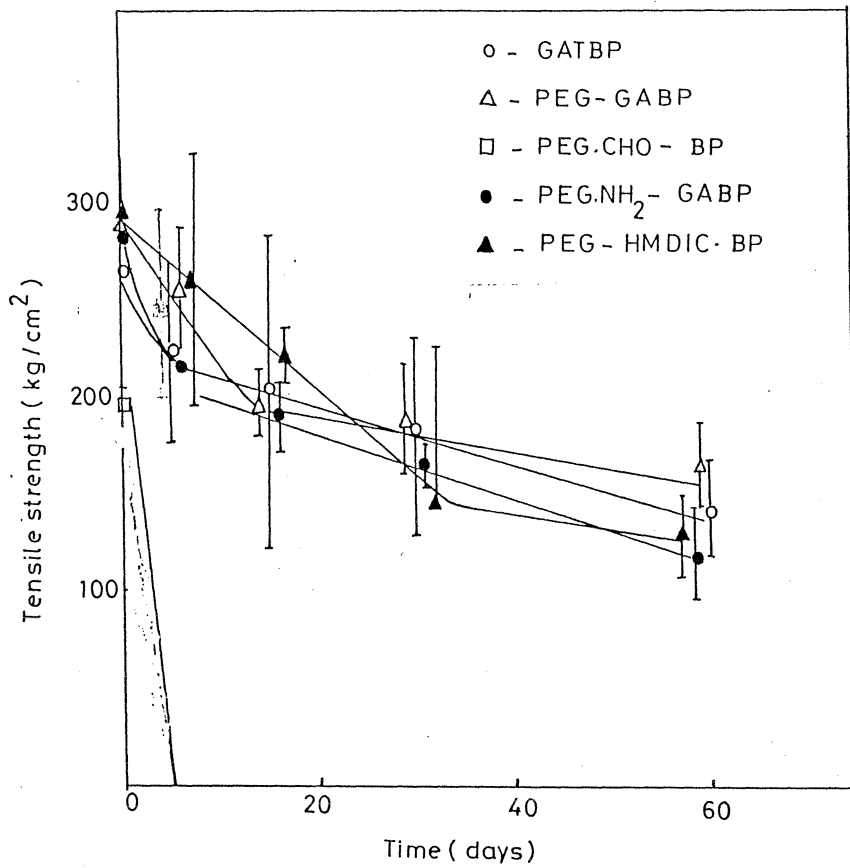


Figure 3.2.1 Effect of collagenase digestion in the tensile strength of PEG grafted bovine pericardium, as a function of time. Bar indicates 95 % confidence limits.

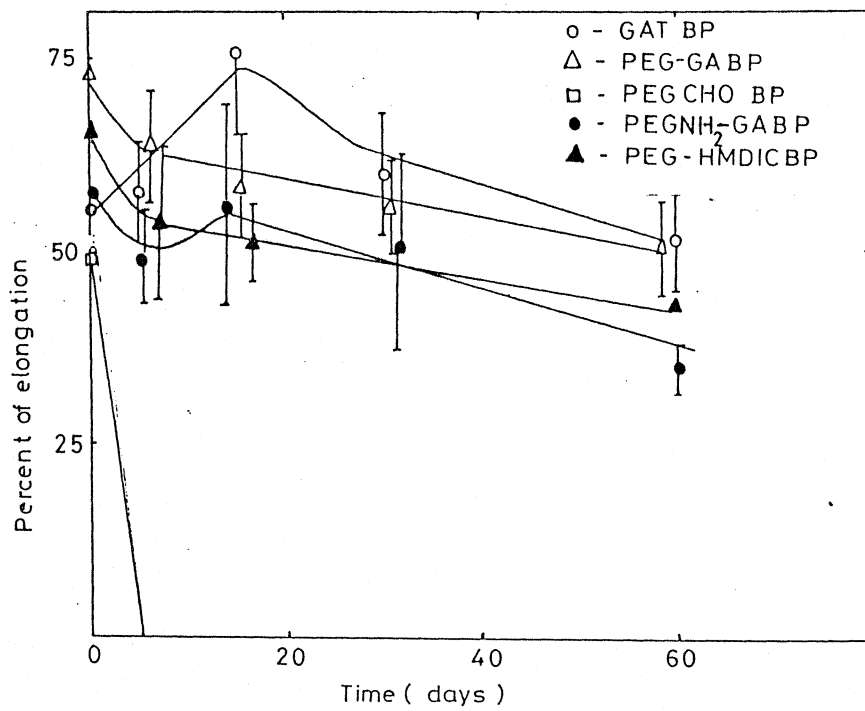


Figure 3.2.2 Effect of collagenase digestion on percent elongation of PEG grafted BP as a function of time. Bar indicates 95% confidence limits.

non-crosslinked pericardial tissues with a variety of functionalities and subsequently their collagenase digestion profile. Bacterial collagenase from *Clostridium histoliticum* was selected as the enzyme for the degradation studies because of its specificity for collagen. As indicated in figure 3.2.1 to 3.2.3, the digestion of PEG modified pericardial tissues varied due to different PEG- grafting techniques. PEG grafting on crosslinked tissue samples PEG-NH₂-GABP, PEG-HMDIC-BP showed resistance to enzymatic digestion. It has been suggested that the collagen molecules are stabilized in the fibrils by covalent intermolecular crosslinks, which provide the fibrillate matrices with an adequate degree of tensile strength and biostability.¹⁹⁶ In this context, glutaraldehyde is an effective crosslinking reagent for crosslinking collagen based biomaterials.⁶⁷ Further, hexamethylene diisocyanate (HMDIC) was introduced by Chvapil et al⁴⁰ for crosslinking collagenous tissues, GA crosslinking involves the formation of short aliphatic chains (Schiff base) and pyridinium compounds, while in HMDIC aliphatic chains containing urea bonds are introduced between two adjacent amine groups.

Both GA and HMDIC crosslinking may lead to the presence of unreacted functional groups (probably aldehyde or amine groups after hydrolysis of isocyanate groups) in the pericardial collagen matrix, which can result in a cytotoxic reaction upon degradation of the collagen. However, in the present system, these functional groups can act as reaction sites for PEG (Scheme 5- 8), and subsequently, direct grafting of the PEG occurs to the tissue. In principle, no

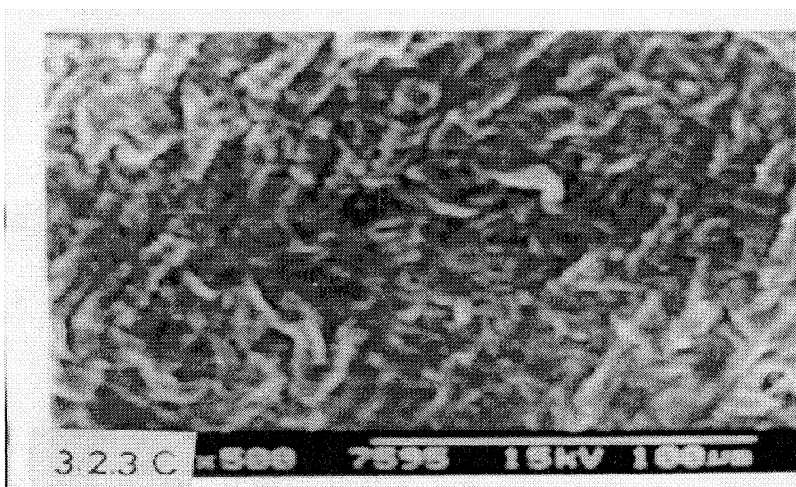
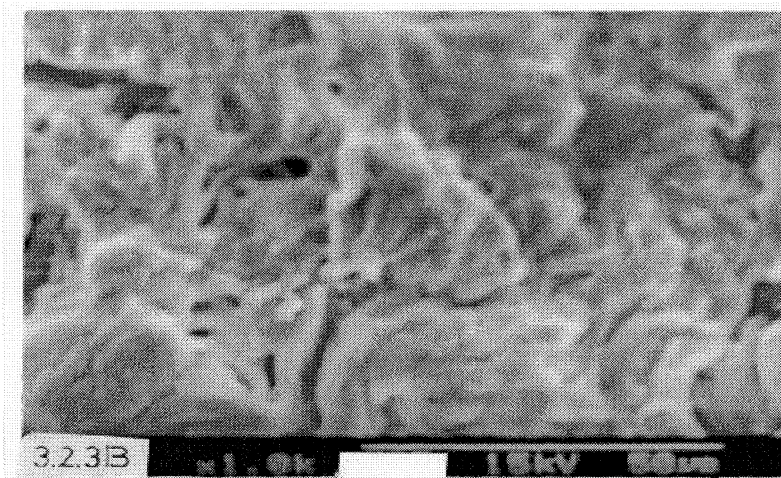
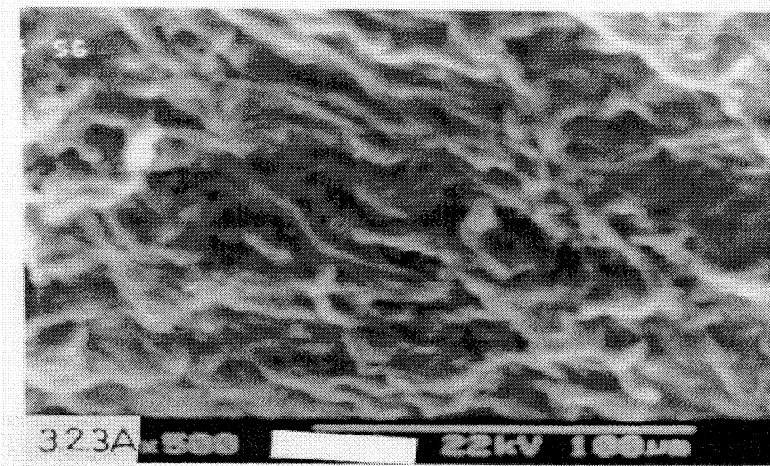
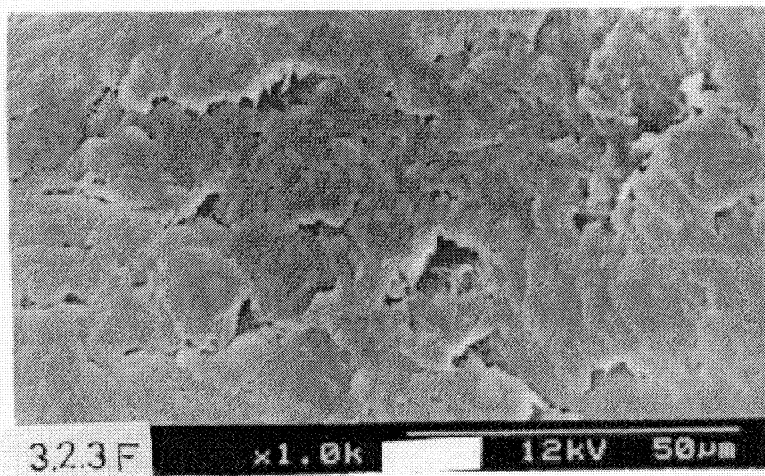
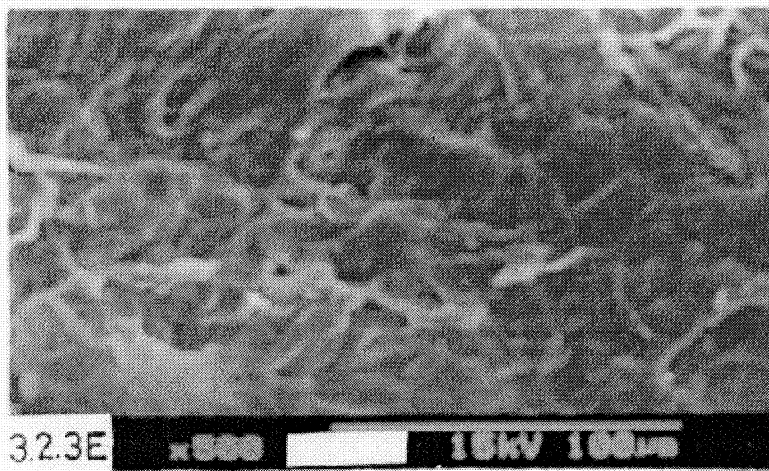
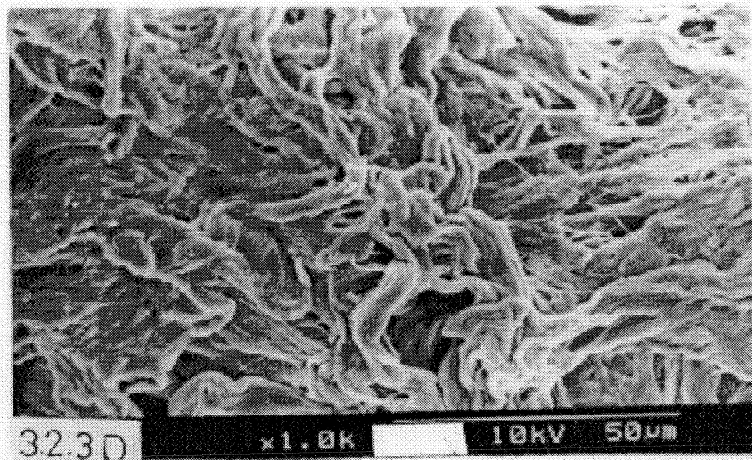


Figure 3.2.3. Scanning electron micrographs of crosslinked bovine pericardium, surface morphology of (A) GA treated BP, (B) its 30 days collagenase digested, (C) PEG grafted BP via GA.



(D) Its collagenase digested; (E) PEG grafted BP via HMDIC,
(F) Its collagenase digested.

unreacted groups may be left in the material after PEG grafting. Thus, crosslinked tissues, grafted with PEG-(PEG NH₂-GABP, PEG-HMDIC-BP) resulted in materials, which had better resistance to degradation by bacterial collagenase compared with ungrafted tissue (GATBP).

3.2.2 Calcium deposition to PEG modified tissues (via various chemical treatments)

The amount of calcium deposited to PEG-6000 grafted BP surfaces incubated in calcium phosphate solution, with time is depicted in figure 3.2.4. PEG-GABP, PEG- NH₂-GABP and PEG-HMDIC showed significant ($0 < 0.01$) reduction in calcification compared to GATBP and PEG-CHO-BP. The amount of phosphorus deposited on modified PEG grafted surface with time is given in figure 3.2.5.

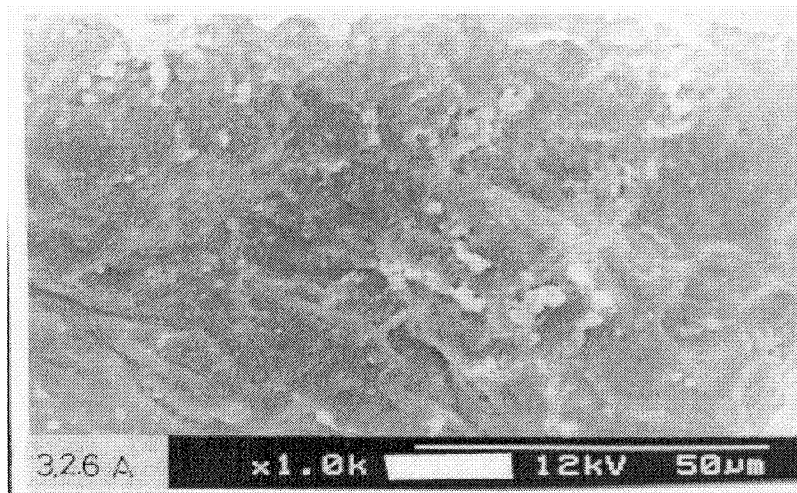
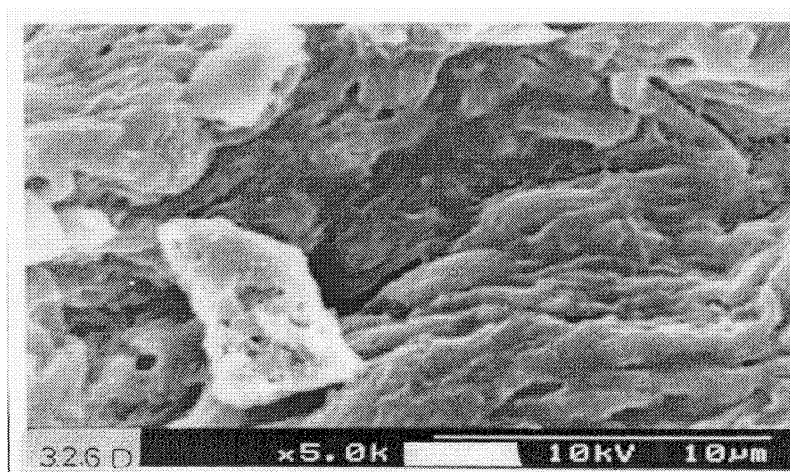
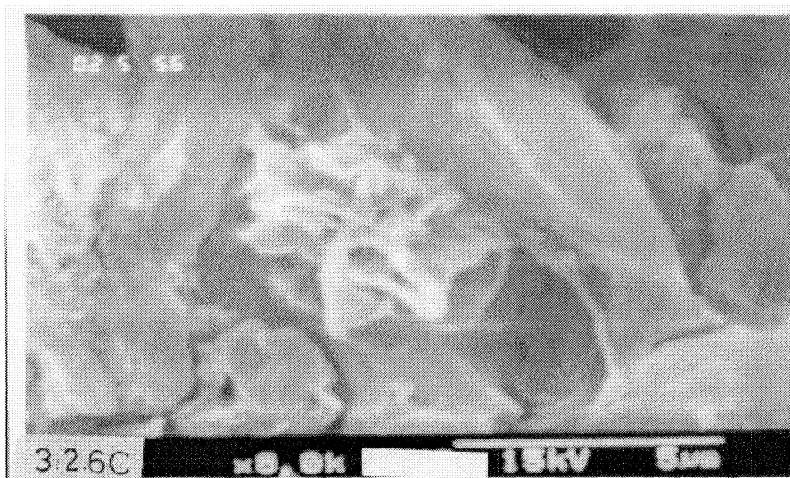
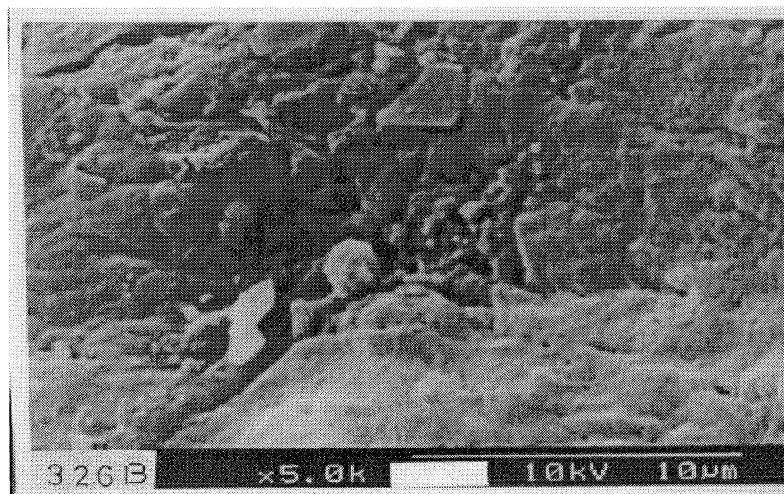


Figure 3.2.6 Scanning electron micrographs of bovine pericardium after 30 days incubation in calcium phosphate solution (A) PEG grafted BP via GA.



- (B) PEG-CHO grafted BP, (C) PEG-NH₂ grafted BP via GA,
(D) PEG grafted BP via HMDIC

Table 3.2 I Percent of grafting and the amount of calcium and phosphorus deposited to PEG-6000 grafted bovine pericardium.

Surfaces	Percent of grafting	Amount of Calcium Deposited in $\mu\text{g}/\text{mg}$ Tissue for (20 days)	Amount of phosphorus Deposited in $\mu\text{g}/\text{mg}$ Tissue (20 days)
GATBP		28.9 ± 0.8	22.4 ± 1.4
PEG grafting			
1% PEG-6000	12.3	$10.1 \pm 1.1^{**}$	$1.4 \pm 0.2^{**}$
3% PEG-6000	14.1	$9.8 \pm 0.2^{**}$	$1.3 \pm 0.1^{**}$
5% PEG-6000	15.8	$9.6 \pm 0.5^{**}$	$1.3 \pm 0.1^{**}$
10% PEG-6000	21.4	$9.5 \pm 0.2^{**}$	$1.3 \pm 0.1^{**}$

0.6% Glutaraldehyde treated (24h) bovine pericardium were incubated with various concentrations of PEG-6000, for 5 hours

** $P < 0.001$ where all PEG-grafted surfaces were compared with GATBP.

Table 3.2.II Data on PEG-modified bovine pericardium.

Surfaces	% of PEG grafting	Contact angle ± SD	Amount of Ca Deposited in µg/mg of Tissue 15 day	% of PEG leaching
GATBP		136.1 ± 11.8	22.4 ± 1.6	
PEG-GABP	15.1 ± 7.9	151.0 ± 4.5	11.6 ± 4.1*	2.8 ± 0.4
PEG.CHO-BP	19.4 ± 8.0	151.3 ± 2.6	17.0 ± 1.1**	4.4 ± 0.8
PEG.NH ₂ -GABP	16.1 ± 7.2	150.2 ± 2.8	9.1 ± 1.1*	3.6 ± 2.5
PEG-HMDIC.BP	18.5 ± 2.8	152.8 ± 3.1	10.5 ± 1.0*	3.2 ± 1.5

* P < 0.001 ** P < 0.01 All PEG-6000 modified surfaces were compared with GATBP.

Scanning electron microscopy of PEG-6000 grafted pericardial surfaces after calcification are depicted in figure 3.2.6. The calcium phosphate crystals were evident on most of the surfaces. Big clusters of calcium phosphate crystals of hydroxyapatite had been observed on GATBP (figure 3.2.6A) while the crystals were rare on PEG-6000 grafted surface. Further, the PEG GABP and PEG-HMDIC BP had significantly reduced the calcium nodulation (figure 3.2.6 B and C).

Percentage grafting of PEG and amount of calcium and phosphorous deposited to BP after 20 days in vitro calcification are shown in Table 3.2.I. The amount of calcium and phosphorous were slightly reduced with per cent of PEG grafting. The grafting per cent had also increased as a function of PEG concentration. Hence an optimum concentration of 5% PEG was selected for our future studies.

Table-3.2.II gives the per cent of PEG grafting, octane contact angle, amount of calcium deposited and percent of PEG leaching. Per cent of PEG grafting was similar to all pericardial samples, even though various techniques were used for grafting. A lowest contact angle was observed for GATBP, and had increased due to PEG grafting. The amount of calcium deposited for 15 days of exposure to metastable calcium phosphate solution had demonstrated a reduction in calcification with PEG-GABP and PEG-HMDIC-BP. However, the calcium deposition to GATBP and PEG-CHO-BP were similar. Per cent leaching of PEG was higher of PEG. CHO BP compared to PEG-GABP and PEG-HMDIC-BP. Hence, it appeared that the PEG-G BP and PEG-HMDIC-BP had more stable PEG on the tissue and their calcification profile was also reduced.

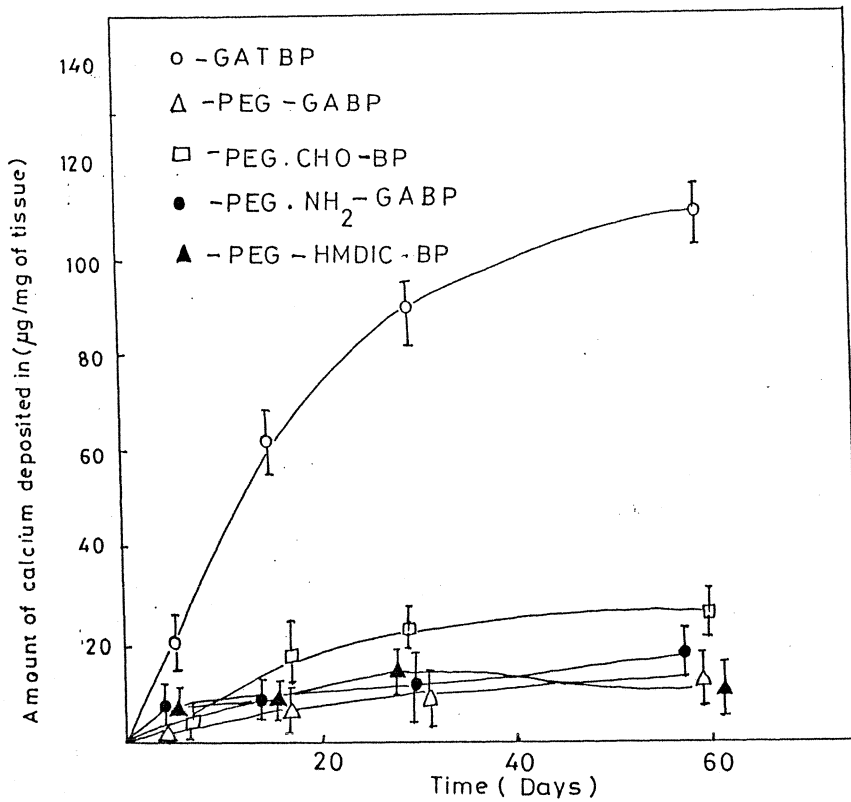


Figure 3.24 Amount of calcium deposited on PEG grafted bovine pericardium as a function of time on exposure to calcium phosphate solution. Bar indicates 95% confidence limits.

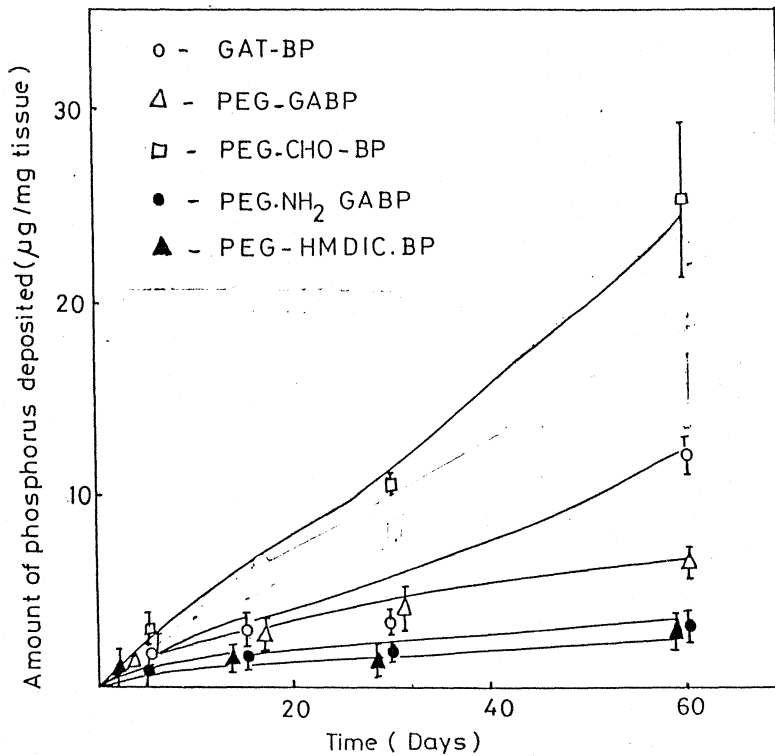


Figure 3.25 Amount of phosphorus deposited on PEG grafted bovine pericardium, as a function of time on exposure to calcium phosphate solution. Bar indicates 95% confidence limits.

The deposition of calcium was least with PEG-GABP and PEG-HMDIC BP as suggested in figures 3.2.4, 3.2.5, 3.2.6 and Table 3.2.II. The reports suggest that the porosity provides a large surface area and volume, which facilitate increased permeation of Ca ions yielding greater calcification.⁶⁴ PEG- modified pericardium appeared to be smooth in its SEM, with less porosity (figure 3.2.3) . Thus, it is conceivable that the PEG grafted tissues could also stabilize the porous structure of collagen and subsequently reduce the calcium mobilization.

Octane contact angle measurements were higher in the case of PEG grafted tissues. The octane contact angle technique is widely used to study the nature of the surface by various investigators, and has been correlated with blood compatibility.⁷ This can provide information related to the hydrophilic or hydrophobic nature of the surface where a higher angle shows the increase in hydrophilic character. Hence, PEG modified pericardium had become hydrophilic and the calcium deposition was also substantially reduced (Table-3.2.II). Hence, it is conceivable that surface modification of bovine pericardium with polyethylene glycol can provide biomaterials with improved stability and resistance to calcification.

From these initial studies, it appears that PEG -6000 grafted BP through glutaraldehyde linkages or hexamethylene diisocyanate pathways had indicated their bacterial collagenase stability and resistance to calcification in in vitro. Hence, further studies were performed via grafting different molecular weight PEGs to BP through glutaraldehyde linkages.

3.2.3 Enzymatic degradation of PEG grafted BP versus PEG molecular weight

Polyethylene glycols having molecular weight range from 600 to 20,000 were grafted on pericardium via glutaraldehyde linkages. These PEG modified pericardia were evaluated for their enzymatic stability and calcification, in an in vitro model system.

The degradation of PEG modified bovine pericardial tissues in the presence of trypsin was studied in vitro in Tris HCl pH 7.4, figure 3.2.7 gives the variation in tensile strength of GA fixed and PEG modified (PEG B 600, 1500, 4000, 6000 and 20000) tissues with time in trypsin. Among the treated surfaces PEG-20,000 grafted BP had shown highest tensile strength. The original tensile strength of GA treated and low molecular weight PEG grafted BP reduced substantially with time. But, the high molecular weight PEG grafted tissue retained most of their original tensile strength even after 70 days of trypsin digestion figure 3.2.7. Figure 3.2.8 shows the reduction in tensile strength of PEG-20000 grafted BP after enzymatic digestion in bromelain, collagenase, chymotrypsin, esterase and trypsin. PEG 20000 modified pericardium have demonstrated the resistance towards enzyme digestion.

The mechanical properties clearly showed a substantial reduction in tensile strength with all tissue samples, after 70 days of trypsin digestion (figure 3.2.7). However, PEG-20,000 grafted pericardium was more susceptible to enzyme digestion and subsequent biodegradation. Thus, it seems that the surface modification of pericardia via GA-PEG grafting may provide new ways of controlling biodegradation.

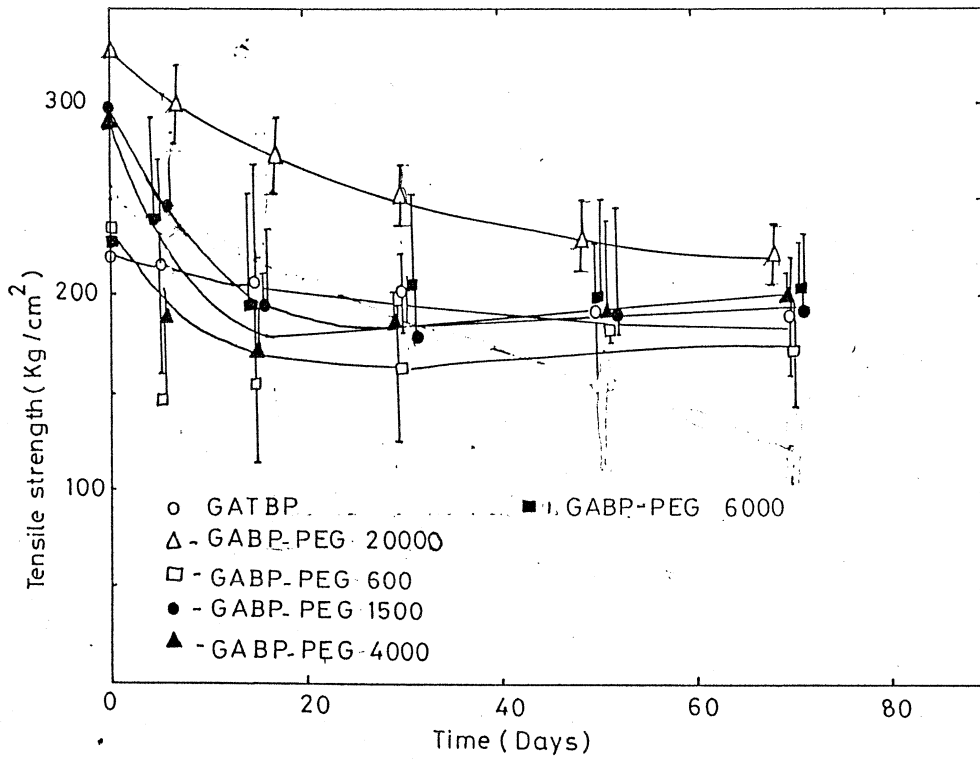


Figure 3.2.7 Effect of Trypsin digestion on the tensile strength of PEG grafted Bovine Pericardium, as a function of time. Bar indicates 95% Confidence limits.

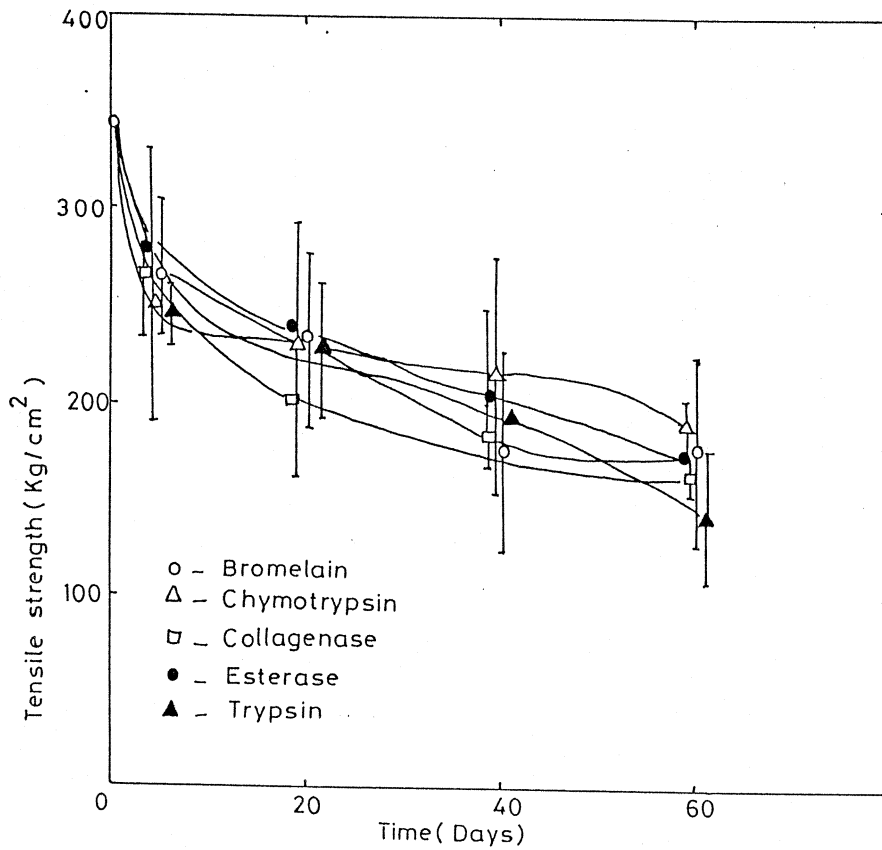


Figure 3.2.8. Effect of various enzymes on the tensile strength of PEG 20000 grafted BP as a function of time. Bar indicates 95% confidence limits

Table 3.2.III Percentage of grafting, mechanical properties, water of hydration of GA fixed and various PEG grafted pericardial tissues.

Surfaces	Percent of grafting	Mechanical properties	Percent water of hydration
GATBP		264.1 ± 29.6	69.0 ± 3.8
PEG-600 grafted BP	19.4 ± 4.3	235.9 ± 39.9	71.3 ± 4.4
PEG-1,500 grafted BP	22.8 ± 6.3	299.1 ± 47.6	70.9 ± 2.3
PEG-4,000 grafted BP	26.7 ± 8.3	295.1 ± 56.0	73.7 ± 6.5
PEG-6,000 grafted BP	15.0 ± 7.9	228.6 ± 29.2	73.5 ± 3.7
PEG-20,000 grafted BP	30.0 ± 7.4	342.3 ± 28.8	79.4 ± 0.2

Values expressed as mean ± SD (from atleast 5 experiments).

The percentage retention in tensile strengths of PEG-20,000 grafted surface was higher compared to GA treated tissue. The other PEG grafted tissues did not show much variation in their retention of tensile strength with trypsin digestion.

Table 3.2.III gives the percentage of grafting, mechanical properties (tensile strength) and water of hydration of GA fixed and various PEG grafted pericardial tissues. Per cent of PEG grafting was similar to all pericardial samples, even though various molecular weight PEGs were used for grafting. However, the water of hydration increased with increase in PEG molecular weights where compared with GA treated cases. A lowest water of hydration was observed for GA treated surface and had increased due to PEG-20000 grafting. The initial tensile strength of BP tissues improved with GA treatment and subsequently increased further with grafting of polyethylene glycols, as evident from Table 3.2.III. In other words, the PEG grafting of BP significantly improved the stability of the pericardial tissues by retarding trypsin digestion.

Scanning electron micrographs (figure 3.2.9) demonstrate the surface morphology of bare and various PEG grafted bovine pericardium. The surface of GA treated BP appeared to be porous in nature, while the PEG crosslinked surfaces had become smooth and compact in nature. The surface pores of the tissue were filled with polyethylene glycols, on grafting as is evident from the figure 3.2.9.

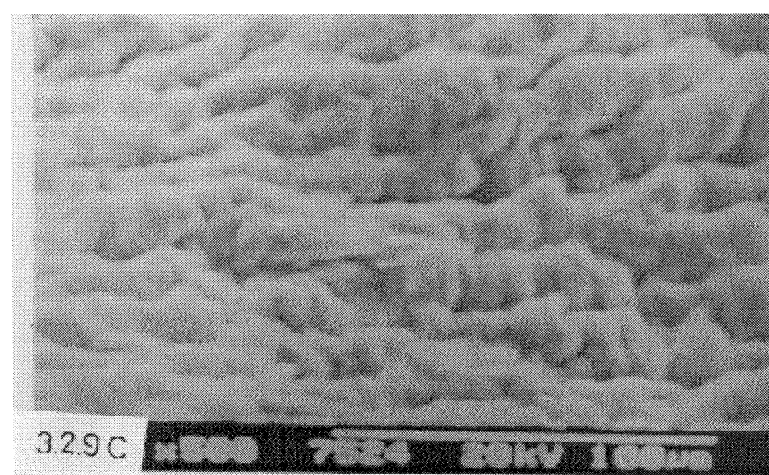
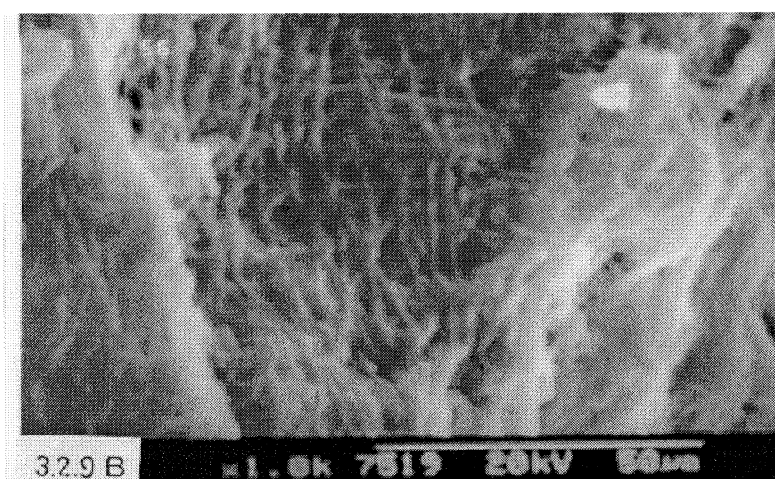
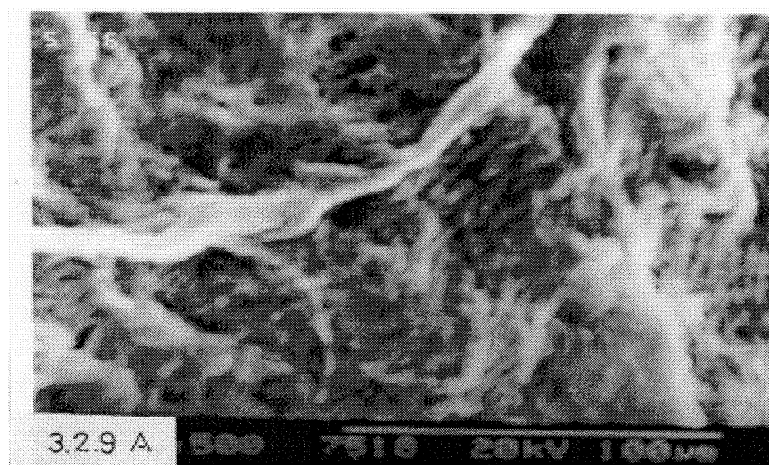
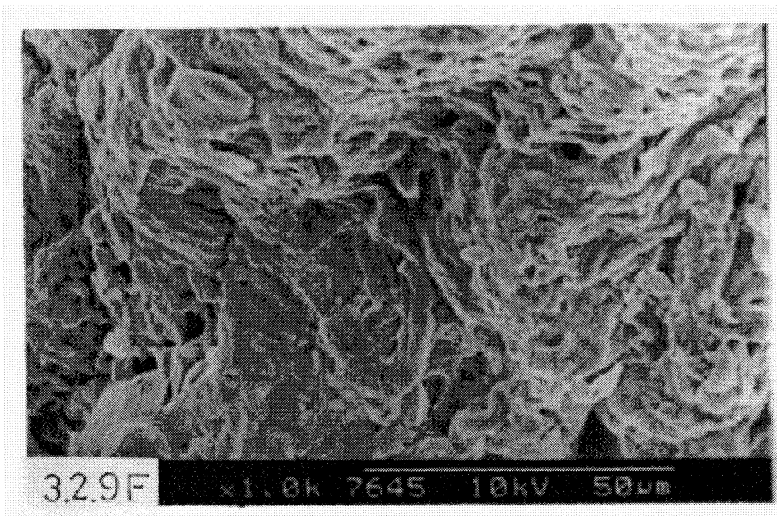
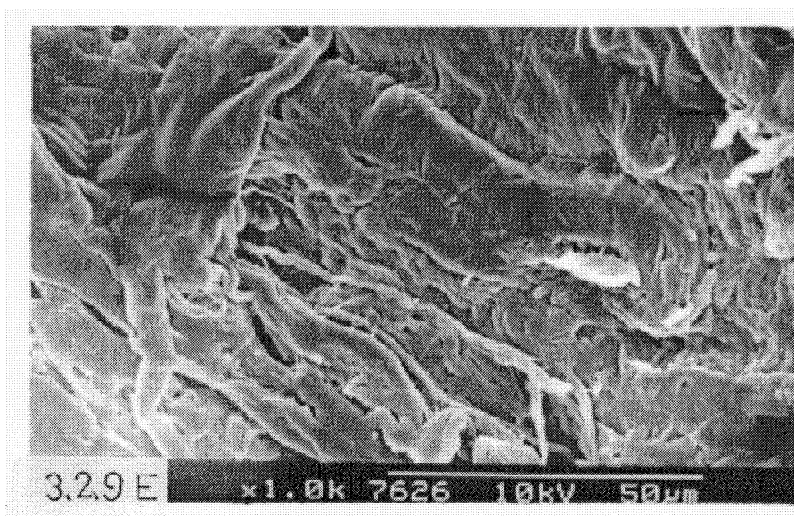
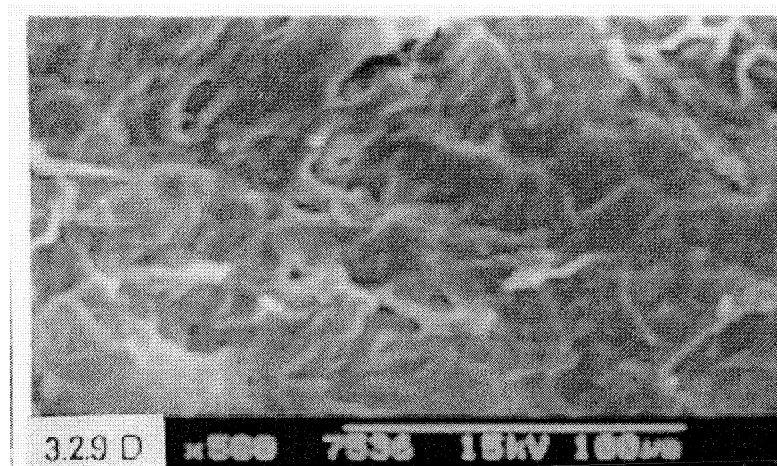


Figure 3.2.9 Scanning electron micrographs of various PEG grafted bovine pericardium (A) PEG-600 grafted BP, (B) PEG-1500 grafted BP and (C) PEG-4000 grafted BP.



(D) PEG-6000 grafted BP, (E) PEG 20,000 grafted BP and (F) its 30 days collagenase digested BP.

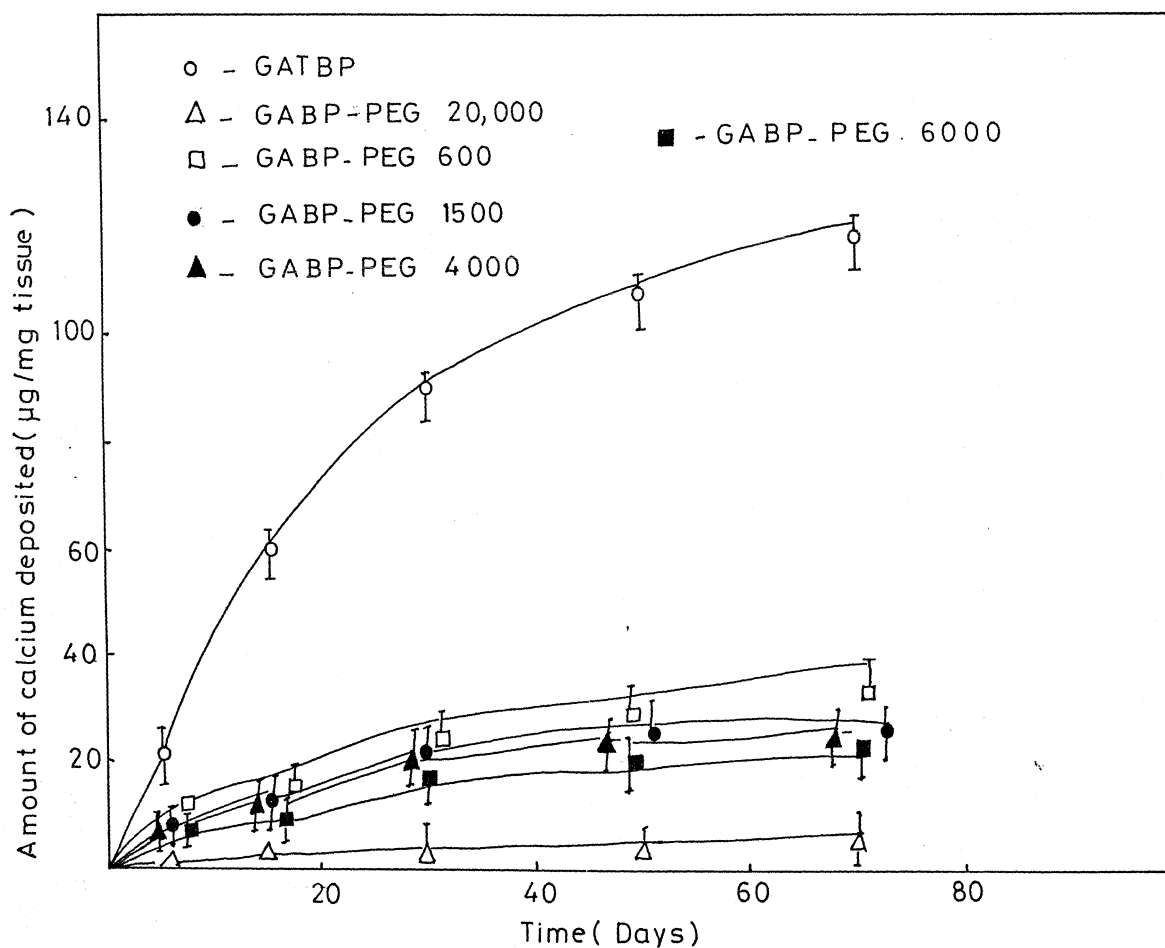


Figure 3.2.10 Amount of calcium deposited on PEG grafted Bovine pericardium as a function of time on exposure to calcium phosphate solution. Bar indicates 95% confidence limits.

3.2.4 Effect of molecular weights of PEG on tissue calcification and cell adhesion:

The amount of calcium deposited to various PEG grafted BP, incubated in calcium phosphate solution, with time is depicted in Figure 3.2.10. In general, the calcium concentration in the GA treated and low molecular weight PEG grafted tissues were much higher than PEG 20,000 grafted BP.

Scanning electron micrographs of various PEG grafted pericardial surfaces after calcification are depicted in figure 3.2.11. The calcium phosphate crystals were evident on most of the surfaces as plaque like deposits. Big clusters of calcium phosphate crystals of hydroxyapatite had been observed on GATBP figure 3.2.11; while the crystals were reduced on PEG grafted surfaces. Further, the reduction in calcification was higher with higher molecular weight PEGs. It is also evident that the PEG-20,000 grafted tissues had substantially inhibited the calcium deposition Figure 3.2.11.

Figure 3.2.12 shows the scanning electron micrographs of the platelets on the bare, and PEG crosslinked bovine pericardium. It appears that platelet adhesion decreased on PEG grafted surfaces compared to bare samples. Platelets on GA treated surfaces extended long pseudopods leading to their complete spreading. While most of the platelets on PEG grafted surfaces retained their discoid shapes. Platelets spreading was maximum on GA treated surfaces. In some case few aggregates were observed.

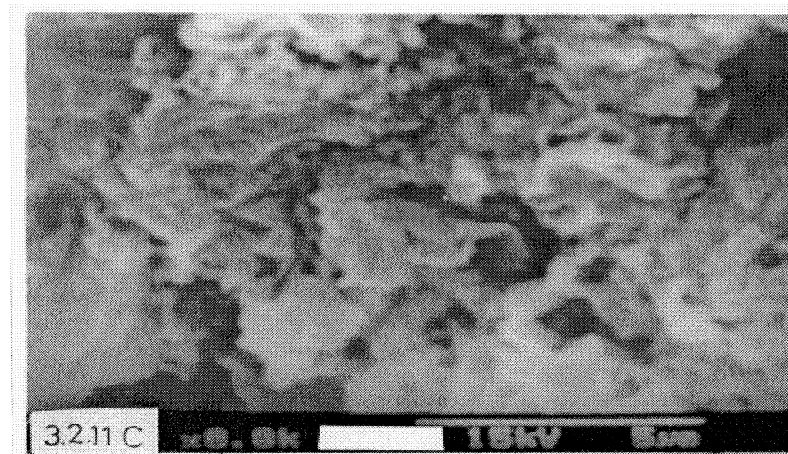
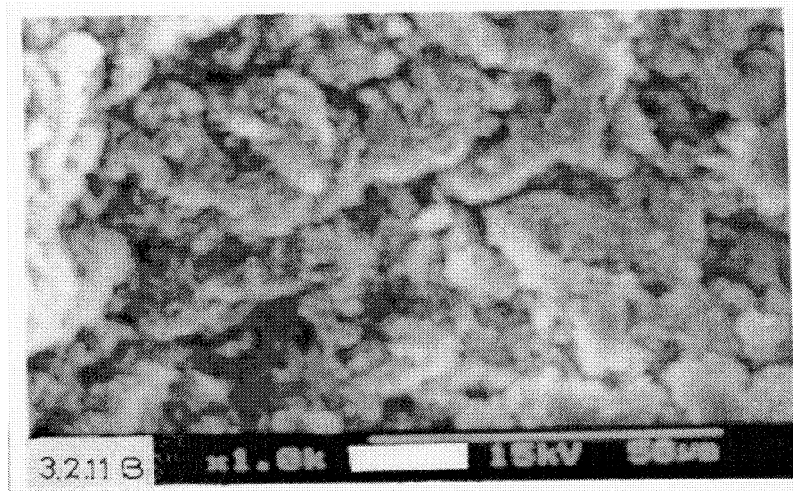
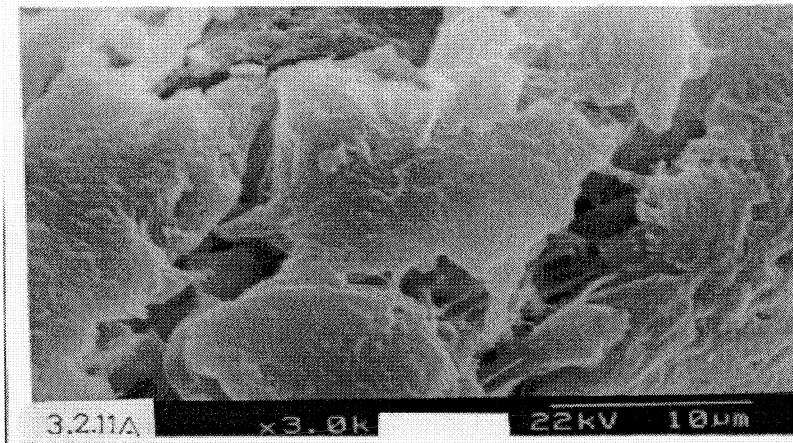
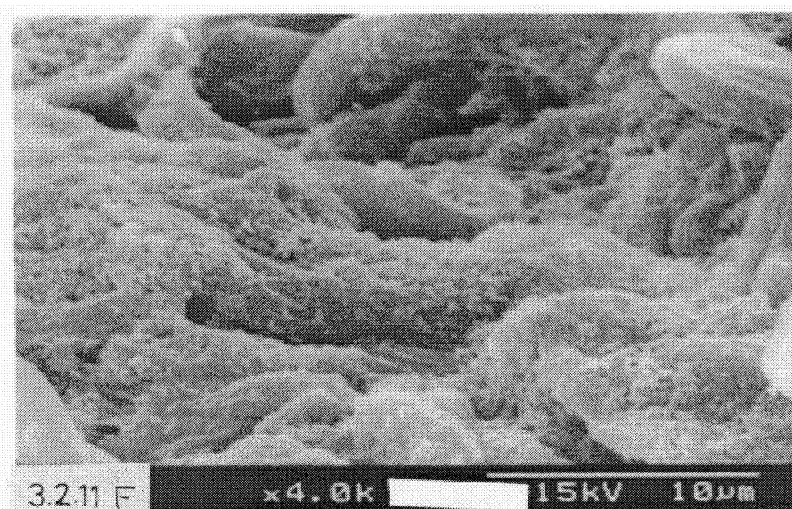
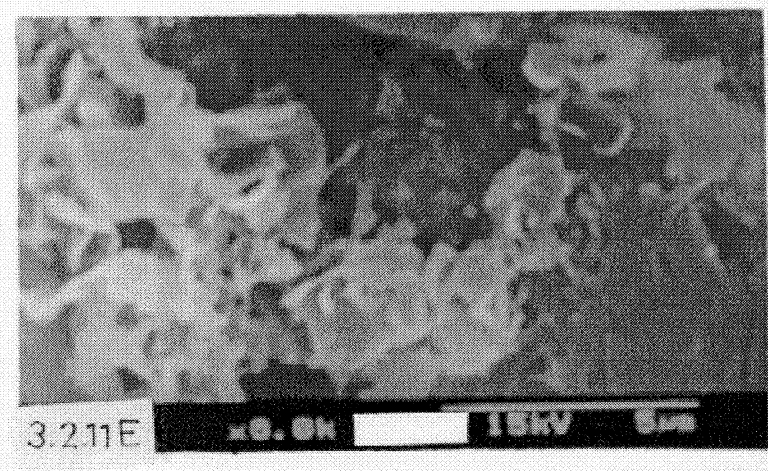
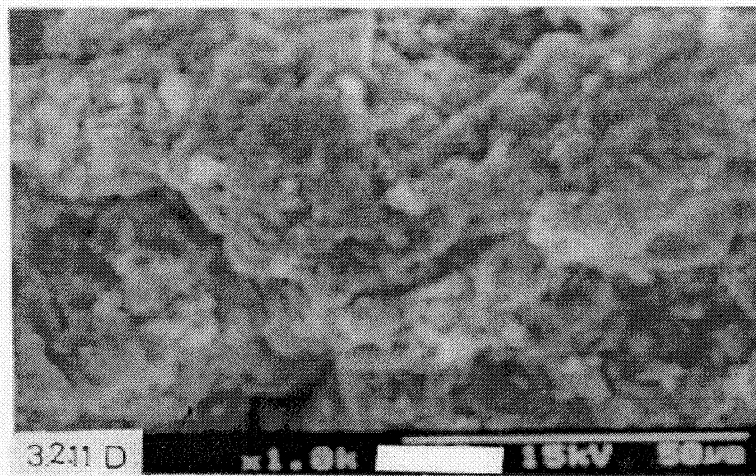


Figure 3.2.11 Scanning electron micrographs of various PEG grafted pericardium after 30 days in vitro calcification. (A) GATBP, (B) PEG 600 grafted BP, (C) PEG 1500 grafted BP.



(D) PEG-4000 grafted BP, (E) PEG-6000 grafted BP, (F) PEG-20,000 grafted BP.

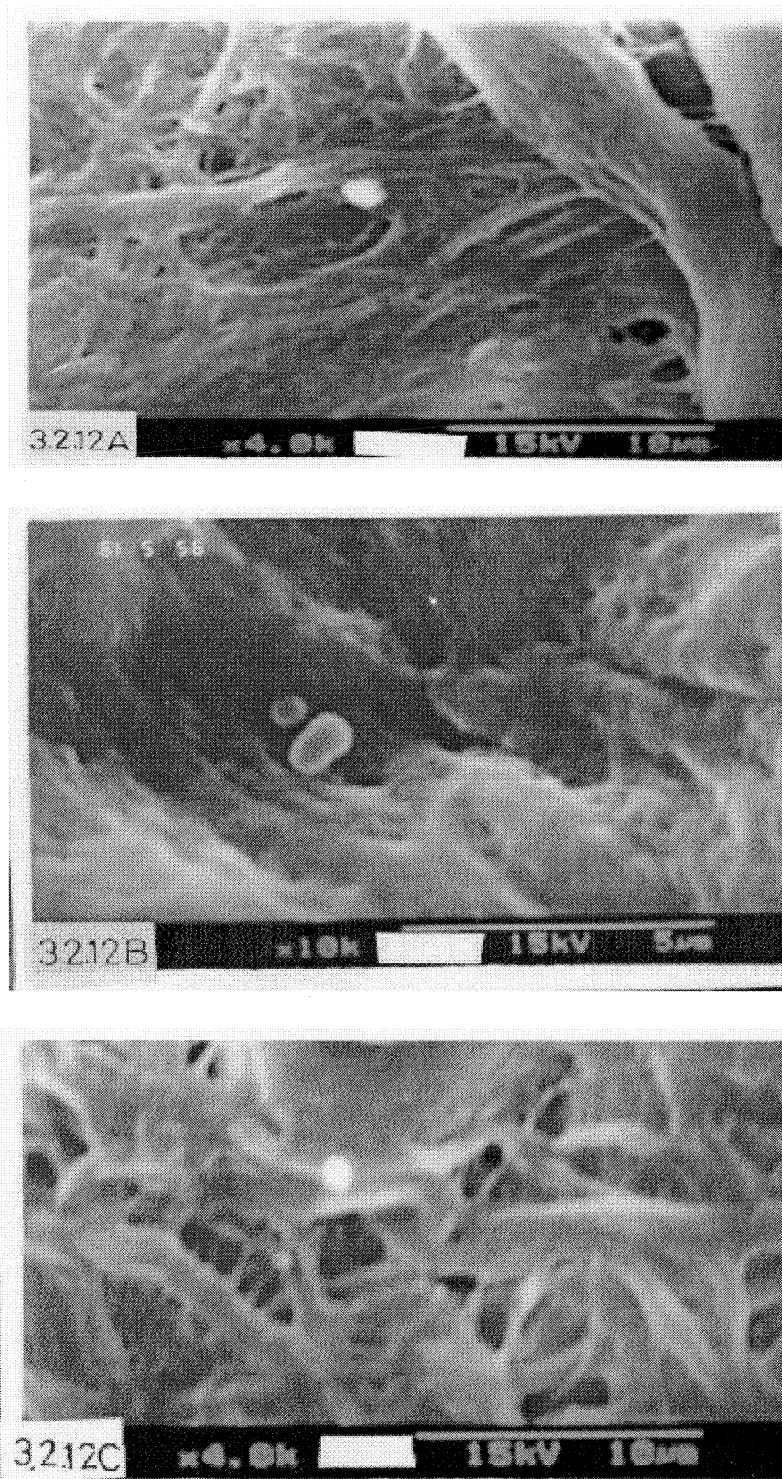
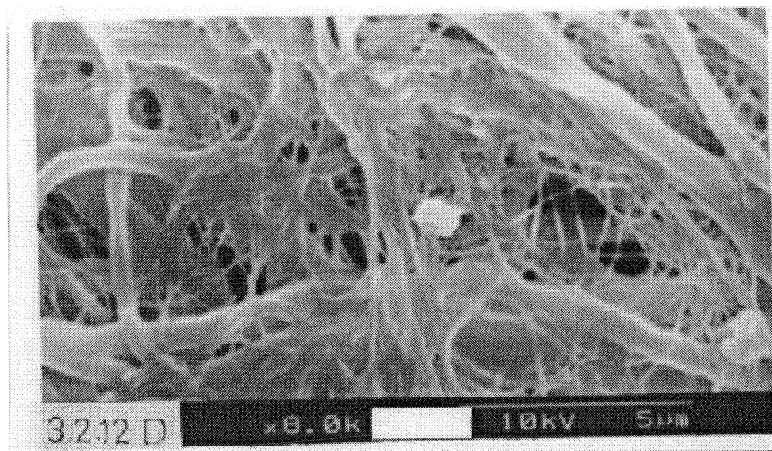


Figure 3.2.12 Scanning electron micrographs of platelet adhered PEG grafted surfaces. (A) PEG-1500 grafted BP, (B) PEG-4000 grafted BP, (C) PEG-6000 grafted BP.



(D) PEG-20,000 grafted BP

Table 3.2.IV gives the contact angle, platelet adhesion and calcium deposition (after 50 days of calcification) to various PEG modified pericardium. Octane contact angles to these tissues indicated an increase with PEG graftings in the order represented below. GA fixed <PEG-600<PEG-4000<PEG-1500<PEG-6000<PEG-20,000. In other words, the GA treated BP showed the lowest octane contact angle, and the PEG-20,000 grafted BP demonstrated the highest octane contact angle. A reverse pattern was observed with the number of platelets seen on the surface. Platelet attachment reduced with the PEG grafting on BP. It is also evident from Table 3.2.IV that the amount of calcium deposited on PEG grafted surfaces had apparently reduced compared with GATBP.

The deposition of calcium was least with PEG grafted surfaces compared to GA fixed surfaces (Figure 3.2.11 and Table 3.2.IV). The reports suggest that the porosity provides a large surface area and volume, which facilitate increased

Table 3.2. IV Contact angle Platelet adhesion, and amount of calcium deposited to various PEG grafted bovine pericardium.

Surfaces ^a	Octane contact angle	Mean platelets per mm ² ± SD	Amount of Ca deposited for 50 days in µg/mg of tissue
GATBP	136.1 ± 1.8	62.6 ± 7.9	106.2 ± 1.8
PEG 600-BP	143.0 ± 2.4*	47.0 ± 8.0*	15.2 ± 4.8**
PEG 1,500-BP	145.1 ± 3.1*	52.6 ± 8.2*	13.1 ± 0.4**
PEG 4000-BP	144.4 ± 2.1*	32.9 ± 7.3**	15.2 ± 5.5**
PEG 6,000-BP	151.0 ± 4.5*	27.7 ± 6.9**	12.1 ± 1.7**
PEG 20,000-BP	155.2 ± 3.4*	18.3 ± 4.6**	9.7 ± 1.0**

- a 5% PEG were exposed to glutaraldehyde activated pericardium.
- b Octane contact angle expressed as mean ± SD (from at least ten observation).
- c Values denoted as the average of the number of platelets attached to the surface per mm² with ± SD (at least 20 observations from triplicate experiments).
- d Values expressed as mean ± SD from at least four experiments.

** P < 0.001, *P < 0.05, where the values of all PEG modified substrates are compared with the GATBP.

permeation of Ca/PO_4 ions yielding greater calcification. Further, more calcium deposits were also observed on thick and porous materials in *in vitro* and *in vivo*.^{26,64,68} Surface morphology of GA treated pericardium appeared to be porous in nature. However, the PEG modified pericardium appeared to be smooth in its SEM with less porosity (figure 3.2.9). It has been reported that PEGs conjugated on to collagen sponges stabilize the porous structure without deactivating biological properties of collagen.⁴⁷ PEGs conjugated with proteins exhibit a decrease in biodegradation and immunogenicity. Further, more PEGs are nontoxic.⁴⁷ Thus it is conceivable that the PEG grafted tissue could also stabilize the porous structure of collagen and subsequently reduce the calcium mobilization.

Doillon et al⁴⁷ have conjugated different concentrations and molecular weights of activated PEGs to collagen sponges. The PEG conjugated onto collagen stabilize the porous structure without deactivating the biological properties of collagen. Hossain and Hubbell⁸⁹ have proposed that calcification of PEG were molecular weight dependent and PEG crosslinking. These observations further strengthen our present observation on PEG modified pericardium towards their biostability and resistance to calcium deposition.

The platelet attachment studies on various PEGs modified pericardium have shown that the cell adhesion was substantially reduced with PEG grafting (Table 3.2.IV). SEM also revealed that platelet adhesion (figure 3.2.12) was less with PEG grafting and the cellular morphology was retained. However, platelets attached

on GATBP had extended their pseudopods (figure 3.2.12). It seems that human platelets possess membrane receptors for a wide variety of materials. These include (a) agents involved in physiologic platelet activators such as ADP, thrombin, collagen and fibrinogen, (b) hormones such as epinephrine, and (c) pathologic agents like endotoxin.^{11,132} Thus it is conceivable that the binding of PEG to pericardium modifies or masks the platelet receptor sites for collagen and causes reduction of platelet densities on the surface.

Table 3.2.IV also provide information related to octane contact angle to various PEG modified tissues. The octane contact angles of PEG-modified surfaces were higher than GA treated tissue. The octane contact angle technique has been widely used by various investigators to study the nature of surfaces, and it has been correlated as one of the factors for blood compatibility.⁷ This can provide informations related the hydrophilic or hydrophobic nature of the surface where a higher angle shows an increase in hydrophilic character. Hence, PEG modified pericardium had became hydrophilic, variably and platelet adhesion also was substantially reduced Table 3.2.IV.. These observations can be supported further with the reports that polyethylene glycol, a hydrophilic polymer, has been widely used for improving blood compatibility and has shown reduced platelet adhesion⁷⁴. Thus it appears that the grafting of PEG to pericardia had dramatically inhibits cell adhesion and spreading. In summary , we find that the PEG-20000 grafted BP substantially inhibited the platelet adhesion, their spreading and had reduced the calcium

deposition. The stability of the PEG modified tissue might be linked to the repulsive properties of PEGs after which their covalent binding to the amino groups of the protein.

Hence, it appears that high molecular weight, PEG modified pericardium is highly blood compatible and a calcium antagonist compared to other chemically treated tissues and is a suitable tissue biomaterial for biomedical applications.

CHAPTER 3.3

EFFECT OF DOUBLE CROSSLINKING TECHNIQUE ON THE ENZYMATIC DIGESTION AND CALCIFICATION OF BOVINE PERICARDIUM

The strength, resorption rate, and biocompatibility of collagenous biomaterials are profoundly influenced by the method and extent of crosslinking. Previous investigations have shown that bifunctional reagents such as carbodiimide, diisocyanates, glutaraldehyde etc. have been applied for the stabilization of collagen based materials.^{37,99,147,196} As discussed earlier the glutaraldehyde treatment of pericardial tissues enhances the biostability, but easily undergoes calcification. However carbodiimide crosslinking of tissues, reduces the calcification profile, but are relatively less stable. Thus, it appears that different crosslinking agents have varied function on the tissue design and subsequent performances. In this chapter we discuss the effect of multiple crosslinking techniques in parallel with PEG grafting for improving the tissue stability and calcification. The modified tissues were evaluated using collagenase digestion and in vitro and in vivo calcification profile.

3.3.1 Effect of collagenase on double crosslinked BP

The degradation of GATBP, GA.PEG.EDC.PEG-BP, EDC.PEG.GA.PEG-BP, GA.PEG.HMDIC.PEG-BP, and HMDIC.PEG.EDC.PEG-BP, in the presence of collagenase were studied in vitro in Tris HCl buffer pH 7.4 as represented in figures 3.3.1 and 3.3.2 respectively. Scanning electron micrographs of the double

crosslinked BP after 60 days collagenase digestion had shown substantial degradation of BP and break down of collagen bundles in GATBP (figure 3.3.1A). HMDIC.PEG.EDC.PEG-BP had also indicated break down of collagen bundles in some areas, however, other crosslinked and PEG grafted BP surfaces had retained most of its structural integrity after collagenase digestion.

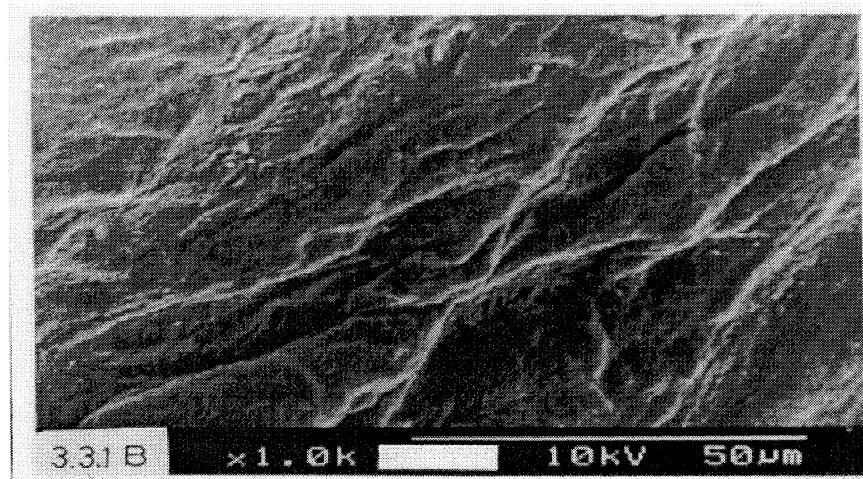
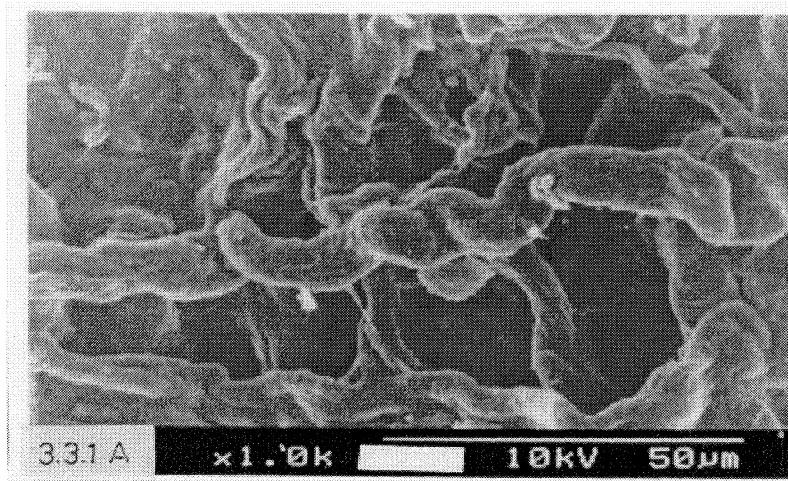
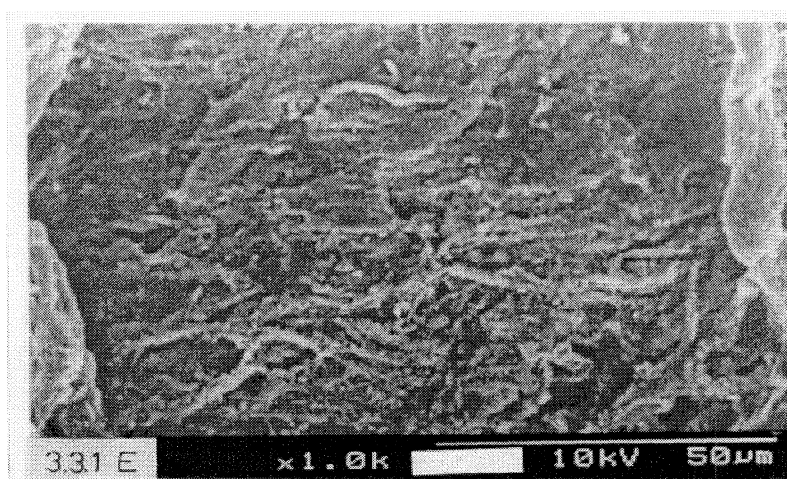
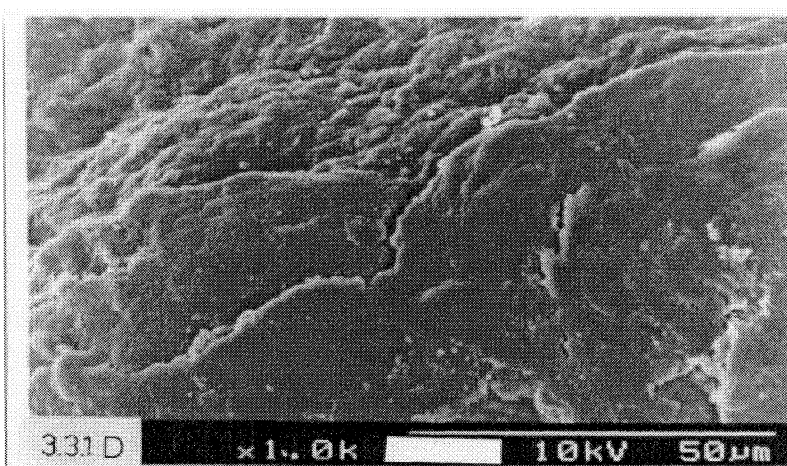
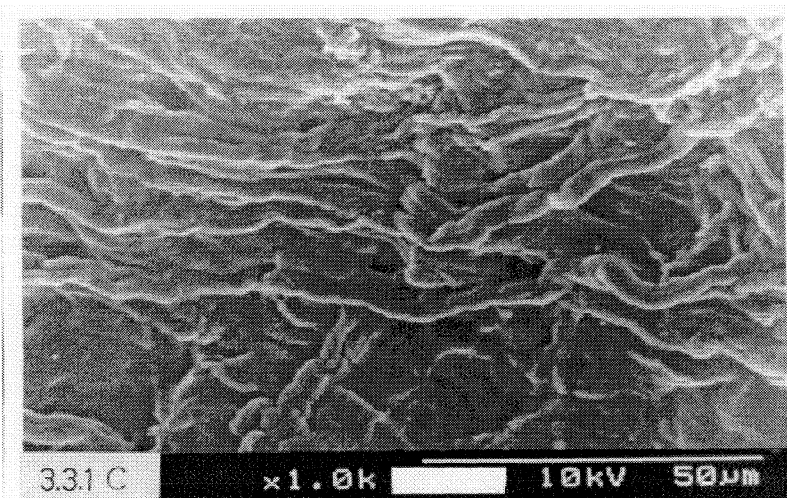


Figure 3.3.1 Scanning electron micrographs of double crosslinked pericardium after 60 days collagenase digestion., (A) GATBP, (B) GA.PEG.EDC.PEG-BP.



- (C) EDC.PEG.GA.PEG-BP, (D) GA.PEG.HMDIC.PEG-BP,
(E) HMDIC.PEG.EDC.PEG-BP.

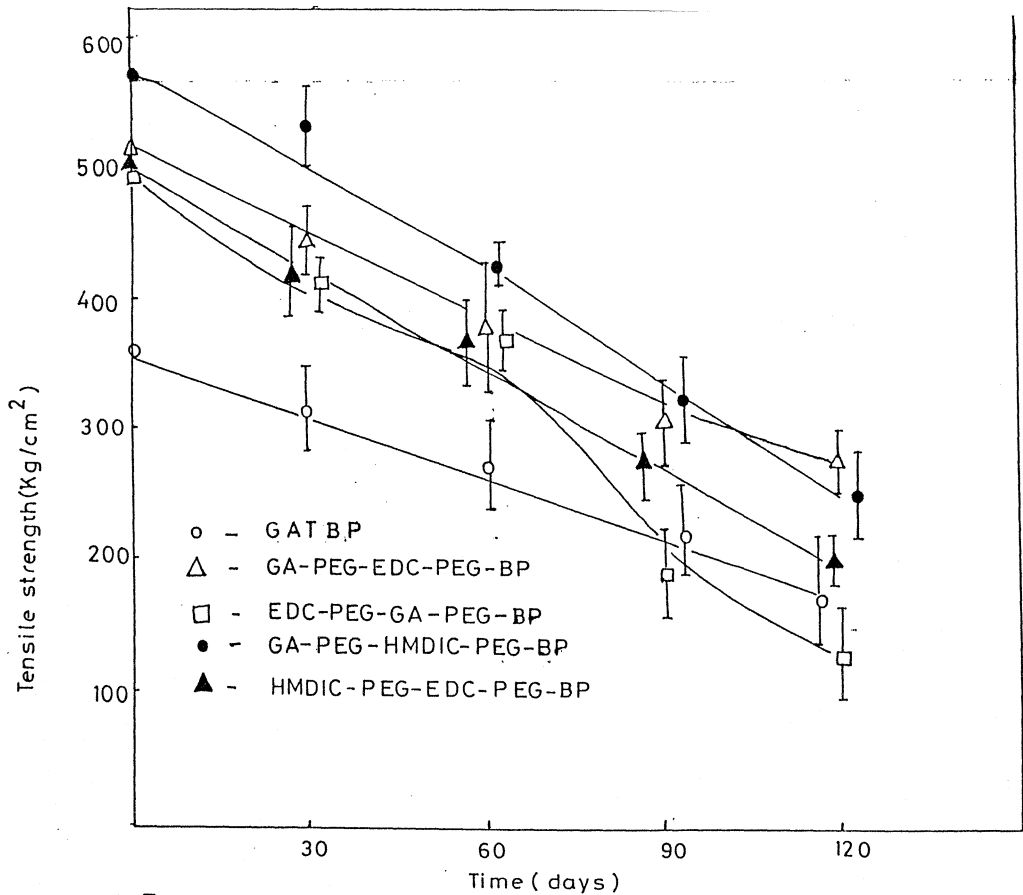


Figure 332 Effect of collagenase on the tensile strength of double crosslinked BP as a function of time. Bar indicates 95% confidence limits.

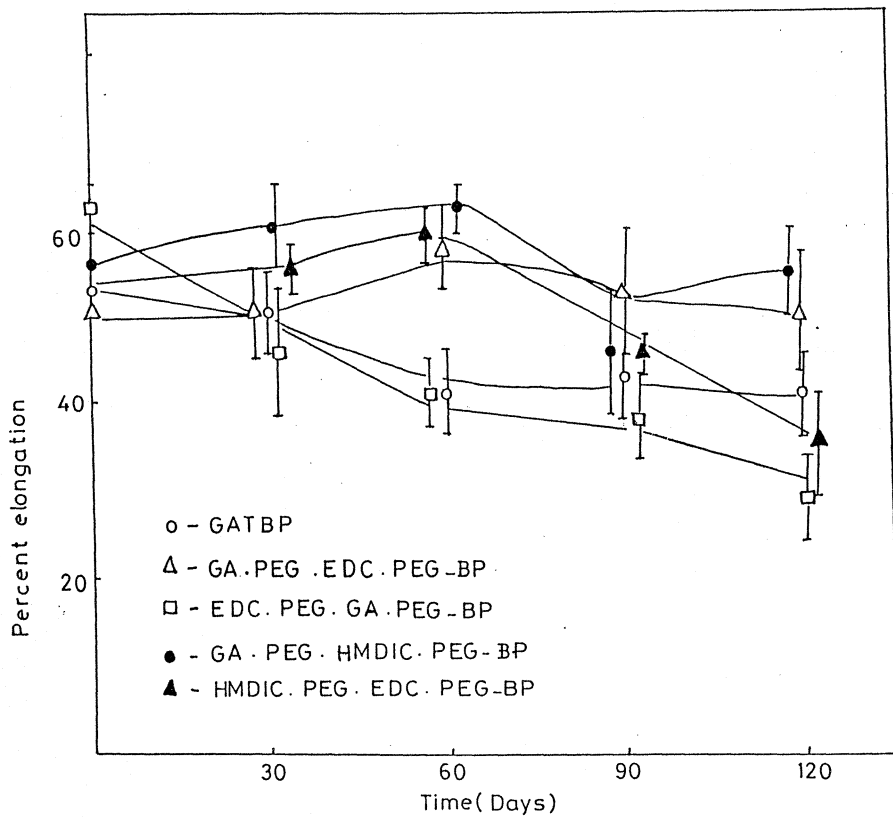


Figure 333 Effect of collagenase digestion on percent elongation of double crosslinked BP as a function of time. Bar indicates 95% confidence limits.

Figure 3.3. 2 shows the reduction in tensile strength of double crosslinked BPs as a function of time due to collagenase digestion. Addition of collagenase to the system variably reduced the tensile strength of all treated tissues. GA.PEG.EDC.PEG and GA.PEG.HMDIC.PEG had shown higher stability towards enzymatic digestion, where as GATBP and HMDIC.PEG.EDC.PEG-BP have had degraded substantially with collagenase.

The per cent elongation of various double crosslinked surfaces under collagenase digestion are shown in figure 3.3.3. Addition of collagenase to these crosslinked tissue system variably reduced the per cent elongation of these tissues . The elongation of EDC.PEG.GA.PEG-BP and GATBP reduced substantially with most of the enzyme systems, as is evident from figure 3.3.3, while GA.PEG.EDC.PEG-BP and GA-PEG. HMDIC.PEG-BP did not exhibit much reduction from their original elongation per cent.

The high enzymatic turnover rate of collagen in the body makes stabilization of collagen-based biomaterials by chemical crosslinking methods necessary to give materials that maintain the desired mechanical properties and stability during the desired implantation period.^{99,147} The extent to which a homobifunctional or homopolyfunctional reagent will cross-link proteins such as collagen is in part geometric, dependent on both protein conformation and the stereology of the cross-linker. Once one side group on the protein (say an ξ -amino group on lysine) has reacted with one reactive group on the reagent, a second reactive group must be

(1) sufficiently close to be reached by another reactive group on the reagent, (2) sterically available, and (3) as yet unreacted with another reagent molecule. Any factor which modulates secondary or tertiary structure in the protein (e.g. temperature, pH, solvent environment, mechanical stress), or any previous modification of reactive groups, can be expected to influence the number of developed cross-links. Thus, multifunctional crosslinkers appears to be more effective in crosslinking protein molecules for stability.

Since the late 1960s and carpentier's²³ identification of glutaraldehyde as a useful fixative agent to prolong the in vivo lifetime of bioprosthetic heart valves, this reagent has become the 'de facto' industrial standard for crosslinking of tissue-derived devices. It appears that glutaraldehyde is a very effective biocide and improves the resistance of collagen to biodegradation. However, GA cannot be considered an ideal reagent for tissue treatment because GA has been identified as potentiating calcification of bioprosthetic materials.^{77,108,128} The desorption or possibly depolymerization of glutaraldehyde may linked to local cytotoxicity and slowed or eliminated repopulation by host cells. These may be modulated by control of strain or stress during crosslinking. But a clear understanding of the relationship between crosslinking and resulting mechanical properties has not yet emerged. Thus, controlled use of GA for optimum crosslinking and reduced calcification may be one of the means for tissue fixing.

This study demonstrated that 0.4% glutaraldehyde fixed pericardium modified with PEG and other crosslinkers like such as EDC or HMDIC indicated smooth surfaces in SEM (figure 3.3.1) without micropores. It seems, the EDC and HMDIC can introduce intra and inter crosslinks between collagen fibrils and the PEG grafting may make the surface smoother. The integrity of the modified surface were maintained even after 60 days collagenase digestion, without any collagen disruption (figure 3.3.1). The second stage treatment of HMDIC or EDC may introduce more crosslinks with free amino acids, phosphates, alcohols or thiols.¹⁹⁶ Thus, the tissue can be fixed completely with bifunctional crosslinkers for better stability.

Bacterial collagenase catalyses hydrolytic cleavage of undenatured collagen in non-polar regions, either in a single α -chain or simultaneously across three chains of the triple helix in lateral fashion.¹⁶⁸ Glutaraldehyde is capable of forming crosslinks either; (i) between adjacent - chains (probably easy) or (ii) between adjacent triple helix molecules or between fibrils. The situation for EDC is quite different. The amino acid triplet (Gly-x-y) typical of collagen, a charged residue (Asp, Glu, Lys, Arg) is matched more often than not by a residue of the opposite charge either in the same triplet or an adjacent¹⁹⁶ triplet. Indeed, within a given α -chain, such charge or "salt" linkages only require that the acid and base group be separated by not more than two other residues. Since charge linkages between adjacent triple helics is fundamental to the stability of the triple helical structure, there are a large number of

appropriate Asp-Lys or Glu-Lys interactions within and between α -chains, which are suitable for crosslink formation by carbodiimide action. Thus, EDC-derived crosslinks may occur within an α -chain, between α -chains or as intermolecular or interfibrillar linkages. This may be the reason for the observed greater resistance towards enzymatic digestion of GA and EDC crosslinking.

According to Weadock et al,¹⁹⁶ more crosslinks formed under EDC than glutaraldehyde treatment and that the extra crosslinks were sufficiently broadly distributed on the collagen to better prevent solubilization of fragments cleaved off by collagenase. Third set of tissue treatment in this study (EDE.PEG.GA.PEG-BP) had shown decrease in the tensile strength and break down of collagen bundles as is evident from figure 3.3.1 and 3.3.2. This may be due to the initial exposure of EDC, which might have masked further sites for GA and PEG interactions; and subsequently have reduced the GA induced crosslinks and the tissue stability.

HMDIC crosslinking involves the formation of aliphatic chains containing urea bonds between two adjacent amine groups in the tissues. The introduction of non-aqueous environments presents a new dimension in the crosslinking of collagenous materials. It is likely to disturb the three-dimensional arrangement of native collagen, and this can lead to crosslinking by virtue of its dehydrating effect, which can alter the side-chain chemistry of collagen.¹⁴⁰ Hence, the bifunctional crosslinkers may be better in crosslinking collagenous materials for better stability.

3.3.2 Calcification on double crosslinked bovine pericardium

Scanning electron micrographs (SEM) of various crosslinked pericardial tissues after 60 days in vitro calcification are depicted in figure 3.3. 4. The bulk deposits of calcium phosphate crystals were evident on GATBP surfaces. However, double crosslinked BP surfaces modified by PEG-20,000 had variably reduced the calcium nodulation and minute foci of calcium phosphate were seen on some cases.

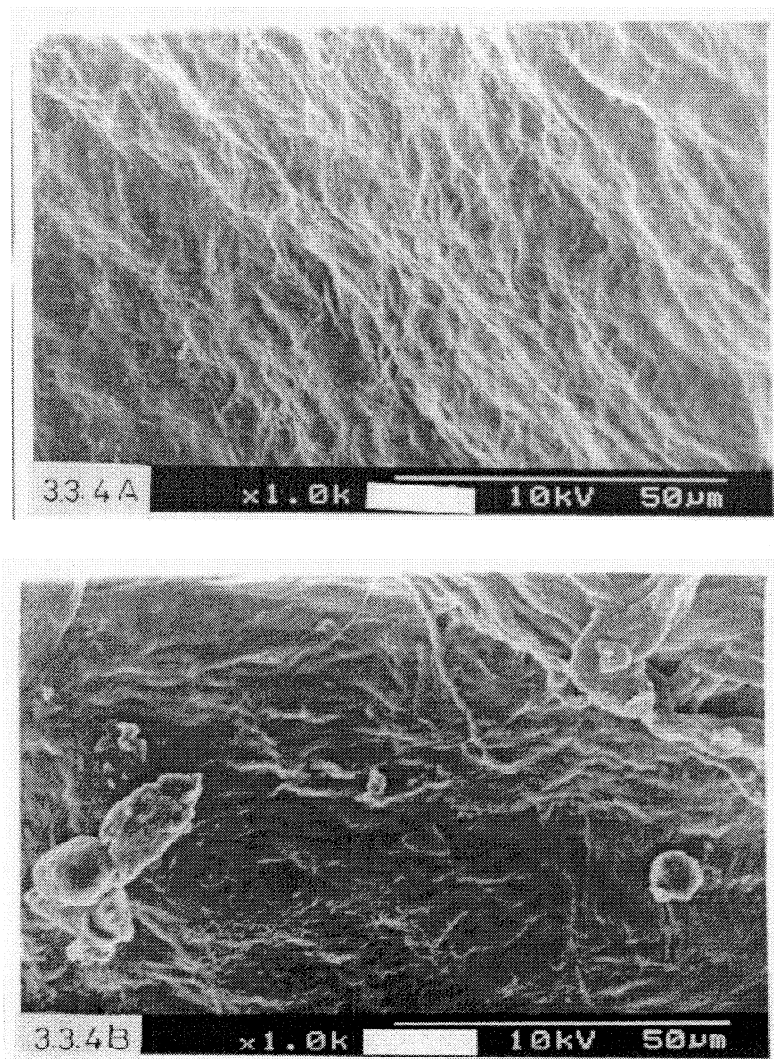
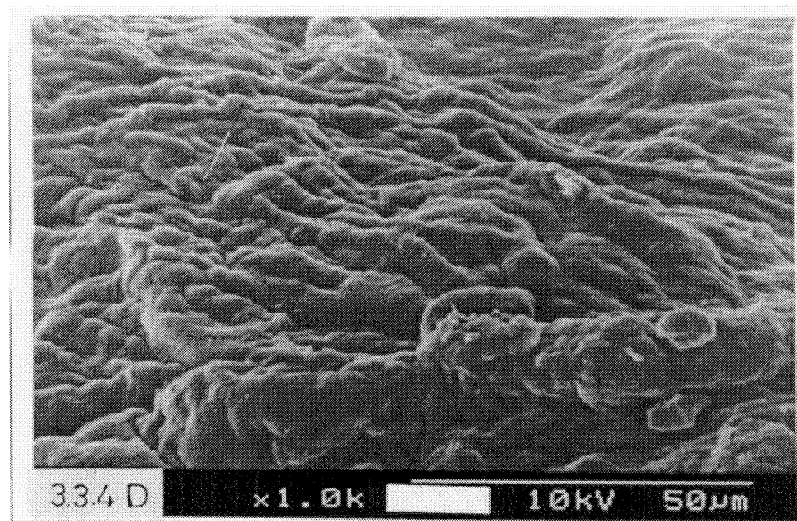
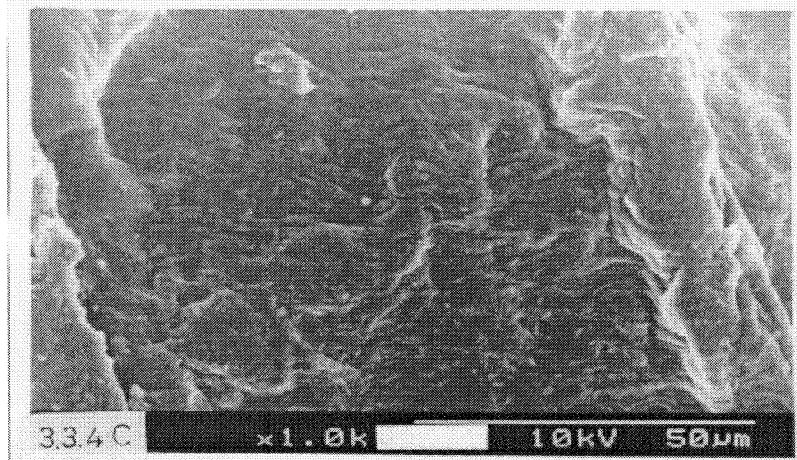


Figure 3.3.4 Scanning electron micrographs of 60 days calcified, double crosslinked pericardium. (A) GA.PEG.EDC.PEC-BP, (B) EDC.PEG.GA.PEG-BP



(C) GA.PEG.HMDIC.PEG-BP, (D) HMDIC.PEG.EDC.PEG-BP.

The amount of calcium deposited to various crosslinked BP specimens incubated in calcium phosphate solution with time is presented in figure 3.3.5. The calcium concentration on the GATBP was significantly higher than PEG modified double crosslinked BP, at all incubation time periods.

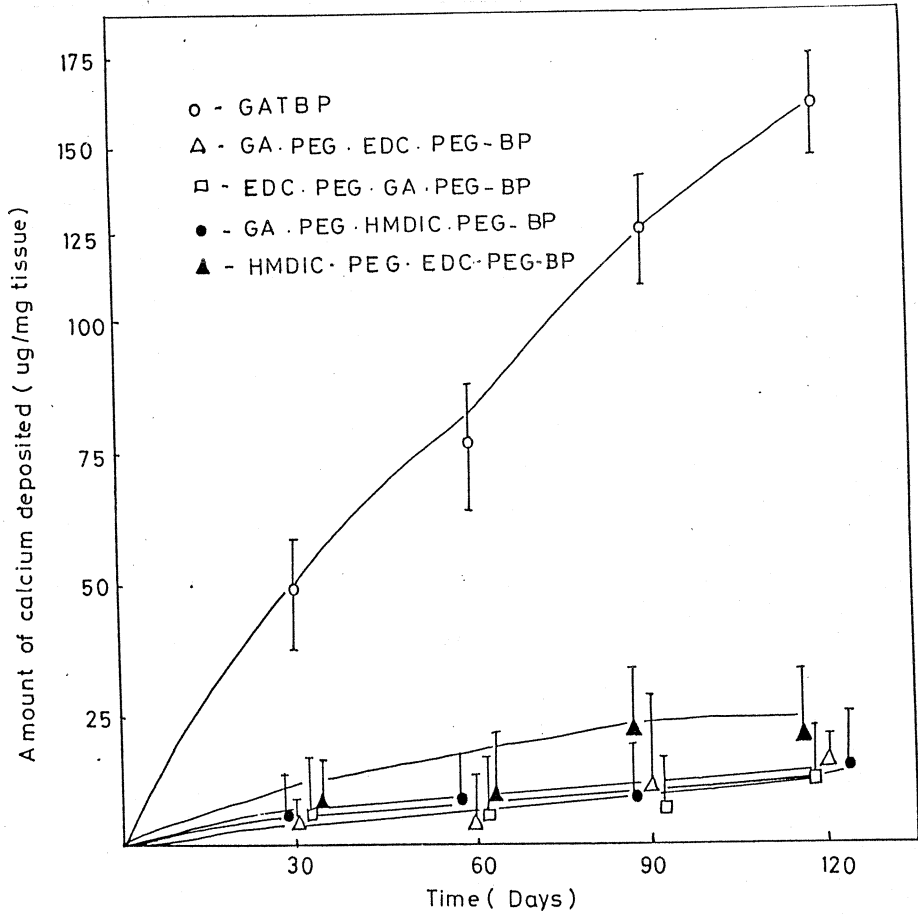


Figure 3.3.5 Amount of calcium deposited on double crosslinked BP as a function of time. Bar indicates 95% confidence limits.

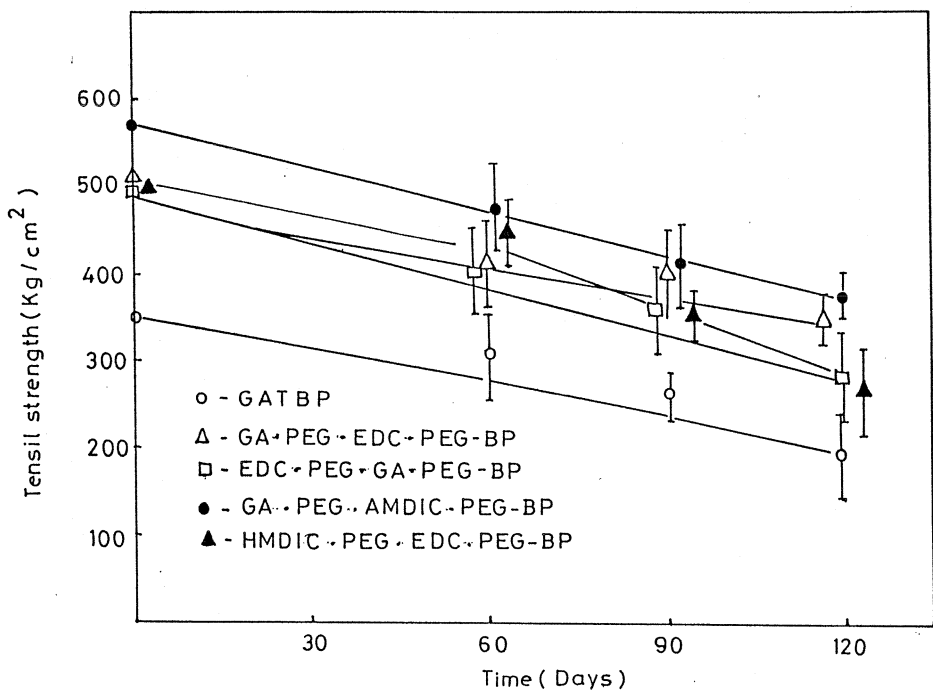


Figure 3.3.6 Effect of calcification on the tensile strength of double crosslinked BP's as a function of time. Bar indicates 95% confidence limits.

The variation in mechanical properties of various crosslinked BP surfaces on incubation in calcium phosphate metastable solution is demonstrated in figure 3.3.6. Due to calcium deposition, GATBP and double crosslinked BP surfaces showed reduction in tensile strength to that of their original strength.

Scanning electron micrograph of retrieved pericardia after 21 days subdermal implantation in rats, are depicted in figure 3.3.7. Break down of collagen bundles as well as plaque deposits of calcium were observed in control (GATBP) pericardial samples (figure 3.3.7 A). However, the calcification and degradation were hardly evident on double crosslinked surfaces. In addition, these double crosslinked BP surfaces modified through PEG were much smoother and without pores or ruptured tissues. In other words, the PEG modified tissues had retained their stability and tissue integrity.

3.3.3 Histological evaluation of subdermal implants

All implants of bovine pericardial tissue had normal architecture and were surrounded by fibroblasts and fibrocytes with an infiltration of macrophages into the peripheral layers of implant. The calcified areas, which stain darkly with von Kossa stain, were present in most samples of pericardial control tissues (GATBP retrieved after 21 days) in the form of confluent areas with breakdown of collagen bundles (figure 3.3.8). There was no evidence of calcification in PEG grafted tissues, when stained with von Kossa. Morphological architecture appeared to be maintained in the modified tissues.

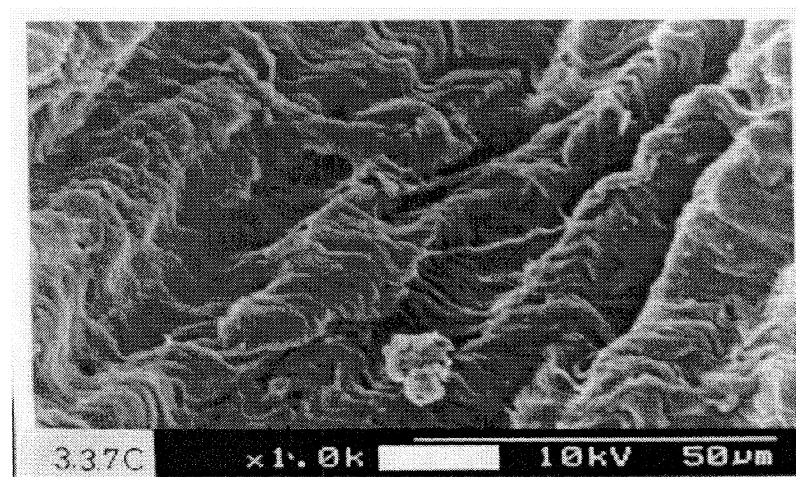
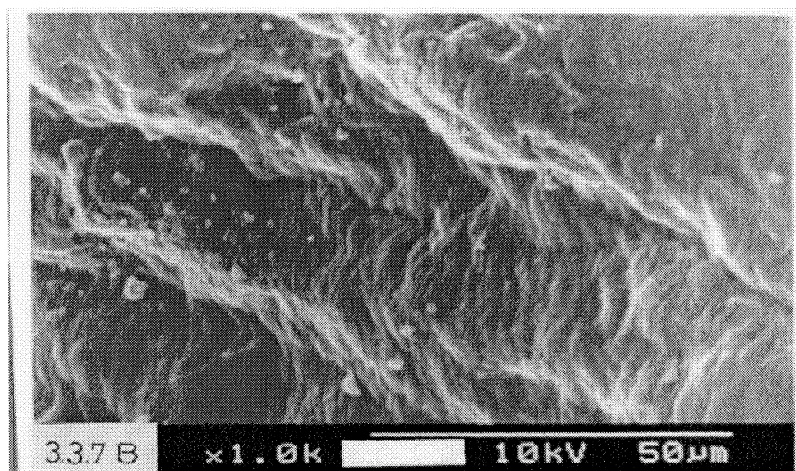
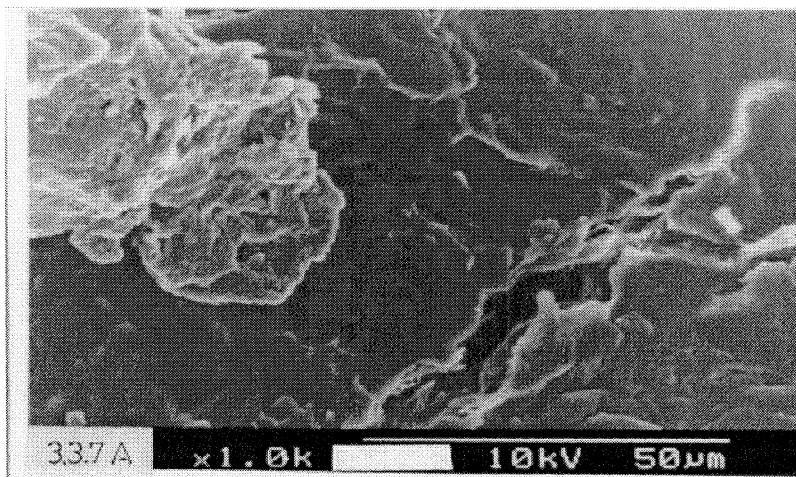
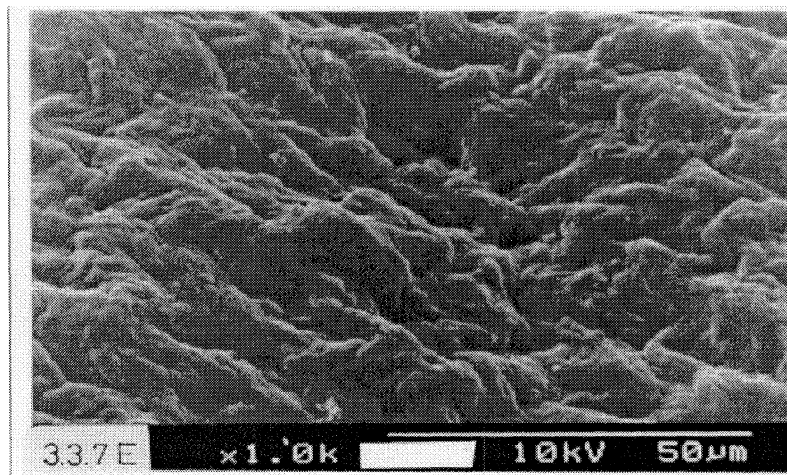
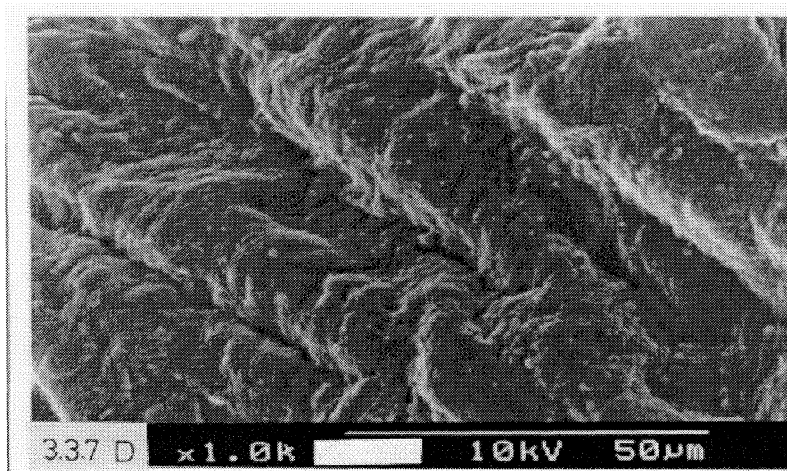


Figure 3.3.7 Scanning electron micrographs of retrieved double crosslinked BP after 21 days rats subcutaneous implantation. (A) GATBP, (B) GA.PEG.EDC.PEG-BP, (C) EDC.PEG.GA.PEG-BP.



(D) GA.PEG.HMDIC.PEG-BP(E) HMDIC.PEG.EDC.PEG-BP

Calcification is the predominant cause in the failure of bioprostheses that has been attributed to the glutaraldehyde process.⁶¹ Calcification is a multi-factorial process and may initiate due to the presence of phospholipids in tissue that can attract calcium ions or voids and cavities in the tissue created by the removal of proteoglycans during processing or cellular degradation. These predeposits of cellular components, in the GA fixed tissue, act as potential points that can trap foreign particles that may lead to nucleation centers for calcium.

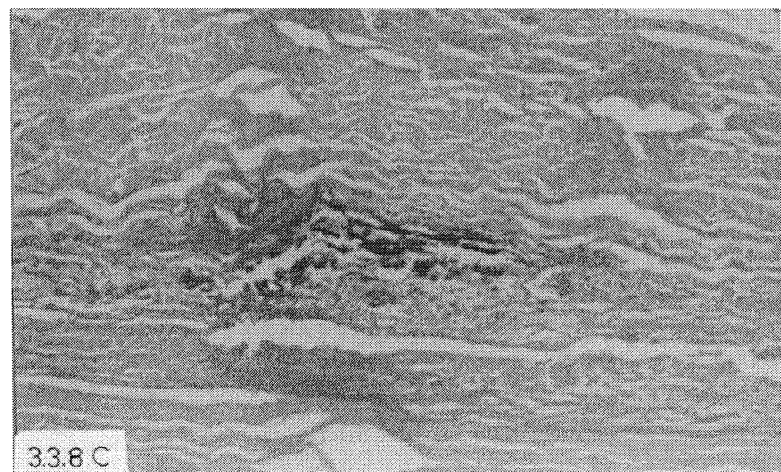
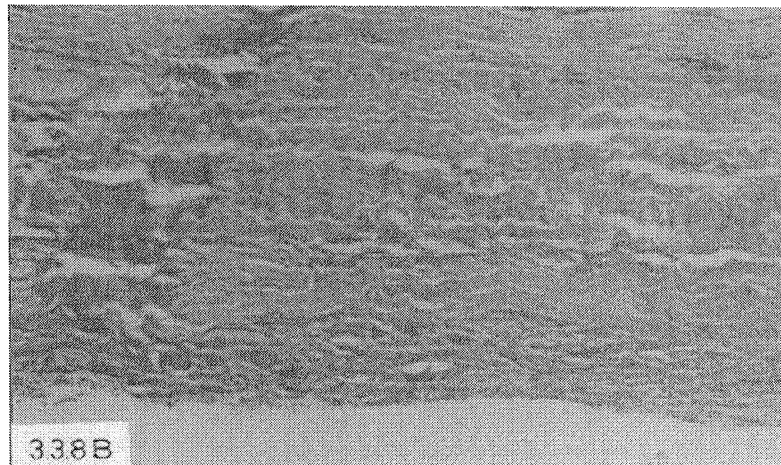
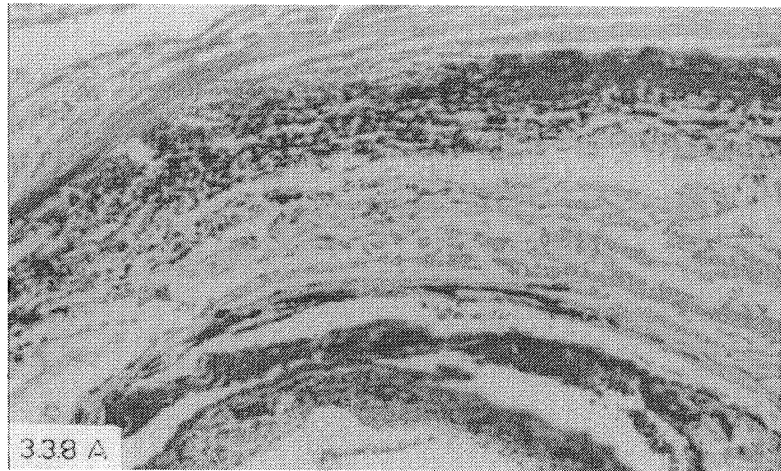
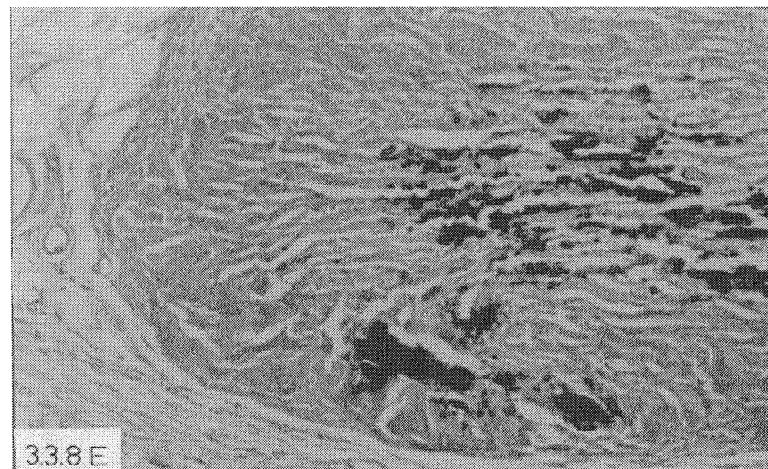
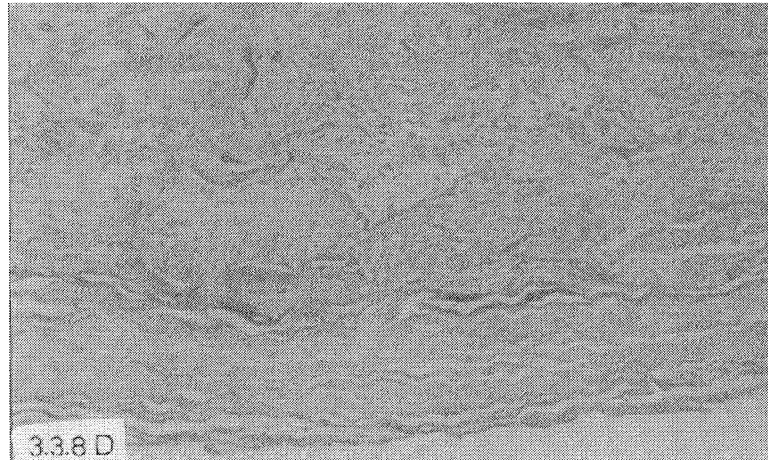


Figure 3.3.8 Histologic demonstration of double crosslinked pericardium stained with von Kossa after 21 days post implantation. (A) GATBP, (B) GA.PEG.EDC.PEG-BP.(C) EDC.PEG.GA.PEG-BP. Original magnification 50X,



(D) GA.PEG.HMDIC.PEG-BP, (E) HMDIC.PEG.EDC.PEG-BP.
Original magnification 50X.

In this study, the deposition of calcium was least with the PEG grafted surfaces compared to GATBP (figure 3.3.4 to 3.3.7). Reports suggest that the porous structures of materials can facilitate increased permeation of CaPO_4 ions yielding greater calcification.^{64,88} PEG modified pericardium via double crosslinking techniques appeared to have smooth surface morphology in its SEM (figure 3.3.8). Thus, it is conceivable that PEG grafted tissue can also stabilize the porous structure

of collagen and subsequently reduce the calcium mobilization. Results from earlier chapter have reported that high molecular weight PEG - a hybrid tissue - may be a suitable material for developing prostheses due to their stability, biocompatibility and immunogenicity. Table 3.3.I shows the effect of EDC HMDIC as an effective double crosslinker along with GA towards biostability and tissue resistance to calcification. It has been reported that carboxy glutamic acid present in vitamin K dependent

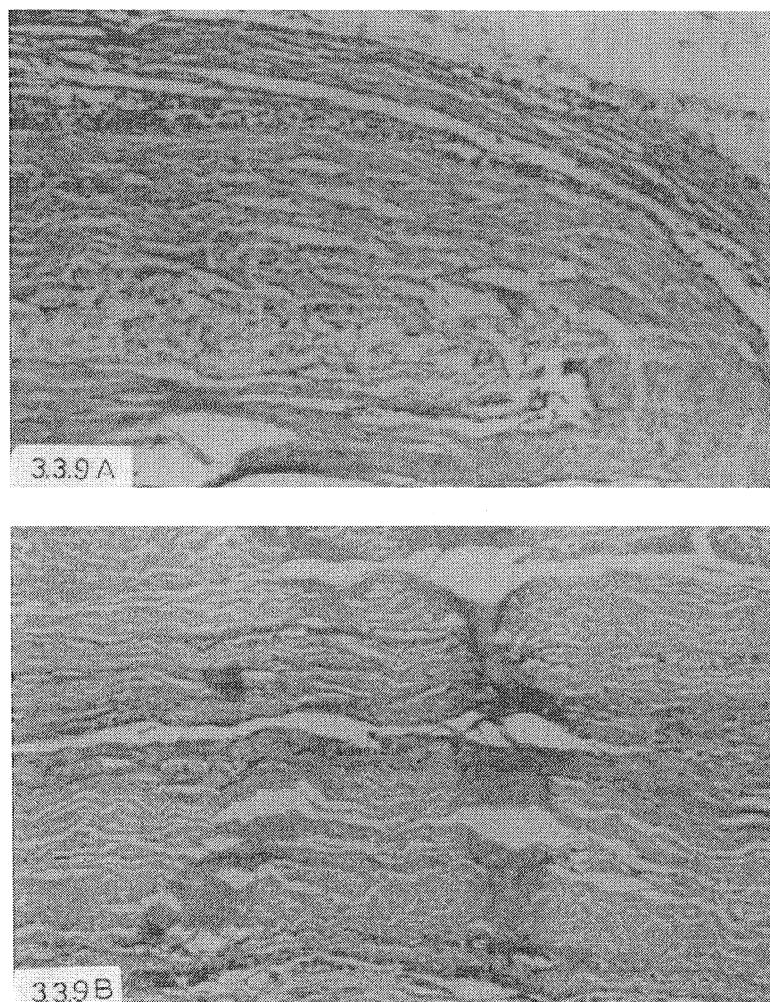
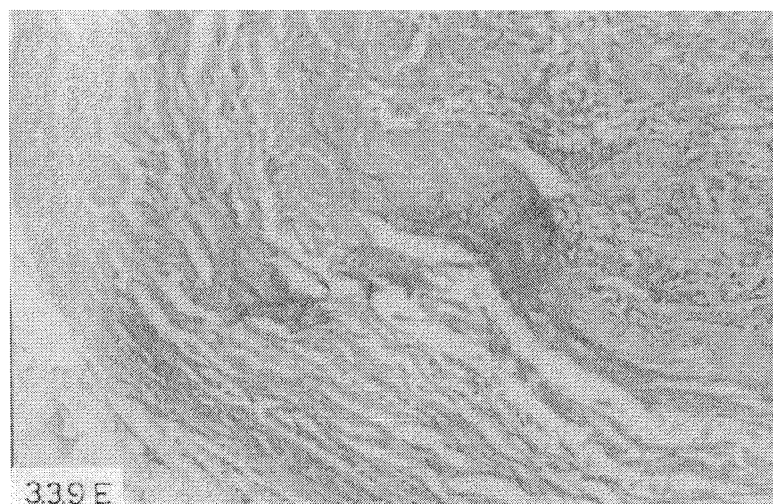
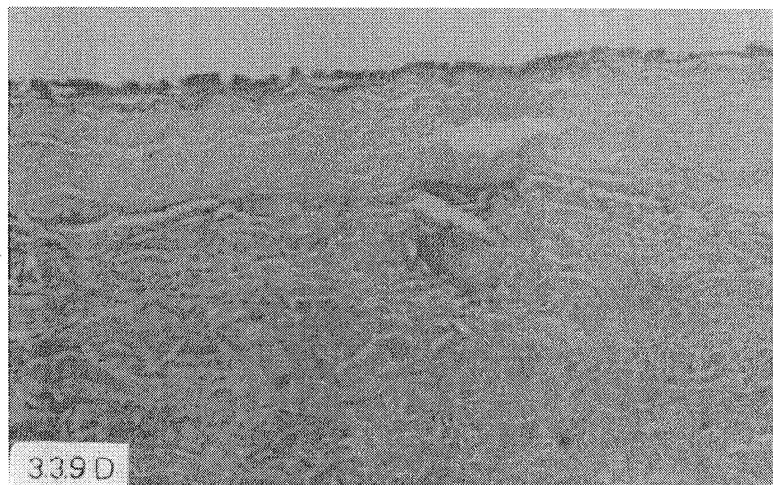
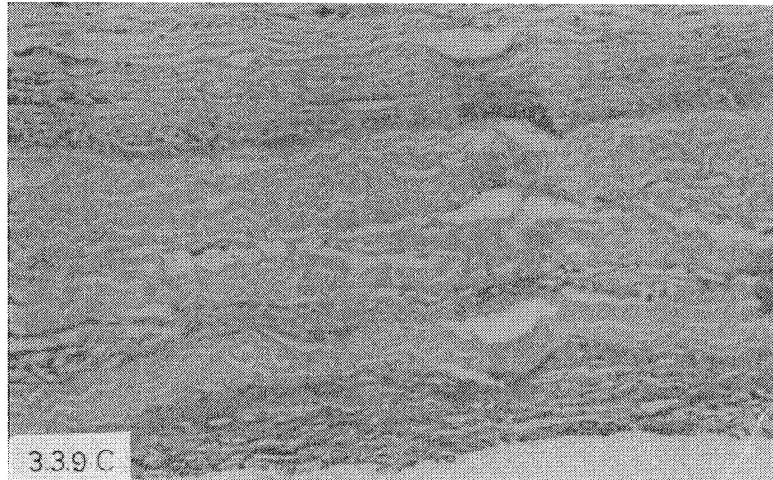


Figure 3.3.9. Histologic demonstration of double crosslinked BP stained with haematoxylin-eosin after 21 days rat subcutaneous implantation. (A)GATBP, (B) GA.PEG.EDC.PEG-BP. Original magnification 50X.



(C) EDC.PEG.GA.PEG-BP, (D) GA PEG.HMDIC.PEG-BP,
(E) HMDIC.PEG.GA.PEG-BP. Original magnification 50X.

Table 3.3.I Contact Angle, Platelet Adhesion, and Amount of calcium deposited on various double crosslinked BP, after 21 days rat subcutaneous implantation.

Surfaces ^a	Contact angle ^a ± SD	Number of platelets ^b adhesion	Amount of Ca ^c deposited in Mg/mg tissue after 21 days implantation.
GATBP	136.1 ± 1.8	58.5 ± 7.5	19.8 ± 2.5
GA.PEG.EDC.PEG	151.3 ± 3.5 *	19.4 ± 2.7*	5.1 ± 1.8*
EDC.PEG.GA.PEG	151.6 ± 2.6*	18.3 ± 1.8*	10.9 ± 1.6*
GA.PEG.HMDIC.PEG	151.8 ± 2.2*	20.2 ± 4.6*	6.3 ± 0.8*
HMDIC.PEG.EDC.PEG	150.9 ± 1.5*	20.8 ± 3.2*	15.6 ± 1.2

a Octane contact angle expressed as mean ± SD (from at least ten observation).

b Values denoted as the average of the number of platelets attached to the surface per mm² with ± SD (at least 20 observations from triplicate experiments).

c Values expressed as mean ± SD from at least four experiments.

** P < 0.005, * P < 0.05 + P < 0.01, where all the values of crosslinked surfaces are compared to GATBP. "P" value <0.05 were considered as statistically significant.

proteins are thought to bind with Ca^{2+} ions.¹⁸² In a similar fashion two neighbouring COO^- groups present at a specific distance can also bind Ca^{2+} ions. In the case of EDC-BP long chain carbodiimide can effectively crosslink intra and inter molecular carboxylic acid groups in BP and subsequently the free COO^- groups may not be available for Ca^{2+} binding.

These may be the reasons for the observed reduction in calcium nodulation on BP with EDC and HMDIC crosslinking. As reported in chapters (chapter 3.2 and 3.5) polyethylene glycol grafted pericardium had improved biostability and resistance to calcification, probably via inhibiting cell adhesion and subsequent cellular involvements.

Table - I also provides information related to octane contact angle, platelet adhesion, and calcium deposited after 21 days in vivo subcutaneous implantation in rats. The octane contact angle of PEG modified surfaces were higher compared to GA treated tissue. This can provide information related to the hydrophilic or hydrophobic nature of the surface where a higher angle shows an increase in hydrophilic character⁸⁷. PEG modified surfaces had become hydrophilic and platelet adhesion was also reduced (Table - 3.3.I). The deposition of calcium was in the order of GA-PEG-EDC-PEG < GA-PEG-HMDIC-PEG < EDC-PEG-GA-PEG < HMDIC-PEG-EDC-PEG < GATBP. HMDIC-PEG-EDC-PEG modified BP had shown hydrophilicity and reduced platelet adhesion, but in vitro and in vivo calcification

were higher. Thus, it appears that suitable selection of double crosslinking techniques may reduce calcification while improving the tissue stability.

Many studies have shown that GA treated pericardial tissue still remains a problem for their implant patency.¹⁴² But GA remains the reagent of choice for bioprosthetic heart valve fabrication because of its superior stability and tissue thromboresistance.

The present study proposes that PEG -modified pericardia through a two step cross-linking procedure involving , very low levels of GA and carbodiimide or hexamethylene diisocyanate, appear to be highly resistant to enzyme digestion (biostable) and calcification in in vitro and in vivo conditions. From these observations, it seems that a suitable selection of bifunctional crosslinking techniques on tissues (combination of crosslinkers) may help to develop stable implants of high patency rates.

CHAPTER 3.4

DEVELOPMENT OF CHITOSAN/POLYETHYLENE VINYL ACETATE CO-MATRIX FOR THE CONTROLLED RELEASE OF DRUG COMBINATIONS

The development of improved methods of drug delivery has received a lot of attention in the last two decades.^{49,103} In many cases, a constant effective nontoxic level of the drug at a particular body location is needed. Controlled release of appropriate drugs alone and in combination is one of the approaches for treating coronary obstructions,^{49,103,154} balloon angioplasty, restenosis associated with thrombosis and calcification. Here the drugs were chosen for controlled release incorporations, based on ameliorating restenosis, thrombosis and calcification.

One approach that has received increasing attention as a means of prolonging drug release has been the incorporation of drugs in solid polymers, such as silicone rubber, ethylene vinyl acetate copolymer, chitosan etc.^{21,144,195} Chitosan a natural polysaccharide, having structural characteristics similar to glycosaminoglycans seems to be non-toxic and bioabsorbable and has been explored for the release of several drugs.^{30,139} Polymers based on polyethylene vinyl acetate and polystyrene butadiene have been widely investigated for therapeutic drug targeting.^{46,109,195} Levy *et al*¹⁹⁵ have used a single matrix of polyethylene vinyl acetate for delivering two drugs having synergistic effects, such as Fe^{3+} and diphosphonate and have found that the released drugs can inhibit the pathological calcification. However, the development

of a co-matrix system for delivering drug combinations for cardiovascular applications have hardly been reported.

This chapter assess the possibility of delivering two drug combinations, such as aspirin- heparin and ferric - magnesium ions from a co-matrix system fabricated from chitosan and polyethylene vinyl acetate. Further, the synergistic effect of these drugs in inhibiting cardiovascular calcification and thrombosis are also investigated.

3.4.1 Controlled release of aspirin-heparin for preventing pericardial calcification and thrombosis

Reports suggest that aspirin, a well known platelet antagonist, and heparin, a bioactive agent for curtailing thrombosis, appear to be effective for various cardiovascular complications.¹⁰⁹ A controlled delivery of aspirin -heparin from a co-matrix system fabricated from aspirin loaded chitosan beads embedded in heparin loaded polyethylene vinyl acetate, was achieved. The synergistic effects of these drugs in inhibiting cardiovascular thrombosis and calcification are reported in these initial studies.

3.4.2 Aspirin/Heparin Delivery

Representative scanning electron micrographs of aspirin/heparin loaded chitosan/PE(VAc) co-matrix systems, are shown in figure 3.4.1. Chitosan beads were embedded within PE(VAc) matrix as per the ultrastructure of the co-matrix (figure 3.4.1 A). The beads were about 900-1100 μ m in size and roughly spherical, in

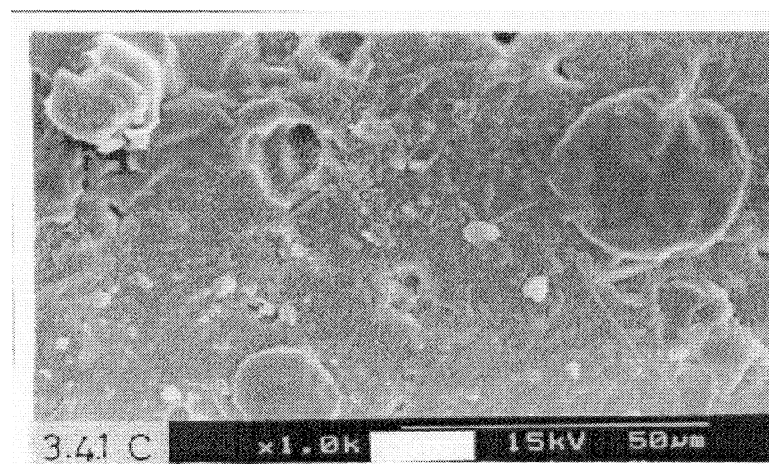
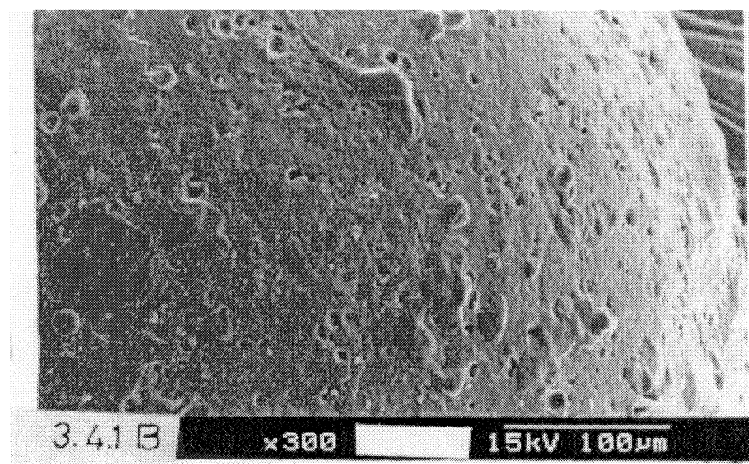
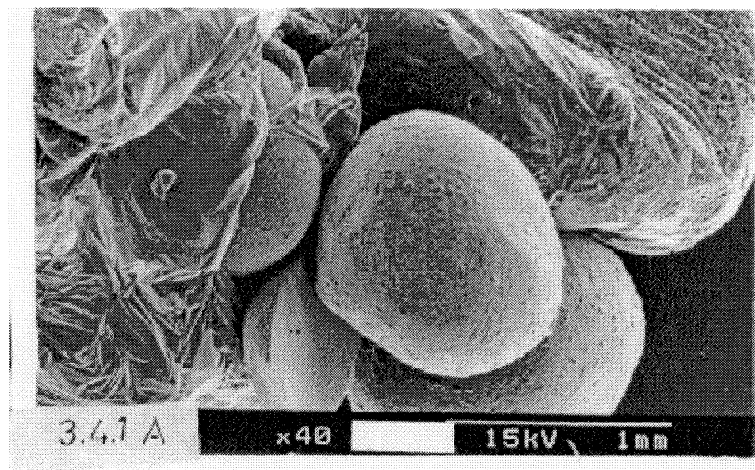
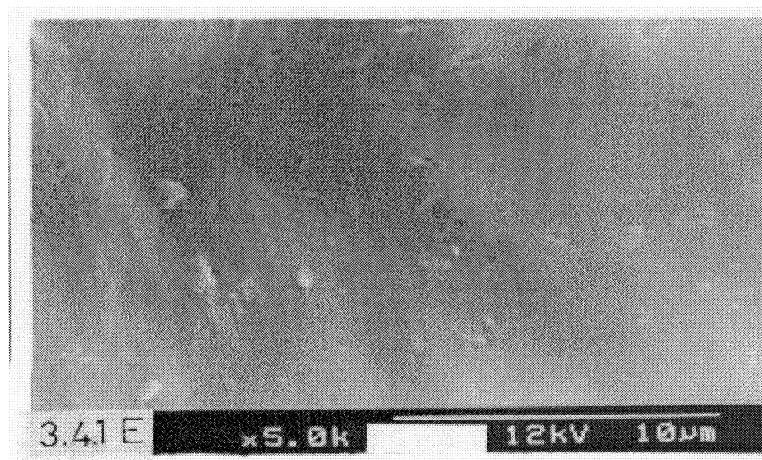
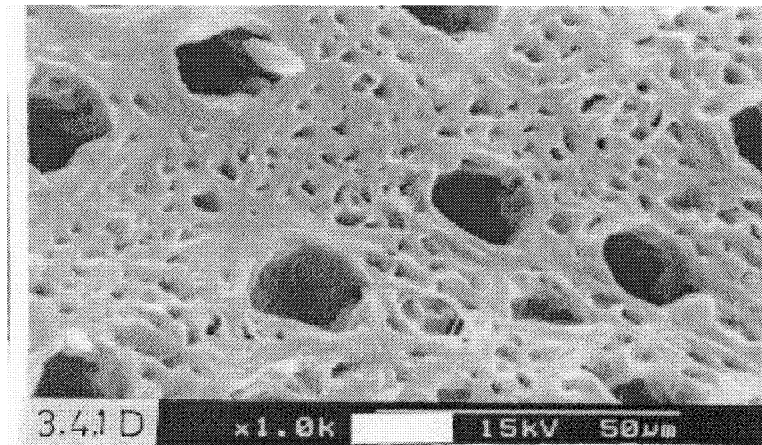


Figure 3.4.1 Scanning electron micrographs of: (A) Aspirin loaded chitosan beads embedded in heparin loaded PE(VAc), (B) Surface morphology of aspirin loaded chitosan beads. (C) Its ultrastructure.



- (D) Surface morphology of co-matrix before SBR coating and
- (E) Surface morphology of co-matrix after SBR coating.

overall shape and had microporous outer surface (figure 3.4.1B). The internal structure also had more micropores (5-10 μm size), where the aspirin had been crystallized and incorporated within these microporous structure of beads (figure 3.4.1C). The ultrastructure of polyethylene vinyl acetate had indicated larger pores (20 μm size) with intermittent microporous structures of (2-3 μm) heparin crystals as demonstrated in figure 3.4.1D. Styrene butadiene rubber (SBR) coating of the co-matrix mask the pores on the surface as is evident in figure 3.4.1E.

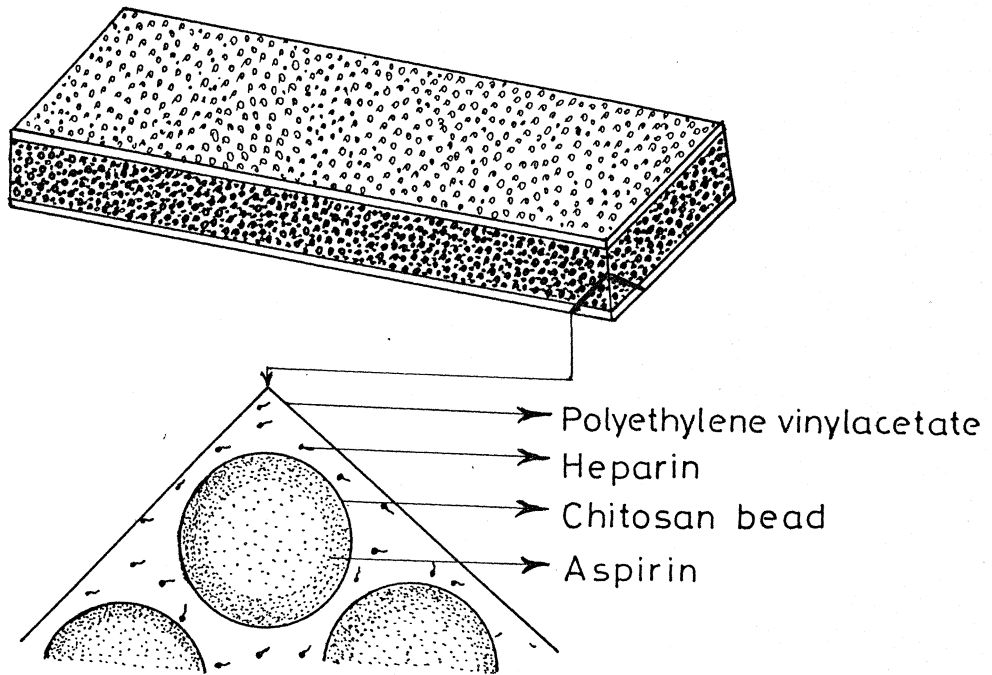


Figure 3.4.2 Schematic diagram of Aspirin/Heparin loaded chitosan/Polyethylene vinylacetate matrix (A), and an enlarged cross section (B).

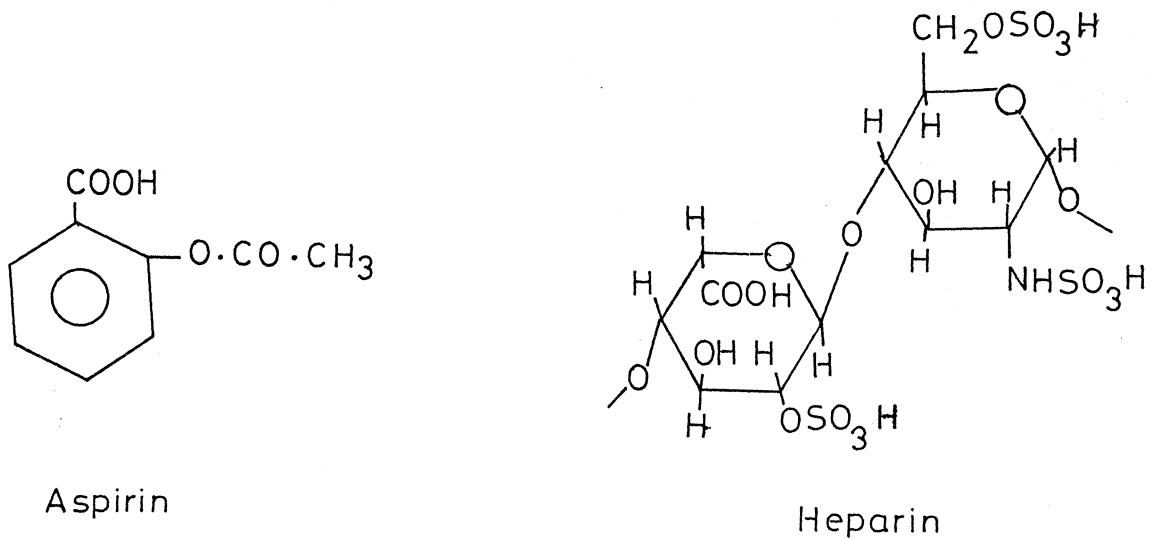


Figure 3.4.2 Structure of drugs used

A schematic diagram of aspirin/heparin loaded chitosan/polyethylene vinyl acetate systems is illustrated in figure 3.4.2. The smaller aspirin molecule (figure 3.4.2C) was incorporated within chitosan beads, which were further embedded in heparin loaded PE(VAc) matrix as depicted in figure 3.4.2B. Figure 3.4.3 demonstrates the amount and per cent of aspirin released from the co-matrix, in Tris HCl buffer at pH 7.4, for various time intervals. Here an initial burst release followed by a constant slow release of aspirin from chitosan/PE(VAc) co-matrix, had been observed for 60 days. It is also evident that the amount and per cent of aspirin release within 24h was much higher (30%) from the co-matrix (figure 3.4.3). Further, amount and percentage of heparin delivery from the co-matrix system is illustrated in figure 3.4.4. Here also an initial burst release followed by a slow release of heparin was evident in Tris HCl buffer.

The initial phase of aspirin and heparin release as a function of exposure time in the Tris HCl buffer pH 7.4 is depicted in figures 3.4. 5 and 3.4.6 respectively. The initial burst release of the drug from the co-matrix system was substantially reduced by the surface modifications of the chitosan/PE(VAc) co-matrix, with polystyrene-butadiene (SBR). Different ratios of styrene-butadiene (5:95), (45:55), (85:15) were used for controlling heparin/aspirin release. Release rates of heparin/aspirin from the co-matrix system were significantly reduced by polystyrene butadiene coatings, in the order, bare co-matrix <85:15 <45:55 <5:95. The initial aspirin release was 32% within 24h of dissolution, for styrene butadiene free matrix, compared to 16 and 21% for various SBR coatings of the PE (VAc) co-matrix (figure 3.4.6).

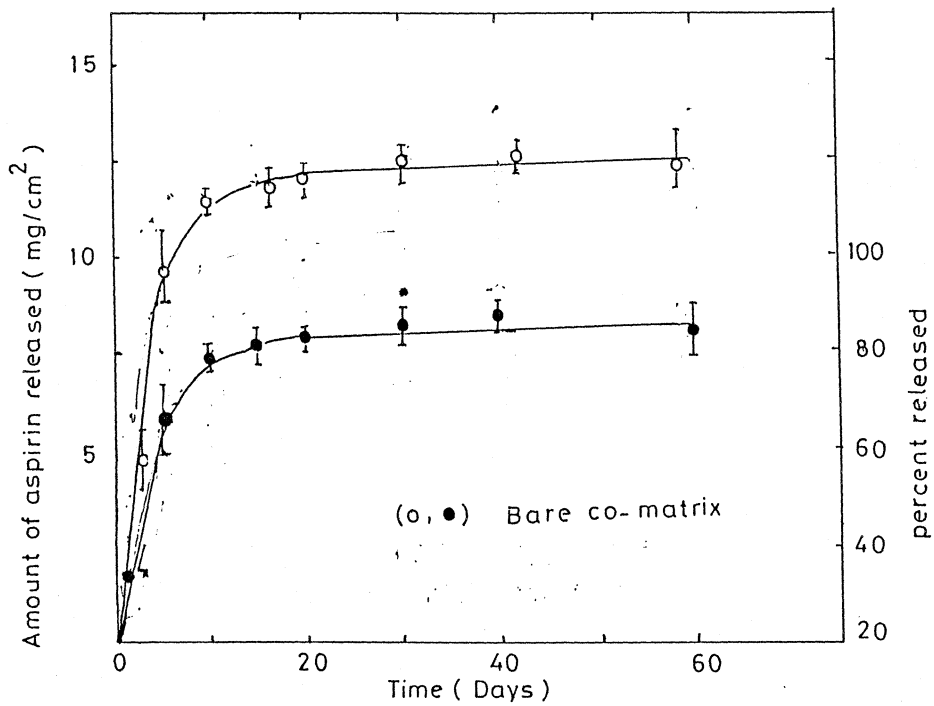


Figure 34.3 Release of aspirin (ASP) from chitosan/PET(VAc) co-matrix (14.45 mg/cm²) as a function of time. Bar indicates 95% confidence limits (o) amount (●) percent released.

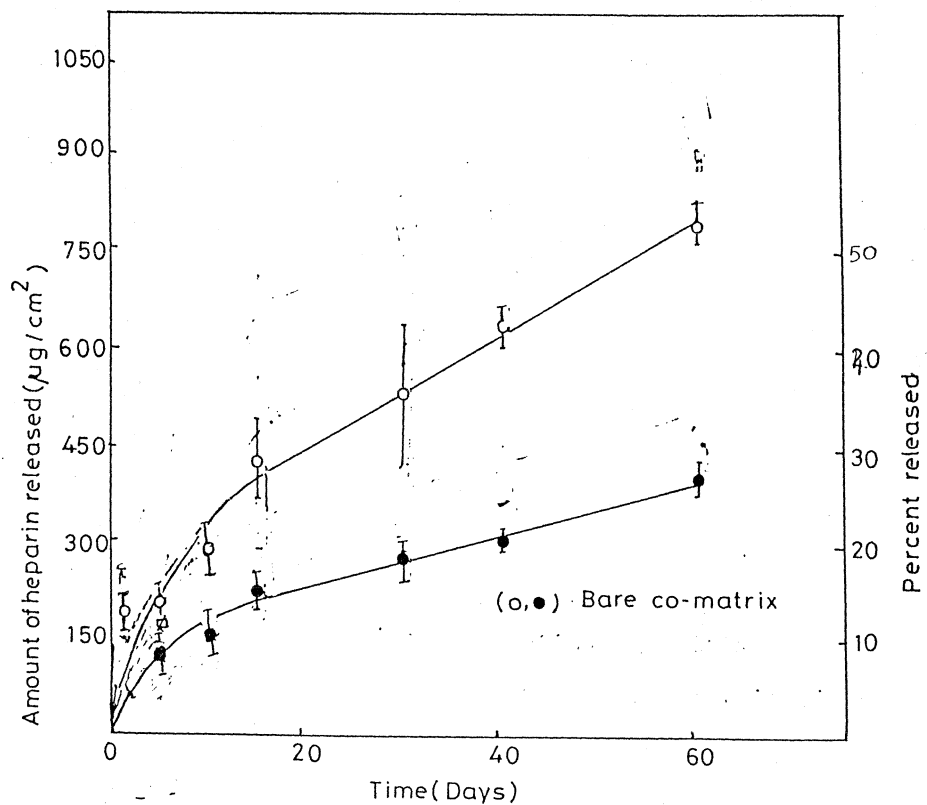


Figure 34.4. Release of heparin (Hep) from chitosan/PET(VAc) Co matrix (11.44 mg/cm²) as a function of time. Bar indicates 95% Confidence limits (o) amount

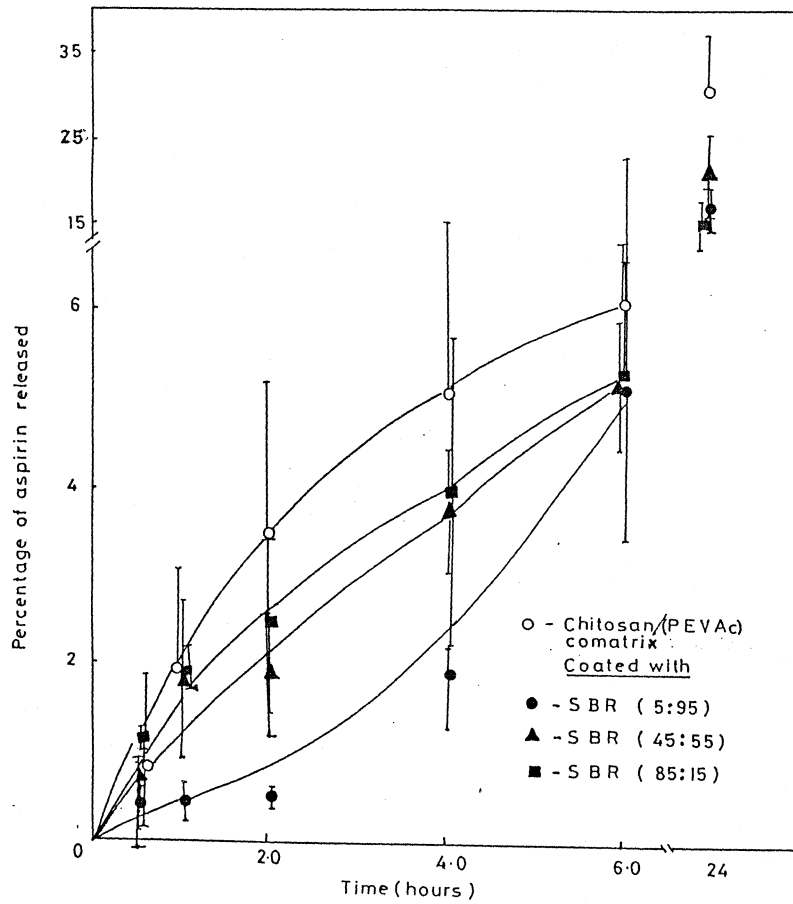


Figure 3.4.5 Initial phase of aspirin release from chitosan / PE(VAc) matrix (14.45 mg/cm²) as a function of time. Bar indicates 95% confidence limits.

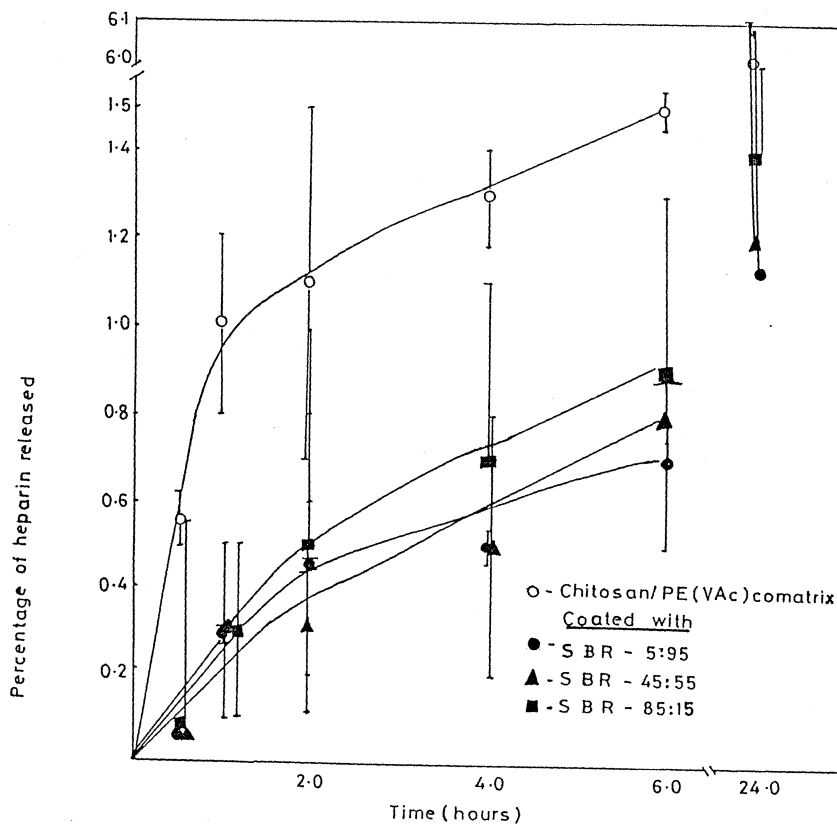


Figure 3.4.6 Initial phase of heparin release from chitosan/PE(VAc) matrix (11.44 mg/cm²) as a function of time. Bar indicates 95% confidence limits.

The present results demonstrate that a chitosan/polyethylene vinyl acetate co-matrix provide near zero order, in vitro release of aspirin and heparin. Rapid initial release of drugs from uncoated chitosan/PE(VAc) co-matrix were noted (figure 3.4.3) and were controlled by the surface modification of the matrix via polystyrene - butadiene coatings (figure 3.4.5 and 3.4.6).

3.4.3 Antithrombotic Properties of released Aspirin/Heparin

Table-3.4.I indicates the amount of aspirin released at specific time intervals from the co-matrix system, and the number of platelets adhered on glass surface. The platelet attachment to glass had been substantially reduced owing to the released aspirin from the co-matrix system. Further, the plasma thromboplastin time had increased, owing to the released heparin from PE (VAc) matrix, as represented in Table-3.4.II. In other words, the released aspirin/heparin had suggested their antiplatelet and anticoagulant properties, demonstrating their specific biological activities.

Antiplatelet activity of released aspirin is evident in Table-3.4.I. The platelet attachment on glass surface has been substantially modified with aspirin release. The pathophysiological mechanisms of restenosis and thrombosis are at present incompletely understood. Platelet thrombi form initially on the surface of the injured artery. Fibrin thrombosis also contributes to acute arterial obstructions and organization and remodeling of the fibrin thrombus, which can further complicate the restenosis processes.^{13,109} Aspirin is a well known platelet antagonist, and has advantages for local release because of its acetylation of the various enzymes

TABLE - 3.4.I : Adhesion of platelets to glass as a function of released aspirin.

Time	Amount of Aspirin released in mg/cm ²	Mean platelets \bar{x} mm ² \pm 50	per
Zero-Bare glass	-	14.9 \pm 2.5	
1st day	4.9 \pm 0.7	8.4 \pm 1.2*	
5th day	9.6 \pm 1.0	7.1 \pm 1.3*	
10th day	11.3 \pm 0.2	6.0 \pm 1.9*	
15th day	11.7 \pm 0.4	5.5 \pm 1.3**	
20th day	11.9 \pm 0.2	5.0 \pm 1.6**	
30th day	12.4 \pm 0.4	5.0 \pm 1.6**	

\bar{x} - Values denoted as the average of the number of platelets attached to the surface per mm² with \pm SD (at least 20 observations from triplicate experiments).

** - $P \leq 0.05$, * $P > 0.05$, where the values of all drug released cases were compared with the bare glass.

TABLE - 3.4.II: Plasma thromboplastin time (PTT) as a function of released heparin.

Time in days	Amount of heparin ≠ released in $\mu\text{g}/\text{cm}^2$	Mean Plasma Thrombolastin ⊕ time (PTT) in seconds \pm SD
Zero (Bare glass)		93.7 \pm 6.7
1	6.6 \pm 0.6 (0.1 ml)	257.4 \pm 22.9*
5	8.2 \pm 1.1 (0.1 ml)	460.2 \pm 18.6*
15	15.0 \pm 2.2 (0.01 ml)	207.8 \pm 14.7**
30	18.7 \pm 4.0 (0.01 ml)	309.2 \pm 8.3**
40	22.8 \pm 0.9 (0.01 ml)	359.4 \pm 27.4**
60	27.6 \pm 1.5 (0.01 ml)	453.6 \pm 36.1**

≠ - 0.1 ml of released heparin (for 1 and 5 days) and 0.01 ml of released heparin (for 15 to 60 days) used for PTT assay.

⊕ - Time in seconds with standard deviation, at least from 5 separate experiments.

** $P \leq 0.05$, * $P > 0.05$, where the PTT values of all heparin released cases were compared with the bare glass.

required for prostaglandin biosynthesis.^{71,109} Hence, it is conceivable that the released aspirin may be useful in preventing platelet-surface attachment and subsequent thrombotic sequale.¹⁹⁹

The coagulation of plasma was substantially inhibited with heparin release (Table 3.4.II). It is well understood that the heparin acts via antithrombin III for its anticoagulant activity and is attributed to the high concentrations of the sulphamate, sulphamide and carboxylic groups and their steric order and confirmation along the chain.^{13,154} The heparin releasing polymers are assumed to improve the thrombo-resistance of foreign surface by providing a high local concentration of heparin. Most recent studies have demonstrated that periarteri drug administration using heparin-ethylene vinyl acetate composites significantly inhibited restenosis in a rat arterial injury model.¹⁰⁹ Thus it is conceivable that release of aspirin/heparin from a co-matrix system appears to be appealing for inhibiting cardiovascular complications. Further, it seems the controlled release of drug combinations from a co-matrix, at the site of a cardio-vascular disease process it can offer an optimal drug action, as well as lowering systemic drug exposure and thereby minimizing the possibility of side effects.¹⁹⁵

3.4.4 Anticalcification effects of released Aspirin/Heparin

Co-matrix system may be advantages over single matrix, for releasing drug combinations having synergistic effects. This may probably reduce the drug - drug

interactions and a low levels of drugs can be released, having varied molecular weights. We have investigated the effect of released aspirin/heparin towards pericardial calcification in an in vitro system. Scanning electron micrographs of the calcification profile of glutaraldehyde treated bovine pericardium in presence of aspirin/heparin delivery is depicted in figure 3.4.7. The deposition of calcium on GATBP was substantially reduced in the presence of aspirin/heparin. In vitro controlled-release drug delivery of aspirin/heparin from chitosan/PE (VAc) co-matrix and the amount of Ca^{2+} deposited on GATBP as a function of time is represented in figure 3.4.8. Further, it indicated that the infusion of aspirin/heparin molecules had inhibited the growth of calcium deposits on GATBP in a concentration dependent manner. The calcium phosphate crystals seen on GATBP surface were roughly spherical in overall shape as is evident from their SEM (figure 3.4.7). However, the calcium deposition was substantially reduced on GATBP samples due to aspirin/heparin delivery in the media. The calcium crystals were rare and only microgranular crystals were evident along with some released aspirin/heparin crystals on the surface of GATBP, as indicates in the SEM micrographs. These initial observations have established the anticalcification effects of antiplatelet aspirin and anticoagulant heparin, in their combinations.

It is interesting to note the deposits of fibrinogen threads within the calcium phosphate crystals on scanning electron micrographs (figure 3.4.7C). The fibrinogen threads might have formed from fibrinogen (Fg) present in the incubating media via

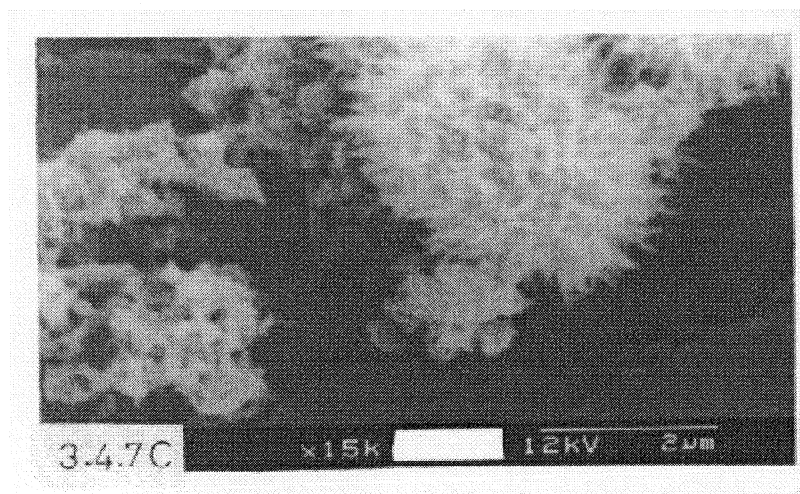
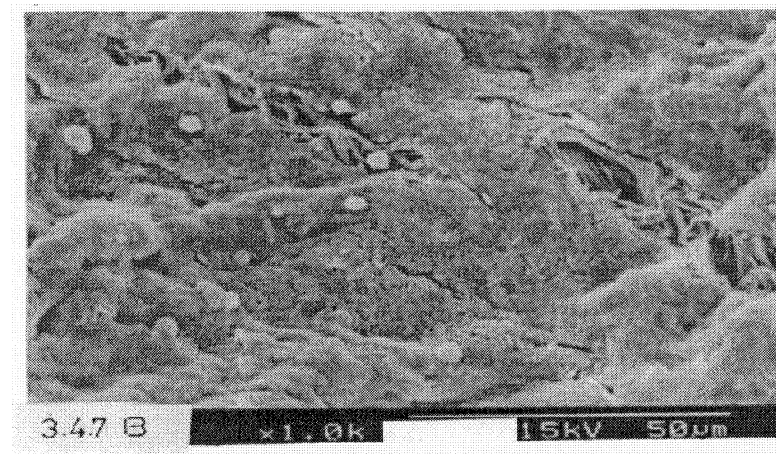
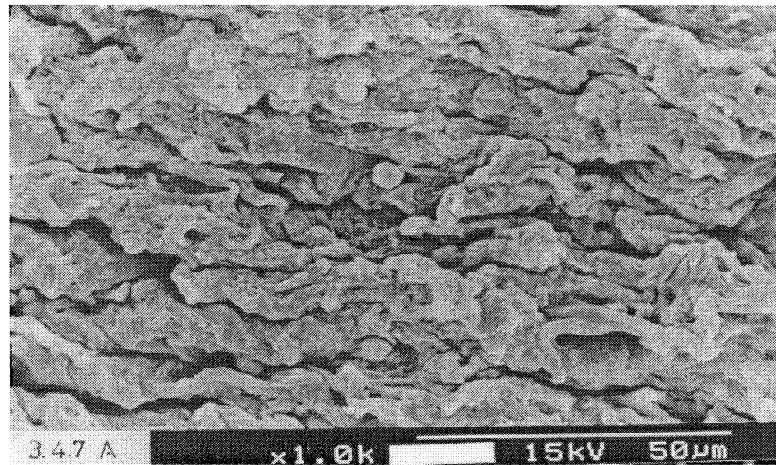


Figure 3.4.7 Scanning electron micrographs of bovine pericardium after 30 days of in vitro calcification: (A) Surface morphology of GA treated BP. (B) Surface morphology of GA treated BP with aspirin/heparin delivery, (C) Calcium phosphate deposits with trapped fibrinogen threads.

involvement of Ca^{2+} crosslinks. The increased deposits of Fg threads may be another reason for more calcium deposition to GATBP. One proposed mechanism for calcification may be the cellular involvements (platelets or bacterial cell deposits) on the implant surface, acting as a site for subsequent calcium phosphate deposition. Vroman¹⁹⁴ has proposed that platelets adhere where they find adsorbed fibrinogen. It may be assumed that the influx of calcium on GATBP may be due to the cellular components via the plasma fibrinogen.

3.4.5 Controlled release of ferric-magnesium ions for preventing calcification

Earlier studies from this laboratory²⁸ have suggested that the metal ions like Fe^{3+} and Mg^{2+} individually and in combinations of low levels significantly reduced the crystallization of calcium phosphates. Hence, we have developed similar co-matrix system for the controlled release of ferric and magnesium ions from chitosan and polyethylene vinyl acetate coated with styrene-butadiene rubber. Amount and percent of ferric ion released in Tris HCl buffer at pH 7.4, for various time intervals are depicted in figure 3.4.9. Here also an initial burst release followed by a constant release of Fe^{3+} ions from the chitosan / PE (VAc) co-matrix had been observed for a 60 days period. Figure 3.4.10 demonstrates the amount and percentage of Mg^{2+} delivery from the co-matrix system, in Tris HCl buffer for various time intervals. In this case an initial burst release followed by a slow release of magnesium was evident in tris buffer. The Mg^{2+} and Fe^{3+} release were substantially reduced due to various surface treatments given to the co-matrix. For that, ferric ion loaded chitosan beads

were crosslinked with glutaraldehyde and were subsequently embedded in PE (VAc) matrix followed by surface coating (SBR) of the co-matrix. Similarly, Mg^{2+} ion release through porous PE (VAc) had also been modulated by masking their pores with SBR coating as is evident in figure 3.4.9 and 3.4.10. The mechanism of ferric/magnesium delivery through chitosan/ PE(VAc) co-matrix is similar to that of aspirin/heparin delivery, proposed earlier.

Ethylene vinyl acetate copolymers have been used for the delivery of various active agents including proteins. It is believed that hydrophilic drugs attract water inside the matrix owing to Donnan equilibrium leading to swelling of the matrix.²¹ The diffusion and dissolution based mechanism for release of hydrophilic drugs from such a hydrophobic polymer having interconnected pores filled with water is well established.^{21,138,195} The present ultrastructural studies of (figure 3.4.1) chitosan/PE (VAc) co-matrix had indicated that the PE (VAc) had macro and microporous internal structures within their matrix (figure 3.4.1D). Hence, it is assumed that the initial burst release observed with heparin through the PE (VAc) matrix, may be owing to the quick diffusion of the molecule through their water swollen interconnected pores. However, as can be seen in figure 3.4.9 and 3.4.10, the initial burst release of the drug were modified with polystyrene butadiene coatings and subsequently a constant drug release was achieved. This may be owing to the thin coating of SBR on the PE (VAc) matrix, which might have concealed their macro and micropores that had been acting as the main channel for drug release. Further, it appears that the 5% styrene

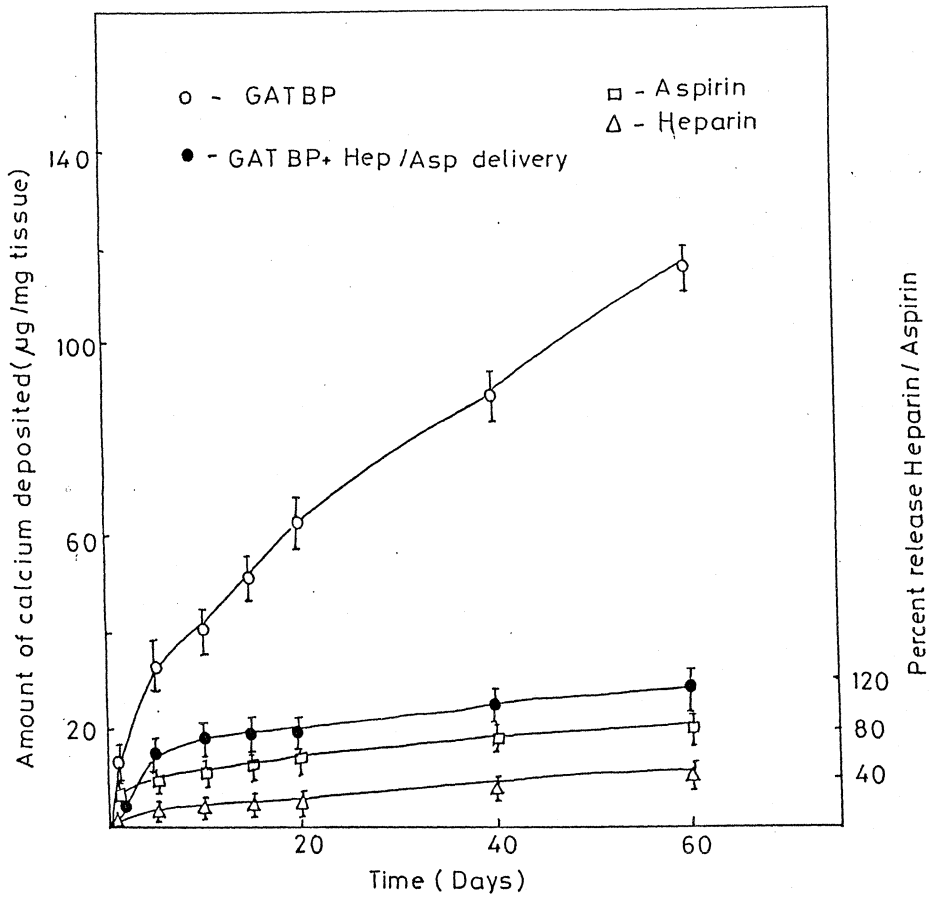


Figure 3.4.8 Amount of calcium deposited to bovine pericardium against the released Hep/Asp as a function of time. Bar indicates 95% confidence limits. (o●) calcium deposited percent Aspirin(□) and heparin(Δ) released.

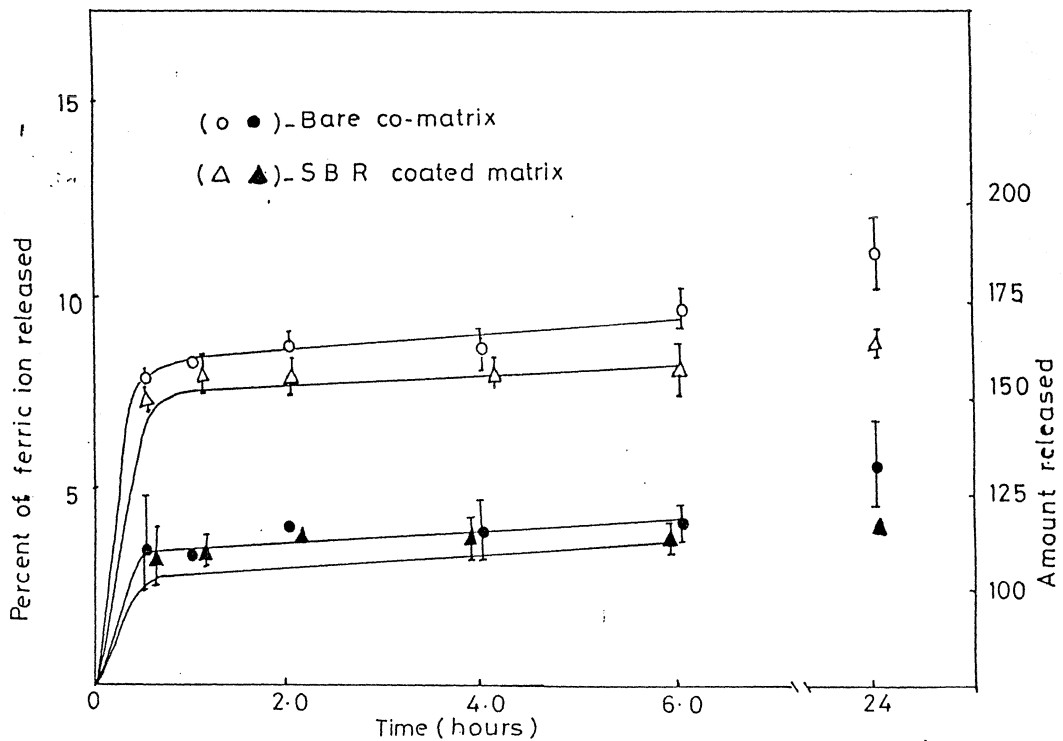


Figure 3.4.9 Initial phase of ferric ion release from chitosan/PE (VAC) co-matrix as a function of time. Bar indicates 95% confidence

containing SBR is most adequate in controlling drug release, probably owing to the maximum hydrophobic nature of rubbery butadiene.

The studies with drug loaded chitosan films had proposed that the rate limiting step in drug release was diffusion through the polymer backbone absorbed with water, rather than degradation of the polymer.¹³⁹ A similar mechanism of aspirin release from chitosan beads is possible in the present system. However, in the case of aspirin loaded CB embedded heparin infused PE (VAc) co-matrix system, the drug release may be slightly different. The smaller aspirin molecules diffuse initially from the swollen outer core of bead, leading to internal mobilization of drugs, causing a constant slow release through the microporous CB, to porous PE (VAc) matrix, and finally diffuses out. The microporous internal structures of the co-matrix (figure 3.4.1) support this interesting release profile.

3.4.6 Anticalcification effects of released Fe^{3+} / Mg^{2+} ions

The anticalcification effects of released ferric/magnesium ions from the co-matrix system was also investigated in an in vitro model. Scanning electron micrographs of the calcification profile of glutaraldehyde treated bovine pericardium, in presence and absence of $\text{Fe}^{3+}/\text{Mg}^{2+}$ delivery is depicted in figure 3.4.11. Bulk deposits of calcium phosphate crystals were evident on the surface of the crosslinked collagen fibrils on exposure to calcium solution. However, the calcium crystals seen on GATBP were substantially reduced with $\text{Fe}^{3+}/\text{Mg}^{2+}$ delivery in the media. The calcium crystals were not evident, and the microgranular deposits were also rare on the surface of GATBP (Figure 3.4.11).

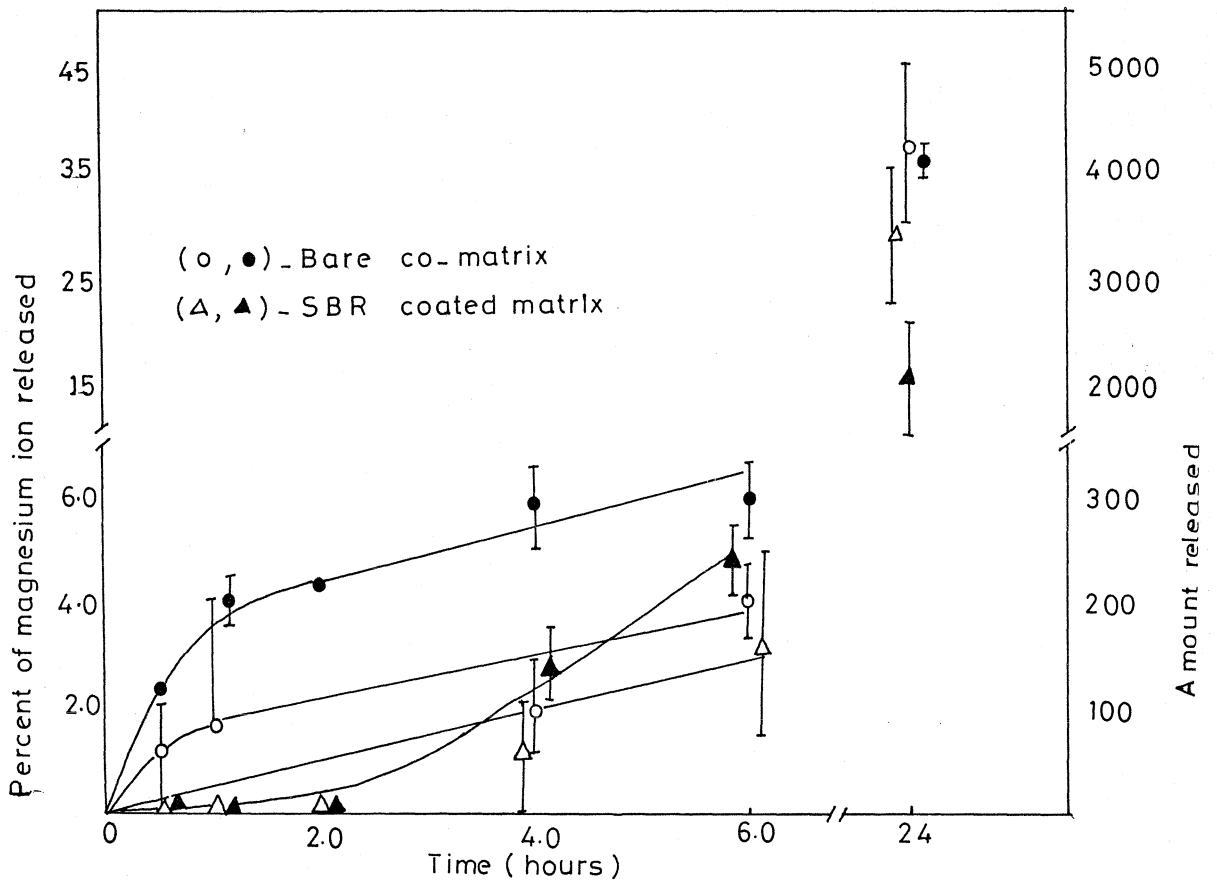


Figure 3.4.10 Initial phase of magnesium ion release from chitosan / PE (VAc) co matrix, as a function of time. Bar indicates 95% confidence limits. (o, Δ) Percent released (●, ▲) amount released

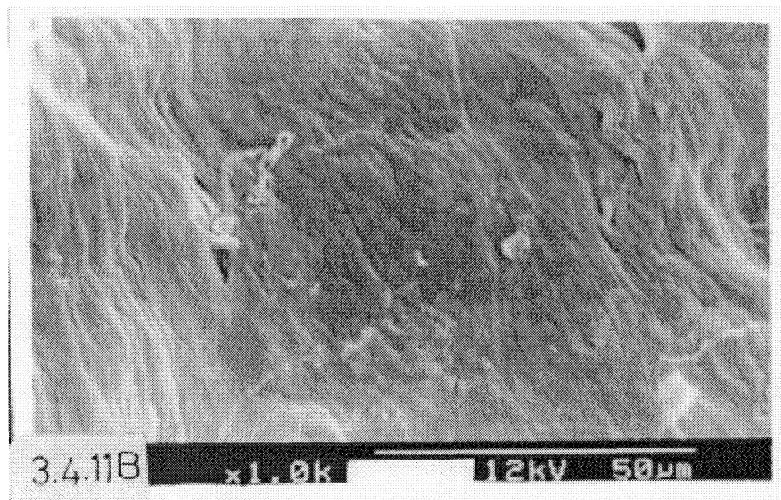
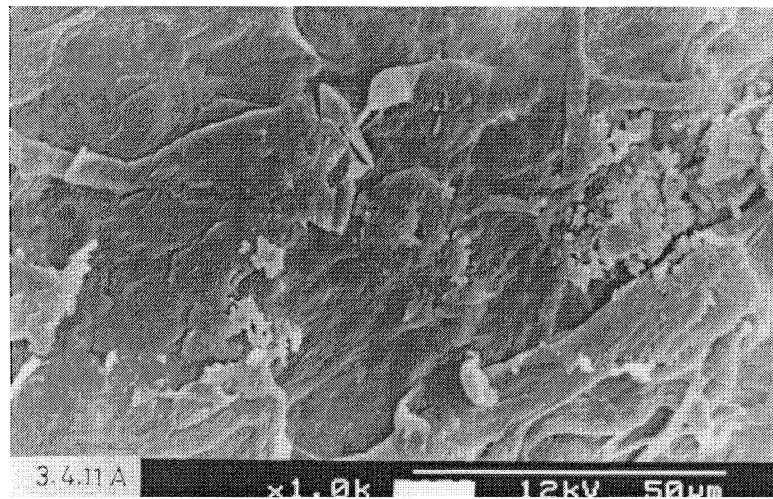


Figure 3.4.11 Scanning electron micrographs of bovine pericardium after 30 days of in vitro calcification (A) Surface morphology of calcified GA treated BP (B) Inhibitor of calcification on GATBP due to $\text{Fe}^{3+}/\text{Mg}^{2+}$ ions delivery from the co-matrix.

Table 3.4.III. Effect of Fe³⁺/Mg²⁺ ions released from the Chitosan/PE (VAc) co-matrix on pericardial calcification.

Surfaces	Amount of Ca ²⁺ deposited for 20 days in µg/mg of tissue	Amount of Fe ²⁺ released in 20 days, in µg/cm ²	Amount of Mg ²⁺ released in 20 days, µg/cm ²	Percent of inhibition
Glutaraldehyde fixed Bovine pericardium (GATBP)	28.9 ± 0.8	—	—	—
GATBP + Fe ³⁺ /Mg ²⁺ loaded Co-matrix	10.1 ± 2.1*	118.3 ± 14.4	9266.7 ± 472.6	63.0 ± 0.7

* P<0.001, where all tissue concentrations and amount of calcium (Fe³⁺/Mg²⁺ ions released), were compared with bare GATBP.

The antagonistic effect of ferric/magnesium ion combinations to GATBP calcification is presented in Table 3.4. III. The 20 days of $\text{Fe}^{3+}/\text{Mg}^{2+}$ delivery from the co-matrix system had significantly inhibited the calcification ($P < 0.001$) profile, when compared to the control pericardium.

These calcification studies on pericardial tissues were performed in an in vitro metastable calcium phosphate solution containing a protein mixture (albumin-25 mg%, γ -globulin-15 mg% and fibrinogen-7.5 mg%) in presence and absence of released ferric and magnesium ions.

Investigations into the use of trivalent metal ions as anti-calcification agents have promoted by reports that some patients undergoing hemodialysis for renal failure developed osteomalacia, caused by the deposition of Al^{3+} in bone as a trace contaminant.¹⁹⁸ Further studies have shown that preincubation of glutaraldehyde pretreated bovine pericardium with Al^{3+} or Fe^{3+} effectively inhibited pathologic calcification in the long term rat subdermal model.¹⁴⁹ Several lines of evidence, support the idea that Mg^{2+} does affect uptake binding and distribution of cellular Ca^{2+} in vascular smooth muscles.¹ It is also suggested that the reduction in Mg^{2+} raise the smooth muscle calcium content, and the elevations in magnesium reverse the effect.¹ The present observations also support this hypothesis, proposing the inhibition of pericardial calcification, by these metal ions.

Hence, this chapter proposes the possibility of delivering drug combinations having synergistic effects for preventing pericardial calcification. This also highlights the use of a co-matrix system for targeting synergistic drug combinations, with least side effects, for therapeutic applications.

CHAPTER - 3.5

SYNERGISTIC EFFECT OF RELEASED ASPIRIN - HEPARIN AND FERRIC - MAGNESIUM IONS FOR INHIBITING POLYETHYLENE GLYCOL MODIFIED PERICARDIAL CALCIFICATION

In the previous chapters we have discussed the in vitro calcification profile of modified pericardium. This in vitro model had been sensitive enough to diagnose the biomaterials propensity to calcify and could serve as a prescreening method to examine calcification mechanisms and methods of prevention. There are a lot of limitations to this in vitro calcification model compared to that of in vivo conditions,^{172,175} since mineralization occurring in in vitro model is mostly restricted to the surface. Other closer methods of experimental models of bioprosthetic tissue calcification include orthotopic tricuspid or mitral valve replacements or conduit mounted valves in juvenile sheep or calves, and heterotopic tissue samples implanted either subdermally or in and around the heart.^{114,116,175} In both circulatory and subcutaneous models, bioprosthetic tissue calcifies progressively, with morphology similar to that observed in clinical specimens, but with markedly accelerated kinetics. Even more dramatic acceleration is achieved in subcutaneous implants of bioprosthetic tissue in young rats, in which levels comparable to those of failed clinical explants occur in 8 weeks or less.

Earlier observations presented in Chapter 3.2 have shown that high molecular weight polyethylene glycol (PEG) modified BP can substantially inhibit in vitro

calcification and enzymatic digestion. Further in Chapter 3.4 we have discussed about chitosan/polyethylene vinyl acetate co-matrix system for the controlled delivery of aspirin/heparin and ferric/magnesium ions and their effects on inhibiting the in vitro calcification. More detailed in vivo studies were undertaken to confirm these in vitro observations, via rat subcutaneous implantation models in 3 weeks old Wistar rats. The histological and biochemical results are discussed here.

3.5.1 SEM of subdermal implants

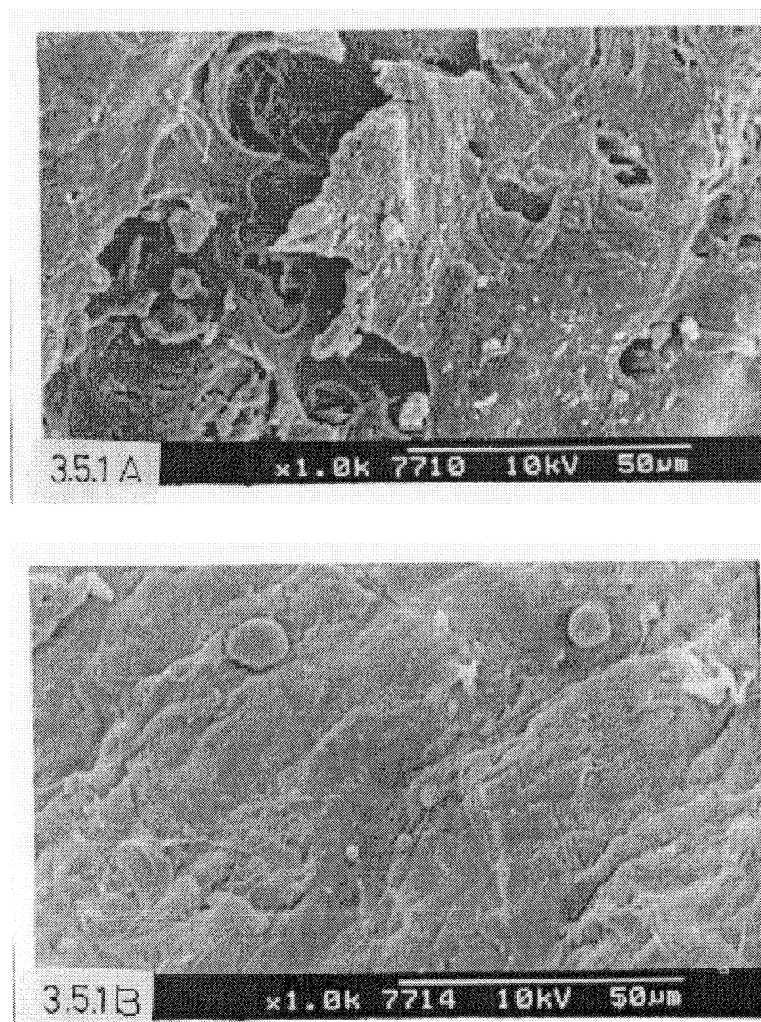
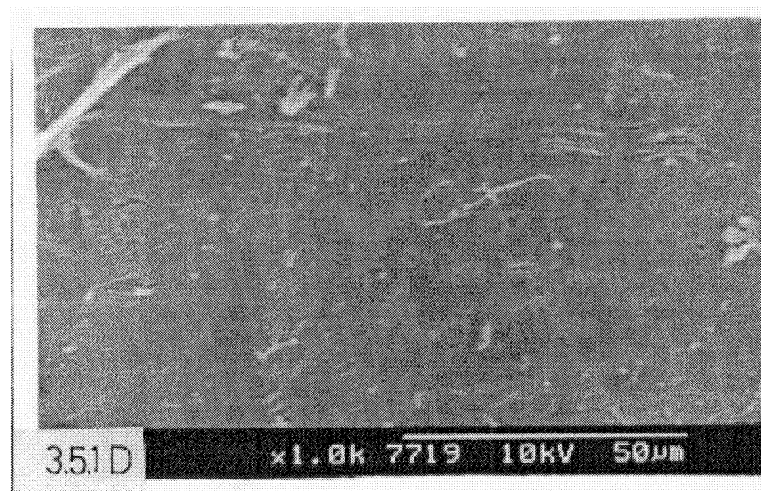
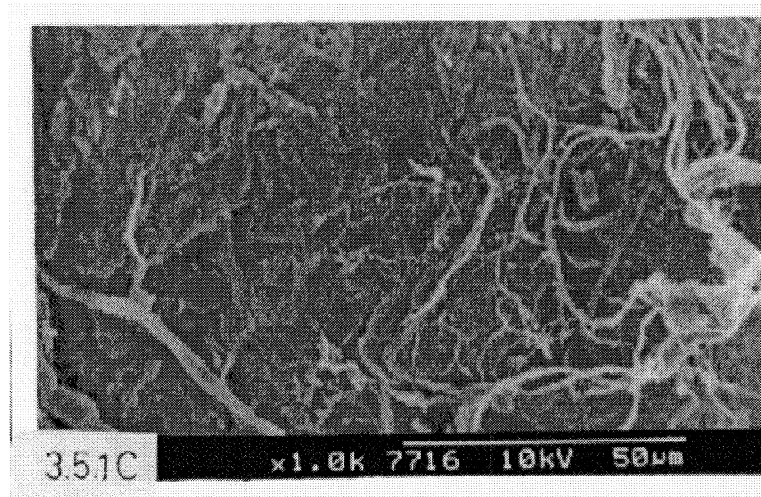


Figure 3.5.1. Scanning electron micrographs of explanted pericardium (A) GATBP, (B) PEG grafted BP



(C) PEG grafted BP with aspirin/heparin delivery

(D) PEG grafted BP with ferric/magnesium ions delivery

Scanning electron micrographs of calcified pericardial tissues after 21 days of rat subcutaneous implantation are depicted in figure 3.5.1. Surface morphology of glutaraldehyde treated BP (figure 3.5.1A) had shown plaque deposits of calcium, adhered platelets and markable break down of collagen bundles. On the other hand, reduced platelet adhesion, calcification and enzymatic digestion were observed on all modified pericardial samples. PEG grafting on BP had shown improved stability to

the pericardial tissue by retarding enzymatic digestion and calcification (figure 3.5.1B). Further, the release of aspirin/heparin or ferric/magnesium ions to PEG BP interfaces had dramatically reduced the calcification and subsequent proliferation of bovine pericardium (figure 3.5.1C and 3.5.1D).

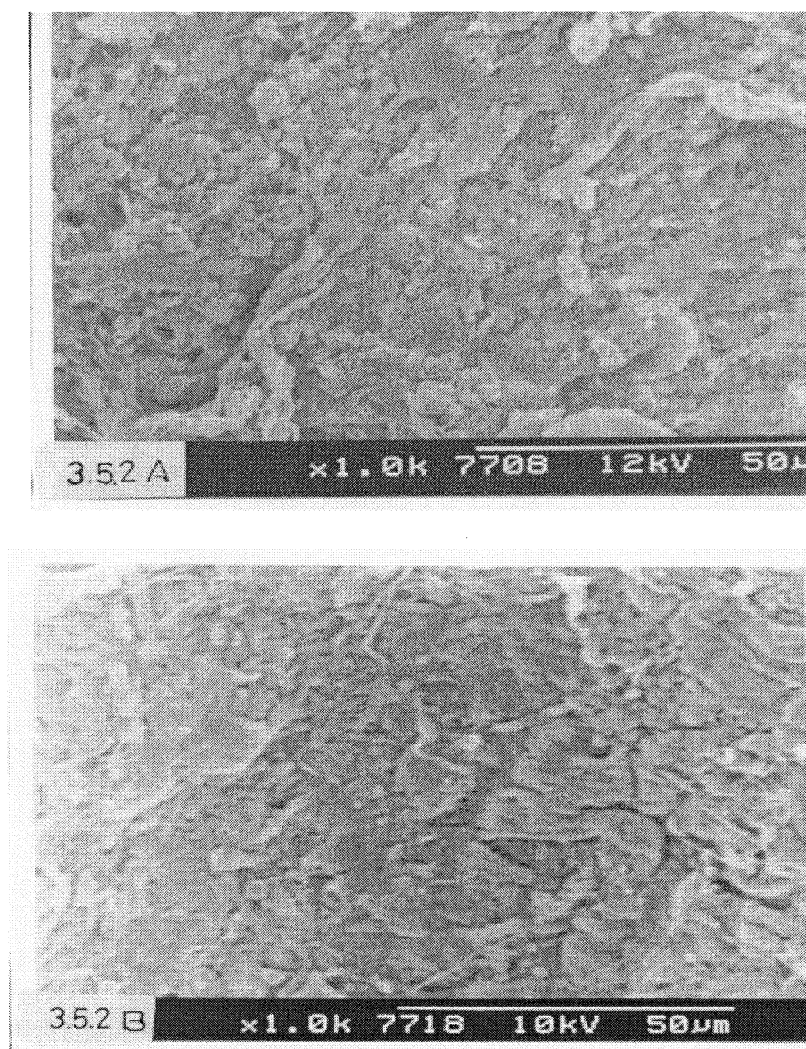
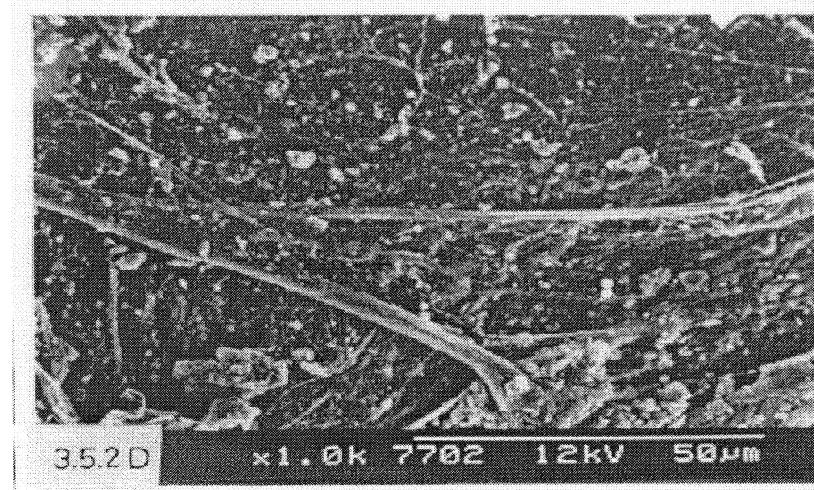
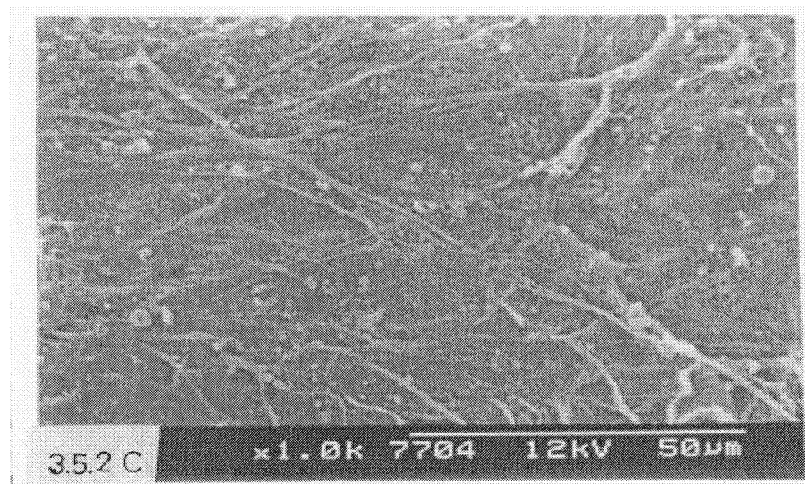


Figure 3.5.2. Scanning electron micrographs of calcified BP after 6 months of implantation (A) GATBP (B) PEG grafted BP.

Scanning electron micrographs of subcutaneous implants retrieved after 6 months in the rat are depicted in figure 3.5.2. Surface morphology of explants have

shown calcified areas and markable breakdown of collagen bundle in almost all samples, but the extent of calcification and degradation were varied. GATBP have shown (figure 3.5.2A) external as well as internal break down of collagen extensively noticed. While PEG modified BP with controlled delivery of asp/hep and ferric/magnesium have shown improved stability of the pericardial tissue by retarding enzymatic digestion and calcification (figure 3.5.2C and 3.5.2 D).



- (C) PEG grafted BP with aspirin/heparin delivery
- (D) PEG grafted BP with ferric/magnesium delivery.

3.5.2 Histological evaluation of Subdermal Implants

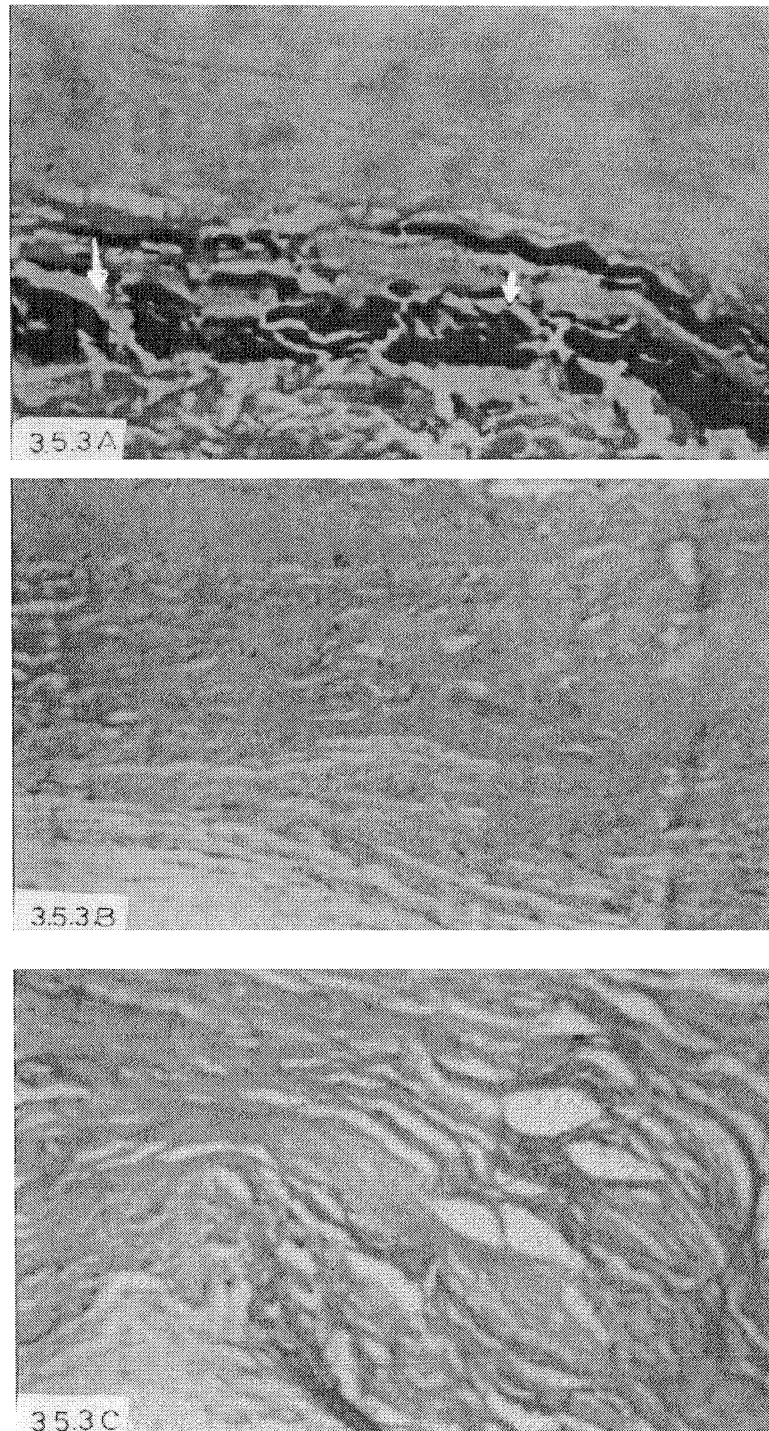
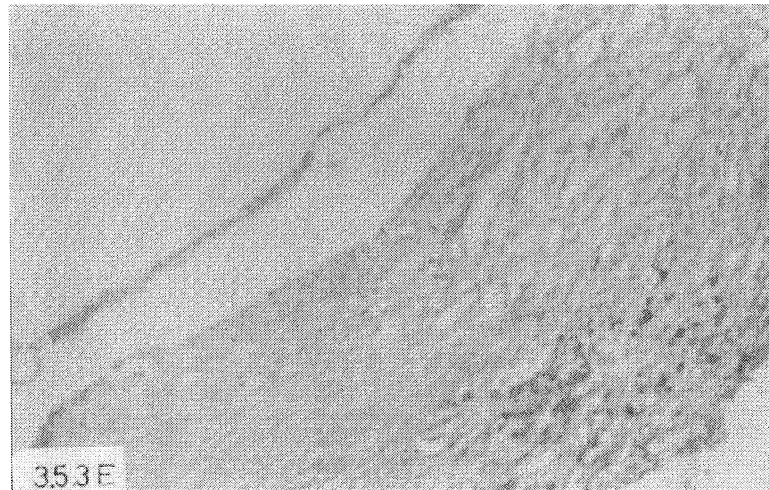
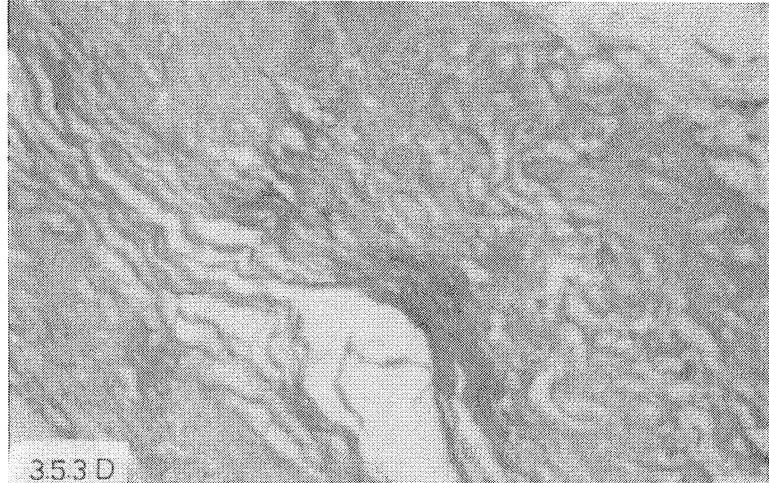


Figure: 3.5.3 Histological demonstration of calcified pericardial samples stained with von Kossa after 21 days post implantation. (A) GAT BP (B) PEG grafted BP. Original magnification-X50 (C) PEG grated BP co-implanted with aspirin/ heparin loaded co-matrix. Original magnification - X100.



- (D) PEG grafted BP co-implanted with ferric/magnesium loaded co-matrix. Original magnification - X100.
- (E) PEG grafted BP co-implanted with ferric/magnesium loaded co-matrix 21 days post implantation stained with Perl's Prussian blue. Original magnification - X50.

All implants of bovine pericardial tissues had normal architecture and were surrounded by fibroblasts and fibrocytes with an infiltration of macrophages into the peripheral layer of implant (figure 3.5.3). The calcified areas which stain darkly with von Kossa, were present in most samples of glutaraldehyde treated BPs (after 21 days)

in the form of minute foci as well as confluent areas. The calcium deposition was substantially reduced with PEG grafted BP (figure 3.5.3B). There was significant inhibition of calcification in PEG-BP implants, due to the release of aspirin/heparin or $\text{Fe}^{3+}/\text{Mg}^{2+}$ ions, as is evident from von Kossa stains (figure 3.5.3C and figure 3.5.3D respectively). Modified pericardia after 6 months (figure 3.5.4B, C & D) have shown foci of calcified areas in almost all retrieved groups. The drug loaded co-matrix of chitosan/polyethylene vinyl acetate was present adjacent to all implants, some of them surrounded by a few fibrocytes. The blue pigmentation seen in the micrographs (Figure 3.5.3 E) of pericardial tissue (after 21 days), due to Perl's Prussian blue stain, may be due to the presence of released ferric ion from the co-matrix.

GATBP have shown complete destruction of collagen bundles due to calcification as is evident from black areas of (von Kossa) figure 3.5.4A. PEG modified BP has also shown some calcified collagen strips (black areas) with significant reduction in degradation of collagen compared to GATBP (control). While marked reduction in calcification and degradation were observed in PEG-20,000 grafted BP along with aspirin/heparin and ferric/magnesium delivery when stained with von Kossa (figure 3.5.4 C and D).

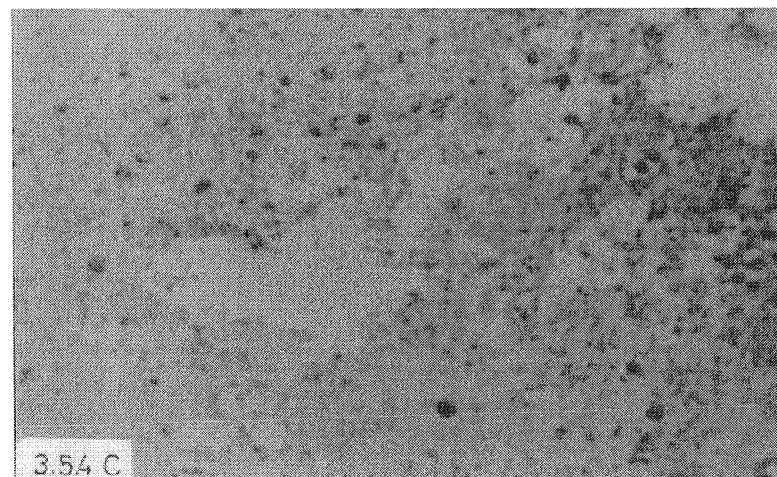
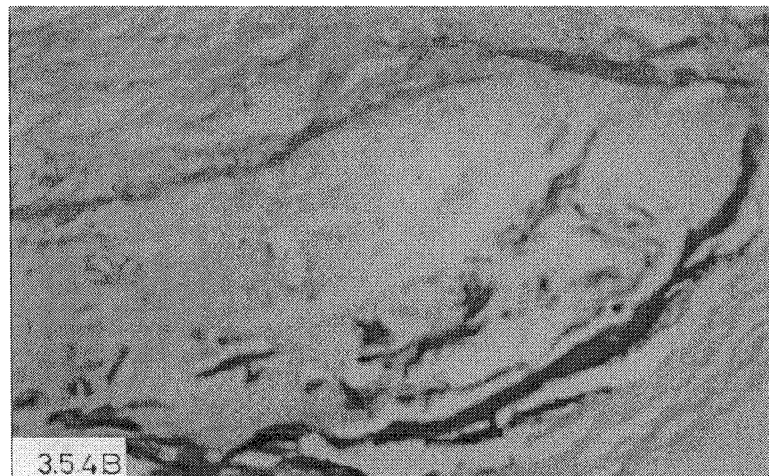
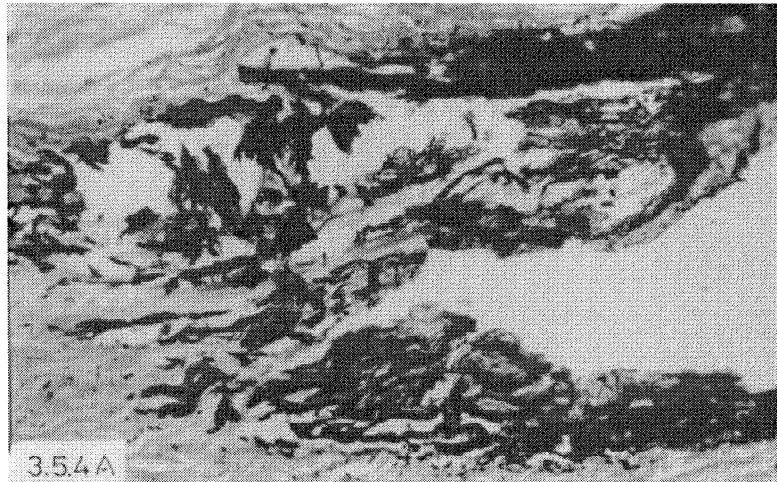
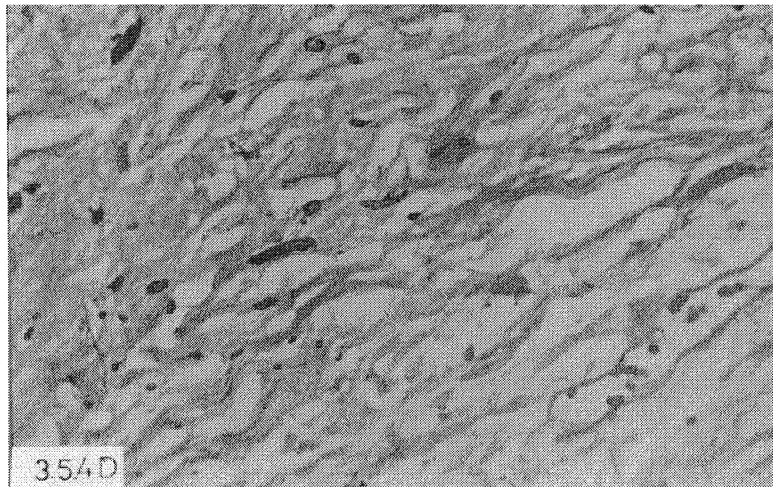


Figure 3.5.4. Histological demonstration of calcified pericardial samples after 6 months of post implantation stained with von Kossa (A) GATBP (B) PEG grafted BP. (C) PEG grafted BP co-implanted with aspirin/heparin delivery. Original magnification x 50



(D) PEG grafted BP co-implanted with ferric/magnesium delivery.
Original magnification x 50.

Haematoxylin-eosin staining of thin paraffin sections of implanted GATBP, PEG modified BP with drug delivery are shown in figure 3.5.5. Evidence of fibroblasts and fibrocytes were observed along one edge, and implants infiltrated with numerous-macrophages, fibroblast, lymphocytes and foreign body type of giant cells along with occasional foci of neutrophils were also observed in 21 days GATBP explants (figure 3.5.5A). The cellular infiltration of the implant had been reduced in the case of PEG modified BP along with aspirin/heparin and ferric/magnesium delivery compared to GATBP samples. The morphological architecture of these modified pericardial implants appeared to be maintained. Further, none of the animals experienced any adverse effects on somatic growth of bone development due to the administration of the controlled-release drugs.

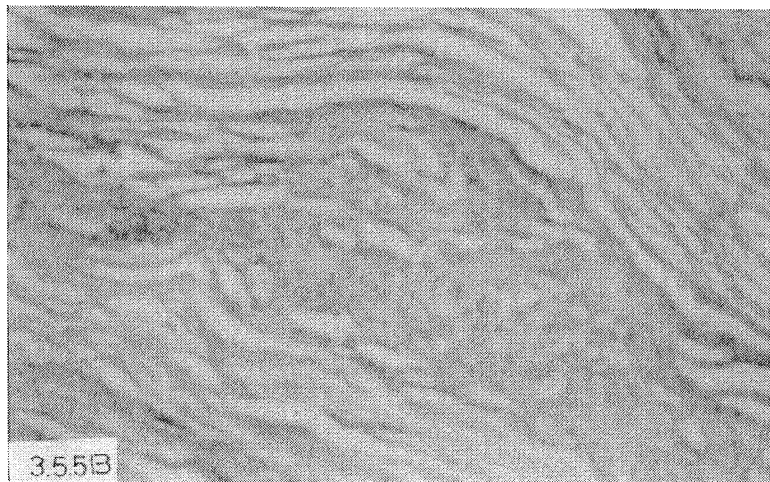
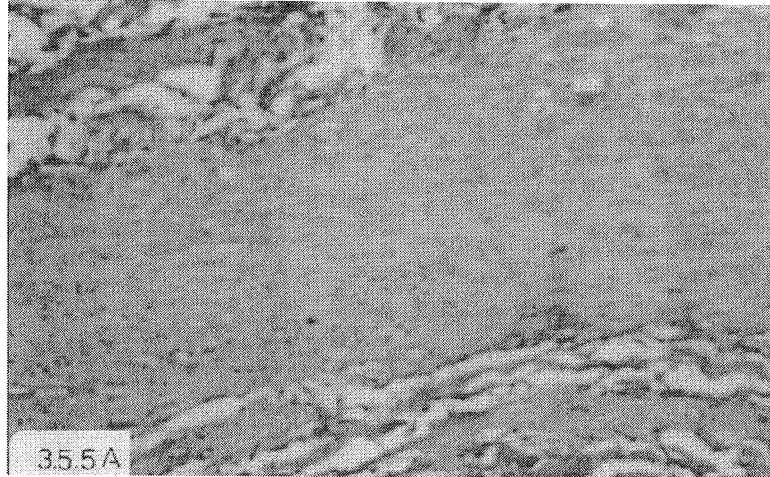
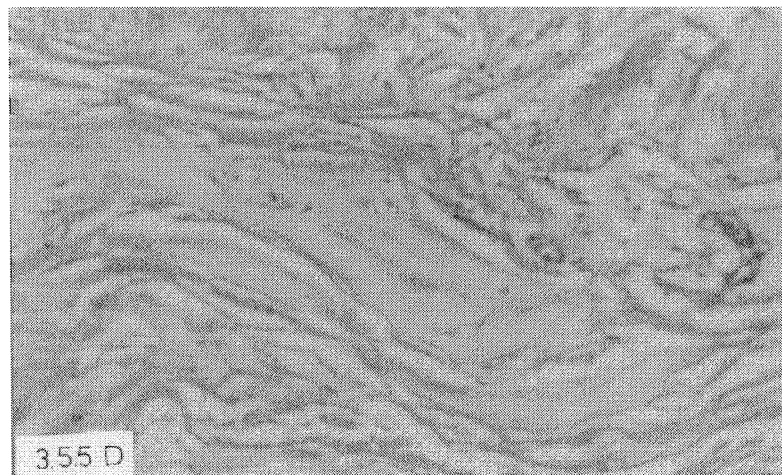
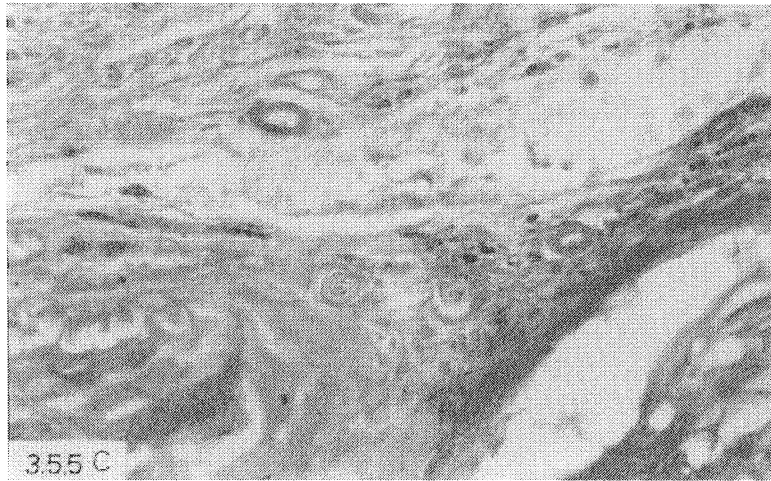


Figure 3.5.5 Histological demonstration of implanted pericardium after 21 days subcutaneous implantation stained by haematoxylin-eosin staining. (A) GAT BP (B) PEG grafted BP. Original magnification A-X50, B-X100.



- (D) PEG grafted BP co-implanted with Ferric/Magnesium.
 - (C) PEG grafted BP co-implanted with aspirin/heparin delivery..
- Original magnification X100.

Table 3.5.I.

Amount of Calcium deposited on bovine pericardium (Group I to IV) after 21 days and 6 months of subcutaneous implantation in rats.

Surfaces	Amount of Ca deposited in $\mu\text{g}/\text{mg}$ dry tissue	
	21 days	6 months
GAT BP	52.4 ± 1.5	240.8 ± 1.6
PEG-GABP	$24.1 \pm 0.8^*$	$51.6 \pm 0.2^*$
PEG-GA BP + aspirin/heparin	$3.4 \pm 0.6^*$	$10.4 \pm 2.1^*$
PEG-GA BP + Ferric/Magnesium	$4.2 \pm 1.0^*$	$14.3 \pm 1.8^*$

Values expressed as mean \pm SD from atleast 6 experimental samples * $p < 0.005$ where all the values of PEG modified surfaces were compared to GAT BP.

3.5.3 In vivo inhibition of calcification: Biochemical studies

The amount of calcium deposited in GATBP (Group I) and PEG modified samples group II, III and IV (refer Chapter II for details of surfaces) after 21 days and 6 months are depicted in Table 3.5.I. Glutaraldehyde treated bovine pericardium showed higher levels of calcium deposition. However, PEG grafting on BP had reduced the deposition of calcium by more than 50%. Further, aspirin/heparin (group III) and $\text{Fe}^{3+}/\text{Mg}^{2+}$ delivery (group IV) from the co-matrix system had substantially inhibited the levels of calcium on PEG-GABP.

This study demonstrated that the released aspirin/heparin from a co-matrix system acted synergistically to inhibit bioprosthetic tissue calcification in the in vivo rat subcutaneous models. The prevention of BP calcification due to these drugs was significant and was comparable to in vitro studies (chapter 3.4). One proposed mechanism for calcification had been the cellular involvements (platelets or cell deposits) on the implant surface, acting as sites for subsequent calcium phosphate deposition. Earlier in vitro observations presented in chapter 3.2 indicated that PEG substantially inhibited platelet adhesion, spreading and reduced the calcium deposition, while retaining biostability. These in vivo studies further confirmed those observations and proposes that the reduced platelet attachment itself may be one of the reason for the observed reduction in calcium deposition on to PEG modified pericardium, through cellular inhibitors.

These *in vivo* studies have also suggested that aspirin and heparin can inhibit the deposition of calcium to GATBP and PEG-GABP, though the exact mechanisms are still unclear to us. It is known that aspirin inhibits platelet release reactions and subsequent adhesion induced by collagenous matrix *in vitro*. Additionally aspirin prolongs the bleeding time.⁷¹ Heparin is a natural anticoagulant responsible for maintaining fluidity of blood. Therefore, it may be expected that aspirin and heparin can exert antithrombotic effect through platelet and coagulation proteins.

Further, Vroman¹⁹³ has indicated that platelets adhere where they find adsorbed fibrinogen. Thus it is assumed that aspirin/heparin can modulate the surface-fibrinogen and subsequently cellular attachment as suggested in chapter 3.4. This itself may be another factor for the inhibition of material associated calcification through cellular involvements. Moreover heparin carries high negative charge due to sulfonate groups which may interact with Ca ions blocking them to form HA crystals to some extent.⁹⁸ Thus, it seems that the antithrombotic drugs may interfere with calcium mobilization and subsequent deposition to tissue interfaces.

3.5.4. Alkaline phosphatase and tissue calcification

Alkaline phosphatase activity reproducibly extractable from the explants of GATBP and PEG modified BP are shown in Table 3.5.II. Explant analyses of PEG grafted pericardium revealed that extractable AP activity (Table 3.5.II) had shown marked reduction compared to GATBP. Moreover, AP activity accumulated rapidly within 72h, following subdermal implantation of all pericardial samples.

Table 3.5.II.

Alkaline phosphatase activity of retrieved samples (Group I to Group IV) after 72 hrs. and 21 days represented as the nano mole of para-nitrophenol liberated per minute per mg protein (units).

Surfaces	Alkaline phosphatase activity (nm pnp/min/mg protein)	
	72 hours	21 days
GAT BP	280.5 ± 1.2	52.1 ± 1.8
PEG-GABP	225.7 ± 3.9	22.2 ± 1.4*
PEG-GA BP + aspirin/heparin	165.2 ± 16.6*	10.2 ± 0.8*
PEG-GA BP + Fe ³⁺ /Mg ²⁺	176.4 ± 9.4*	12.0 ± 1.5*

Values expressed as mean ± SD from at least 6 experiment samples

* p < 0.005 where all the values of PEG modified surfaces were compared to GATBP

Table 3.5.II suggests that the activity of AP is markedly increased in the first 72h in the GATBP rat subcutaneous implants, during which calcification is initiated. This may involve both intrinsic AP activity associated with the site of the initial calcific deposits and absorbed extrinsic AP. Absorbed AP could rapidly hydrolyse the phospho-esters, to provide a rapid rise in regional phosphate concentration leading to mineralization. This enhanced AP activity appeared to normalize within 21 days of implantation (Table 3.5.II). The mechanistic relationships between aspirin/heparin mediated mitigation of calcification on the one hand and inhibition of AP on the other are incompletely understood. However, this mechanism could in part be responsible for the reduction of calcification noted in the present study. However, it seems that aspirin/heparin, and $\text{Fe}^{3+}/\text{Mg}^{2+}$ ions may directly quench the chemical activity of AP. Biochemical studies revealed that 72h explants have intense AP activity, this may be due to the cellular injury associated with surgery and which may not be a reason for initiation of calcification.

AP is present in blood, extracellular fluid and urine. Hence, AP could be readily adsorbed into many implantable biomaterials. Calcification of bioprosthesis may occur in association with the deposition of devitalized cells and cellular debris,^{48,61,100,145} and perhaps adherent blood platelets, which also contain high levels of AP activity. In this case PEG grafting on BP in combination with aspirin/heparin delivery can substantially inhibit the cellular attachment and subsequently their extrinsic calcification. This itself may be one of the reasons for reduced AP activity

which subsequently reduces calcification. Hence, aspirin/heparin delivery can inhibit the bioprosthesis induced thrombosis and calcification. However, more detailed studies are needed to understand the possible interrelation between alkaline phosphatase and platelets in surface mediated calcification.

Earlier in vitro observations from our lab have shown²⁸ that preincubation of the metal ions like Fe^{3+} and Mg^{2+} individually and in combination of low levels can significantly reduce the crystallization of calcium phosphate. The present in vivo studies have further confirmed this hypothesis by proposing the inhibition of pericardial calcification through controlled release of these metal ions. Blumenthal¹⁴ has proposed, on the basis of in vitro studies that the co-ordination of Fe^{3+} ions to oxygen atoms in the growth site of hydroxyapatite (HA) crystals can slowdown or retard the calcification process by delaying the proper formation of HA. However, Mg^{2+} was believed to disrupt the growth of HA by replacing Ca^{2+} by distorting the structure of embryonic HA crystals leading to their break down.¹⁴ Both Fe^{3+} and Mg^{2+} restrict the crystalline growth of hydroxyapatite in in vitro.^{14,28} Furthermore, from the present in vivo studies it is conceivable that Fe^{3+} and Mg^{2+} may act to interfere with AP and perhaps the AP contribution to mineralization, by multiple independent mechanisms.

Thus, compiling the in vitro studies (chapter 3.2 and 3.4) and the present in vivo observations, it appears that the synergistic drug combinations such as $\text{Fe}^{3+}/\text{Mg}^{2+}$, aspirin/heparin delivery can inhibit the tissue associated AP activity and

subsequent calcification. PEG grafting with subsequent aspirin/heparin delivery to pericardial interface can reduce the localized cellular attachment and mineralization. $\text{Fe}^{3+}/\text{Mg}^{2+}$ may also act in the latter stages of anticalcification through their independent mechanisms. In conclusion it is proposed that a combination therapy via surface modification in parallel with synergistic drug delivery is an attractive option to prevent bioprosthesis associated calcification and thrombosis.

CHAPTER 4

CONCLUSION AND FUTURE OUTLOOK

Over the last twenty years, the use of bioprosthetic heart valves to replace diseased natural valves has become an important alternative to the use of completely synthetic materials. Enthusiasm for the biologic valve fluctuates as cardiac surgeons are attracted to the obvious advantages of their superior flow characteristics and lack of thromboembolism, but at the same time they are deterred by the questionable durability, possible antigenicity, and the difficulty in achieving a surgically acceptable level of sterility. Undoubtedly valve durability due to calcification emerges as the most persistent criticism of biologic valves. Thus there is an ever increasing need for newer novel; tissue based smart biomaterials for replacing diseased heart valves.

4.1 Development of a hybrid biomaterial (PEG-BP)

The present investigation suggests that the double crosslinked BP with high molecular weight polyethylene glycol (PEG - 20,000) grafting, produces a highly blood compatible and anticalcifying material, with improved immunogenicity and biostability. Among the various crosslinking techniques tried, a combination of glutaraldehyde • PEG • carbodiimide • PEG - BP and GA • PEG • hexamethylene diisocyanate - PEG - BP appeared to be appealing as a novel hybrid material.

The exact mechanism of PEG in inhibiting calcification, is not well understood. However, one possibility may be polyethylene glycol binds to

glutaraldehyde pretreated bioprosthetic tissues, presumably as the result of an acetal reaction. Due to non-availability of free-CHO groups in GA treated pericardium when crosslinked with PEG, inhibit calcification. One proposed mechanism for calcification had been the cellular involvements (platelets or cell deposits) on the implant surface, acting as sites for subsequent calcium phosphate deposition.^{48,61,116} PEG modified surfaces have shown an increase in albumin surface binding and substantial reduction in fibrinogen attachment.⁴⁷ Vroman¹⁹³ has proposed that platelets adhere where they find adsorbed fibrinogen. These studies have also indicated that PEG substantially inhibited platelet adhesion, spreading and reduced the calcium deposition, while keeping biostability. Thus it appears that the PEG modifies the cellular adhesion and subsequently the tissue associated calcification. These multifunctionalities of PEG may provide biostability and resistance to tissue calcification.

4.2 Prevention of pericardial calcification via synergistic drug delivery

This study proposes the possibility of delivering aspirin/heparin and Ferric/Magnesium combinations through chitosan/PE(VAc) matrix for inhibiting pericardial thrombosis and calcification. The exact mechanism of action of antiplatelet aspirin and anticoagulant-heparin in the calcification profile is not well defined. Studies have shown that aspirin can inhibit platelet functions in vivo and in vitro due to the modulation of platelet receptor sites.^{49,71} Further, it has been demonstrated that heparin/aspirin infusion can cause an increase in albumin or

decrease in fibrinogen surface binding, on incubation with protein mixture.^{29,71} Thus it is assumed that aspirin-heparin can modulate the surface-fibrinogen and subsequent cellular attachment. This may be one of the factors for inhibition of material associated calcification through cellular involvements.

Previous work has shown that regional controlled release of Al^{3+} and Fe^{3+} effectively inhibited tissue calcification.¹¹⁴ However, the release of a single drug can lead to certain unwanted side effects, since a higher concentration of the drug is needed for therapy. The therapeutic approach proposed in this study may be appealing i.e. a combination drug therapy - via synergistic drugs such as aspirin/heparin or $\text{Fe}^{3+}/\text{Mg}^{2+}$ to the implant site for preventing calcification.

4.3 Surface modification and drug delivery

PEG grafted pericardium through glutaraldehyde linkages in parallel with aspirin/heparin or $\text{Fe}^{3+}/\text{Mg}^{2+}$ delivery can inhibit the tissue associated calcification. Park *et al*¹⁴⁷ have recently modified the biological porcine tissue by the direct coupling of sulphonated poly(ethylene oxide) containing amino end groups after glutaraldehyde fixation. The calcification was substantially reduced in such modified tissues, when investigated by in vivo rat subcutaneous model. Chanda *et al*²⁴ have found that coupling of heparin through an intermediate surface-bound substrate containing amino groups, can prevent the calcification of glutaraldehyde treated porcine pericardium implanted subdermally in weanling rats. These interesting observations further support our present conclusions. A promising therapeutic

approach may be a combination therapy via surface modification of the implant with anticalcifying agents (PEG grafting and controlled delivery of drug combinations aspirin/heparin to the implant site, while avoiding systemic side effects).

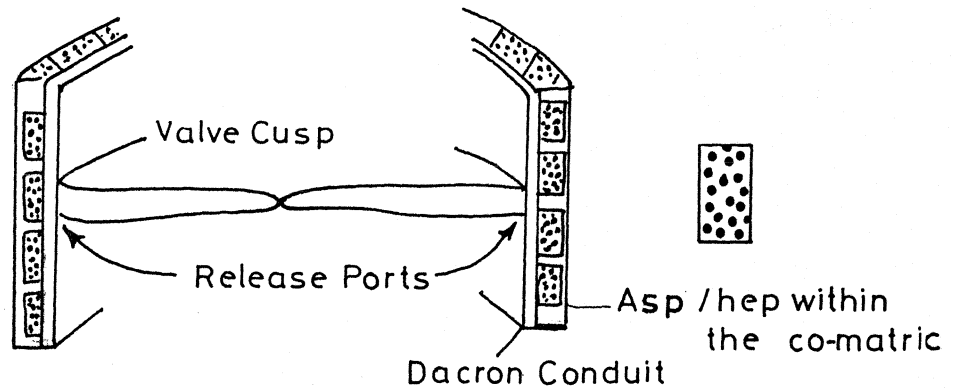
4.3.1 Site Specific drug delivery

Where the drug matrices can be incorporated in a tissue valve is a critical issue for consideration. The drug should be delivered directly into the valve cusps (the initial sites for calcification), to minimize or eliminate a washout effect by the blood stream. One possible approach may be to load the controlled-release matrix containing aspirin/heparin around the attachment ring of the valve (Figure 4.1). The polymeric matrix containing the drugs could surround the attachment ring and this configuration would result in drug delivery at the valve annular attachment area, a site where calcification often appears to originate and is most intense.

Bioprosthetic heart valve calcification is an important clinical and experimental problem. Understanding its pathogenesis and physiology can lead to the means to improve the outcome of cardiac valve replacement and provide a therapeutic approach to reduce pathological calcification in general. A direct outcome from the present research has been the development of the hybrid-tissue material with parallel site - specific - controlled - release drug delivery for cardiovascular implants. An approach which may provide to be useful for anticalcification therapy and tissue biostability.

CONTROLLED RELEASE OF ASPIRIN / HEPARIN FROM
CO-MATRIX

I. Pre release



II. Ongoing Release

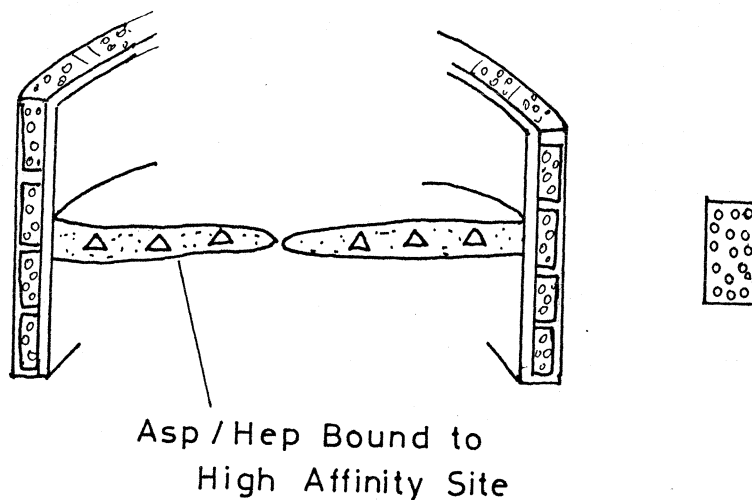


Figure. 4.1. Schematic diagram of controlled release co matrix situated at the valve-anular junction in bioprosthetic heart valve conduit with selective release at the a affinity sites.

FUTURE OUTLOOK

4.4.1 In vitro wear testing

The durability of the cardiovascular biomaterials, we have developed can be tested by accelerated life cycle testing to study their mechanical wear resistance and fatigue properties. To test new designs at normal heart rates, whether in mechanical systems or in animal models for periods over 10 years is totally unrealistic. Several methods of accelerated testing of prosthetic valves can be used including pneumatic cycling, several variations of mechanical cycling, hydraulic cycling and a combination of these. At the end of the test, the valves can be dismantled and then inspected for signs of wear or other degradation and in vitro calcification profile.

4.4.2 Circulatory Animal Models

There are lot of limitations to the in vitro calcification model^{26,68} and in vivo rat subcutaneous implantation models, compared to that of circulatory implants in particularly. When calcific deposits have been noted to be localized to sites of maximum dynamic physical stress, where there is thought to be damage to the elastomeric blood contact surface, with microscopic cellular debris and other blood components probably accumulating in the material defects; this may lead to nucleation of hydroxyapatite deposits. Stress-induced potentiation of bioprosthetic heart valve calcification is commonly noted and may also be due to material damage

and a related enhancement of calcification; In vitro or rat subcutaneous implantation methods cannot give stress mediated calcification. One possible approach may be the orthotopic heart valve replacements in either the mitral or tricuspid positions in sheep or calf which provide a pathological picture comparable to that seen clinically. Such studies are time consuming and very expensive, but can provide the exact situation in a circulatory environment. Thus, more in vivo studies with modified hybrid tissue is needed in the circulatory animal models to find out the exact mechanisms of calcification and tissue stability to evaluate long term patency.

4.4.3 Development of the tissue engineered valves.

Since open heart surgery began in the 1960s, repair and replacement of diseased heart valves has become an established practice. Prosthetic heart valves have been designed and evolved over the years, resulting in enhanced valve performance. While significantly superior to first generation devices, the prosthetic heart valves of today leave room for improvement. A tissue valve from hybrid tissue (PEG - BP) combined drug delivery (Asp/Hep) would be developed and studied for future to come to use them in clinical conditions. These valves may recreate the structure and function of native valves via naturalization that contribute to healthy valve performance.

BIBLIOGRAPHY

1. Altura BM, Altura BT. Influence of magnesium on drug induced contractions and ion content in rabbit aorta. *Am. J. Physiol* 1971; 220: 938-944.
2. Anderson HC. Calcific diseases. *Arch. pathol. Lab Med.* 1983; 107: 341-348
3. Anderson HC. Vesicles associated with calcification in the matrix of epiphyseal cartilage. *J. cell. Biol.* 1969; 41: 59-62.
4. Andrade JD, King RN, Gregonis DE, Coleman DJ. Surface characterization of poly (hydroxy ethyl methacrylate) and related polymer I contact angle methods in water, *J. Polym. Sci. Polym. Symp.* 1979; 66: 313-321.
5. Arbustini E, Jones M, Moses RD et al. Modification by the Hancock T6 process of calcification of bioprosthetic valves implanted in sheep, *Am. J. Cardiol.* 1984; 53: 1388-1393.
6. ASTM-D638-80, Annual Book of ASTM Standards. 1982; 35: 250-252.
7. Bagnall RD, Annis JAD, Sherliker SJ. Adsorption of plasma proteins on hydrophobic surface IV contact angle studies on implanted polymers. *J. Biomed. Mater. Res.* 1980; 14: 1-10.
8. Bancroft JD. Enzyme histochemistry. Theory and Practice of Histological Techniques 3rd (Ed) Churchill Livingstone. 1980; pp. 384-385.
9. Bartek IT, Holden MP, Ionescu MI. Frame mounted tissue heart valves Techniques of construction. *Thorax* 1974; 29: 51-55.
10. Bashey RI, Jimenez SA. Collagen in heart valves In: Nimni ME(ed) Collagen, Vol. 1: Biochemistry 1988; 257-274.
11. Baumgartner HR, Haudenschild C. Adhesion of platelets to subendothelium *Ann NY Acad. Sci.*, 1972; 201: 22-36.
12. Bjork VO. The improved Bjork -Shiley tilting disc valve prosthesis. *Scand. J. Thorac. Cardiovasc. Surg.* 1978; 12: 18-19
13. Bjornsson TD, Levy G. Pharmaco Kinetics of heparin I studies of dose dependence in rats. *J. Pharm Pharmacol Expert Ther.* 1979; 210: 237-242.

14. Blumenthal NC Binding of aluminium hydroxyapatite and amorphous calcium phosphate as a model for aluminium associated osteomalacia in the Chemistry and Biology of Mineralized Tissues (Ed. WT Buttler) Ebsco Press, Birmingham, AL, USA, 1985; p. 385.
15. Blumenthal N C. Mechanism of inhibition of calcification Clin. Orthop. Rel. Res. 1989; 27: 279-289.
16. Blumenthal NC, Posner AS, Rosenberg LC. Further studies on the inhibition of hydroxyapatite formation by proteoglycans, Trans Orthop. Res. Soc. 1980; 5: 10-16.
17. Bodnar E, Bowden NL, Drury PJ, Olsen EGJ, Durmaz I, Ross DN. Bicuspid mitral bioprosthesis. Thorax 1981; 36: 45-51.
18. Boyan-Salyer BP, Boskey AL, Relationship between proteolipids and calcium phospholipid phosphate complexes in bacterionema matrucholi calcification, calcif. Tissue Res. 1980; 30: 176-182.
19. Broom ND, Thomson FJ. Influence of fixation conditions on the performance of glutaraldehyde treated porcine aortic valves: towards a more scientific basis. Thorax. 1979;34: 166-176.
20. Butterfield M, Fisher J, Davies GA, Kearney JM, Sureta F, Watson DA. Fresh glutaraldehyde preserved frame mounted homograft and porcine bioprosthetic heart valves: leaflet geometry, dynamics and function. In: Heimke G, Sottesz U, Lee AJC eds Clinical Implant materials Advances in Biomaterials Amsterdam: elsevier. 1990; 9: 523-528.
21. Carelli V, Di Colo G. Effect of different water soluble additives on water sorption in the silicone rubber. J. Pharm. Sci 1983; 72: 316-317.
22. Carpentier A, Dubost C, Lane E, Nashef A, Carpentier S, Relland J, Deloche A, Fabiani JN, Chauvaud S, Perier P, Maxwell S. Continuing improvement in valvular prosthesis. J. Thorac. Cardiovasc. Surg. 1982; 83: 27-42.
23. Carpentier A, Lemaigre G, Ladislav R, Dubost C. Biological factors affecting long term results of valvular heterografts. J. Thorac. Cardiovasc. Surg. 1969; 58: 467-474.
24. Chanda J, Kuribayashi R, Abe T. Heparin in calcification prevention of porcine pericardial bioprostheses. Biomaterials. 1997; 18: 1109-1113.

25. Chanda J. Pretreatment with amino compounds effective in prevention of calcification of glutaraldehyde treated pericardium *Artif. Organs.* 1994; 18(5): 408-410.
26. Chandy T, Kumar BA, Sharma CP. Inhibition of in vitro calcium phosphate precipitation in the presence of polyurethane via surface modification and drug delivery. *J. Appl. Biomater.* 1994; 5: 245-254.
27. Chandy T, Mohanty M, John A, Rao SB, Sivakumar R, Sharma CP, Valiathan MS. Structural studies on bovine bioprosthetic tissues and their in vivo calcification: Prevention via drug delivery. *Biomaterials.* 1996; 17: 577-585.
28. Chandy T, Sharma CP. Anesthetic and ferric Magnesium in combination as calcium antagonists for glutaraldehyde treated pericardial tissues. *Clinical Materials* 1994; 17: 165-172
29. Chandy T, Sharma CP. Changes in protein adsorption on polycarbonate due to ascorbic acid. *Biomaterials.* 1985; 6: 416-420.
30. Chandy T, Sharma CP. Chitosan matrix for oral sustained delivery of ampicillin. *Biomaterials* 1993; 14: 939-944.
31. Chandy T, Sharma CP. Effect of liposome- albumin coatings on ferric ion retention and release from chitosan beads. *Biomaterials* 1996; 17(1): 61-66.
32. Chandy T, Sharma CP. Effect of plasma glow glutaraldehyde and carbodiimide treatments on the enzymic degradation of poly (L-lactic acid) and poly (benzyl-L-glutamate) films. *Biomaterials.* 1991; 12: 677-682.
33. Chandy T, Sharma CP. Platelet adhesion on polycarbonate changes due to L-ascorbic acid. *J. colloid - Interface. Sci.* 1983; 92: 102-104.
34. Chandy T, Sharma CP. Structural relevance of adsorbed aminosugers on poly carbonate antithrombogenicity. *Thromb. Res.* 1984; 3: 105-115.
35. Chandy T, Vasudev SC, Sharma CP. Changes in polyurethane calcification due to antibiotics. *Artif. Org.* 1996; 20(7): 752-760.
36. Chen W, Kim JD, Schoen FJ, Levy RJ. 2-amino oleic acid derivitization of glutaraldehyde pretreated bioprosthetic tissues for counteracting calcification. A review and comparison of its efficacy and mechanism in various animal models, *Cells and Materials.* 1994; 4: 419-428.

37. Cheung DT, Nimni ME. Mechanism of crosslinking of proteins by glutaraldehyde II. Reactions with monomeric and polymeric collagen *Connective Tissue Res.* 1982; 10: 201-216.
38. Cheung DT, Perelman N, Ko EC, Nimni ME. Mechanism of crosslinking of proteins by glutaraldehyde. III: Reaction with collagen in tissues *Connect. Tissue Res.* 1985; 13: 109-115.
39. Christoffersen MR, Christoffersen J. The effect of aluminium on the rate of dissolution of calcium hydroxyapatite - a contribution to the understanding of aluminium induced bone diseases. *Calcif. Int.* 1985; 37: 673-676.
40. Chvapil M, Speer DP, Holuber H, Chvapil TA, King DH. Collagen fibers as a temporary scaffold for replacement of ACL in goats. *J. Biomed. Mater. Res.* 1993; 27: 313-325.
41. Coleman D. Mineralization of blood pump bladders. *Am. Soc. Artif. Intern. Organs*, 1981; 27: 708-713.
42. Collins D, Lindberg K, Mc Lees B, Pinnell S. The collagen of heart valves *Biochem. Biophys. Acta.* 1977; 495: 129-139.
43. Conceicao AN, Puig LB, Verginetti G, Iryia K, Bittencourt D, Zerbini EJ. Homologous dura mater cardiac valves -Structural aspects of eight implanted valves. *J. Thorac. Cardiovasc. Surg.* 1975; 70: 499-508.
44. Courtman DW, Perira CA, Kashef V, Mc Comb D, Lee JM, Wilson GT. Development of a pericardial acellular matrix biomaterial Biochemical and mechanical effects of cell extraction. *J. Biomed. Mater. Res.* 1994; 28: 655-666.
45. Dahm M, Lyman WD, Schwell Ab, Factor SM, Frater RWM. Immunogenicity of glutaraldehyde tanned bovine pericardium. *J. Thorac. Cardiovasc. Surg.* 1990; 99: 1082-1090.
46. Dicolo G. Controlled drug release from implanted matrices based on hydrophobic polymers *Biomater.* 1992, 13, 850-856.
47. Doillon CJ, Cote MF, Pietrucha K, Laroche G, Gaudreault RC. Porosity and biological properties of polyethylene glycol conjugated collagen materials *J. Biomater. Sci. Ploymer. Edn* 1994; 6: 715-728.
48. Dzemeshevich SL. Heart valve Bioprosthesis causes and pathogenesis of calcification. *Biomaterial Living system interactions.* 1994; 2: 149-159.

49. Ebert C, Mc Rea J, Kim SW. Controlled release of antithrombotic agents from polymer matrices in controlled release of Bioactive Materials. 1980; pp 107-122.
50. Fadali AM, Ramos MD, Topaz SR, Gott VL. The use of autogenous peritonium for heart valve replacement, *J. Thorac. Cardiovasc. Surg.* 1970; 60: 188.
51. Feher JJ, Briggs FN. The effect of calcium load on the calcium permeability sarcoplasmic reticulum, *J. Biol. Chem.* 1982; 257: 10191-10193.
52. Ferrans VJ, Hilbert SL, Tomita Y, Jones M, Roberts WC. Morphology of collagen in bioprosthetic heart valve. In Nimni M(ed): *Collagen*. Boca Raton FL, CRC Press. 1988; 3: 145-189.
53. Fishbein M, Levy RJ, Nashef A, Ferrans VJ, Dearden LC, Goodman AP, Carpentier A. Calcification of cardiac valve bioprostheses: Histological, ultrastructural and biochemical studies in subcutaneous implantation model system. *J. Thorac. Cardiovasc. Surg.* 1982; 83: 602-605.
54. Fisher J, Gorham SD, Howie AM, Wheatley DJ. Examination of fixative penetration in glutaraldehyde treated bovine pericardium by stratigraphic analysis of shrinkage temperature measurements using differential scanning calorimetry. *Life Supp. Sys.* 1987; 5: 189-193.
55. Fleisch H, Neuman WF, Mechanism of calcification role of collagen, polyphosphate and phosphatase, *Am. J. Pathol.* 1961; 200: 1296-1301.
56. Gallop PM, Lian JB, Hauschka PV. Carboxylated calcium-binding proteins in vitamin-K. *N. Engl. J. Med.* 1980; 302: 1460-1466.
57. Gallucci V, Borotolotti U, Milano A, Valfre C, Mazzucco A, Thiene G. Isolated mitral valve replacement with the Hancock bioprosthesis A 13 year appraisal. *Ann. Thorac. Surg.* 1984; 38(6): 571-578.
58. Geha AS, Salaymel MT, Davis GL, Baue AE. Replacement of the aortic valve with molded autogenous grafts grown in response to implanted silastic. *J. Thorac. Cardiovasc. Surg.* 1977; 60: 661-665.
59. Genge BR, Sauer GR, Wu LNY, Mc Lean FM and Wuthier RE. Correlation between loss of AP activity and accumulation of calcium during matrix vesicles mediated mineralization. *J. Biol. Chem.* 1988; 263: 18513-18519.

60. Gerosa G, Mc Kay R, Ross DN. Replacement of the aortic valves or root with a pulmonary autografts in children. *Am. Thorac. Surg.* 1991; 51: 424-429
61. Girardot MN, Torrianni M, Dillehay D, Girardot JM. Role of glutaraldehyde in calcification of porcine heart valves comparing cusp and wall. *J. Bimed. Mater. Res.* 1995; 29: 793-801.
62. Glimcher MJ. Composition, structure and organization of bone and other mineralized tissues and the mechanism of calcification. In RO Greep and ED Astwood (eds), *Hand Book of Physiology*, vol 2, American Physiological Society. Washington DC, 1976; pp. 25-116.
63. Glimcher MJ. On the form and function of bone from molecules to organs. Wolff's law revised 1981 in A Veis (ed), *The Chemistry and Biology of Mineralized Connective Tissue*, Elsevier North - Holland, Amsterdam 1981; 617-673.
64. Golomb G. Calcification of polyurethane based biomaterials implanted subcutaneously in rats: role of porosity and fluid absorption in the mechanism of mineralization. *J. Mater. Sci. Mater. Med.* 1992; 3: 272-247.
65. Golomb G, Egra V, Prevention of bioprosthetic heart valve tissue calcification by charge modification. Effects of protamine binding by formaldehyde *J. Bimed. Mater. Res.* 1991; 25: 85-98.
66. Golomb G, Langer R, Schoen FJ, Smith MS, Choi YM, Levy RJ. Controlled release of diphosphonate to inhibit bioprosthetic heart valve calcification: Dose response and mechanistic studies. *J. Control. Release.* 1986; 4: 181-194.
67. Golomb G, Schoen FJ, Smith MS, Linden J, Dixon M, Levy RJ. The role of glutaraldehyde induced crosslinks in calcification of bovine pericardium used in cardiac valve bioprosthesis. *Am. J. Pathol.* 1987; 127: 122-130.
68. Golomb G, Wagner D. Development of a new a in vitro model for studying implantation polyurethane calcification *Biomaterials* 1991; 12: 397-405.
69. Gong G, Ling Z, Seifter E. Aldehyde tanning. The villain in Bioprosthetic calcification, *European Journal of Cardio-thoracic surg.* 1991, 5: 288-299.
70. Gottschalk N, Jaenicke R, Chemically crosslinked lactate dehydrogenase stability and reconstitution after glutaraldehyde fixation *Biotech. Appl. Biochem.* 1987; 9: 389-400.

71. Haak JC. Mechanisms of action Aspirin. *Thromb. Res. Suppl.* 1983; IV: 47-57.
72. Hagler HK, Lopez LE, Murphy ME, Greico CA, Buja LM et al. Quantitative X-ray microanalysis of mitochondrial calcification in damaged myocardium. *Lab. Invest.* 1981; 45: 241-247.
73. Hamilton WC. A technique for the characterization of hydrophilic solid surfaces. *J. Colloid. Interface. Sci.* 1972; 40: 219-222.
74. Han DK, Jeong SY, Kim YH. Evaluation of blood compatibility of PEO grafted and heparin immobilized polyurethanes. *J. Biomed. Mater. Res. Appl. Biomater.* 1989; 23: 211-228.
75. Harasaki H, Mc Mahon J, Richards T, Goldcamp J, Kiraly R, Nose Y. Calcification in cardiovascular implants: Degraded cell related phenomena, *Trans. Am. Soc. Artif. Intern. Org.* 1985; 31: 489-494.
76. Harasaki H, Mortiz A, Uchida N, Chen JF, Mc Mahon JT, Richards TR, Smith WA, Murabayashi S, Kambic HE, Kiraly RJ, Nose Y. Inhibition and growth of calcification in polyurethane coated blood pump. *Trans. Am. Soc. Artif. Intern. Org.* 1987; 33: 643-649.
77. Hardy PM, Nicholls AC, Rydon HN. The nature of the crosslinking of proteins by glutaraldehyde. Part I. Interaction of glutaraldehyde with the amino groups of 6 amino hexanoic acid and of -N-acetyl-lysine. *J. Chem. Soc. Perkin Trans.* 1976; 958-962.
78. Harper E, Berger A, Katchalski E. The hydrolysis of poly (L-prolyl-glycyl-L-prolyl) by bacterial collagenase. *Biopolymers*, 1972; 11: 1607-1612.
79. Harris JM. *Polyethylene Glycol Biotechnical and Biomedical Applications.* Edited by Plenum Press, New York. 1992.
80. Harris JM, Struck EC, Case MG, Paley MS, Yalpani M, Van Alstine JM, Brooks D. Synthesis and characterization of poly(ethylene Glycol) Derivatives. *J. of Poly. Sci.: Poly. Chem. Edition.* 1984; 22: 341-352.
81. Harris HF. On the rapid conversion of haematoxylin into haematein in staining reaction. *J. of Applied Microscopic Laboratory Methods* 1990; 3: 777-778.
82. Henry RJ, Dryer RL. *Standard Methods of Clinical Chemistry* Acad. Press New York. 1963; pp 205-206.

83. Herring GM. The organic matrix of bone in the *Biochemistry and Physiology of Bone* Bourne GH. Ed Academic Press, New York. 1972; 128-132.
84. Highman W.J, Calcified bodies and the intrauterine device *ACTA Cytol* 1971; 15: 473-475.
85. Hirsch D, Drader J, Pathak VY, Yee R, Schoen FJ, Levy RJ. Synergistic inhibition of the calcification of glutaraldehyde pretreated bovine pericardium in a rat subdermal model by FeCl₃ and ethane hydroxy diphosphonate: preincubation and polymeric controlled release studies. *Biomaterials*. 1993; 14: 705-711.
86. Hirsch D, Drader J, Thomas TJ, Schoen FJ, Levy JT, Levy RJ. Inhibition of calcification of glutaraldehyde pretreated porcine aortic valve cusps with sodium dodecyl sulfate: Preincubation and controlled release studies *J. Biomed. Mater. Res*. 1993; 27: 1477-1484.
87. Holly FJ, Refojo MF, Wettability of hydrogels Poly (2-hydroxy ethyl methacrylate) *J. Biomed. Mater. Res*. 1975; 9: 315-326.
88. Hopwood D. Theoretical and practical aspects of glutaraldehyde fixation, 1972, 4: 267-303.
89. Hossaing SFA, Hubbell JA. Molecular weight dependence of calcification of polyethylene glycol hydrogels. *Biomaterials*. 1994; 15: 921-925.
90. Ionescu MI, Tandon AP, Mary DAS, Abid A. Heart valve replacement with the Ionescu-Shiley pericardial xenograft. *J Thorac. Cardiovasc. Surg*. 1977; 73: 31-35.
91. Ionescu MI (ed): *Tissue Heart valves*, London Butter Worth 1979; 91-93
92. Jamieson WRE, Allen P, Miyagishima RT, Gerein AN, Muro AI, Burr LH, Janusz MT, Ling H, Tutassaura H, Tyers GFO. The Carpentier- Edwards standard porcine bioprosthesis- A first generation tissue valve with excellent long term clinical performance. *J Thorac Cardiovasc. Surg*. 1990; 99: 543-561.
93. Jamieson WRE, Allen P, Janusz MT, Germann E, Chan F, Mac Nab J, Munro AI, Miyagishima RT, Gerein AN, Burr LH, Tyers GFO. First-generation porcine bioprosthetic valves: Proceedings of the Third International Symposium, New York, Yoke Medical Books. 1986; pp 105-115.

94. Jamieson WRE, Gerein AN, Tyers GFO, Janusz MT, Muro AI, Jyrala AJ, Miyagishima RT, Allen P Carpentier- Edwards Supra annular porcine bioprosthesis Clinical experience and implantation characteristics. *J. Thorac. Cardiovasc. Surg.* 1986; 91: 555-565.
95. Johnes M, Eidbo EE, Hilbert SL, ferrans VJ Clack RE. Anticalcification treatments of bioprosthetic heart valves in vivo studies in sheep, *J. Cardiac. Surg.* 1949; 4: 69-73.
96. Johnes SJ, Boyde A. Scanning electron microscopy of the tissue response to polymers. *Techniques of biocompatibility testing boca Raton CRC Press Inc.* 1986; 131-146.
97. Johnston TP, Schoen FJ, Levy RJ. Prevention of calcification of bioprosthetic heart valve leaflet by calcium diphosphanate pretreatment, *J. Pharm. Sci.* 1988; 77: 740-744.
98. Joshi RR, Frautschi JR, Phillips RE, Levy RJ. Immobilized heparin and heparin-Bisphosphonate prevent polyurethane calcification and thrombosis. In vitro and in vivo studies. Fifth World Biomaterial Congress, Toronto, Canada. 1996; 610.
99. Khor E. Methods for the treatment of collagenous tissue for bioprosthesis. *Biomaterials* 1997;18: 95-105
100. Kim K M, Role of membranes in Calcification, *Surv. Synth. Pathol Res.* 1983; 2: 215-228.
101. Lam CR, Aram HH, Munnell ER. An experimental study of the aortic valve homografts surgery, *Gynecology and Obsterics*, 1952; 94:129-134.
102. Langdell RD, Wagner RH, Brinkhous KM. Effects of antihaemophilic factor on one stage clotting test, *J. Lab. Clin. Med.* 1953; 41: 637-642.
103. Langer R, Polymeric delivery systems for controlled drug release. *Chem. Eng. Commun* 1980; 6: 1-48.
104. Lee JM, Edwards HHL, Pereira CA, Sami SI, Crosslinking of tissue derived biomaterials in 1-ethyl-3-(3-dimethyl amino propyl)-carbodiimide (EDC). *J. Mater. Sci. Mater. Med.* 1996; 7: 531-541.
105. Lee JM, Haberer SA, Boughner DR, The bovine pericardial xenograft: I. Effect of fixation in aldehydes without constraint on the tensile viscoelastic

- properties of bovine pericardium. *J. Biomed. Mater. Res.* 1989; 23: 457-475.
106. Lefrak EA, Starr A (Eds). Caged ball valves. In *cardiac valve Prostheses* New York, Appleton- Century-Crofts, 1979; pp 67-166.
 107. Levy RJ, Bolling SF, Siden R, Kadish A, Pathak Y, Dorostkar P, Sintov A, Golomb G, Johnston TP. Polymeric controlled release of cardiovascular drugs in CG Gebelein (Ed) *Cosmetics and Pharmaceutical applications of polymers* Plenum Press, New York, 1991; 231-238.
 108. Levy RJ, Glutaraldehyde and the calcification Mechanism of bioprosthetic Heart valves. *The J of Heart valve Diseases* 1994; 3: 101-104.
 109. Levy RJ, Golomb G, Trachy J, Labhasetwar V, Muller D and Topol E. Strategies for treating arterial restenosis using polymeric controlled release implants. In *Biotechnology and Bioactive polymers*, eds C. Gebelein and C. Carraher, Plenum Press, New York. 1994; 259-268.
 110. Levy RJ, Gudberg C, Scherinman R. The identification of the vitamin K-dependent bone protein osteocalcin as one of the gamma-carboxy glutamic acid containing protein present in calcified atherosclerotic plaque and mineralized heart valves atherosclerosis 1983; 46: 49-56.
 111. Levy RJ, Hawley MA, Schoen FJ, Lund SA, Liu PY. Inhibition by diphosphonate compounds of calcification of porcine bioprosthetic heart valve cusps implanted subcutaneously in rats, *Circulation* 1985; 71: 349-356.
 112. Levy RJ, Labhasetwar V, Song C, Lerner E, Chen W, Vyavahare N, Qu X. Polymeric drug delivery system for treatment of cardiovascular calcification, arrhythmias and restenosis *J. Control. Relea.* 1995; 36: 137-147.
 113. Levy RJ, Lian JB, Gallop PM, Atherocalcin, a carboxyglutamic acid containing protein from atherosclerotic plaque, *Biochem. Biophys. Res. Commun.* 1979; 41: 41-48.
 114. Levy RJ, Schoen FJ, Anderson HC, Harasaki H, Koch H, Brown W, Lian JB, Cunning R, Gavin JB. Cardiovascular implant calcification: a survey and update. *Biomaterials* 1991; 12: 707-714.
 115. Levy RJ, Schoen FJ, Flowers WB, Staelin ST. Initiation of mineralization in bioprosthetic heart valve; Studies of alkaline phosphatase activity and its inhibition by AlCl₃ or FeCl₃ preincubation. *J. Biomed. Mater. Res.* 1991; 25: 905-935.

126. Locke KJ, Fisher J, Juster NP, Davies GA, Watterson K. Biomechanics of glutaraldehyde treated porcine aortic roots and valves, *J. Thorac. Cardiovasc. Surg.* 1994; 108: 1037-1042.
127. Lowry OH, Rosebrough NO, Farr AL. Protein measurement with the Folin phenol reagent. *J. Biol. Chem.* 1951; 193: 265-275.
128. Lynn LH, Huang Lce, David DT, Cheung DT, Nimni ME. Biochemical changes and cytotoxicity associated with the degradation of polymeric glutaraldehyde derived crosslinks. *J. Biomed. Mater. Res.* 1990; 24: 1185-1201.
129. Macmanus Q, Mets droff MT, Grukemeier GL, Starr A. Thrombotic and embolic complications with silastic ball prosthetic valves. *Eur. Heart. J.* 1984; 5: 59-63.
130. Maranto AR, Schoen FJ. Alkaline phosphatase activity of glutaraldehyde treated bovine pericardium used in bioprosthetic cardiac valves, *Circ. Res.* 1988; 63: 844-848.
131. Maranto AR, Schoen FJ. Phosphatase enzyme activity is retained in glutaraldehyde treated bioprosthetic heart valves. *Trans. Am. Soc. Artif. Inter. Organs.* 1988; 34: 827-830.
132. Marguerie GA, Arclaillon N, Cherel G, Plow EI. The binding of fibrinogen to its platelet receptor involvement of the D domain. *J. Biol. Chem.*, 1982; 257: 11872-11878.
133. Merrill EW, Salzman EW. Polyethylene oxide as a biomaterial. *J. Am. Soc. Artif. Intern. Organ.*, 1983; 6(2): 60-64.
134. Metsdorff MT, Grunkemeier GL, Pinson CW, Starr A. Thrombosis of mechanical cardiac valves: A quantitative comparison of the silastic ball valve and the tilting disc valve. *J. Am. Coll. Cardiol.* 1984; 4: 50-53.
135. Milano AD, Bortolotti U, Mazzucco A, Guerra F, Stellin G, Talenti E, Thiene G, Gallucci V. Performance of the Hancock porcine bioprosthesis following aortic valve replacement considerations based on a 15 year experience. *Ann. Thorac. Surg.* 1988; 46: 216-222.
136. Milano AD, Bortolotti V, Talenti E, Valfre C, Arbustini E, Valente M, Mazzucco A, Gallucci V, Thiene G. Calcific degeneration as the main cause of porcine bioprosthetic valve failure. *Am. J. Cardiol* 1984; 53: 1066-1070.

137. Miller EJ. Chemistry of the collagen and their distribution In: Extracellular Matrix Biochemistry Amsterdam. Elsevier 1984; 41-81.
138. Miller ES, Peppas NA, Winslow DN. Morphological changes of ethylene vinyl acetate based controlled delivery system during release of water soluble solutes. *J. Member Sci.* 1983; 14: 79-92.
139. Muzzarelli R, Baldassarre V, Contio F. et al. Biological activity of chitosan, Ultrastructural study *Biomaterials* 1988; 9: 247-252.
140. Naimark WA, Pereira CA, Tsang K, Lee JM. HMDC Crosslinking of bovine pericardial tissue: A potential role of the solvent environment in the design of bioprosthetic materials. *J. Mater. Sci., Mater. Med.* 1995; 6: 235-241.
141. Neuman WF, Distefano V, Mulryan BJ. The surface chemistry of bone III observations on the role of phosphatase, *J. Biol. Chem.* 1951; 193: 227-235.
142. Nimni ME, Chering D, Strates B, Kodama M, Skeikh K. Chemically modified collagen a natural biomaterial for tissue replacement *J. Biomed. Mater. Res.* 1987; 21: 741-771.
143. Nimni ME. Collagen in cardiovascular tissues In: Hastings GW (ed) *Cardiovascular Biomaterials*. London: Springer-Verlag 1992; 81-141.
144. Nishimura K, Nishimura S, Scott, Nishi N, Tokura S, Azuma I. Macrophage activation with multi porous beads prepared from partially deacetylated chitin. *J. Biomed. Mater. Res.* 1986; 20: 1359-1372.
145. Nose Y, Harasaki J, Murray J. Mineralization of artificial surfaces that contact blood *Trans. Amer. Soci. Artif Oryans.* 1981; 27: 714-720.
146. Olde Damink LHH, Dijkstra PJ, Van Luyn MJA Van Wachem PB, Nieuwen Huis P, Feijen J. Changes in the mechanical properties of dermal sheep collagen during in vitro degradation. *J. Biomed. Mater Res.* 1995; 29: 139-147.
147. Olde Damink LHH, Dijkstra PJ, Van Luyn MJA, Van Wachem PB, Nieuwe Huis P, Feijen J. Crosslinking of dermal sheep collagen using a water soluble carbodiimide *Biomaterials* 1996; 17: 765-773.
148. Park KD, Lee WK, Yun JY, Han DK, Kim SH, Kim YH, Kim HM, Kim KT. Novel anti-calcification treatment of biological tissues by grafting of sulphonated poly (ethylene oxide). *Biomaterials*, 1997; 18: 47-51.

149. Pasquino E, Pascale S, Andreon M, Rinaldi S, Laborde F, Galloni M, Bovine pericardium for heart valve bioprosthesis in vitro and in vivo characterization of new chemical treatments. *J Biomed. Mater. Res.* 1994; 5: 850-854.
150. Pathak Y, Boyd V, Schoen FJ, et al. Prevention of calcification of glutaraldehyde pretreated bovine pericardium through controlled release polymeric implants; Studies of Fe^{3+} , Al^{3+} protamine sulfate and levamisole, *Biomaterials.* 1990; 118: 718-723.
151. Pereira CA, Lee JM, Haberer SA. Effect of alternative crosslinking methods on the low strain rate viscoelastic properties of bovine pericardial bioprosthetic material. *J. Biomed. Mater. Res.* 1990; 24: 345-361.
152. Perress NS, Anderson HC, Sajdera SW. The lipids of matrix vesicles from bovine fetal epiphyseal cartilage. *Calcif. Tiss. Res.* 1974; 14: 275-281.
153. Phillips RE, Thomas RJ. Metal ion complexation of polyurethanes: a proposed mechanism for calcification. In planck H, Syre I, Dauner M, Egbers G eds. *Polyurethanes in Biomedical Engineering, 2 Progress in Biomedical Engineering, 3* Amsterdam Elsevier. 1987; 91-108.
154. Plate NA, Valuev L. On the mechanism of enhanced thromboresistance of polymeric materials in the presence of heparin. *Biomaterials.* 1983, 4: 14-20.
155. Posner AS. The mineral bone. *Clin. Orthop.* 1985; 200: 87-99.
156. Price PA, Williamson MK, Haba T, Dell RB, Lee WSS. Excessive mineralization with growth plate closure in rats on chronic warfarin treatment *Proc. Natl Acad. Sci. USA.* 1982; 72: 7734-7739.
157. Prockop DJ, Kivirikko KI. Collagen Molecular Biology, diseases and potentials for therapy. *Ann. Rev. Biochem* 1995; 64: 403-434.
158. Ramos G, Aspeitia D, Romero EG, Castillo-Olivares JL, Figurea D. Evaluation of physiological properties of biological tissues that can be used for reconstruction of cardiac valves. An experimental study *J. Thorac Cardiovasc. Surg.* 1973; 65: 359-365.
159. Ratner BD, Johnston AB et al. Biomaterials surfaces. *J. Biomed. Mater. Res. Appl. Biomat.* 1987; 21: 59-89.

160. Rehul H. In: Plank H et al (eds) Polyurethane in biomedical engineering Elsevier Science Publishers, Amsterdam 1984; pp. 257-277.
161. Reiman W, Benkenkamp J. In treatise on Analytical Chemistry, 5, Part II, Edited by Kolthoff and Elving, Wiley, New York. 1961; pp. 317-402.
162. Reis RL ,Hancock WD, Yarbrough JW, Galncy DL, Morrow AG. Flexible stent J. Thorac Cardiovasc. Surg. 1971; 62: 683-689.
163. Robbins SL, Cotran RS, Kumar V (eds): Pathologic Basis of Disease, WB Saunders. 1984; pp. 35-36.
164. Roberts D, Bake B, William Olsson G. Improved red cell survival in patients with chronic subclinical hemolysis due to artificial heart valve. Scand. J. Thorac. Cardiovasc. Surg. 1984; 18: 115-118.
165. Ross DN. Homograft replacement of the aortic valve, Lancet 1962; 2: 488-489.
166. Ruben M, Tripathi RC, Winder AF. Calcium deposition as a cause of spoilation of hydrophilic soft contact lenses, Br. J. Ophthalmol. 1975; 59: 141-148.
167. Sacks MS, Chuong CJC, More R. Collagen fiber architecture of bovine pericardium ASAIO. 1994; 40: M632-M637.
168. Seifter S, Harper EH. In Methods in enzymology. Vol. 19, Proteolytic enzymes edited by GE Perlmann and L Lorand (Academic Press, New York 1979; pp. 613-635.
169. Schoen FJ, Biomaterial associated infection, neoplasia, and calcification. Clinicopathologic features and pathophysiological concepts. Trans. Am. Soc. Artif. Intern. Organs 1987; 33: 8-18.
170. Schoen FJ. Cardiacvalve prostheses: Pathological and bioengineering consideration J Cardiac. Surg 1987; 2: 65-108.
171. Scheuer PJ, Chalk BT. Clinical Tests Histopathology published by Wolfe Medical Publications Ltd. 1986; 120: pp. 84-85.
172. Schoen FJ, Harasaki H, Kim KM, Anderson HC, Levy RJ. Biomaterial associated calcification: Pathology mechanisms, and strategies for prevention. J Biomed. Mater. Res: Appl. Biomater. 1988; 22: 11-36.

173. Schoen FJ, Kujovich JL, Levy RJ. St. John Sutton M. Bioprosthetic valve failure cardiovasc. Clin. 1988; 18(2): 289-317.
174. Schoen FJ, Levy RJ Bioprosthetic heart valve failure pathology and pathogenesis Cardiol. Clin. 1984; 2: 217-223.
175. Schoen FJ, Levy RJ, Nelson AC, Bernhard WF, Nashef A, Hawley MA. Onset and progression of experimental bioprosthetic heart valve calcification. Lab. Invest. 1985; 52: 523-532.
176. Schoen FJ, Tsao JW, Levy RJ. Calcification of bovine pericardium used in cardiac valves bioprosthesis :role of glutaraldehyde modified structural components in bioprosthetic tissue mineralization. Am. J. Pathol. 1986; 123: 143-154.
177. Shantora V, Huang RYM. Separation of liquid mixtures by using polymer membrane III. Grafted polyvinyl alcohol membranes in vacuum permeation and dialysis. J. of Applied Polymer Sci. 1981; 26: 3223-3243.
178. Silver MD, Hudson REB, Trimble AS. Morphologic observations on heart valve prostheses made of fascia lata. J. Thorac. Cardiovasc. Surg. 1975; 70: 360-366.
179. Simionescu D, Simionescu A, Deac R. Mapping of glutaraldehyde-treated bovine pericardium and tissue selection for bioprosthetic heart valves. J. Biomed. Mater. Res. 1993; 27: 697-704.
180. Smith PK, Mallia AK, Hermanson GT. Calorimetric method for the assay of heparin content in immobilized heparin preparations. Analytical Biochemistry 1980; 109: 466-473.
181. Snell FD. Photometric and fluorometric methods of analysis-metals. A Wiley - Interscience Publication Iron, Chapter 18.
182. Stenflo J, Fermlund P, Egan W. Roepstorff P. Vitamin K dependent modifications of glutamic acid residues in prothrombin Proc. Nat. Acad. Sci. 1977; 71: 2730-2733.
183. Steven FS. "Polymeric collagen fibrils : An example of substrate - mediated steric obstruction of enzymic digestion, Biochem. Biophys. Acta 1976; 452: 151-160.
184. Tang Z, Yilum Y. Crosslinkage of collagen by polyglycidyl ethers. ASAIO. 1995; 41: 72-78.

185. Tan WM, Loke WK, Tan BL, Khor AWE, Gohi KS. Trivalent metal ions in the prevention of calcification in glutaraldehyde treated biological tissues. Is there a chemical correlation? *Biomaterials*. 1993;14:1003-1007.
186. Tew WP, Malis CD, Howard JE, Lehninger AL. Phosphocitrate inhibits mitochondrial and cytosolic accumulation of calcium in kidney cells in vivo. *Proc. Natl. Acad. Sci. USA* 1981; 78: 5528.
187. Thubrikar MJ, Deck JD, Aouad J, Nolan SP. Role of mechanical stress in calcification of aortic bioprosthetic valves. *J. Thorac. Cardiovasc. Surg.* 1983; 86: 115-125.
188. Tindale WB, Trowbridge EA. Evaluation in vitro of prosthetic heart valves: Pulsatile flow through a compliant aorta. *Life supp. Syst.* 1983; 1: 173-185.
189. Tu R, Lu CL, Thyagarajan K, Wang E, Nguyen H, Shen S, Hata C, Quijano RC. Kinetic study of Collagen fixation with polyepoxy fixatives. *J. Biomed. Mater. Res.* 1993; 27: 3-9.
190. Valente M, Bortolotti U, Thiene G. Ultrastructural substrates of dystrophic calcification in porcine bioprosthetic valve failure. *Am. J. Pathol.* 1985; 119: 12-21.
191. Van Buskirk JJ, Kirsch WM, Kleyer DL, Barkely RM, Koch TH. Aminomalonic acid identification in *Escherichia coli* and atherosclerotic plaque. *Proc. Natl. Acad. Sci. USA.* 1984; 81: 722-725.
192. Varley H. *Practical Clinical Biochemistry* William Heinemann. Medical Books Ltd. (London) and Interscience Books Inc. New York. 1967; 480-483.
193. Vroman L, Adams AL, Fisher GC, Munoz C, Stanford M. Proteins, Plasma and blood in narrow space, of clot promoting surface *Adv. Chem* 1982; 199: 266-276.
194. Vroman L, Adams AL, Klings M, Fischer GC, Munoz PC, Solensky R. Reactions of formed elements of blood with plasma proteins at interfaces *Ann. NV. Acad. Sci.* 1977; 283: 65-76.
195. Vyavahare NR, Qu X, Lee M, Bihari P, Schoen FJ, Levy RJ. Synergism of calcium-ethane hydroxy bis phosphonate (CaEHBP) and FeCl₃ Controlled release polymers for preventing calcification of bioprosthetic aortic wall. *J. of controlled release.* 1995; 34: 97-110.

196. Weadock K, Olson RM, Silver TH. Evaluation of collagen crosslinking techniques, *Biomat. Med. Dev. Art. Org.* 1983-84; 11:2 93-318.
197. Webb CL, Flowers WE, Boyd J, Rosenthal EL, Schoen FJ and Levy RJ. Al^{3+} binding studies and metallic actions effects on bioprosthetic heart valve calcification in the rat subdermal model, *Trans. Am. Soci. Artif. Intern. Org.*, 1990; 36: 56-59.
198. Webb CL, Schoen FJ, Flowers WE, Alfrey AC, Horton C, Levy RJ. Inhibition of mineralization of glutaraldehyde pretreated bovine pericardium by $AlCl_3$. *Am. J. Pathol.* 1991; 138: 971-981.
199. Webb CL, Schoen FJ, Levy RJ. Covalent binding of aminopropanehydroxy diphosphonate to glutaraldehyde residues in pericardial bioprosthetic tissue stability and calcification inhibition studies. *Exp. Mol. Pathol.* 1989; 50: 291-302.
200. Weiss HJ, Aledort LM, Kochwa S. The effect of salicylates on the haemostatic properties of platelets in man. *J. Clin. Invest.* 1968; 47: 2169-2172.
201. Williams DF, Mort E. Enzyme Accelerated hydrolysis of polyglycolic acid. *J. Bioeng.* 1977; 1: 231-238.
202. Williams DF. Enzymic hydrolysis of polylactic acid. *Eng. Med.* 1981; 10: 5-7.
203. Wolff J, *Das Gesetz der Transformation der Knochen*, Quarto Berlin. 1892, 1-10.
204. Woodroof EA. The Chemistry and Biology of aldehyde treated tissue heart valve xenografts In *Tissue Heart valves* Ed. By MI Ionescu London, Butterworths 1979; 347-362.
205. Yamada T, Nakumura K, Iwaku M et al. The extent of the odontoblast process in normal and carious human dentin, *J Dent Res* 1983; 62: 798.
206. Yoganathan AP, Reul H, Black MM. Heart valve replacement: Problems and Developments in Cardiovascular Biomaterials. Springer-Verlag, London Berlin Heidelberg, Garth Hastings(Ed) New York 1992; pp 173-183.

APPENDIX A

LIST OF PUBLICATIONS FROM THIS THESIS

1. C.V. Sindhu, T. Chandy, C.P. Sharma, Bioprosthetic tissue calcification. Actiological factors and prospects for prevention Trends in Biomat. & Artif. Organs 1995; 9:34-51.
2. C.V. Sindhu, T. Chandy, C.P. Sharma Polyethylene glycol modified bovine pericardium A novel calcium resistant hybrid material. Trends in Biomat. Artif. Organs 1996; 10:1-15.
3. C.V. Sindhu, T. Chandy, C.P. Sharma Development of chitosan/polyethylene vinyl acetate co-matrix controlled release aspirin/heparin for preventing cardiovascular thrombosis. Biomaterials 1997, 18(5) 375-381.
4. C.V. Sindhu, T. Chandy. Effect of alternative crosslinking technique on the enzymatic degradation of bovine pericardium and their calcification J. Biomed. Mater. Res. 1997; 35:357-369.
5. C.V. Sindhu, T. Chandy, C.P. Sharma. Influence of polyethylene glycol grafting on the in vitro degradation and calcification of bovine pericardium. J. Biomat. Appl. 1997,11,430-452.
6. C.V. Sindhu, T. Chandy, C.P. Sharma, Polyethylene glycol grafted bovine pericardium - A novel hybrid tissue resistant to calcification J. of Mater Sci. Mater. Med (In Press).
7. C.V. Sindhu, T. Chandy controlled release of Ferric/Magnesium ions from chitosan/polyethylene vinylacetate co-matrix for prevention of pericardial calcification. Drug Delivery (accepted).
8. C.V. Sindhu, T. Chandy, C.P. Sharma. Synergistic effect of aspirin / heparin for preventing bovine pericardial calcification. Artif. Organs. (communicated) (Abstract presented in ISAO, conference held at USA).
9. C.V. Sindhu, T. Chandy, C.P. Sharma. Synergistic inhibition of bovine pericardial calcification via controlled release of ferric/magnesium ions (Abstract presented in ISAO conference held at USA) communicated to Artif. Organs.

APPENDIX - B

LIST OF ABBREVIATIONS

ADP	-	Adenosine diphosphate
AOA	-	2 Amino Oleic Acid
AP	-	Alkaline Phosphatase
APD	-	Amino hydroxy diphosphonate
Asp	-	Aspirin
ASTM	-	American Society for Testing
BP	-	Bovine Pericardium
BPHV	-	Bioprosthetic heart valve
CB	-	Chitosan bead
CRT	-	Cathode Ray Tube
DMSO	-	Dimethyl Sulphoxide
EDC	-	Ethyl -3(3-Dimethyl aminopropyl) carbodiimide
EHDP	-	Ethanehydroxy diphosphonate
Fg	-	Fibrinogen
GA	-	Glutaraldehyde
GABP	-	0.6% GA treated BP for 24h
GATBP	-	GABP treated for 2 weeks in 0.2% GA
Hep	-	Heparin
HMDIC	-	Hexamethylene diisocyanate
µg	-	Microgram
µm	-	Micrometer
PEG	-	Polyethylene glycol
PE(VAc)	-	Polyethylene vinyl Acetate
PMSF	-	Phenyl methane sulphonyl fluoride
PTMG	-	Polytetra methylene glycol
rpm	-	rotation per minute
SBR	-	Styrene butadiene
SDS	-	Sodium dodecyl Sulphate
SEM	-	Scanning electron Micrographs
Tris HCl	-	Tris (hydroxy methyl amine methane)